



EU Cost Action FA1306 - The quest for tolerant varieties: phenotyping at plant and cellular level

Poster book of the 3rd general meeting

Oeiras, Portugal, 27-28 March 2017

Organization

Sponsors



<http://www.spfv.pt>



Organising Committee

Carla **Pinheiro**

Jorge Marques da **Silva**

Joaquim Miguel **Costa**

Inês **Chaves**

Ana Sofia **Fortunato**

Leonor **Guerra-Guimarães**

Célia **Miguel**

Scientific Committee

Astrid **Junker**

Carla **Pinheiro**

Carl-Otto **Ottosen**

Célia **Miguel**

Diego **Rubiales**

Dionysia **Fasoula**

Estelle **Goulas**

Eva **Rosenquist**

Inês **Chaves**

Joaquim Miguel **Costa**

Jorge Marques da **Silva**

Leonor **Guerra-Guimarães**

Rick **van de Zedde**

Sebastien **Carpentier**

Ulrich **Schurr**

Contribution list

Number	Name	Affiliation	Country	Contact
PL_1	Elisa Liras	Bayer Crop Science	FR	elisa.liras@bayer.com
OC1	Gerrit Polder	Wageningen University & Research	NL	gerrit.polder@wur.nl
OC11	Marta W. Vasconcelos	Escola Superior de Biotecnologia, Universidade Católica Portuguesa	PT	mvasconcelos@porto.ucp.pt
P2	Stanislaw Weidner	University of Warmia and Mazury in Olsztyn	PL	weidner@uwm.edu.pl
P4	Marijana Acanski	Faculty of Technology, University of Novi Sad	RS	macanski@tf.uns.ac.rs
P6	Radmila Stikic	Faculty of Agriculture, University of Belgrade	RS	rstikic@agrif.bg.ac.rs
P15	Ayse Sen	Faculty of Science, Istanbul University	TR	senayse@istanbul.edu.tr
P17	Stefanie Wienkoop	University of Vienna	AT	stefanie.wienkoop@univie.ac.at
P18	Jasmine Zorrilla	KU Leuven	BE	jasmine.zorrilla@kuleuven.be
P20	Carla Pinheiro	FCT-NOVA & ITQB-NOVA	PT	cm.pinheiro@fct.unl.pt
P24	Vicent Arbona	Universitat Jaume I	ES	arbona@uji.es
P29	Sofija Bozinovic	Maize Research Institute Zemun Polje	RS	sofija_bozinovic@yahoo.com
P30	Gonçalo Laureano	BIOISI-Faculdade de Ciencias, Universidade de Lisboa	PT	goncalo186@gmail.com
P31	Miguel Gaspar	LEAF and BioISI Universidade de Lisboa, Portugal	PT	miguel.fragoso.gaspar@gmail.com
P32	Jelle van Wesemael	KU Leuven	BE	jelle.vanwesemael@kuleuven.be
P34	Daniela Ferreira	Faculdade de Ciências da Universidade de Lisboa	PT	danielaajferreira@gmail.com
P37	Eduardo Feijão	Faculdade de Ciências da Universidade de Lisboa	PT	eduardomof@gmail.com
P38	Rui Nascimento	Faculdade de Ciências da Universidade de Lisboa	PT	rui_nascimento93@hotmail.com
P39	Elias Alisaac	Institute of Crop Science and Resource Conservation, University of Bonn	DE	alisaac@uni-bonn.de
P40	Kristina Loziene	Nature Research Centre, Institute of Botany	LT	kristina.loziene@gmail.com
P41	Natalia Valasevich	Central European Institute of Technology, Masaryk University	CZ	239948@mail.muni.cz
P42	Inês Diniz	CIFC - LEAF, Instituto Superior Agronomia da Universidade Lisboa	PT	inesdiniz@gmail.com
P43	Ankica Kondic-Spika	Institute of Field and Vegetable Crops	RS	ankica.spika@nsseme.com
P44	Ana Jeromela	Institute of Field and Vegetable Crops	RS	anamarjanovicjeromela@gmail.com
P52	Paula Coelho	INIAV - Instituto Nacional de Investigação Agrária e Veterinária	PT	paula.coelho@iniav.pt
P53	Lijuan Zhang	VBCF - Vienna Biocenter Core Facilities	AT	lijuan.zhang@vbcf.ac.at
P58	João Carreiras	MARE - Marine and Environmental Sciences Centre	PT	joaoalbuquerquecarreiras@gmail.com
P60	Pavel Vítámvás	Crop Research Institute	CZ	vitamvas@vurv.cz
P61	Olfa Zarrouk	ITQB-NOVA	PT	zolfaz@itqb.unl.pt
P62	Paula Scotti-Campos	INIAV - Instituto Nacional de Investigação Agrária e Veterinária	PT	paula.scotti@iniav.pt
P63	Tomás Ochôa Cruz	Faculdade de Ciências da Universidade de Lisboa	PT	fc50244@alunos.fc.ul.pt
P66	Cintia Macedo	Faculdade de Ciências da Universidade de Lisboa	PT	cintiamac0802@hotmail.com
P67	MManuela Veloso	INIAV - Instituto Nacional de Investigação Agrária e Veterinária	PT	mveloso.inrb@gmail.com
P69	Clara Pinto	INIAV - Instituto Nacional de Investigação Agrária e Veterinária	PT	clara.pinto@gmail.com
P72	Jorge Marques da Silva	Faculdade de Ciências da Universidade de Lisboa	PT	jmlsilva@fc.ul.pt
P73	Rick van de Zedde	Wageningen Food & Biobased Research Institute	NL	rick.vandezedde@wur.nl
P74	Marina Dermastia	National Institute of Biology	SI	Marina.Dermastia@nib.si
P76	Jenny Renaut	Luxembourg Institute of Science and Technology	LU	jenny.renaut@list.lu



Science For A Better Life

Phenotyping at Bayer HyperCare Farms

Elisa Liras

B&TD Field Phenotyping Global Manager

Crop Efficiency at Bayer

Crop Efficiency: The use of technologies to modulate plant metabolism or improve plant nutrition with the primary intention of increasing yield



Yield Increase

Intrinsic yield enhancement



Yield Preservation

Abiotic stress tolerance (e.g. drought)



Yield Maximization

Nutrient use efficiency (e.g. inoculants)

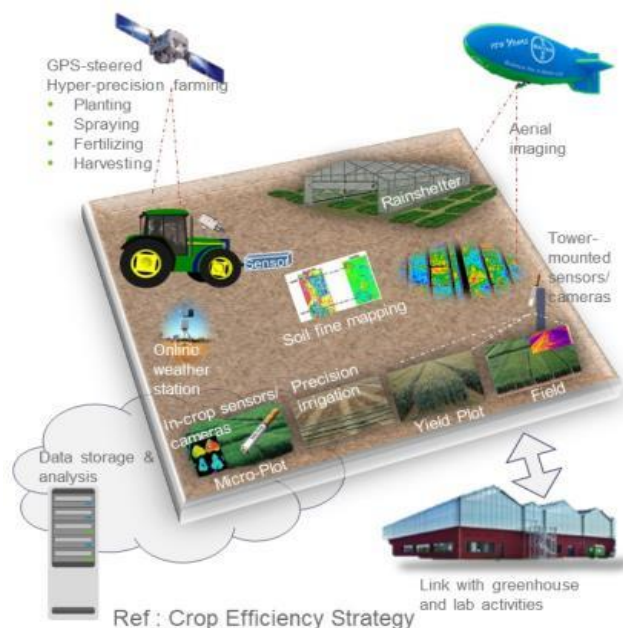
HyperCare Farm concept

HyperCare Farm concept

A high-resolution assessment of plant performance, under target conditions, by measuring phenotypic traits/parameters

Controlled treatment conditions

Adapted data collection, storage, processing & analysis




Precision phenotyping tools

Environment monitoring

Hyperspectral and 3D imaging for disease detection in seed potatoes

EU Cost Action FA1306, PhenomenAll, 3rd general
meeting, Oeiras, Portugal, 27-28 March 2017

Gerrit Polder, Pieter M. Blok, Dirk Otten,
Pieter Kastelein, Jan M. van der Wolf



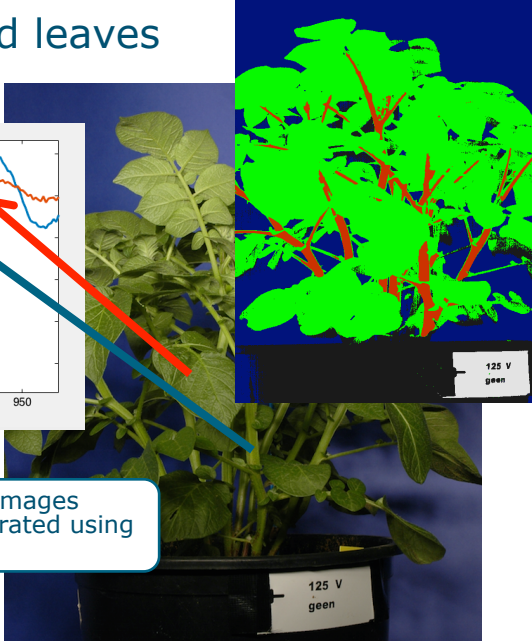
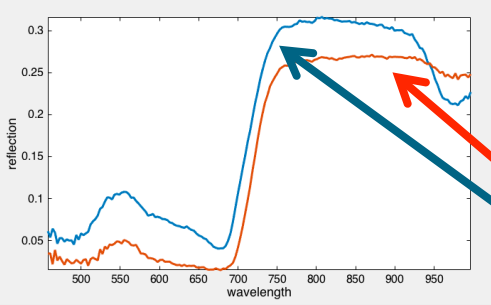
WAGENINGEN UR For quality of life

COST EUROPEAN COOPERATION IN SCIENCE AND TECHNOLOGY

PhenomenAll COST

FA1306

Separate stem and leaves

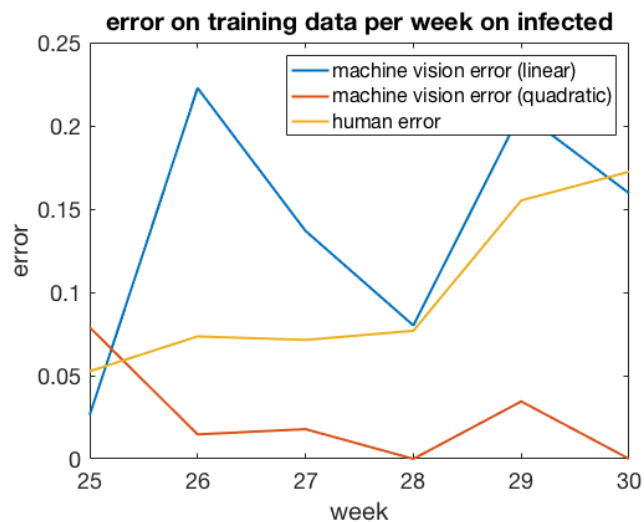


Based on a few example images
leaves and stem are separated using
a simple linear classifier.

WAGENINGEN UR For quality of life

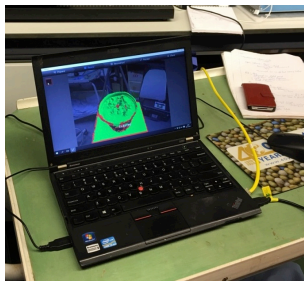
125 V geen

Analysis bacterial infection - results

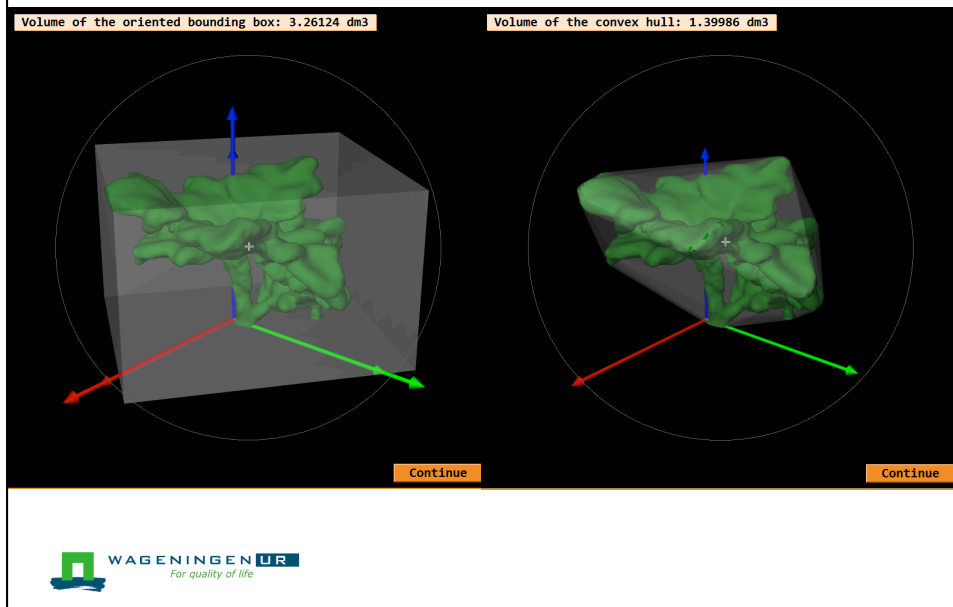


3D plant volume

- Primesens Carmine sensor (larger FOV than Kinect)
- Skanect 1.8
- 30-60s scanning time/ plant



3D plant volume



Future outlook

- More data (plants) is needed in order to fruitfully apply machine learning techniques.
- Plants needs to be in their natural growing conditions.
- Therefore we planned to do a real field experiment in June-July 2017.
- Currently we are working on a field measurement box mounted in front of a tractor utilizing an Ensenso 3D camera and Specim FX10 hyperspectral camera.





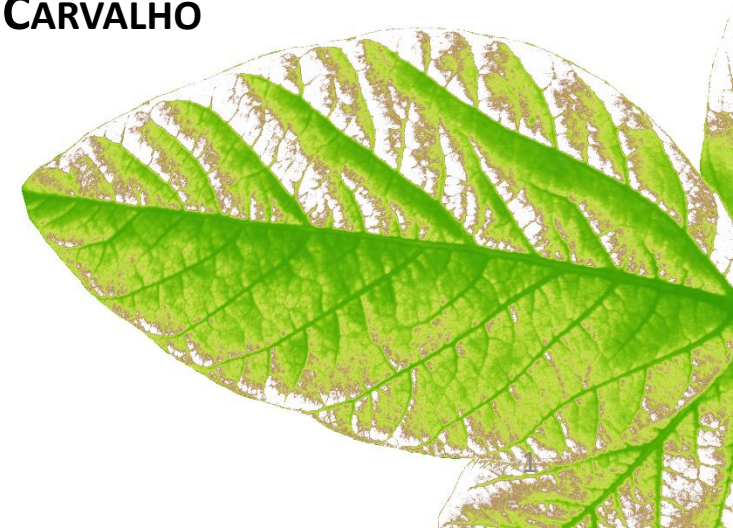
CATOLICA
FACULTY
OF BIOTECHNOLOGY

PORTO

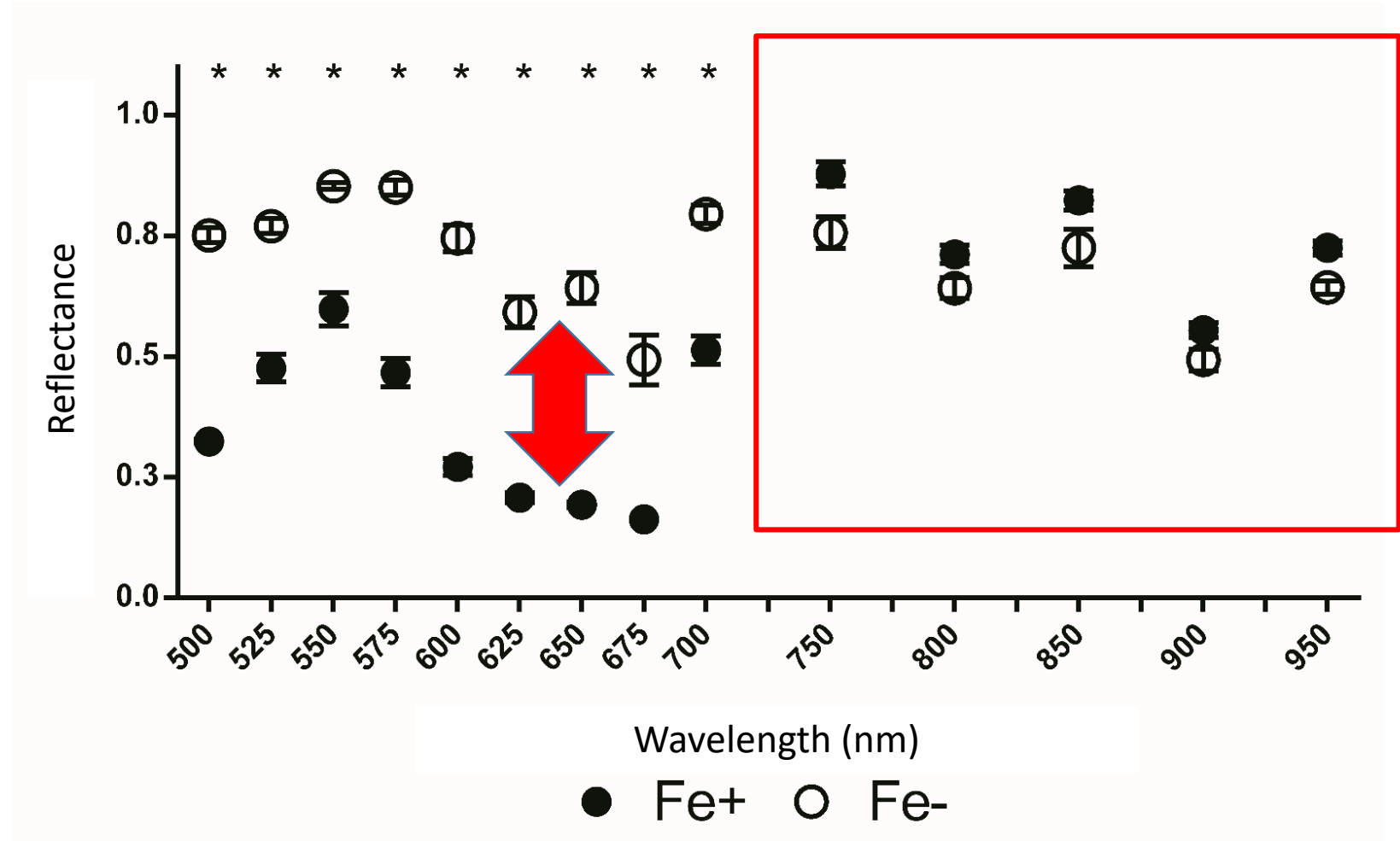
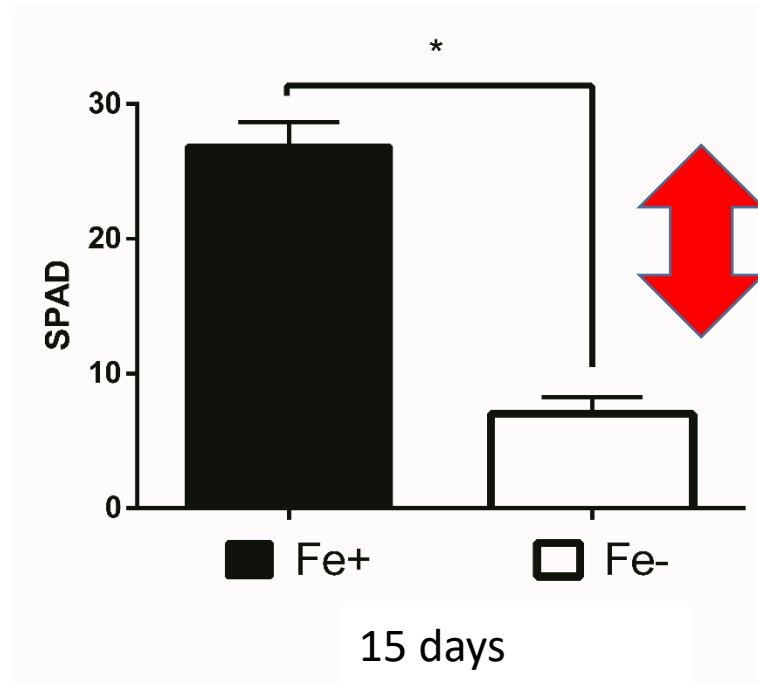


MULTISPECTRAL IMAGING + CONVENTIONAL ANALYSIS FOR EARLY STAGE IDENTIFICATION OF Fe DEFICIENCY IN SOYBEAN

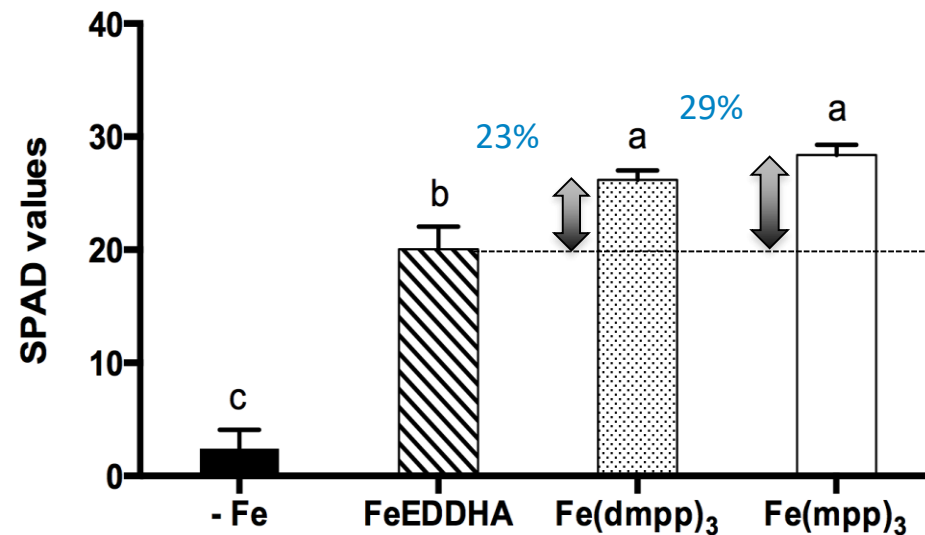
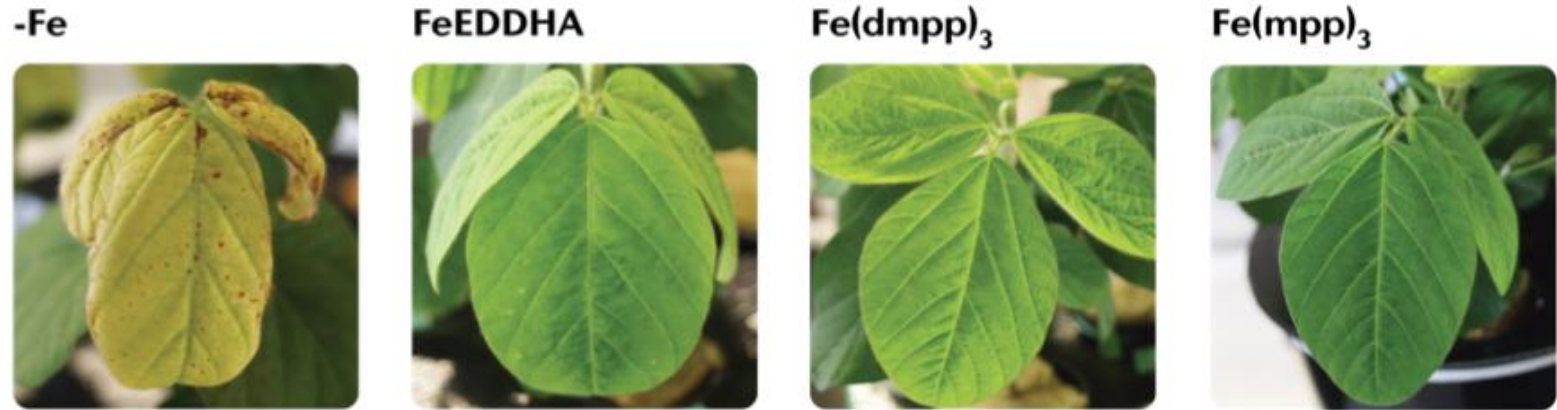
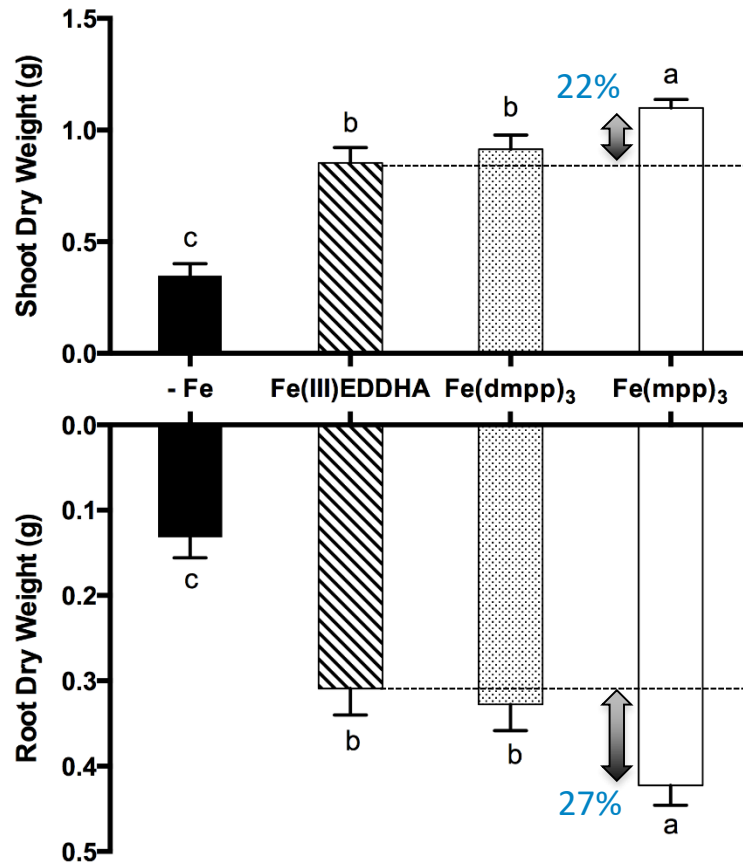
MARTA W. VASCONCELOS, DAVID ARAÚJO, CARLA SANTOS, SUSANA CARVALHO
OEIRAS, MARCH 27TH 2017



Validation in a non-efficient line



New iron chelators (for field application)





Alterations in root proteome of salt-sensitive and tolerant barley lines under salt stress conditions

Agnieszka Mostek^a, Andreas Börner^b, Anna Badowiec^a, Stanisław Weidner^a

^aDepartment of Biochemistry, Faculty of Biology and Biotechnology, University of Warmia and Mazury in Olsztyn, Oczapowskiego Street 1a, 10-957 Olsztyn, Poland.

^bLeibniz Institute of Plant Genetics and Crop Plant Research, Corrensstrasse 3, 06466 Gatersleben, Germany.

Introduction

Crop plants are often exposed to various biotic and abiotic stresses, greatly reducing the productivity of the crop worldwide. Soil salinity is among the main abiotic stresses and effects more than 800 million hectares of land, equivalent to more than 6% of the total global area of the Earth. This is a serious problem, considering the growing global population and, consequently, the increased demand for food. Therefore improving salt tolerance of crop plants is one of the current issues of global breeding program. To date, there is lack of studies describing the proteome changes under seed-applied salt stress in the roots of two barley lines contrasting in salinity tolerance.

Materials and methods

Germinating conditions

Seeds of salt-tolerant (DH187) and salt-sensitive genotype (DH14) were obtained from Leibniz Institute of Plant Genetics and Crop Plant Research (Gatersleben, Germany). Salinity sensitive and tolerant lines of barley belong to the mapping population, created in terms of salinity tolerance. Seeds germination was conducted in a growth chamber at the constant temperature of 20 °C for 6 days on the tissue-paper placed in glass cylinder. The seeds that constituted the control samples of sensitive (Cs) and tolerant (Ct) barley lines were germinated in Mili-Q water. Salt stressed samples of sensitive (Ss) and tolerant (St) barley lines were germinated in 100 mM NaCl solution. One hundred seeds were sown per every biological replication. After the appointed time the roots were cut and immediately frozen in liquid nitrogen. All experiments were performed in three biological replicates (n=3).

Protein extraction

Harvested roots were ground in liquid nitrogen using mortar and pestle. Proteins were extracted with a buffer containing 7 M urea, 2 M thiourea, 4% CHAPS, 2% IPG buffer pH 3–11 NL (GE Healthcare), 120 mM dithiothreitol, protease inhibitors cocktail (Sigma). The protein extraction was carried out for 1 h on the laboratory shaker at 4 °C. After the incubation time samples were centrifuged (14.000 x g, 10 min, 4 °C) and protein extracts were purified using DOC/TCA precipitation.

Two-dimensional electrophoresis

Extracted proteins were separated using IEF/SDS-PAGE. Each sample, containing 400 µg of protein in rehydration buffer, was loaded onto 24 cm Immobiline DryStrip Gels (GE Healthcare) with the non-linear pH gradient 3–11. Isoelectric focusing was performed in the Ettan IPGphor 3 system (GE Healthcare). The running conditions were as follows: 30 V/10 h (active rehydration at 20 °C), 500 V/1 h (step and hold), 1000 V/1 h (gradient), 8000 V/3 h (gradient), 8000 V/ 4:30 h (step and hold).

Protein digestion and MALDI-TOF/TOF analysis

Spots containing the proteins of interest were manually cut out from the gels with a scalpel blade. Prior to digestion, the proteins were washed and destained. Proteins were dried in a vacuum centrifuge and digested using a trypsin solution (Promega) containing 15 ng.µl-1 trypsin in 25 mM ammonium bicarbonate. The digestion was carried out overnight at 37 °C. Samples were subsequently sonicated for 5 min and briefly centrifuged. A 1 µl aliquot of each peptide mixture was applied onto the ground steel MALDI target plate.

Results

Fresh and dry weight measurement

The effect of salinity on barley seedlings growth was investigated in terms of differences in root fresh and dry weight content. The applied salinity stress significantly affected fresh and dry weight of the roots in both barley lines (Fig. 1

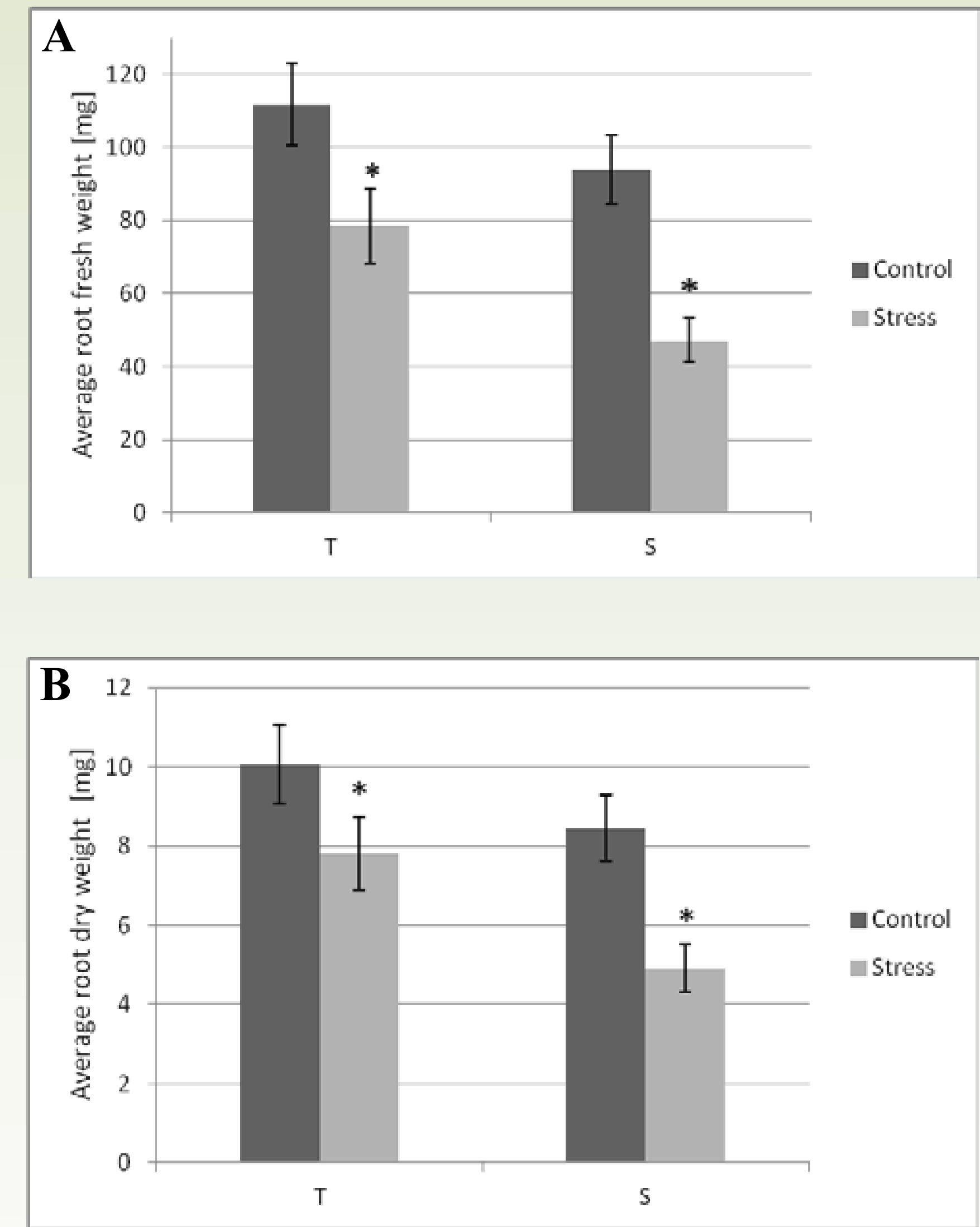


Fig. 1. Changes fresh (A) and dry weight (B) of barley roots isolated from sensitive (S) and tolerant (T) lines germinating under optimal (Control) or salt stress conditions (Stress). Results are presented as means ±SD. The statistically significant differences (p < 0.05) between control and stress samples were marked with an asterisk.

and 2). However, the average root fresh weight of the tolerant line (78.6 mg) was substantially higher than that of the sensitive line (47.2 mg) under salt stress. The root fresh weight in the tolerant line was reduced by about 29% (Fig.1A) while in sensitive line was reduced to a greater extent, by about 49%. Similar trend was also observed for root dry weight (Fig.1B). The dry weight in tolerant and sensitive lines was decreased by about 21% and 42% respectively, under salt stress conditions.

Identification of salt-responsive proteins

The aim of this study was to investigate changes in protein patterns, occurring under salt stress in the roots of salt-sensitive and salt-tolerant barley lines. To separate and identify differentially expressed salt-responsive proteins, IEF/SDS-PAGE, coupled with MALDI TOF/TOF mass spectrometry were used. Among the controls and salt-treated samples of the two barley lines, more than 1800 reproducible protein spots were detected on gel replicates of which more than 1000 could be matched in the compared gels. Among the matched spots of both barley lines, the abundance levels (%vol) of 72 protein spots were changed more than 1.75-fold (p < 0.05), 47 spots were successfully identified by spectrometric analysis. The identified proteins are summarized in Tab.1. The total number of salt-responsive proteins was higher in tolerant (35 proteins) than in sensitive line (22 proteins). Most of the salt-responsive proteins in tolerant line were up-regulated (28 proteins). The number of up- and down-regulated proteins in sensitive line was comparable, amounting 12 and 10 proteins respectively.

Functional distribution of salt-responsive proteins

The identified proteins were classified according to their function into several groups such as: proteins involved in carbohydrate and energy metabolism, amino acid metabolism, signal transduction, detoxification processes, translation cell wall metabolism, proteins of chaperone and other functions as well as hypothetical or putative proteins with unknown functions. The up-regulated proteins in the sensitive line were assigned to 4 functional groups: carbohydrate and energy metabolism (37%), amino acid metabolism (27%) chaperones (27%) and cell wall (9%) (Fig. 3A). The tolerant line showed accumulation of proteins associated with 9 functional groups: amino acid metabolism (19%), signal transduction (15%), cell wall metabolism (12%), translation (12%), chaperones (11%) carbohydrate and energy metabolism (11%), detoxification (8%), other (8%) and unknown (4%) (Fig. 3B.). It should be emphasized that the up-regulation of proteins involved in signal transduction and translation was observed only in tolerant line. Most of the proteins showing down-regulation in sensitive line is associated with a detoxification processes (Fig. 3C), whereas the majority of down-regulated proteins in tolerant line were assigned as unknown (Fig 3.D).

Conclusions

One of the most challenging issues in present plant research is to explain the molecular basis of plant adaptation to environmental stress and our results may greatly improve the understanding of mechanisms leading to salt tolerance in barley. In this experiment it was demonstrated that the sensitive and tolerant barley lines respond differently to salt stress. A number of salt-responsive proteins with various functions were identified. The most significant differences concerned proteins involved in signal transduction (annexin, translationally-controlled tumor protein homolog, lipoxygenases) detoxification processes (osmotin, vacuolar ATP-ase) and protein folding (protein disulfide isomerase), which were up-regulated only in the tolerant line under salt stress. Presumably enhanced salinity tolerance of DH187 line results mainly from increased activity of signal transduction mechanisms leading to the accumulation of stress protective proteins and changes in cell wall structure. The results suggests that salinity tolerance may be highly dependent on the efficiency of salt stress signal transduction mechanisms which should be subjected to more detailed examinations in the future experiments.

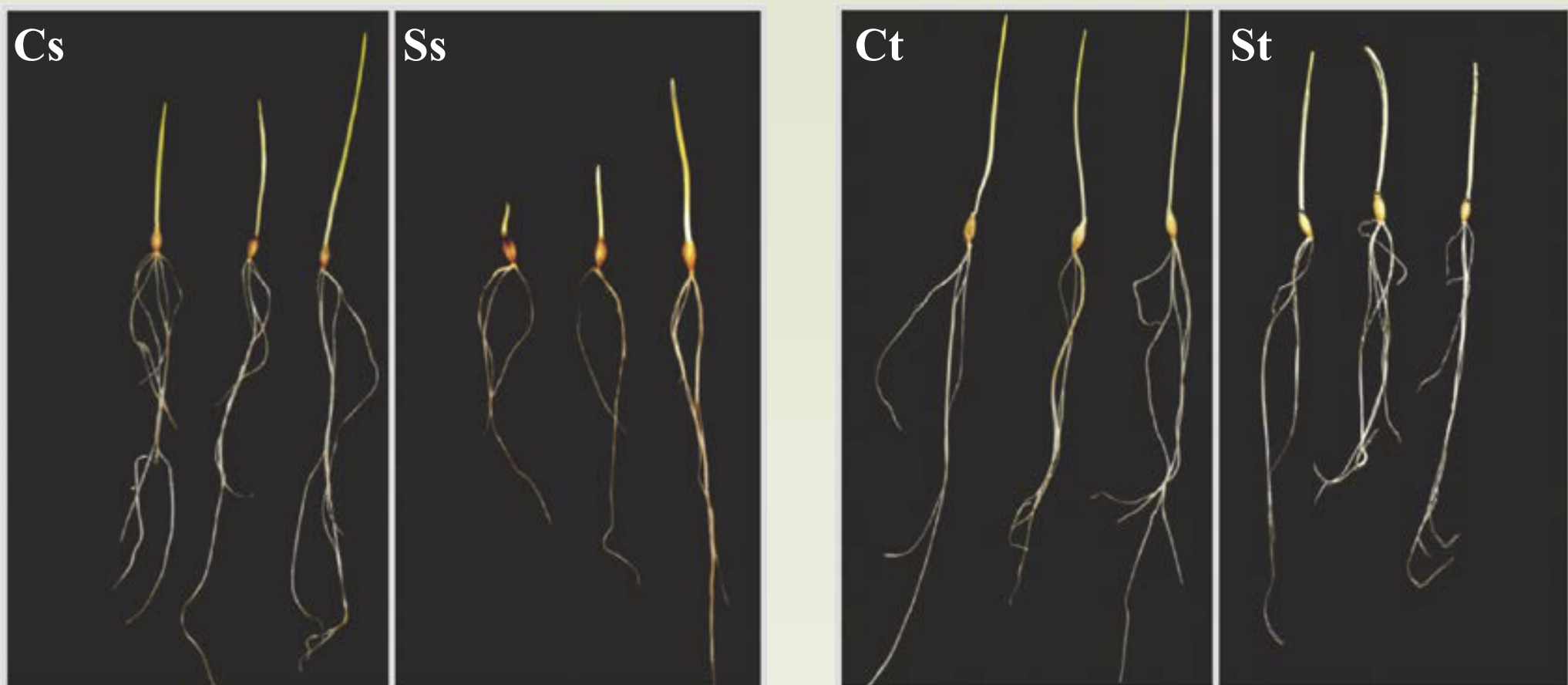


Fig. 2. Phenotypes of 6-days old barley seedlings of salt-sensitive and tolerant lines germinating under control and salt-stress conditions. Cs- control sample sensitive line; Ss- stress sample of sensitive line; Ct- control sample of tolerant line; St- stress sample of tolerant line.

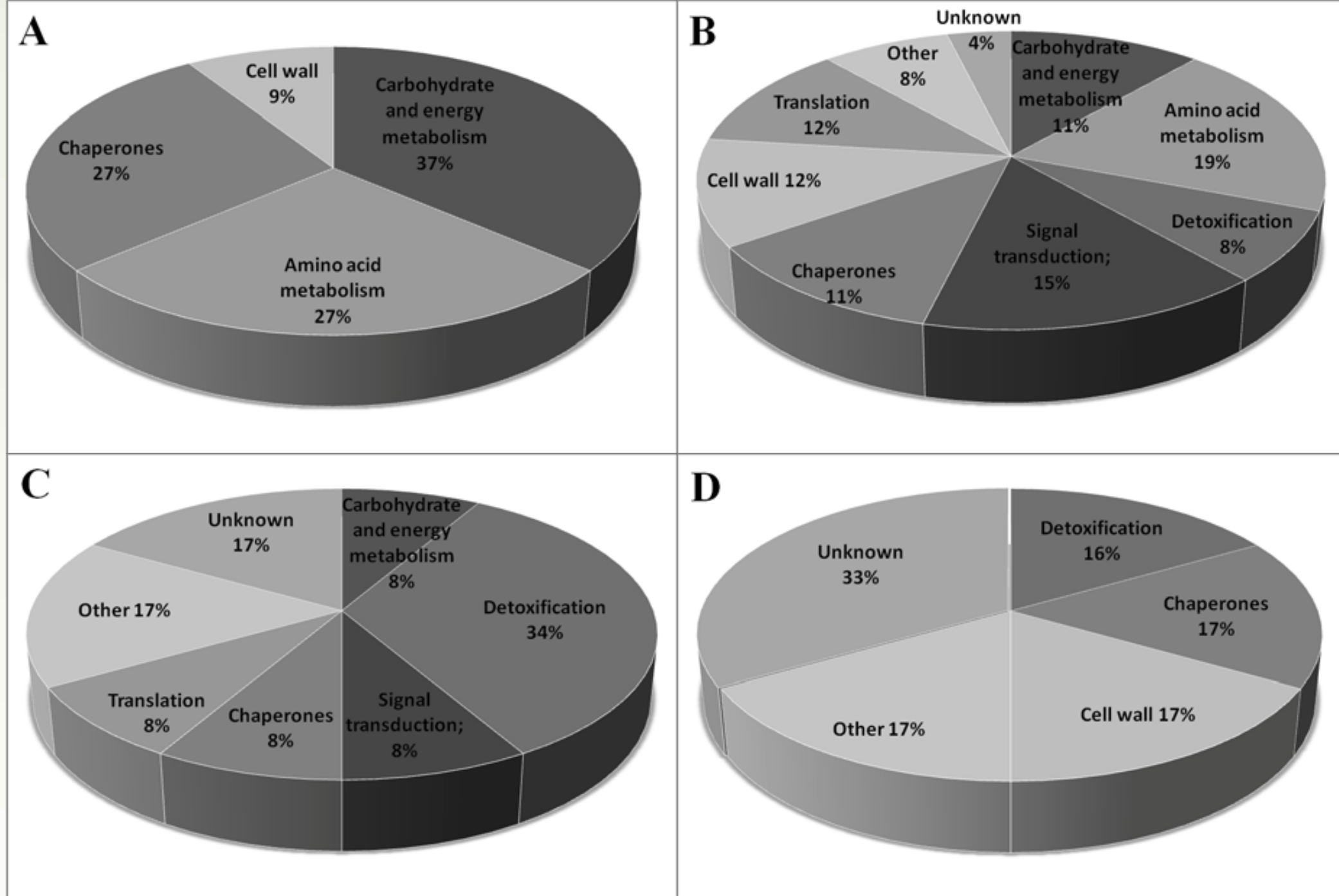


Fig. 3. Pie chart showing the functional distribution of salt-responsive proteins in the root of salt sensitive and tolerant barley lines. Proteins up-regulated in sensitive line (A); proteins up-regulated in tolerant line (B); proteins down regulated in sensitive line (C); proteins down-regulated in tolerant line (D).

Tab.1. Salt stress-responsive proteins identified in roots of salt-sensitive and tolerant barley lines.

Spot no. ^a	Protein name	Function	Species	Accession no.	score ^b	Pept. no. ^c	Exp. MW ^d	Calc. pI ^e	Calc. MW ^e
Proteins up-regulated under salt stress in both sensitive and tolerant barley lines									
782/783	S-adenosyl-L-homocysteine hydrolase	Amino acid metabolism	<i>H. vulgare</i>	gi 68655456	378	19	5.5/51	5.8/49.9	
901/907	Nucleotide pyrophosphatase	Cell wall	<i>H. vulgare</i>	gi 51592190	144	8	6.0/72.3	5.5/40.3	
748/728	Serine-hydroxymethyltransferase	Amino acid metabolism	<i>T. urartu</i>	gi 474154142	141	17	6.5/54.8	9.5/77.2	
765/748	Serine-hydroxymethyltransferase	Amino acid metabolism	<i>monococcum</i>	gi 115589736	122	12	6.6/55.3	8.2/56.2	
933/966	Heat shock protein 90	Chaperone	<i>T. aestivum</i>	gi 82582811	105	11	4.8/85.3	5.09/75.9	
36/726	Cyclophilin A, chain A	Chaperone	<i>T. aestivum</i>	gi 471270462	152	9	8.4/14	8.75/22.5	
Proteins up-regulated under salt stress only in the sensitive barley line									
909*	Heat shock cognate 70 kDa	Chaperone	<i>T. urartu</i>	gi 473983421	133	11	5.2/78	5.1/82.9	
678*	Citrate synthase	Carbohydrate and energy metabolism	<i>T. urartu</i>	gi 474326909	123	13	6.2/49	8.5/58.8	
148*	Stem 28 kDa glycoprotein	Other	<i>T. urartu</i>	gi 473808028	93	6	9.5/22	9.57/23.5	
846*	Pyrophosphate-fructose-6-phosphate-1-phosphotransferase	Carbohydrate and energy metabolism	<i>B. distachyon</i>	gi 357124641	129	16	6.1/61	6.18/61.4	
548*	Pyruvate dehydrogenase E1 component subunit alpha, mitochondrial	Carbohydrate and energy metabolism	<i>T. urartu</i>	gi 474166845	226	25	6.5/41.7	7.16/39.2	
942*	Asconitate hydratase, putative	Carbohydrate and energy metabolism	<i>T. urartu</i>	gi 473887274	259	23	5.9/94.2	6.04/93.8	
Proteins up-regulated under salt stress only in the tolerant barley line									
959	Methionine synthase 2	Amino acid metabolism	<i>H. vulgare</i>	gi 686555500	383	18	6/85.1	5.97/84.7	
976	Methionine synthase	Amino acid metabolism	<i>H. vulgare</i>	gi 50897038	164	16	5.6/90	5.68/84.7	
770	Enolase	Carbohydrate and energy metabolism	<i>T. aestivum</i>	gi 461744058	139	14	5.3/51.2	5.49/48.5	
544	Phosphoglycerate kinase	Carbohydrate and energy metabolism	<i>H. vulgare</i>	gi 473781647	193	6	5.85/43.6	5.9/45.2	
519	UDP-glucuronate decarboxylase	Cell Wall	<i>T. urartu</i>	gi 474071954	166	16	6.9/43.1	7.1/39.2	
988	Linolate 9S-lipoxygenase 1	Signal transduction	<i>H. vulgare</i>	gi 5325272	196	16	5.7/94	5.73/96.4	
979	Lipoxygenase 2	Signal transduction	<i>H. vulgare</i>	gi 2429087	217	25	6.1/94	6.25/96.8	
980	Lipoxygenase 2	Signal transduction	<i>H. vulgare</i>	gi 2429087	181	12	6.2/92	6.34/96.6	
126	Thaumatin-like protein (osmotin)	Detoxification	<i>H. vulgare</i>	gi 56682582	112	9	6.9/19	6.04/25.8	
402	Annexin	Signal transduction	<i>T. urartu</i>	gi 474139853	105	6	6.5/35	6.15/35.5	
912	β-D-glucan exohydrolase	Cell Wall	<i>H. vulgare</i>	gi 1203832	85	8	7/79.7	7.96/67.8	
943	Vacuolar proton ATP-ase	Detoxification	<i>H. vulgare</i>	gi 11527563	92	8	5.1/81.2	5.23/68.7	
832	ATP-synthase subunit beta, mitochondrial-like	Carbohydrate and energy metabolism	<i>B. distachyon</i>	gi 357135971	334	14	5/56.1	5.95/97.3	
812	UDP-glucose pyrophosphorylase	Cell Wall	<i>H. vulgare</i>	gi 6136111	192	15	5.05/56.5	5.2/51.7	
677	Predicted actin-1-like	Other	<i>B. distachyon</i>	gi 357151587	206	11	4.7/48.3	5.3/42	
90	Translationally-controlled tumor protein homolog	Signal transduction	<i>H. vulgare</i>	gi 20140865	233	11	4.05/8	4.53/18.9	
723	Tubulin alpha-1 chain	Other	<i>O. sativa</i>	gi 108710846	107	8	4.9/49	4.89/46.5	
994	Elongation factor 2	Translation	<i>T. urartu</i>	gi 474416088	111	13	5.9/96	5.96/97.3	
780	Eukaryotic translation initiation factor 4A-3-like protein, partial	Translation	<i>M. sinensis</i>	gi 379054892	230	11	5.2/65	6.3/43	
46	Eukaryotic translation initiation factor 5A1	Translation	<i>T. aestivum</i>	gi 74048999	139	11	5.5/16.2	5.7/17.5	
532	Protein Disulfide Isomerase-like protein, putative	Chaperones	<i>T. aestivum</i>	gi 299469378	131	12	5.9/40	6.17/40.5	
936	Predicted protein	Unknown	<i>H. vulgare</i>	gi 326526063	105	8	5.5/79	6.07/81.2	
Proteins down-regulated under salt stress in both sensitive and tolerant barley line									
640/625	Heat shock cognate 70 kDa	Chaperones	<i>T. urartu</i>	gi 474012573	166	8	4.92/5.1	5.07/71.4	
492/464	Glutelin type-1A1-like, predicted	Other	<i>H. vulgare</i>	gi 357134819	94	10	5.7/38	6.02/38.2	
617/598	Predicted protein	Unknown	<i>H. vulgare</i>	gi 326519550	129	14	4.6/43	4.83/40.4	
116/-	Ascorbate peroxidase	Detoxification	<i>H. vulgare</i>	gi 3688398	181	14	5.6/22.5	5.85/27.5	
Proteins down-regulated under salt stress only in the sensitive barley line									
150*	L-ascorbate peroxidase	Detoxification	<i>O. sativa</i>	gi 15808779	156	14	4.8/23.5	5.1/27.9	
62*	Eucaryotic translation initiation factor 5A1	Translation	<i>T. aestivum</i>	gi 74048999	142	9	5.9/17	5.7/17.5	
248*	Glyceraldehyde-3-phosphate dehydrogenase 2	Carbohydrate and energy metabolism	<i>H. vulgare</i>	gi 120668	122	12	6/24.9	6.2/33.4	
357*	Root peroxidase	Detoxification	<i>T. aestivum</i>	gi 194425591	103	9	8/31.2	8.59/32.9	
469*	Lipoxygenase 1	Signal transduction	<i>H. vulgare</i>	gi 30025164	180	22	5.85/37	6.29/40.6	
281*	Predicted protein	Unknown	<i>H. vulgare</i>	gi 326493760	185	16	5.1/25	5.43/40.3	
Proteins down-regulated under salt stress only in the tolerant barley line									
188	UDP-D-glucuronate decarboxylase	Cell wall	<i>H. vulgare</i>	gi 50659026	82	9	5.2/22	7.1/39	
464	Predicted protein	Unknown	<i>H. vulgare</i>	gi 326494746	126	9	5.4/39	5.66/38.3	
355	Predicted protein	Unknown	<i>H. vulgare</i>	gi 326511695	96	9	6.2/34	9.97/35.1	

^a Spot ID of sensitive line are marked with an asterisk (*); ID numbers separated by a slash refers to other spots with the same gi-number.
^b Statistical probability of the predicted protein calculated by MASCOT including PMF and ion scores; scores above 72 (p < 0.05) are considered significant.
^c The number of matched peptides.
^d Experimental values of isoelectric point and molecular mass of the protein.
^e Theoretical values of isoelectric point and molecular mass of the protein.

Classification of various cold-pressed plant oils using a new semi-quantitative analytical approach

Marijana M. Ačanski 1, Kristian A. Pastor 1 and Ana M. Marjanović-Jeromela 2

1 University of Novi Sad, Faculty of Technology, Bulevar cara Lazara 1, 21000 Novi Sad, Serbia

2 Institute of Field and Vegetable Crops, Maksima Gorkog 30, 21000 Novi Sad, Serbia

Corresponding author: *e – mail: macanski@tf.uns.ac.rs

Aims

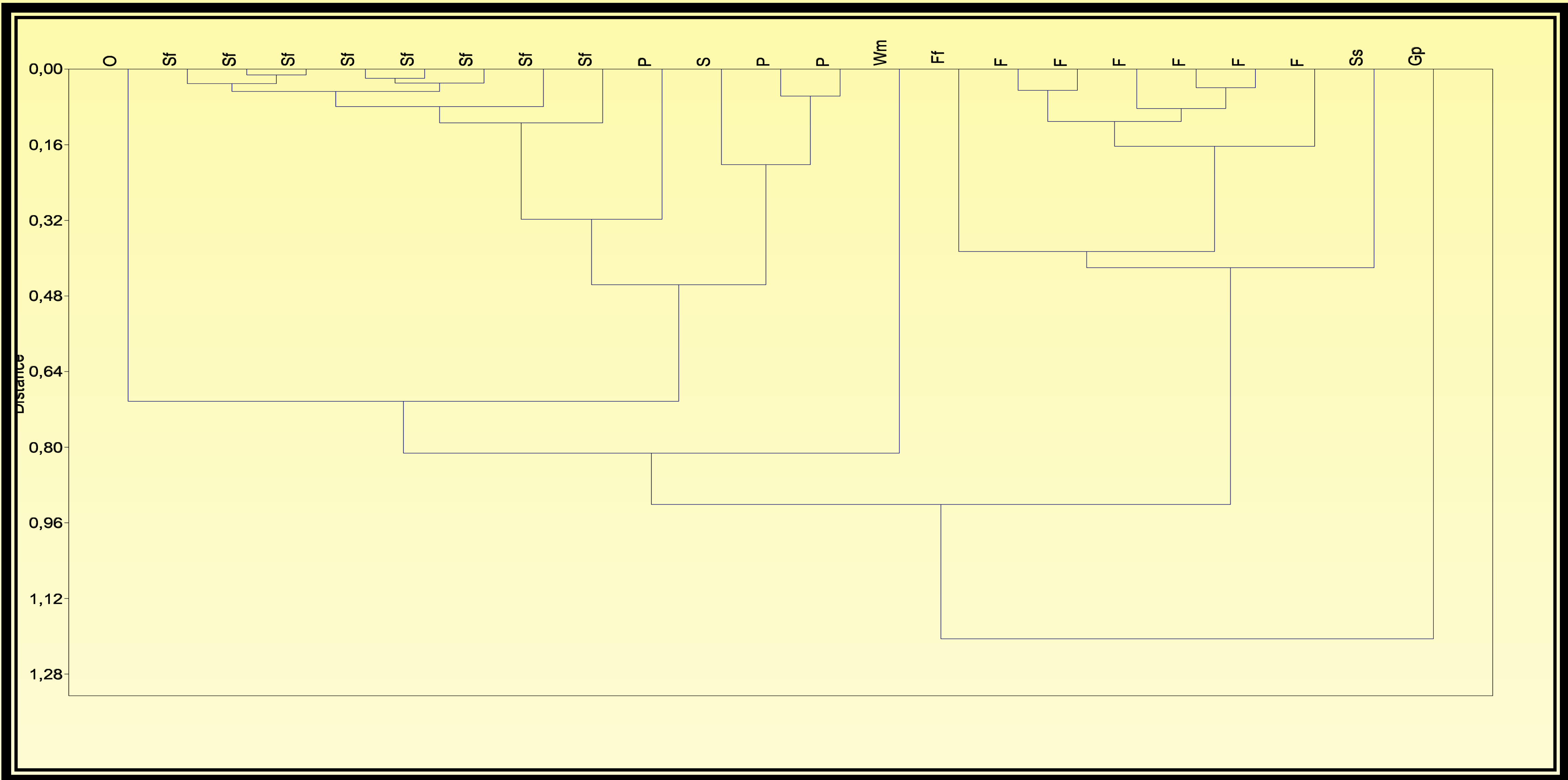
The aim of this work has been the development of a new, semi-quantitative analytical approach in order to differentiate and classify the samples of various plant oils according to their corresponding botanical origin, by using GC/MS system and multivariate analysis. The following plant species were included in the analysis: **safflower Sf** (*Carthamus tinctorius*), **flaxseed F** (*Linum usitatissimum*), **pumpkin P** (*Cucurbita pepo*), **sesame S** (*Sesamum indicum*), **false flax Ff** (*Camelina sativa*), **okra O** (*Abelmoschus esculentus*), **gopher purge Gp** (*Euphorbia lathyris*), **summer savory Ss** (*Satureja hortensis*), and **white mustard Wm** (*Sinapis alba*).

Experimental

The volume of 10 µL of each cold-pressed plant oil sample was derivatized using TMSH solution (Trimethylsulfonium hydroxide, Merck) and analyzed on a GC/MS system under appropriate chromatographic conditions. After GC analysis, the eluting derivatized lipid components were identified using a mass spectrometer, by comparing their fragmentation spectra with mass spectra libraries. Chromatographic data of specific fatty acids were introduced into PAST program, in order to perform exploratory data analysis, i.e. hierarchical cluster analysis.

Results and discussion

The obtained dendrogram shows strong separations between investigated samples of cold-pressed plant oils using Chord distancesimilarity measure with corresponding cophenetic correlation coefficient of 0.97, thus suggesting that the presented tree represents the dissimilarities among observations very faithfully. Very high similarity was observed among the samples of flaxseed, wild flax and summer savory oil, as well as the samples of pumpkin and sesame seed oil, with the gopher purge oil being the most separated of all analyzed samples. It is worth mentioning that among the analyzed plant oil samples, gopher purge represents the only one being non-edible and toxic.



Conclusions

Obtained results show that it is possible to classify plant oil samples of various oilseed species, according to the corresponding botanical origin, in a rapid way, on a GC/MS instrument with contemporary data analysis tools, successfully avoiding the application of analytical standards and time-consuming qualitative and quantitative determinations.



Use of infrared thermography for detection of drought stress in potato and tomato

Radmila Stikić¹, Milena Marjanović¹, J. Miguel Costa² and Zorica Jovanović¹

¹Faculty of Agriculture, University of Belgrade, Belgrade, Serbia

²Instituto de Tecnologia Química e Biológica, Universidade Nova de Lisboa, Portugal

INTRODUCTION

Infrared (IR) thermal imaging (also known as IR thermography), is a specialized branch of IR thermometry. This imaging technique permits to measure IR radiation emitted by objects at ambient temperature over a large amount of points and processing those measurements to form a thermal map of the target surface, including leaf surface. Leaf temperature can be a good indicator of leaf stomatal conductance and plant water regime. Thermal infrared camera visualizes increase in leaf temperature for analyses and diagnosis of the plant water regime and degree of drought stress that plants are exposed. The advantage of IRT comparing to other methods is that is non-destructive and fast and could be used for early quantification of crop stress in large irrigation areas.

The aim of presented study was to test the IRT method for monitoring water regime of potato and tomato plants exposed to drought. IRT method is introduced as a result of bilateral scientific cooperation between Serbia and Portugal.

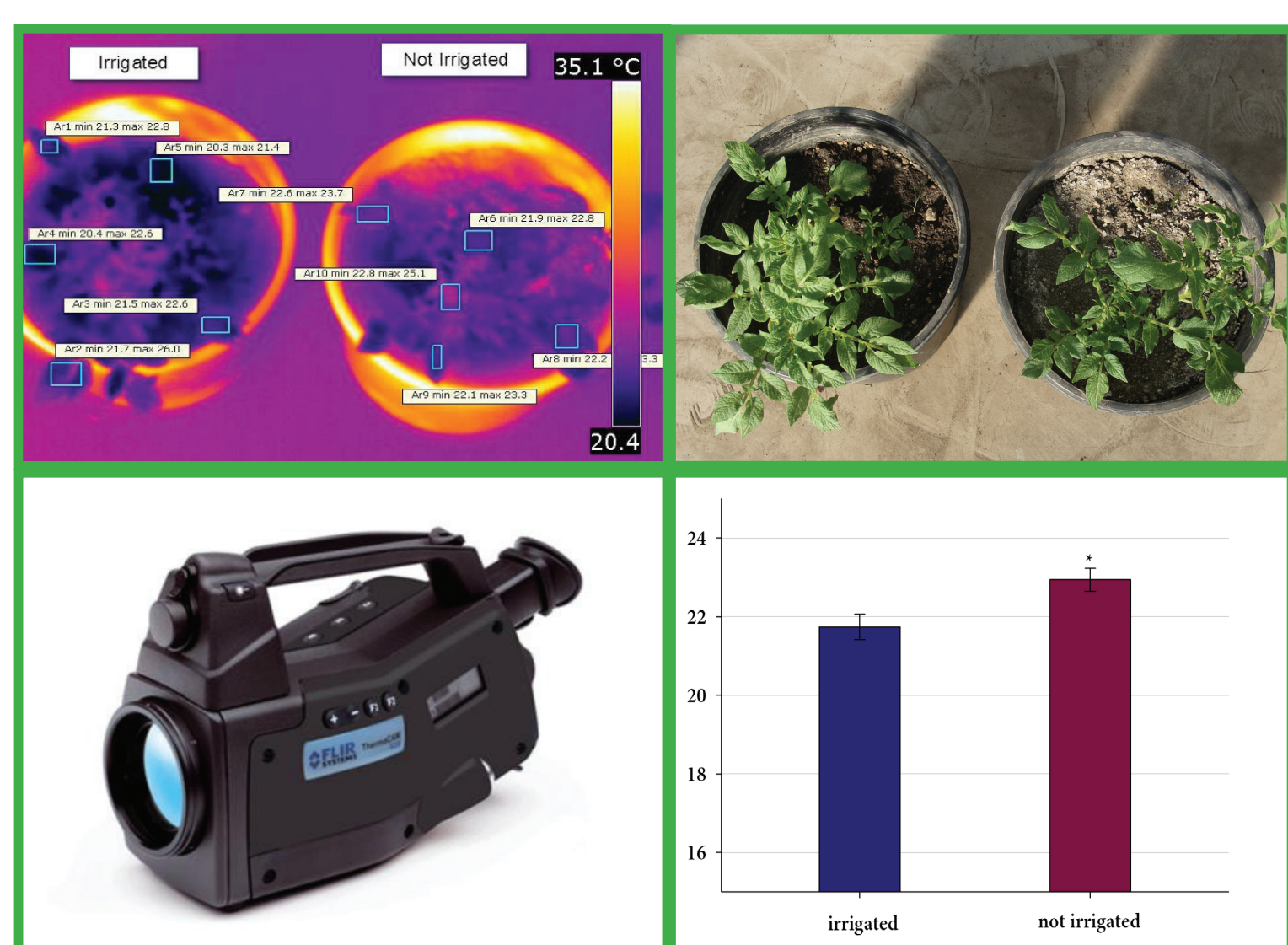


Figure 1. Thermal image of two potato plants irrigated and not irrigated (up left) taken with a Thermo CAM B20 (down left); and visible image of the same plants (up right). Leaf temperature based on thermal imaging from potato plants, t-test(*-P<0.05) (down right)



Figure 2. Visible image and thermal image (FLIR B425) for the ABA deficient mutant *flacca* and Ailsa Craig (up). Stomatal conductance and leaf temperature measured for the ABA deficient mutant *flacca* and Ailsa Craig (down)

MATERIAL

- Potato experiment - Potato plants (*Solanum tuberosum* L.) were grown in a greenhouse at Institute of Chemical and Biological Technology (ITQB), Oeiras, Portugal. When the plants were in the stage of 7 leaves developed on main shoot they were subjected to drought by withholding water for 5 days. In the same time control plants were fully irrigated.

- Tomato experiment - plants of four different genotypes of tomato (*Solanum lycopersicum*) and tomato *flacca* mutant (deficient in ABA content) were grown in pots in a climate chamber of Faculty of Agriculture, University of Belgrade. Plants were subjected to two irrigation treatments: deficit irrigation at 50% and well irrigated plants.

Measured parameters

Stomatal conductance was measured by leaf porometer (AP4, Delta-T, Cambridge, U.K). Measurements were done on the third fully developed leaf on main shoot immediately after thermal imaging measurements.

Leaf temperature was measured by using thermal imaging.

The statistical analyses of the results was performed with SigmaPlot software (version 11.0) using Student's t-test.

CONCLUSION

Thermal imaging results obtained confirmed that in the leaves of plants exposed to drought the temperature of leaf surface was higher compared to the well watered leaves. This difference was due to the fact that in the leaves exposed to drought the reduced stomatal conductance and transpiration reduced evaporative cooling of their surface and, consequently, led to an increase in temperature of their surface. Both the visual estimation with the thermal infrared camera and calculated temperature data, confirmed that leaf temperature is a reliable indicator of drought stress in the leaves of potato and tomato plants. These results showed that IRT method could be very efficient and non-destructive tool for monitoring potato and tomato water regime. Also it could be relevant approach to manage water supply in modern irrigated horticulture.

REFERENCES

- Costa et al. (2010). Methodologies and Results in Grapevine Research, pp. 135-150, New York: Springer.
- Costa et al. (2012). Functional Plant Biology, 179-189.
- Jones, H. (1999a). Agricultural and Forest Meteorology, 135-149.
- Jones, H. (1999b). Plant, Cell and Environment, 1043-1055.
- Jones, H. (2004). Advances in Botanical Research, 107-163.
- Jones et al (2002). Journal of Experimental Botany, 2249-2260.



Figure 3. Leaf temperature measured for potted plants of tomato of four different genotypes : 102, 106, 109 and 114, under deficit irrigation (white bars) and under well irrigated conditions (grey bars) (up). Thermal camera used for measurements FLIR B425 (down).

Evaluation of drought tolerant mutant lines under saline environment based on some agronomic and biochemical parameters



Ayşe SEN

Istanbul University, Faculty of Science, Department of Biology, 34134, Vezneciler, Istanbul, Turkey
(E-mail: senayse@istanbul.edu.tr)

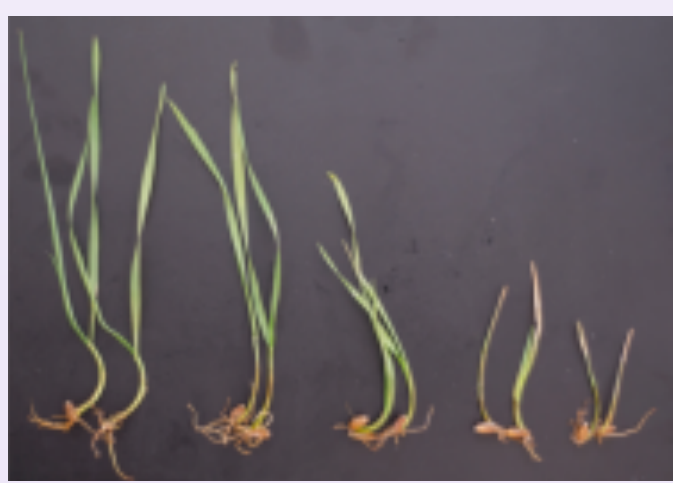
BACKGROUND

Salinity is a major abiotic stress, which greatly reduces the photosynthetic capacity of plant leaves and increases the production of reactive oxygen species, and as a result of all of this, the loss of product and yield in agricultural plants occurs. It is a problem in many regions worldwide. Therefore, the development of varieties with an increased salt tolerance is one of the strategies to meet the growing food demand. Mutation-assisted breeding has been proven to be an effective way of improving cultivars with a high resistance/tolerance to various abiotic and biotic stresses. In this study, the morphological and physiological responses of M₅ generation gamma irradiation- induced drought-tolerant Sagittario mutant lines under salinity have been studied and which line(s) are more suitable for the Advanced National Breeding Program in terms of releasing new bread wheat cultivar(s) tolerant to both drought and salinity has been determined. For this purpose, the previously detected threshold NaCl concentration has been applied to screen one control and five candidate drought tolerant lines against salinity under greenhouse conditions based on some of agronomic (Flag Leaf Area, Main Shoot Length, Spike Length, Weight of Grains per Spike, Number of Grains per Spike and 100-Grain Weight) and biochemical (Total Chlorophyll, Carotenoid, Proline, SOD, CAT, POX, Carbonylated Protein Content and K⁺/Na⁺) parameters. Additionally, linkage associations analysis between SSR data and agronomic and biochemical parameters were done under saline and drought environment.

EXPERIMENTAL PROCEDURE

Determining of NaCl threshold concentration

Table: Fresh weights and plant heights of 28-day-old Sagittario cultivar after NaCl application



Experimental Groups	Average Plant Heights (cm)	Plant Heights %	Average Plant Fresh Weights (g)	Plant Fresh Weights %
Control	21.03 ^a	100	1.252 ^a	100
50 mM NaCl	18.61 ^b	88.49	0.957 ^b	76.44
100 mM NaCl	12.68 ^c	60.29	0.758 ^c	60.54
150 mM NaCl	8.38 ^c	39.85	0.292 ^d	23.32
200 mM NaCl	4.67 ^d	22.21	0.158 ^d	12.62

Means that are followed by a different letter are significantly different *p < 0.05 (Student-Newman Keuls test).

According to the results of the regeneration ratios, plant heights and fresh weights of the 28-day-old cultures about 75 mM NaCl were detected as a threshold concentration under greenhouse environment.

Phenotyping with Biochemical Parameters

Table: Biochemical performances of control and drought tolerant mutant lines during vegetative and flowering stages determined in control and saline environment under greenhouse condition

	Control							75 mM NaCl				
Parameters	Control and Mutant Lines											
Vegetative Stage												
	Control	ML5	ML8	ML9	ML10	ML11	Control	ML5	ML8	ML9	ML10	ML11
Total Chlorophyll	2.56	2.88	2.81	2.71	2.76	2.65	1.89	2.55	2.43	2.21	2.53	2.23
Carotenoid	0.43	0.44	0.47	0.46	0.47	0.47	0.52	0.63	0.68	0.63	0.65	0.65
POX	51.92	62.89	62.76	66.01	63.15	65.76	67.89	88.89	91.23	103.45	111.22	98.87
CAT	15.17	16.23	16.56	17.21	17.46	18.89	21.05	33.43	35.67	38.54	35.18	41.23
SOD	30.57	39.77	43.61	44.44	45.67	40.11	48.06	61.23	63.43	65.77	68.93	66.66
Proline	5.36	6.11	5.89	6.23	6.58	6.44	11.23	18.99	21.34	24.62	25.46	27.56
Carbonylated	2.03	2.11	2.07	1.92	1.89	1.95	4.38	3.61	3.74	3.57	3.27	3.18
Protein Content												
Na ⁺	0.21	0.19	0.21	0.20	0.19	0.20	1.85	1.75	1.83	1.82	1.67	1.64
K ⁺	2.67	2.67	2.63	2.68	2.73	2.71	1.05	1.20	1.21	1.35	1.28	1.25
K ⁺ /Na ⁺	12.71	14.05	12.52	13.40	14.37	13.55	0.57	0.69	0.66	0.74	0.77	0.76
Flowering Stage												
Total Chlorophyll	3.06	3.33	3.41	3.43	3.26	3.33	2.07	2.73	2.65	2.77	2.71	2.81
Carotenoid	0.52	0.55	0.58	0.56	0.57	0.61	0.73	0.83	0.88	0.81	0.85	0.88
POX	81.12	102.09	92.96	96.91	103.11	105.86	117.09	198.79	191.73	213.05	226.62	231.87
CAT	17.11	19.29	19.91	19.11	19.66	19.81	29.77	41.93	44.67	48.04	51.68	52.03
SOD	41.07	55.07	53.11	58.41	55.07	60.01	61.76	81.28	83.43	85.77	91.96	93.06
Proline	6.06	7.71	7.19	7.43	7.88	7.84	15.63	26.09	31.04	34.02	35.41	37.54
Carbonylated	2.71	2.72	2.75	2.65	2.58	2.68	5.18	4.57	4.83	4.98	4.43	4.45
Protein Content												
Na ⁺	0.31	0.27	0.28	0.31	0.26	0.27	2.25	2.25	2.21	2.22	2.18	2.20
K ⁺	2.98	3.07	3.11	3.09	3.15	3.14	1.21	1.45	1.38	1.42	1.48	1.53
K ⁺ /Na ⁺	9.6	11.37	11.11	9.97	12.12	11.63	0.54	0.64	0.62	0.64	0.68	0.70

To chose best line(s), the activities of SOD (Umg⁻¹ protein), CAT (Umg⁻¹ protein) and POX (ΔA₄₇₀ mg⁻¹ protein), and the contents of Proline (μmolmg⁻¹protein) , total Chlorophyll (mg(gfw)⁻¹, Carbonylated Protein (nmolmg⁻¹protein), Na⁺ (nmol(gdw)⁻¹) and K⁺ (nmol(gfw)⁻¹) were determined in vegetative and flowering stages under control and salt stress conditions. According to the majority of biochemical parameters, the mutant line 10 and 11 gave better performance than the others. These results confirmed by agronomical parameters.

Phenotyping with Agronomic parameters

Table: Agronomic parameters of control and drought tolerant mutant lines under control and salt stress conditions in greenhouse environment

Control							75 mM NaCl					
Parameters	Control and Mutant Lines											
	Control	ML5	ML8	ML9	ML10	ML11	Control	ML5	ML8	ML9	ML10	ML11
Flag Leaf Area (cm²)	21.9	18.2	18.6	19.1	18.7	19.3	12.5	11.2	11.7	11.9	13.4	14.1
Main Shoot Length (cm)	90.5	75.2	83.6	88.8	79.4	75.4	58.6	63.2	65.5	73.2	67.8	65.8
Spike Length (cm)	9.2	8.3	9.1	9.2	8.9	8.8	5.8	5.8	7.5	7.5	7.7	7.5
Weight of Grains per Spike (g)	2.2	2.3	2.4	2.1	2.3	2.4	1.1	1.8	1.6	1.7	1.9	1.8
Number of Grains per Spike	36.3	37.8	36.6	35.8	35.6	34.8	22.7	29.2	29.7	28.7	30.1	29.5
100-Grain Weight (g)	4.93	4.88	4.95	5.11	5.14	4.98	3.18	3.31	3.59	3.62	3.95	3.87

According to agronomic performances, the mutant line 10 and 11 gave better performance than the others.

Linkage associations analysis between SSR markers and Phenotyping Parameters

Table : Analysis of variance for SSR data, agronomic and biochemical parameters under saline and drought environment

No	Primer Name	FLA	MSL	SL	WGS	NGS	100-GW	Chl	Car	POX	CAT	SOD	Proline	CarPC	K ⁺ /Na ⁺
1	Xubc859a	ns	ns	ns	ns	ns	ns	ns	*	ns	ns	ns	ns	ns	ns
2	Xgwm10	ns	ns	ns	*	*	*	ns	ns	ns	ns	ns	ns	ns	ns
3	Xwmc261	ns	ns	ns	ns	ns	ns	ns	*	ns	*	ns	ns	ns	ns
4	Xgwm294b	ns	ns	ns	ns	ns	ns	ns	ns	ns	ns	*	ns	*	ns
5	Xfca2121b	ns	ns	ns	*	*	*	ns	ns	ns	ns	ns	ns	ns	ns
6	Xwmc296	ns	ns	ns	*	*	*	ns	ns	*	ns	ns	ns	ns	ns
7	Xgwm515	ns	ns	ns	ns	ns	ns	ns	ns	ns	ns	ns	*	ns	ns
8	Xgwm95	ns	ns	ns	ns	ns	ns	ns	ns	*	ns	ns	ns	ns	ns
9	Xwmc170	ns	ns	ns	ns	ns	ns	ns	ns	ns	ns	ns	*	ns	*
10	Xwmc445d	ns	ns	ns	ns	ns	ns	ns	ns	ns	ns	ns	ns	ns	*
11	Xwmc11	ns	ns	ns	*	*	*	ns	ns	ns	ns	ns	ns	ns	ns
12	Xgwm403	*	*	*	ns	ns	ns	*	ns	ns	ns	ns	ns	ns	ns
13	Xcfd9	ns	*	*	ns	ns	ns	ns	ns	ns	ns	ns	ns	*	ns
14	Xgwm6	ns	*	*	*	*	*	ns	ns	ns	ns	*	ns	ns	ns
15	Xgwm538	ns	*	*	*	*	*	ns	*	ns	*	ns	ns	ns	ns
16	Xwmc413	ns	ns	ns	*	*	*	ns	ns	ns	ns	ns	ns	ns	ns
17	Xgwm194	*	ns	ns	*	*	*	ns	ns	ns	ns	ns	ns	ns	ns
18	Xgwm624	ns	ns	ns	*	*	*	ns	ns	*	ns	*	ns	ns	ns
19	Xgwm540	ns	ns	*	ns	ns	ns	ns	ns	ns	ns	ns	ns	ns	ns
20	Xcfd18	ns	*	*	ns	ns	ns	ns	ns	ns	ns	ns	ns	ns	ns
21	Xcfd183	ns	*	*	ns	ns	ns	ns	ns	ns	ns	ns	ns	ns	ns
22	Xcfd080	ns	ns	ns	ns	ns	ns	ns	ns	ns	ns	ns	ns	ns	*
23	Xgwm626	ns	ns	*	ns	ns	ns	*	ns	ns	ns	ns	ns	ns	ns
24	Xgwm88	ns	ns	ns	ns	ns	ns	*	ns	ns	ns	*	ns	*	ns
25	Xwmc416	ns	ns	ns	ns	ns	ns	ns	ns	ns	ns	ns	*	ns	ns
26	Xwmc83	ns	ns	ns	ns	ns	*	*	ns	ns	ns	ns	ns	ns	ns
27	Xgwm4	*	*	*	ns	ns	ns	ns	*	ns	*	ns	ns	ns	ns
28	Xcfd6	*	*	*	ns	ns	ns	ns	ns	ns	ns	ns	ns	ns	ns

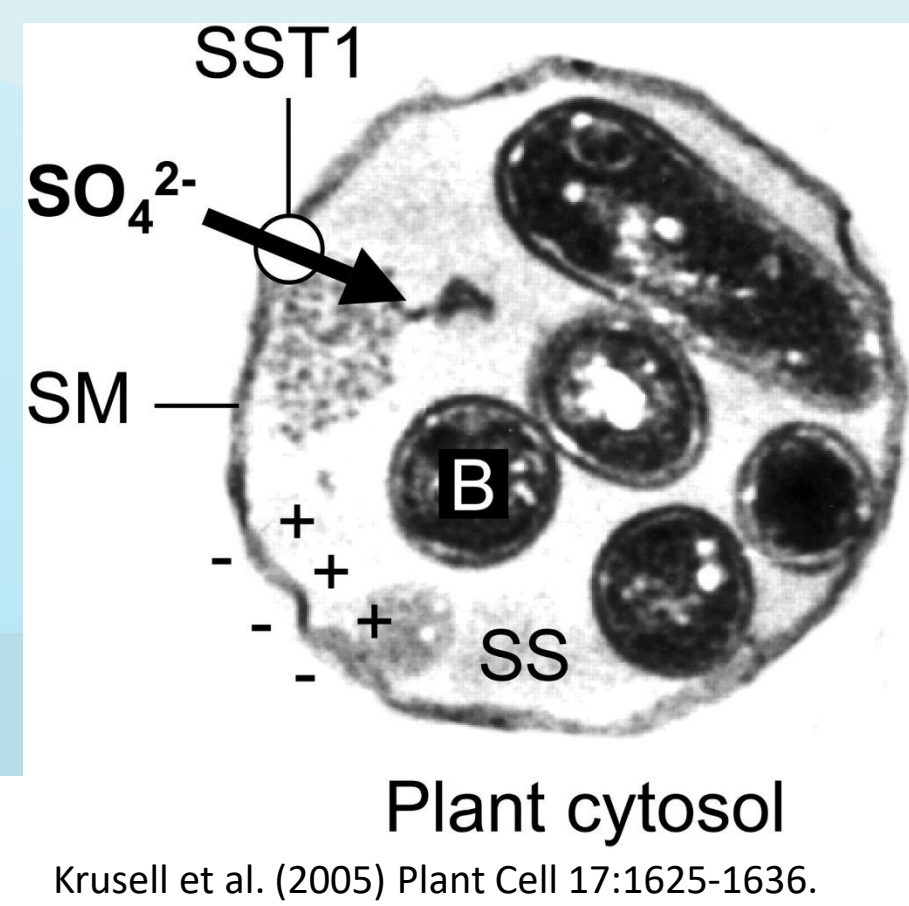
FLA: Flag Leaf Area, MSL: Main Shoot Length, SL: Spike Length, WGS: Weight of Grains per Spike, NGS: Number of Grains per Spike, 100-GW: 100-Grain Weight, Chl: Total Chlorophyll, Car: Carotenoid, POX: Guaiacol peroxidase, CAT: Catalase, SOD: Superoxide dismutase, CarPC: Carbonylated Protein Content, ns: not significant, *: significant at 5% probability level.

Linkage disequilibrium mapping is a valuable strategy for describing associations between markers and useful traits for crop improvement. In this study over the twelve mutant lines improved by gamma irradiation either putative salt or drought tolerant were screened over 150 SSR markers. The preliminary results were given above.

FUTURE WORK

Induced mutations are necessary to enhance rate of genetic variability since spontaneous mutation rate is very slow and that prevents breeders to exploit them in plant breeding programs. Selecting new cultivar(s) against tolerance to either salt or drought stress is generally evaluated using phenotypic observations. To find out a specific phenotype which is carrying a trait that is linked to stress resistance/tolerance has become a must for sustainable plant breeding. At this point, biochemical or metabolic phenotyping with high precision can be utilized to promote standard phenotyping approaches. Additionally, phenotyping combined with Linkage Disequilibrium (LD) Mapping can be offered valuable strategy for crop improvement. A major advantage of LD over the conventional QTL mapping in that it does not require specific genetic population. To contribute the Advanced National Breeding Program, this study has focused on developing a new strategy combining with mutagenesis, pre-field phenotyping and LD association approaches for selecting the best performing line(s) under multi-environmental conditions. Hereafter, it will continue to produce seeds from candidate lines for field trials.

Tracing the Sulfur-Proteome of Nitrogen-Fixing Root Nodules of *Lotus japonicus*



Sebastian Schneider and Stefanie Wienkoop
Dept. of Ecogenomics and Systems Biology, University of Vienna, Austria

Background

Lotus japonicus establishes nitrogen-fixing nodules in symbiosis with *Mesorhizobium loti*. The root nodules harbor the bacteroids that are surrounded by a peribacteroid membrane (PBM) formed from the plant plasma membrane. The PBM plays a central role in the metabolic exchange between the organisms. Besides nitrogen and sugars, the sulfur metabolism seems to play an important role for the functioning of the nitrogen fixation process (1). Several studies support this: (2) the sulfate transporter (SST1) was found one of the most abundant PBM proteins; (3) evidence for a regulatory role of sulfate during drought acclimation and ethylene biosynthesis in nodules was presented as well as the nodule function as important source of cysteine for the whole plant (4). However, the role of sulfur during nodule protein-synthesis and -functional regulation remains unclear.

Approach - Proteomics

Using a high throughput mass spectrometry based proteomics approach, we initially detected 1031 sulfur (cysteine or methionine) containing nodule proteins (Figure 1A) corresponding to 2685 different peptides (Figure 1B). From those, 923 were plant and 1204 bacteroid specific (Figure 2). A high coverage, since the percentage of cysteine/methionine of the plants proteome is about 2.6/1.9 and of rhizobia 0.9/2.5, respectively (UniProt database 2016).

We extracted a number of 42 proteins, functionally annotated to the sulfur metabolism, such as several plant and bacteroid specific cysteine synthase isoforms (Figure 3). Thus, S-metabolism-regulation enzymes seem themselves to be regulated by the synthesis of cysteine and methionine.

Sulfur Turnover Dynamics of the Nodule Proteome

We then analyzed the incorporation of reduced sulfur into the nodule proteome (plant and bacteroids) by using ³⁴S-metabolic labelling and mass spectrometry. Samples were taken 24, 48 and 72 hours after pulse labelling. Sulfur turnover dynamics are being presented for a rhizobial Methionine synthase (Figure 3) and the Nitrogenase (Figure 4). It is the first proof for the incorporation of SO₄²⁻, taken up by the plant, into rhizobial proteins.

References

- (1) Krusell et al. (2005) Plant Cell 17:1625-1636.
- (2) Wienkoop & Saalbach (2003) Plant Physiol. 131:1080-1090.
- (3) Larrainzar et al. (2009) MPMI 22(12):1565-1576.
- (4) Kalloniati et al. (2015) Plant Cell. 27(9):2384-2400.

⇒ **FIRST EVIDENCE!**

SO₄²⁻, taken up by the plant, is actually used for rhizobia protein synthesis!

FIGURE 1

Venn chart comparison of all identified cysteine and/or methionine containing proteins (A) and peptides (B) of roots versus nodules.

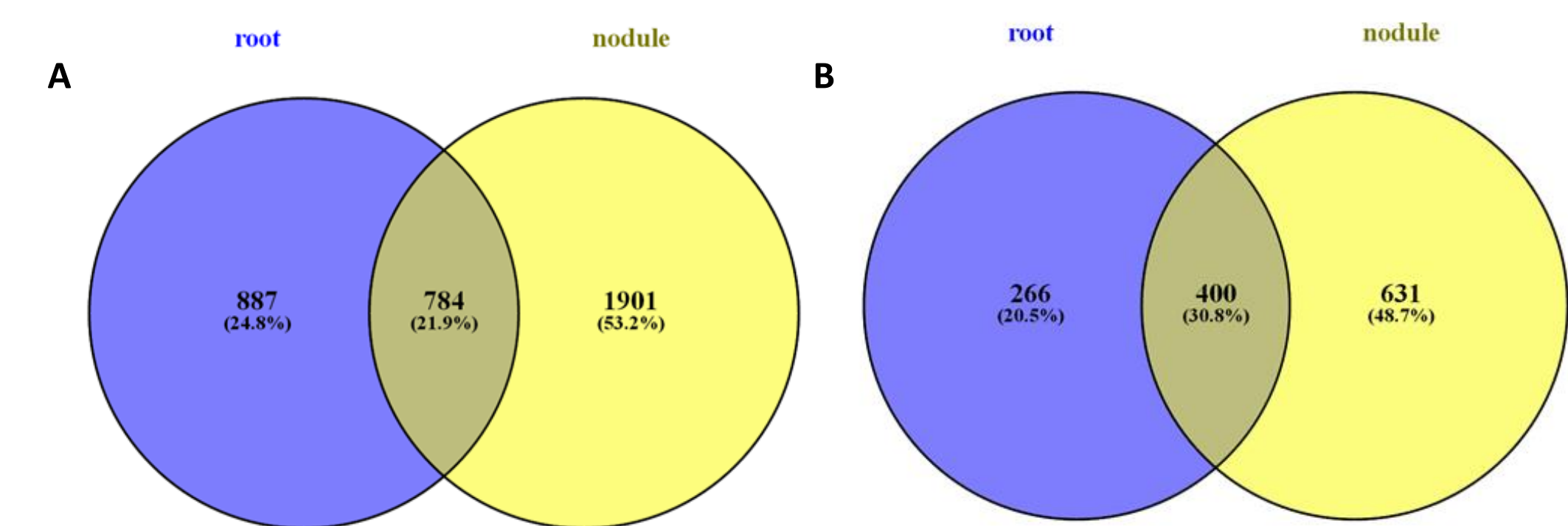


FIGURE 2

Venn chart comparison of all identified cysteine and/or methionine containing plant vs. bacteroid peptides (B) of nodules.

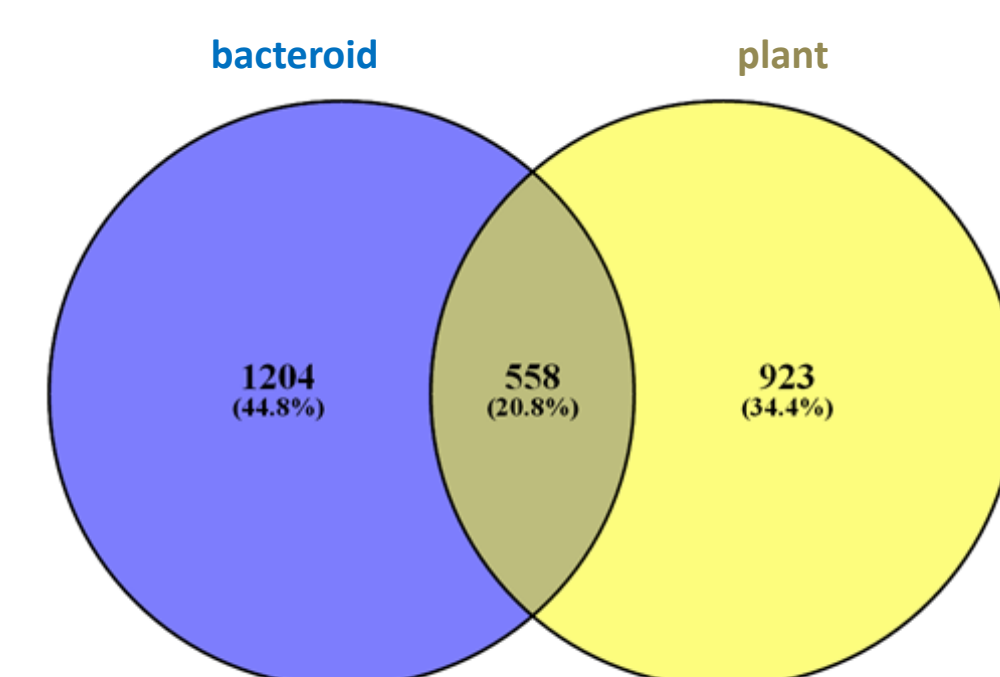
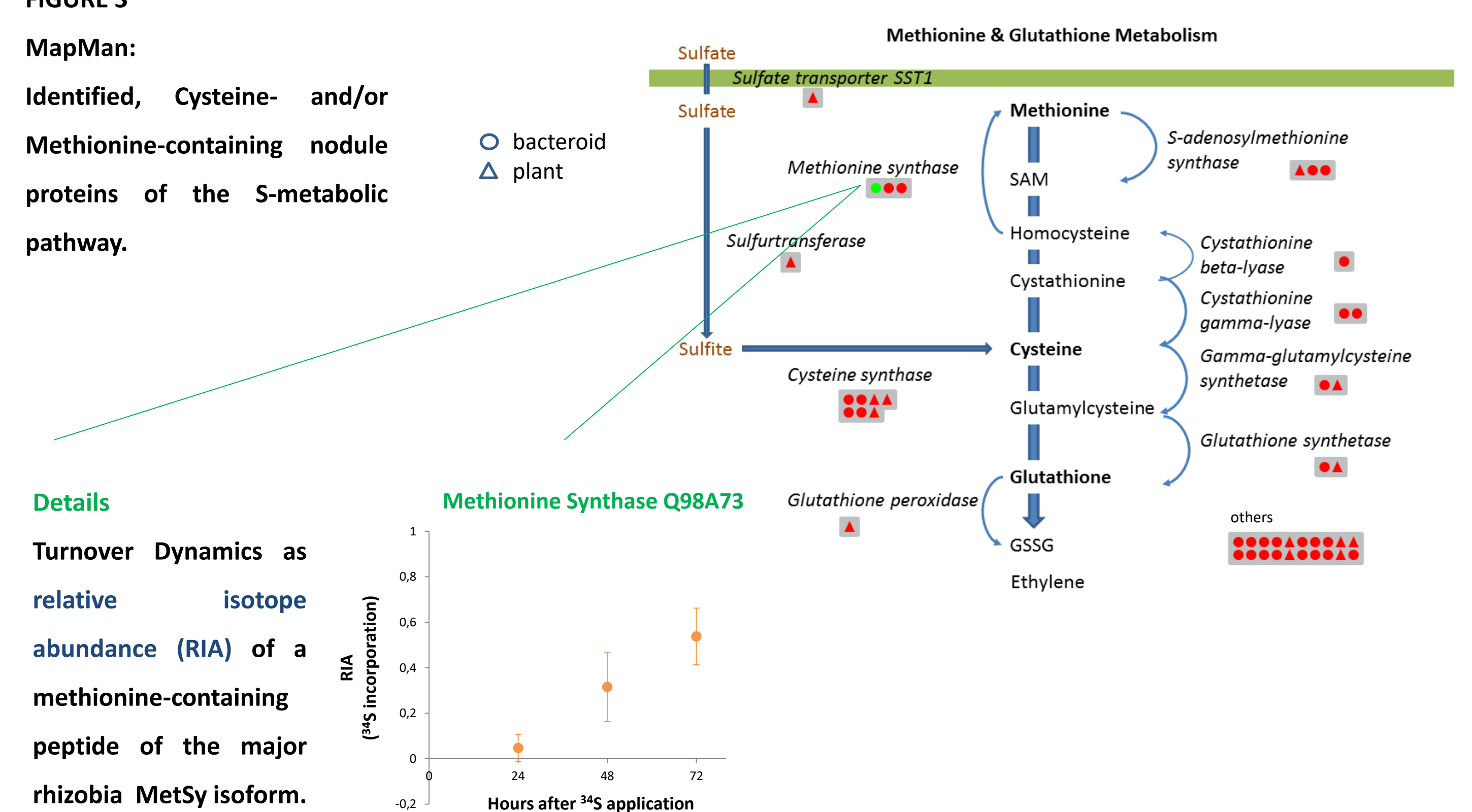


FIGURE 3

MapMan:

Identified, Cysteine- and/or Methionine-containing nodule proteins of the S-metabolic pathway.

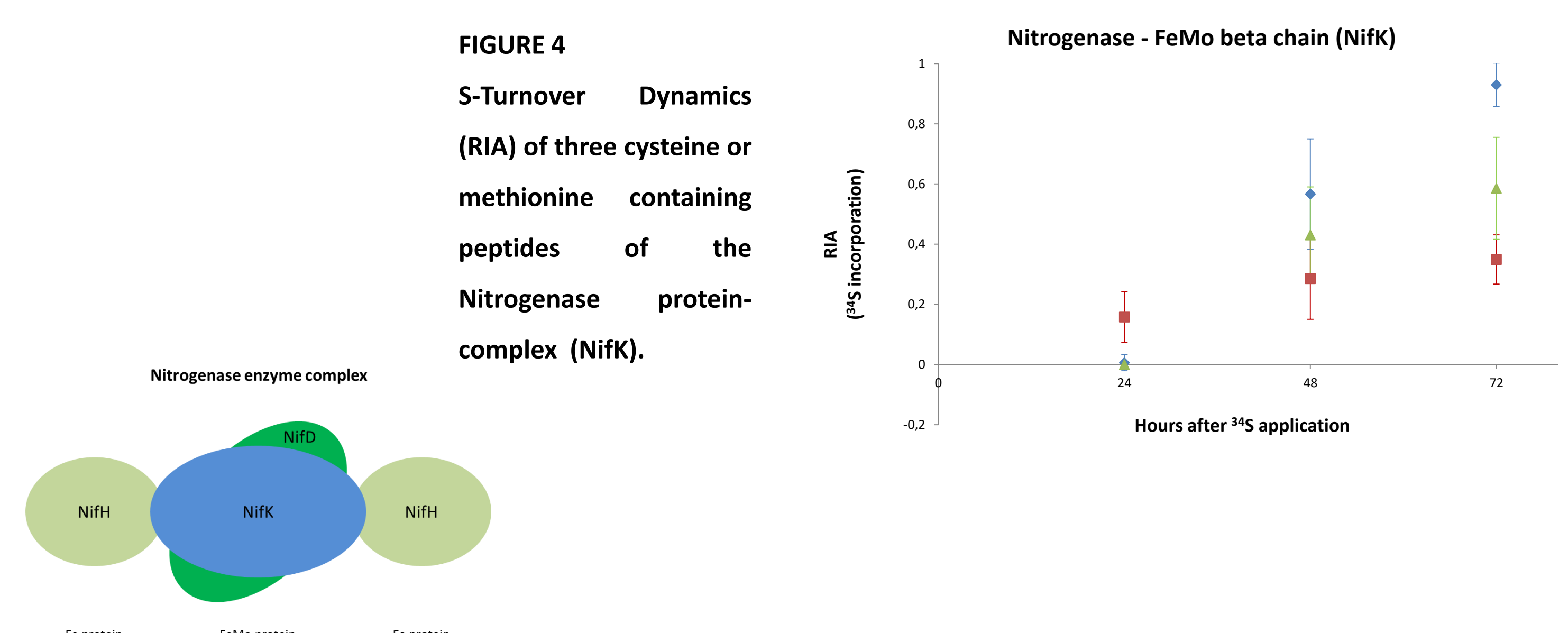


Details

Turnover Dynamics as relative isotope abundance (RIA) of a methionine-containing peptide of the major rhizobia MetSy isoform.

FIGURE 4

S-Turnover Dynamics (RIA) of three cysteine or methionine containing peptides of the Nitrogenase protein-complex (NifK).



Conclusion

- S-containing proteins/peptides are found enriched in nodules mostly coming from the bacteroid fraction. This suggests a higher demand of S for rhizobia protein biosynthesis.
- S-metabolism seems regulated by the synthesis of Cysteines and Methionines itself.
- for the Nitrogenase, data reveal that all subunits are containing S-peptides but only the molybdenum-iron protein β-subunit (NifK) shows high Cysteine incorporation dynamics (~90% after 3 days).

<http://homepage.univie.ac.at/stefanie.wienkoop/>

FWF Project DK+



Department
Molecular Systems Biology



universität
wien

University of Vienna | Faculty of Life Sciences | Althanstrasse 14 | 1090 Vienna | Austria

FWF

Der Wissenschaftsfonds.



universität
wien

The role of glycolysis and fermentation during drought stress in a polyploid crop. Confirmation of a lab model in a greenhouse model

INTRODUCTION

In banana (*Musa* spp.) even mild-drought conditions are responsible for considerable yield losses. First results from plants grown under autotrophic conditions in a growth chamber pointed to an up-regulation of genes involved in glycolysis, fermentation, carbon allocation, (an)aerobic respiration and ROS detoxification in roots under osmotic stress (Figure 1; Zorrilla-Fontanesi *et al.* 2016). To validate this outcome, we performed a greenhouse experiment where plants of the same genotypes were subjected to water deprivation until the soil reached a pF value of 2.8-3.1, which has proven to induce drought in field (Kissel *et al.*, 2015). We have measured the expression levels in root of 13 key genes (and their paralogs) related to the above mentioned pathways, and observed their induction in the greenhouse model. Correlations among the expression patterns of these genes confirmed the interlink between these pathways and also the shift to a more anaerobic metabolism during stress (Figure 2). We then focused on the analysis of the alcohol dehydrogenase family in *Musa* (*MaADH*; Table 1; Figure 3) and the role of ethanolic fermentation in stressed roots, as this process is clearly induced in both models (lab and greenhouse).

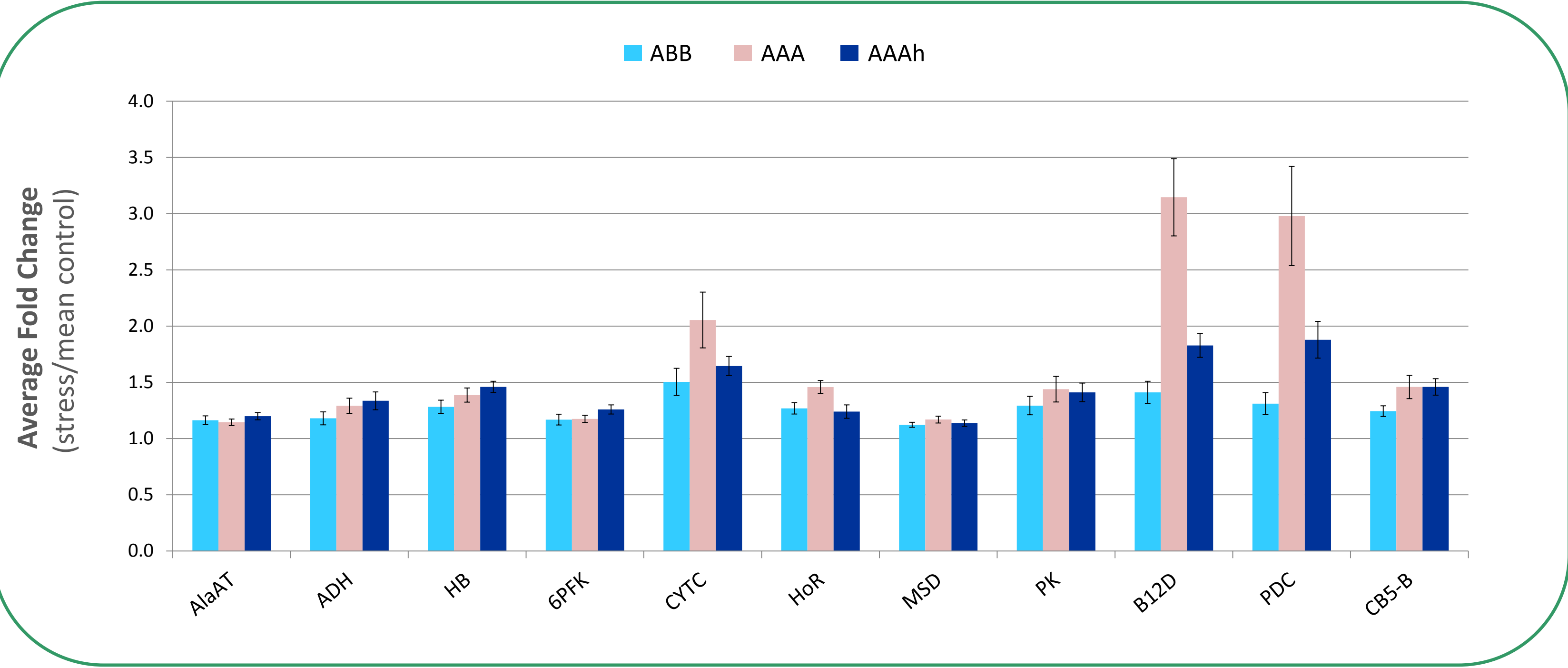


Figure 1. Expression levels of 11 genes involved in (an)aerobic metabolism in roots in a lab model. RT-qPCR results expressed as Fold Change of log-transformed data. *Musa* genes ribosomal protein L2, Actin-1 and Tubulin beta-1 chain were used as internal controls to normalize the expression values. Function abbreviations: AlaAT: alanine aminotransferase; ADH: alcohol dehydrogenase; HB: class I non-symbiotic haemoglobin; 6PFK: 6-phosphofructokinase; CYTC: cytochrome c; HoR: hypoxia responsive family protein; MSD: manganese superoxide dismutase; PK: pyruvate kinase; B12D: B12D protein; PDC: pyruvate decarboxylase; CB5-B: cytochromes b5.

Table 1. ANOVA results showing the significance level of the genotype, treatment and genotype × treatment effects for the *MaADH* paralogs analyzed by RT-qPCR in roots in a greenhouse model. Genotypes tested: ABB (tolerant), AAA (intermediate) and AAHh (sensitive). Blue color: gene down-regulated in all 3 genotypes. Red color: gene up-regulated in all 3 genotypes. Number of biological replicates (stress/control): n = 18/18. ns: not significant. -: gene not expressed.

<i>MaADH</i> paralogs	<i>p</i> -value		
	Genotype	Treatment	Genotype × treatment
<i>MaADH1</i>	2×10^{-4}	ns	ns
<i>MaADH2</i>	2×10^{-3}	1×10^{-7}	ns
<i>MaADH3</i>	4×10^{-2}	1×10^{-2}	ns
<i>MaADH4</i>	1×10^{-14}	1×10^{-13}	2×10^{-2}
<i>MaADH5</i>	-	-	-

RESULTS

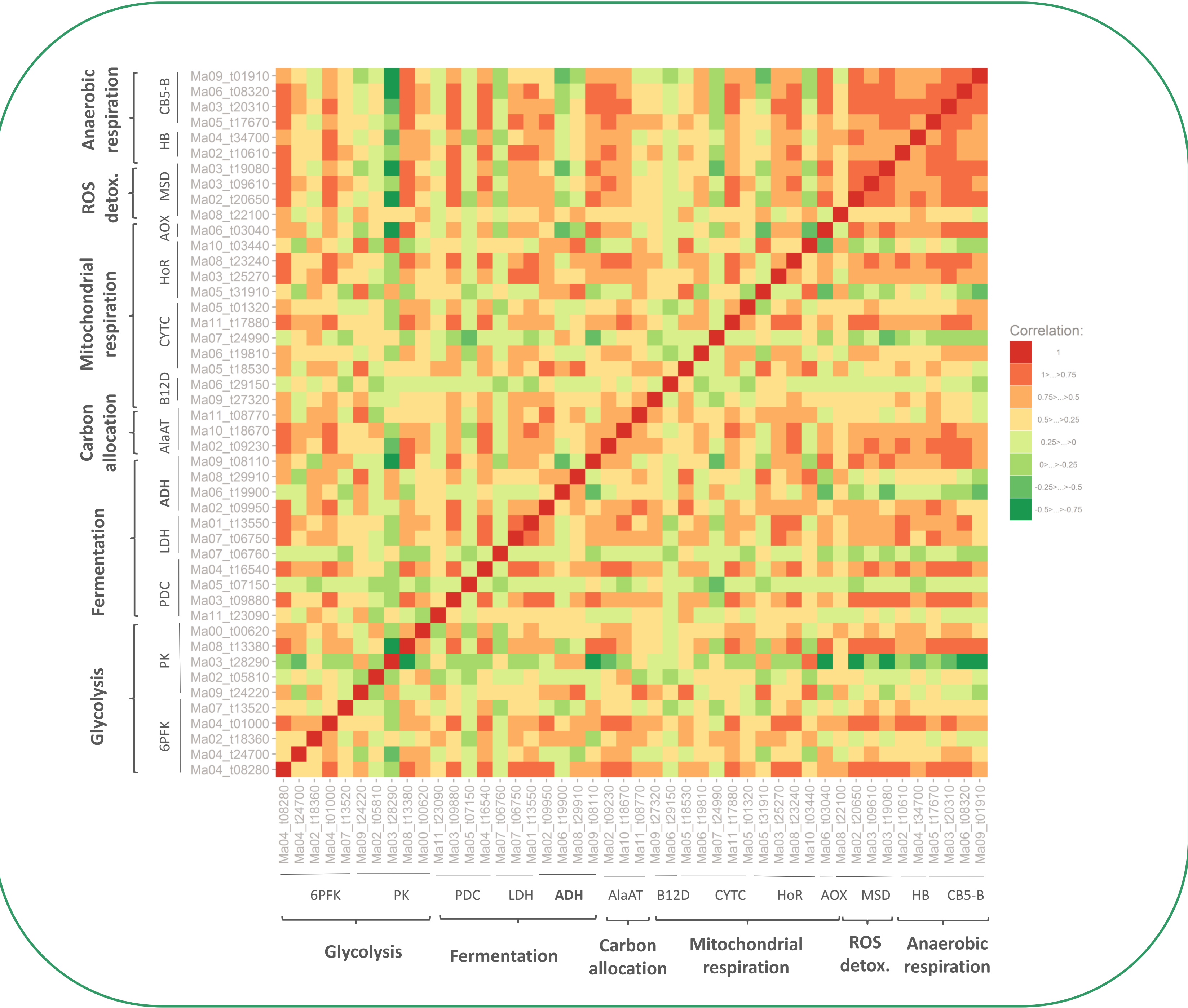


Figure 2. Pearson correlations among expression levels of 13 key genes (and their paralogs) involved in (an)aerobic metabolism in roots in a greenhouse model. Expression levels measured by RT-qPCR in genotype AAHh. Gene IDs according to the *M. acuminata* reference genome Version 2 (Martin *et al.*, 2016). Function abbreviations are the same as in Figure 1, but including LDH: lactate dehydrogenase, and AOX: alternative oxidase.

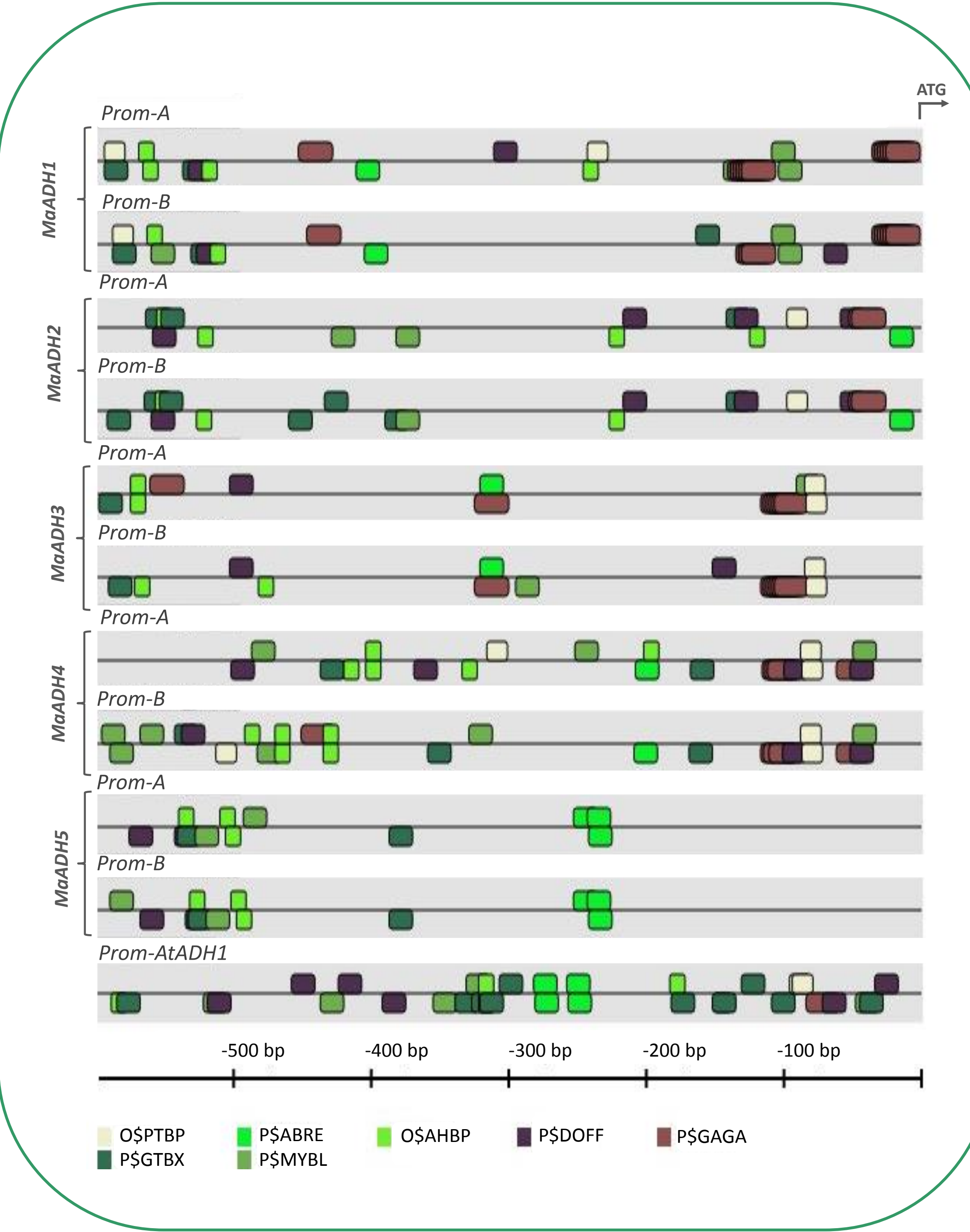


Figure 3. Elements found in the promoters of *MaADHs* and comparison to the *Arabidopsis* ADH promoter (*AtADH1*) using MatInspector (https://www.genomatix.de/online_help/help_matinspector/matinspector_help.html). Prom-A: promoter sequence in the A genome; Prom-B: promoter sequence in the B genome. O5PTBP: Plant TATA binding protein factor; P5ABRE: ABA response elements; P5AHBP: *Arabidopsis* homeobox protein binding site; P5DOFF: DNA binding with one finger; P5GAGA: GAGA elements; P5GTBX: GT-box elements; P5MYBL: MYB-like proteins binding site.

CONCLUSIONS

- ✓ Glycolysis, fermentation and (an)aerobic respiration were induced in banana roots exposed to water deficit, as previously observed in a lab model. These pathways are interconnected and the underlying genes belong to families with several paralogs.
- ✓ The alcohol dehydrogenase family in *Musa* has four paralogs expressed in roots. Differences in expression levels across genotypes and treatments can be explained by differences in the promoter regions.
- ✓ Binding sites for MYB transcription factors seem to play a role in the significant up-regulation of *MaADH4* during drought stress.

References

Kissel E., *et al.* Scientia Horticulturae 185, 175-182 (2015).
Martin G., *et al.* BMC Genomics 17:243 (2016).
Zorrilla-Fontanesi Y., *et al.* Scientific reports 6, 22583 (2016).
The authors would like to thank Hien Do, Els Thiry and Saskia Windelinx for technical assistance. Financial support from the Bioversity International project 'Adding value to the ITC collection through molecular and phenotypic characterization' (financed by the Belgian Directorate-General for Development Cooperation (DGDC)) is gratefully acknowledged.

Quercus suber phellogen: what INFERNO reveals

Carla Pinheiro^{1,2}, Stefanie Wienkoop³, João Feio de Almeida¹, Olfa Zarrouk², Cecilia Brunetti^{4,5}, Sébastien Planchon⁶, Antonella Gori^{4,5}, Massimiliano Tattini⁴, Cândido Pinto Ricardo², Jenny Renaut⁶, Rita Teresa Teixeira⁷

¹ Faculdade de Ciências e Tecnologia, Universidade NOVA de Lisboa, Portugal; ² Instituto de Tecnologia Química e Biológica, Universidade NOVA de Lisboa, Portugal;

³ Department of Molecular Systems Biology, University of Vienna, Austria; ⁴ The National Research Council of Italy; ⁵ University of Florence, Italy;

⁶ Luxembourg Institute of Science and Technology, Luxembourg; ⁷ Virginia Polytechnic Institute and State University, USA

Cork is a highly valuable, and renewable, non-wood forest product, and plays an important role in the Portuguese economy. Cork is extracted from *Quercus suber* trees (Figure 1). Cork is extracted from *Q. suber* trees every nine years. Not all trees produce cork of good quality (GQC; Figure 1), but only GQC is highly valuable by the market.

Molecular analysis of *Q. suber* phellogen

Samples were collected from five trees from producing type cork of good quality and from a minimum of five trees producing bad quality cork (BQC). Immediately after debarking, the phellogen was collected.



Figure 1. A representative *Quercus suber* tree. The cork produced by trees is ranked according to its quality. It ranges from good quality cork (GQC) to bad quality cork (BQC). During its life cycle, a given tree typically produces the same type of cork.

Photo credits:

commons.wikimedia.org/wiki/File:Cork_oak,_Vale_da_Azinheira,_25_June_2016.JPG

Teixeira et al J Exp Bot 2014 doi: 10.1093/jxb/eru252

www.corklink.com/wp-content/uploads/2013/10/natural-cork-qualities.jpg

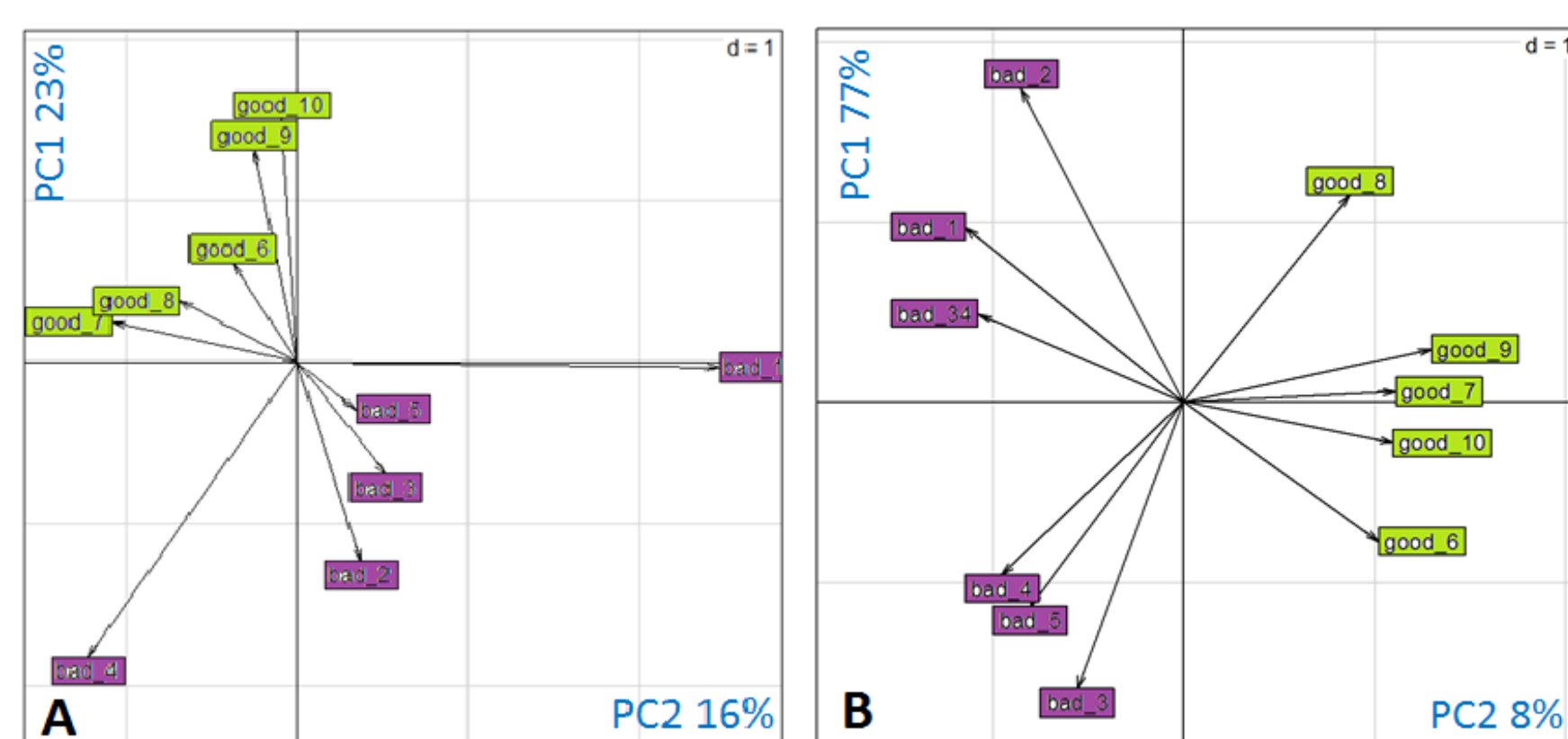


Figure 2. Principal components analysis (ade4, R platform) using the protein profile obtained by 2DE (A) and phenolic compounds profile (B).

The data set reveal an interesting pattern, supporting the characterization with distinct omics methodologies and the integration of the several datasets for data analysis. While discrimination between GQC and BQC at transcriptomic level was found to be minimal (Teixeira et al J Exp Bot 2014), it was possible to discriminate between GQC and BQC at the proteomic level (Figure 2A). At the phenolics level (Figure 2B), such difference is particularly evident.

The combined use of the proteomic and phenolic datasets, using InfernoRDN (v1.1.6044, Popitiya et al. 2008 Bioinformatics, 1556-8), allowed to highlight the proteins and the phenolic compounds discriminating the GQC and the BQC (Figure 3).

This approach allowed to relate 14 proteins with cork quality. Twelve of these proteins were identified through MS/MS, and in order to confirm annotation each peptide pool was scanned for uniqueness, and collinearity. Consolidated sequences were submitted to similarity search through standard BLASTP from among the plant entries in the NCBI Protein database, and localized InterPro annotation transfer. This approach allowed to refine the annotation detail and better assess the role of these proteins in the cell.

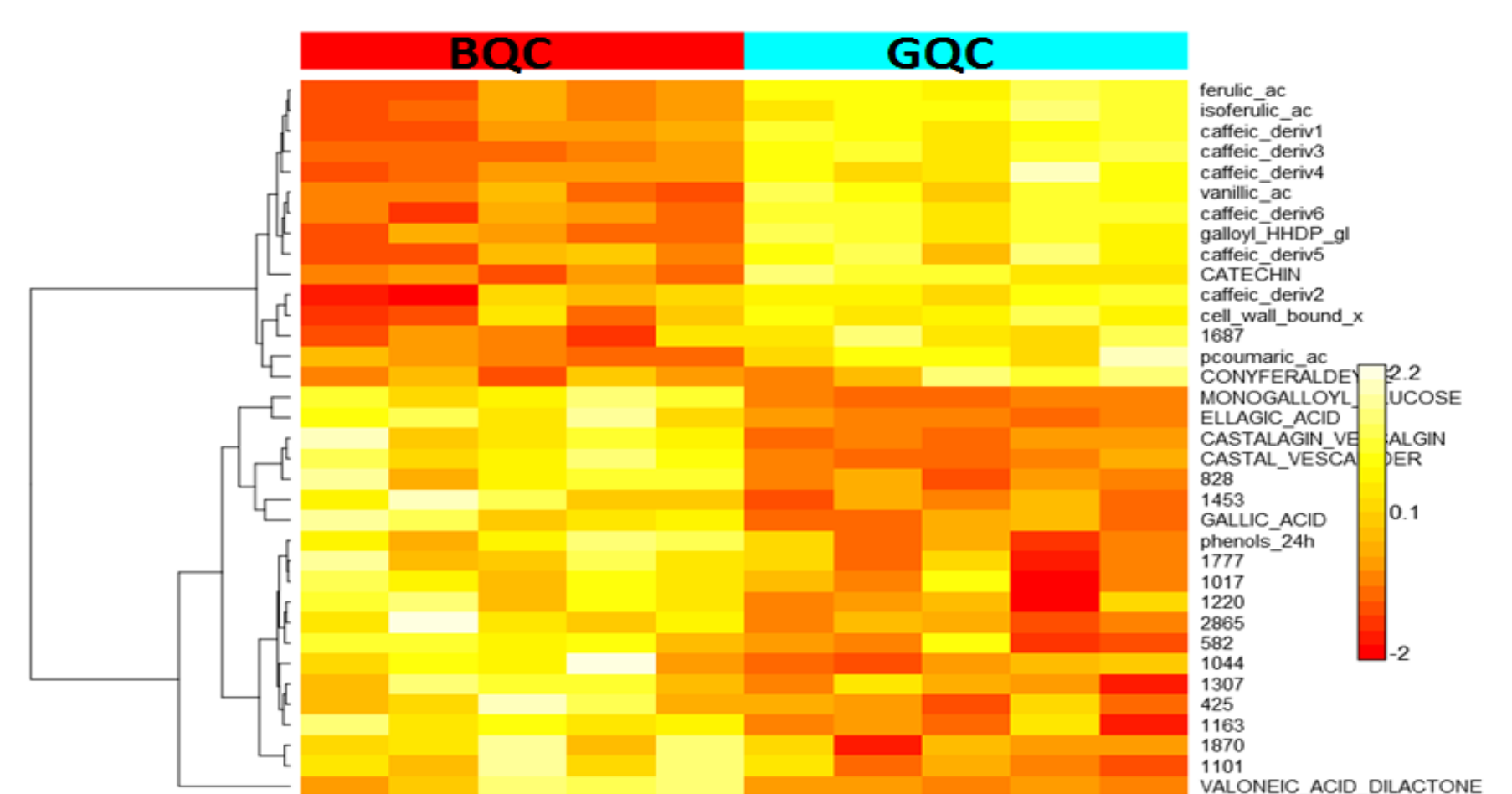


Figure 3. Heat map cluster with Pearson correlation ($p < 0.05$) obtained with InfernoRDN.

Conclusion & future prospects

The phellogen proteome and phenolics profile discriminate between good quality cork and bad quality cork producers. Currently, we found good candidates for such discrimination. Our next goal is to build a model for phellogen biochemistry at the cellular level. The main goal is to increase our knowledge on the phellogen production and how distinct types of cork are built.

Physiological and metabolic responses of citrus associated to tolerance to combined heat stress and drought conditions

Sara I. Zandalinas, Aurelio Gómez-Cadenas, Vicent Arbona
Ecofisiologia i Biotecnologia. Departament de Ciències Agràries i del Medi Natural.
Universitat Jaume I. E-12071 Castelló de la Plana. SPAIN.
 E-mail: arbona@uji.es

Climate change refers to a variation in the global average climate conditions associated to anthropic activity.

In Europe and North America, drought and high temperatures will be the predominant conditions in the near future.

The objective in this work is to characterize the physiological and biochemical responses of citrus to combined stress conditions and identify potential tolerance traits.

- Physiological and Biochemical Characterization: *identification of tolerant and sensitive phenotypes*
- Analysis of hormonal regulation: *regulation of the physiological response*
- Metabolite profiling: *analysis of potential effectors*

Carrizo was categorized as tolerant and Cleopatra as sensitive.

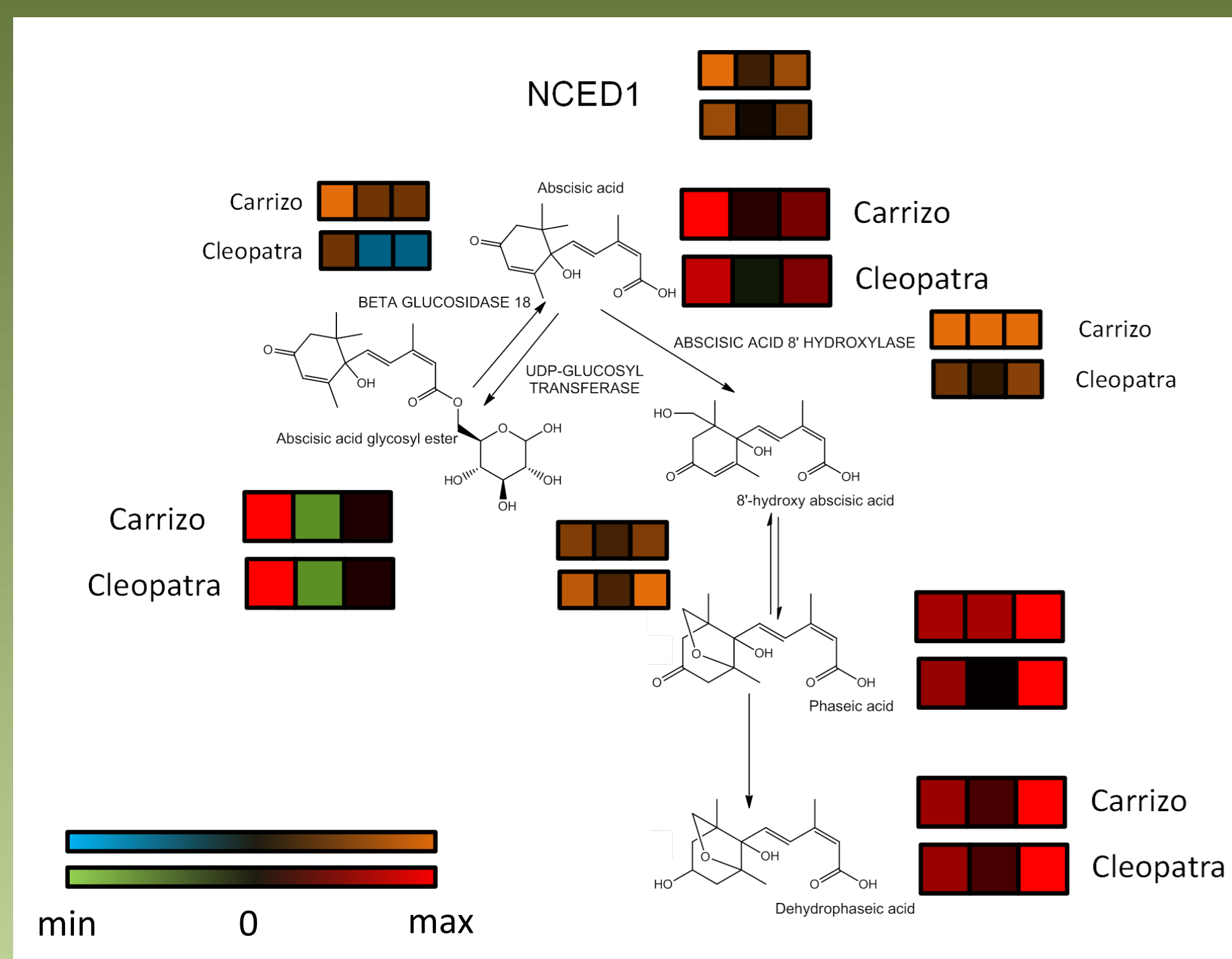


Figure 4. Absciscic acid (ABA) metabolism: gene expression (blue/orange) and accumulation of ABA, its catabolites and conjugated forms (green/red).

ABA metabolism was associated to different stomatal movements upon HS or WS+HS in Citrus.

Different secondary metabolite profiles were observed in Carrizo and Cleopatra.

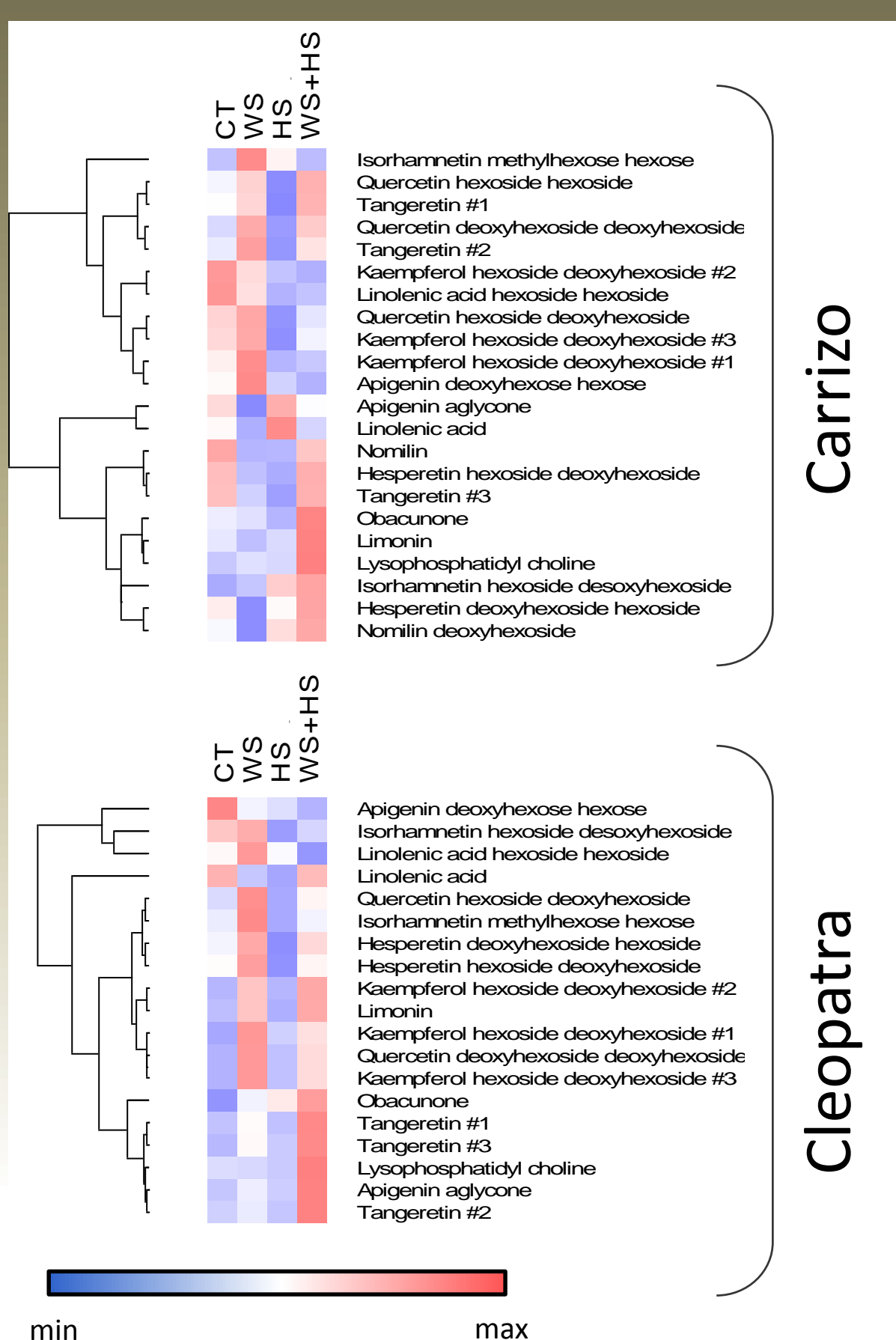


Figure 6. Secondary metabolism.

Sensitive Cleopatra showed higher levels of protective phenylpropanoids (scopolin) and flavonoids (quercetin derivatives).

Tolerant Carrizo induced metabolic pathways involved in lignin biosynthesis.

Seedlings of Carrizo citrange (*P. trifoliata* x *C. sinensis*) and Cleopatra mandarin (*C. resnyi*) were subjected to high temperatures (HS) and drought (WS) separately or in combination.

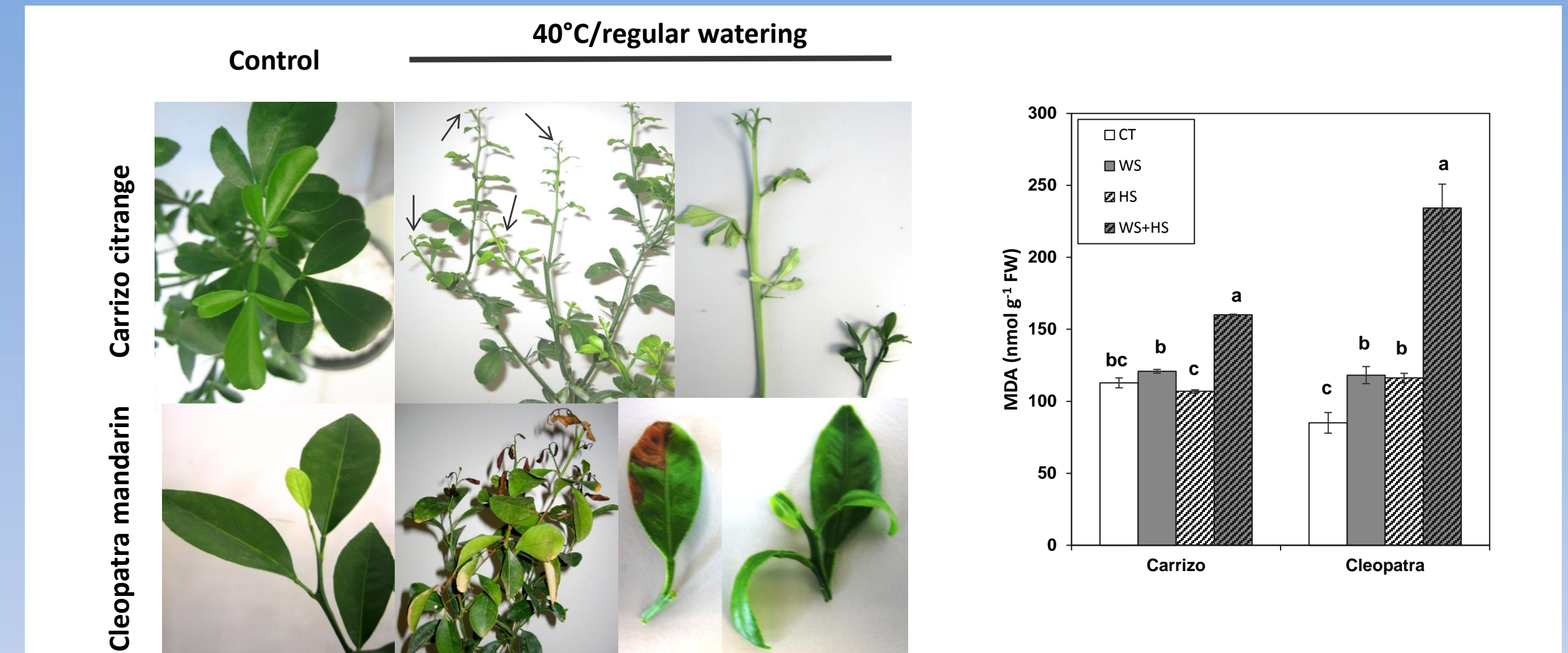


Figure 2. Leaf symptoms developed upon heat stress imposition, malondialdehyde (MDA) accumulation in leaves.

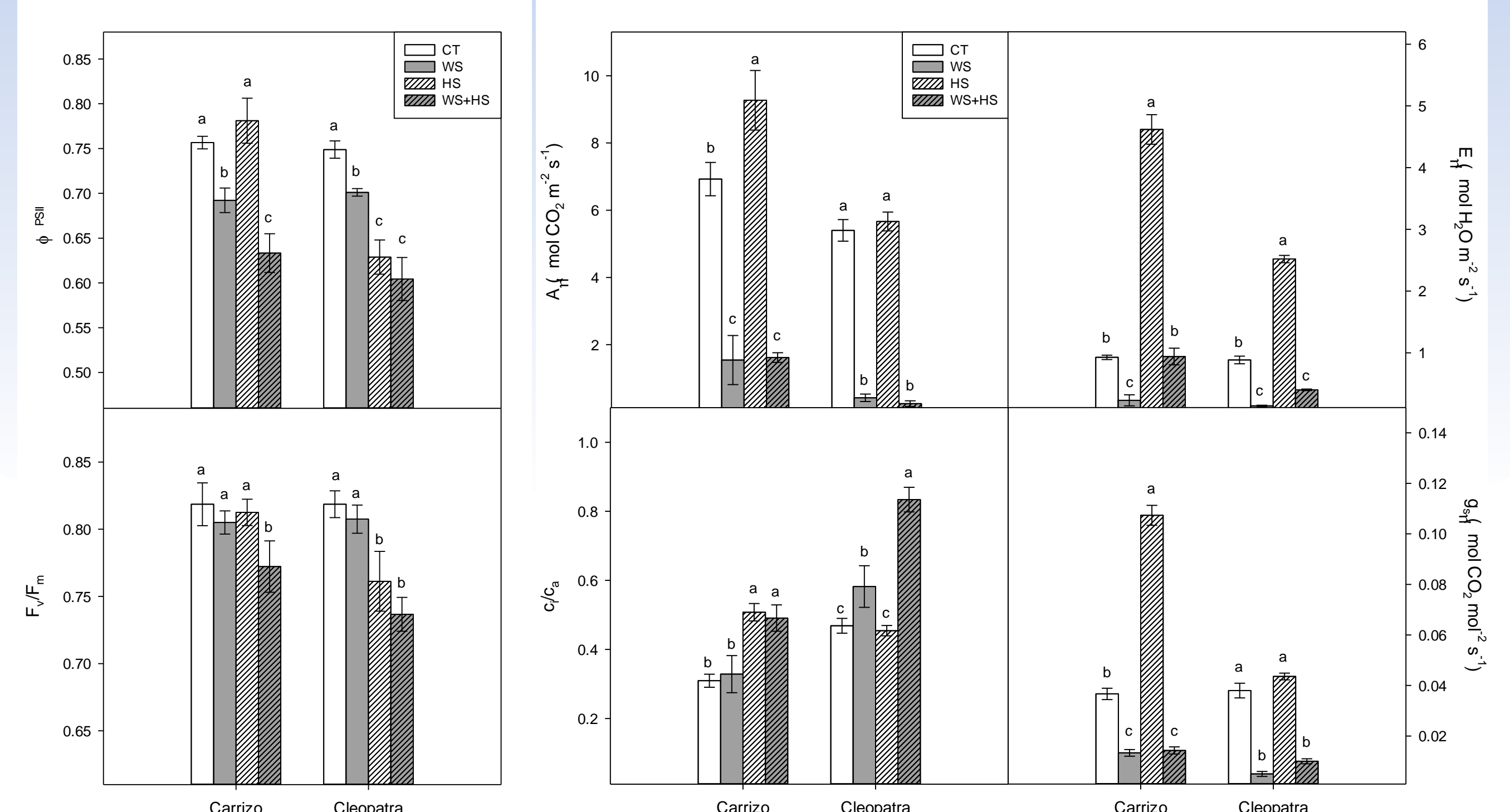


Figure 3. Photosynthesis. Chlorophyll fluorescence and gas exchange parameters.

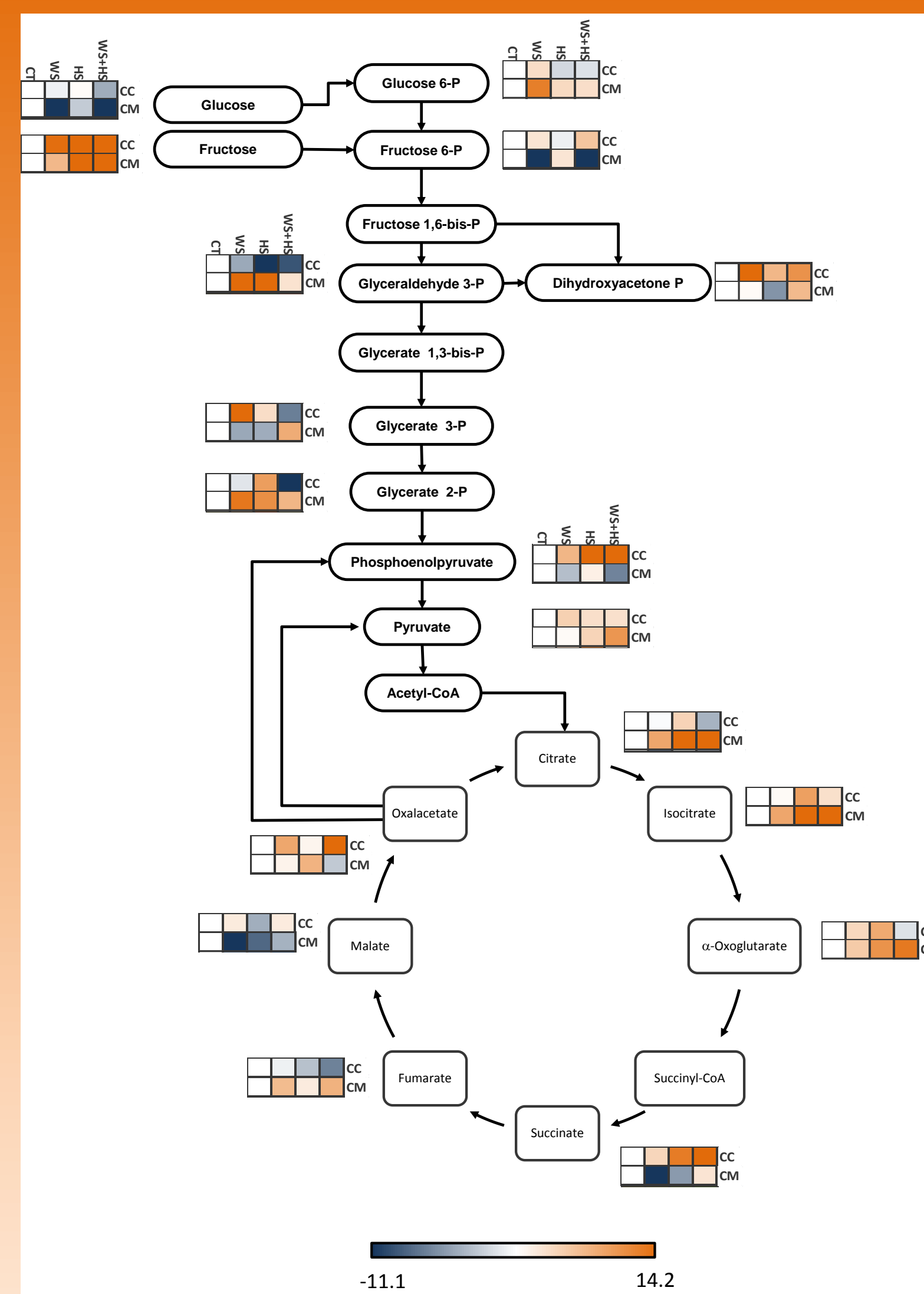


Figure 5. Primary metabolism: glycolysis and TCA cycle.

Upon imposition of stress, Cleopatra mandarin (CM) showed an enhanced energy metabolism.

This activation in CM was linked to increased MDA accumulation and sensitivity.

References

- Zandalinas SI, Rivero RM, Martínez V, Gómez-Cadenas A, Arbona V (2016). BMC Plant Biol 16:105. doi: 10.1186/s12870-016-0791-7
- Zandalinas SI, Sales C, Beltran J, Gómez-Cadenas A, Arbona V (2017). Front Plant Sci 7:1954. doi: 10.3389/fpls.2016.01954

The relationship between drought tolerance in maize in vegetative and reproductive stage

Sofija Božinović¹, Ana Nikolić¹, Jelena Vančetović¹, Dragana Ignjatović Micić¹, Astrid Junker², Kathleen Weigelt-Fischer², Dejan Dodig¹, and Thomas Altmann²

¹*PlantBreeding Department, Maize Research Institute ZemunPolje, Belgrade, Serbia*
²*Research group Heterosis, Dept. of Molecular Genetics, Leibniz Institute of Plant Genetics and Crop Plant Research (IPK) Gatersleben, Germany*

INTRODUCTION

A set of 20 maize (Zea mays L.) inbred lines, including 15 tolerant and five susceptible to drought stress, were chosen for the experiment. Twelve out of 15 tolerant inbred lines are introduced from different countries and belong to the drought tolerant mini core collection of Maize Research Institute Zemun Polje gene bank. The genotypes were defined either as drought tolerant or drought susceptible according to their response to water deficiency during early reproductive stage in the field conditions, with the grain yield as the main parameter. One of the objectives of this research was to relate the obtained data with our previous studies in the field.

THE EXPERIMENT

- Genotypes were grown in a greenhouse under optimal conditions until V6 growth stage
- From V6: start of treatments and automated phenotyping for four weeks (LemnaTec Scanalyzer, IPK Gatersleben)
- Randomized Block Design with eight replications and four treatments:
 - optimum ammount of water and nitrogen (control)
 - optimum amount of water + nitrogen stress
 - optimum amount of nitrogen + water stress
 - combined water and nitrogen stress
- Optimum and stress water level = 75% and 30% of the field capacity
- Nitrogen stress level = no nitrogen fertilizer added during the experiment
- TRAITS: morphological and physiological - extracted from visible, near-infrared and fluorescence images being taken every day; leaf number and chlorophyll content, fresh and dry biomass, water and nitrogen use efficiency and relative water content - manually measured.



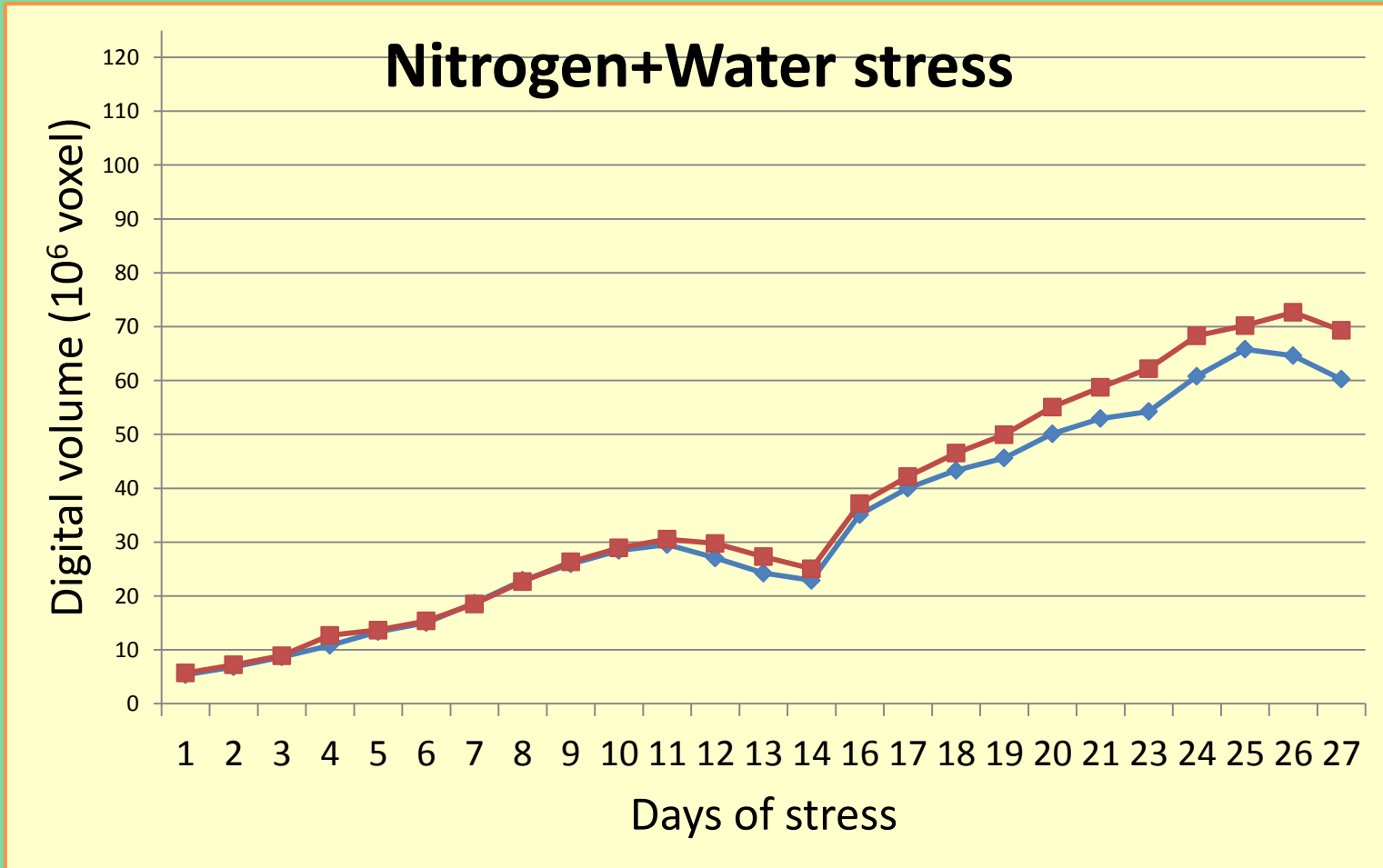
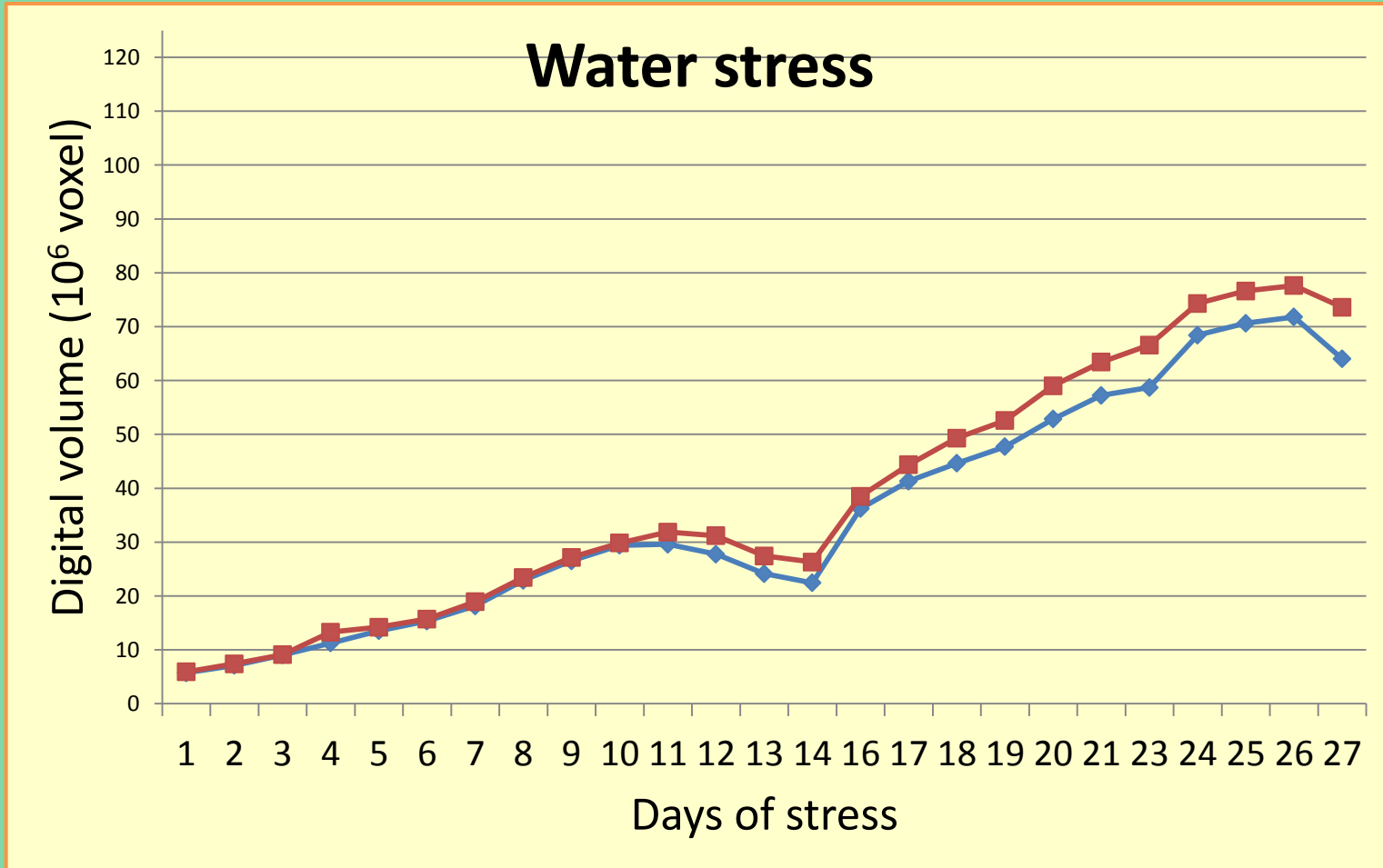
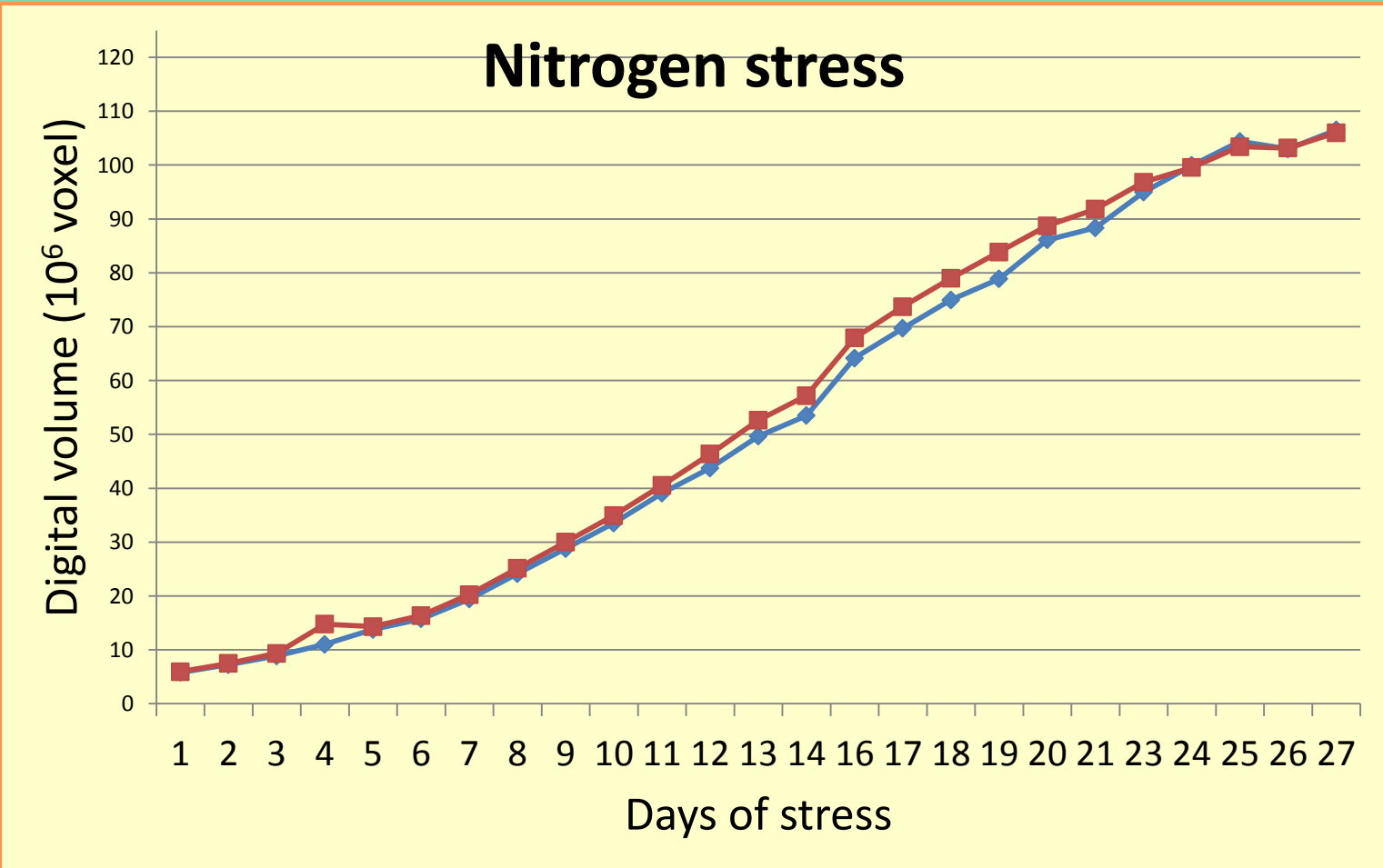
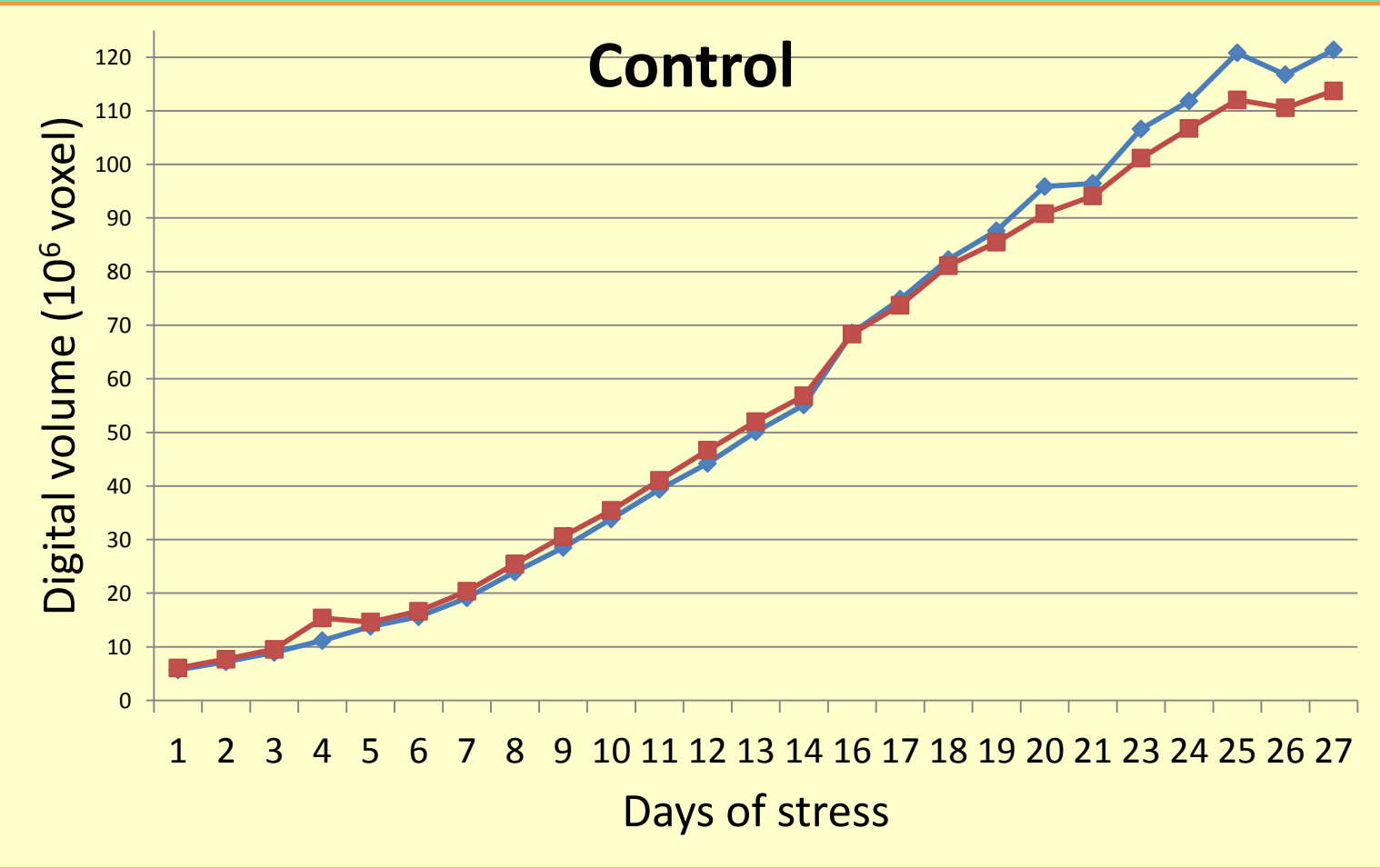
RESULTS

Table 1. Means and ranges over treatments of the chosen traits for susceptible vs. tolerant genotypes at the end of the experiment

TREATMENT	GENOTYPE	WUE		FW		DW		DMS		RWC		LN		CHL		VOL	
		range	mean	range	mean	range	mean	range	mean	range	mean	range	mean	range	mean	range	mean
C	S	2.81-3.35	3.07	378.0-489.9	452.4	40.2-58.5	48.4	9.1-12.0	10.7	92.8-94.8	93.8	13.-16.1	14.3	29.7-36.1	31.8	101.70-146.79	121.34
	T	2.2-3.38	2.97	318.2-633.8	414.7	31.8-67.5	47.2	9.5-13.6	11.4	91.9-96.5	94.2	12.1-15.2	13.9	27.9-36.1	32.1	85.58-150.07	113.73
N	S	2.85-3.37	3.04	354.2-454.3	415.9	37.9-55.1	45.2	9.2-12.2	10.9	92.4-94.2	93.3	12.8-15.2	13.9	26.2-32.0	29	95.14-117.13	106.51
	T	2.22-3.31	2.94	317.3-539.8	393.9	30.9-55.9	44.7	9.7-13.6	11.4	91.8-96.1	94	11.8-14.8	13.6	25.3-33.0	29.4	82.13-129.76	106.01
W	S	3.51-3.92	3.67	254.3-301.3	273.8	25.0-27.7	26.1	8.5-10.6	9.6	82.1-90.5	85	11.9-14.3	12.9	39.9-46.1	42.5	45.89-73.58	64.03
	T	3.22-4.67	3.81	222.1-318.7	280.1	22.7-34.6	28	9.1-11.4	10	79.6-91.2	85.4	11.7-14.3	13.2	28.2-44.2	38.1	57.06-93.45	73.59
N+W	S	3.37-3.79	3.59	233.9-292.8	254.9	23.1-27.1	25	8.9-11.0	9.9	79.8-90.6	84.3	11.4-13.7	12.6	39.8-46.3	41.7	52.61-70.94	60.25
	T	3.19-4.41	3.72	213.3-297.5	262.8	22.4-31.2	26.5	9.1-11.5	10.1	79.3-91.5	85.4	11.4-14.4	12.7	31.1-43.9	38	56.86-81.78	69.32

C- control; N- nitrogen stress; W- water stress; N+W- combined nitrogen and water stress; S- susceptible to drought stress; T- tolerant to drought stress; WUE- water use efficiency (mg/g); FW- fresh weight (g); DW- dry weight (g); DMS- FW/DW ratio; RWC- relative water content (%); LN- leaf number at the end of experiment; CHL- chlorophyll content at the end of experiment (SPAD units) ; VOL- image based plant digital volume (10⁶ voxel).

Under optimal and N limited conditions susceptible lines showed higher values for WUE, FW, DW and LN on average, while under W and N+W limited conditions these parameters were higher for tolerant genotypes (Table 1). Relative water content was similar for both groups of genotypes, although slightly higher for the tolerant lines in all the treatments. Chlorophyll content under optimal and N limited conditions was similar for both groups of genotypes, but tolerant lines had lower chlorophyll content at the end of the experiment in W and N+W limited conditions. This was probably due to the fact that the SPAD value specifies relative, but not the absolute content of chlorophyll within the sample leaf. As a response to the stress, leaf tissue of a susceptible lines probably shrunk more than those of tolerant lines, so the chlorophyll concetration, but not the absolute content, in these lines was higher.



Volume, also termed „digital biomass“, represents one of the most important image based traits and is calculated from a top and a side camera views. Preliminary data analysis showed that volume was highly correlated with FW and DW and also significantly influenced by all the treatments in our experiment. Under optimal conditions susceptible genotypes had somewhat higher volume than the tolerant ones, while under N limited condition both groups had the same volume on average at the end of the experiment. Although both susceptible and tolerant lines showed significant effect of limited W and N+W supply on volume, tolerant lines on average had higher volume after four weeks of stress. The dynamics of the digital biomass growth clearly shows higher sensitivity of susceptible lines to all the limiting factors (Graphs).

This research has been done under the frame of EPPN project funded by the European Union under FP7 Capacities Programme. Grant Agr. No. 284443.

Fatty acids profile in phenotypic characterization of grapevine resistance against *Plasmopara viticola*

Gonçalo Laureano¹, Joana Figueiredo^{1,2,3}, Ana Rita Matos¹, Andreia Figueiredo¹

¹ Biosystems & Integrative Sciences Institute (BioISI), Plant Biology Department, FCUL, Portugal

² Laboratório de FTICR e Espectrometria de Massa Estrutural, FCUL, Portugal

³ Centro de Química e Bioquímica, FCUL, Portugal

Introduction

Fatty acids (FAs) and fatty acid-derived metabolites are not only major structural and metabolic constituents of the cell but they also function as modulators of a multitude of signal transduction pathways evoked by biotic stresses. Emerging evidence identifies as second messengers, regulators of signal transducing molecules or transcription factors, regulators of cell survival and plant cell death (PDC). The domesticated grapevine (*Vitis vinifera*) is prone to several diseases, being downy mildew one of the major treats of modern viticulture. In our previous studies [1, 2, 3] we have shown that *Vitis vinifera* resistance to *Plasmopara viticola* is mediated by jasmonic acid (JA, Fig. 1). We have also shown that in the first hours of inoculation, a synergism between JA and salicylic acid (SA) exists (Fig. 1).

Materials and Methods

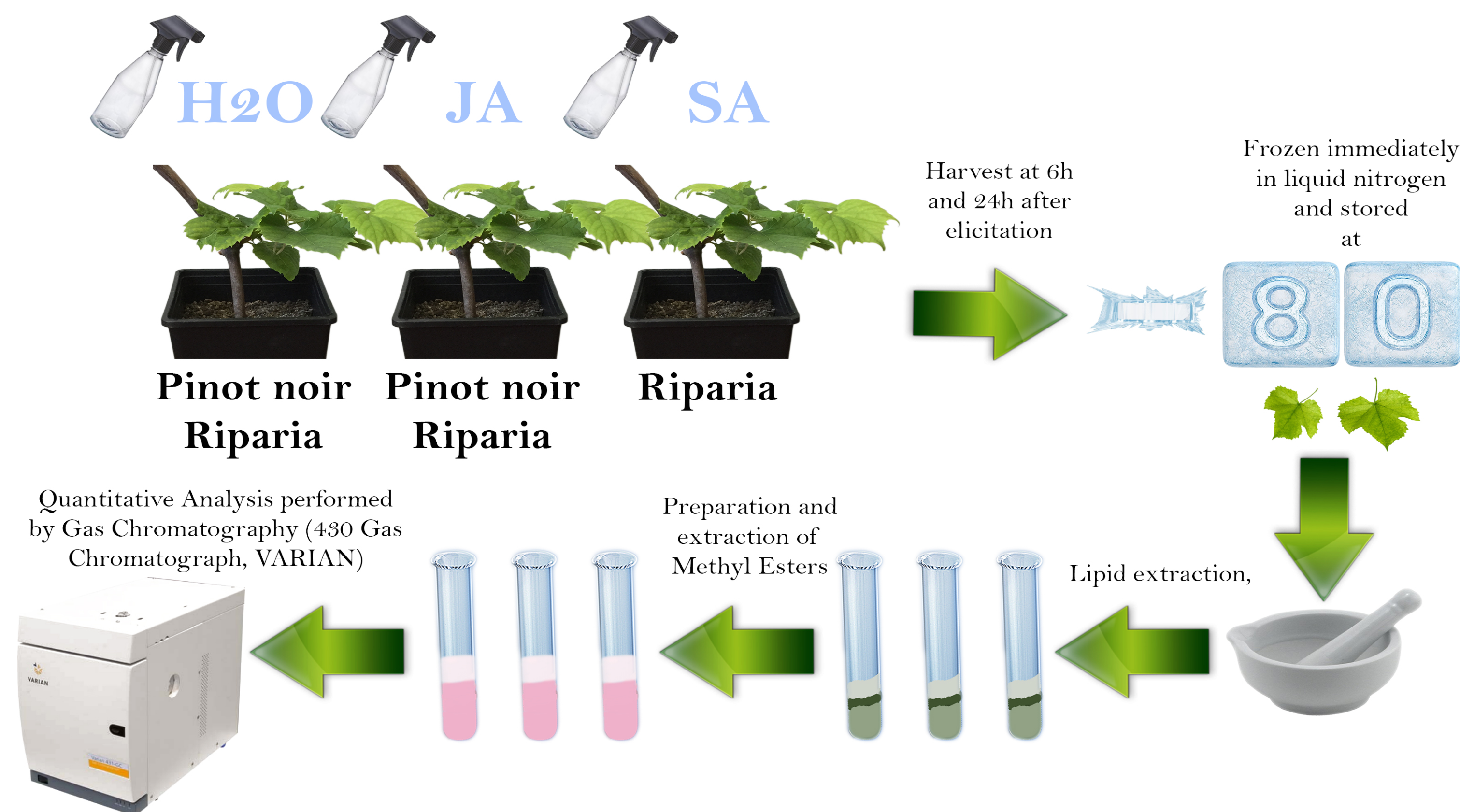


Fig. 2- Experimental procedure for grapevine elicitation, lipid extraction, methylation and quantitative analysis of fatty acids content.

Vitis riparia

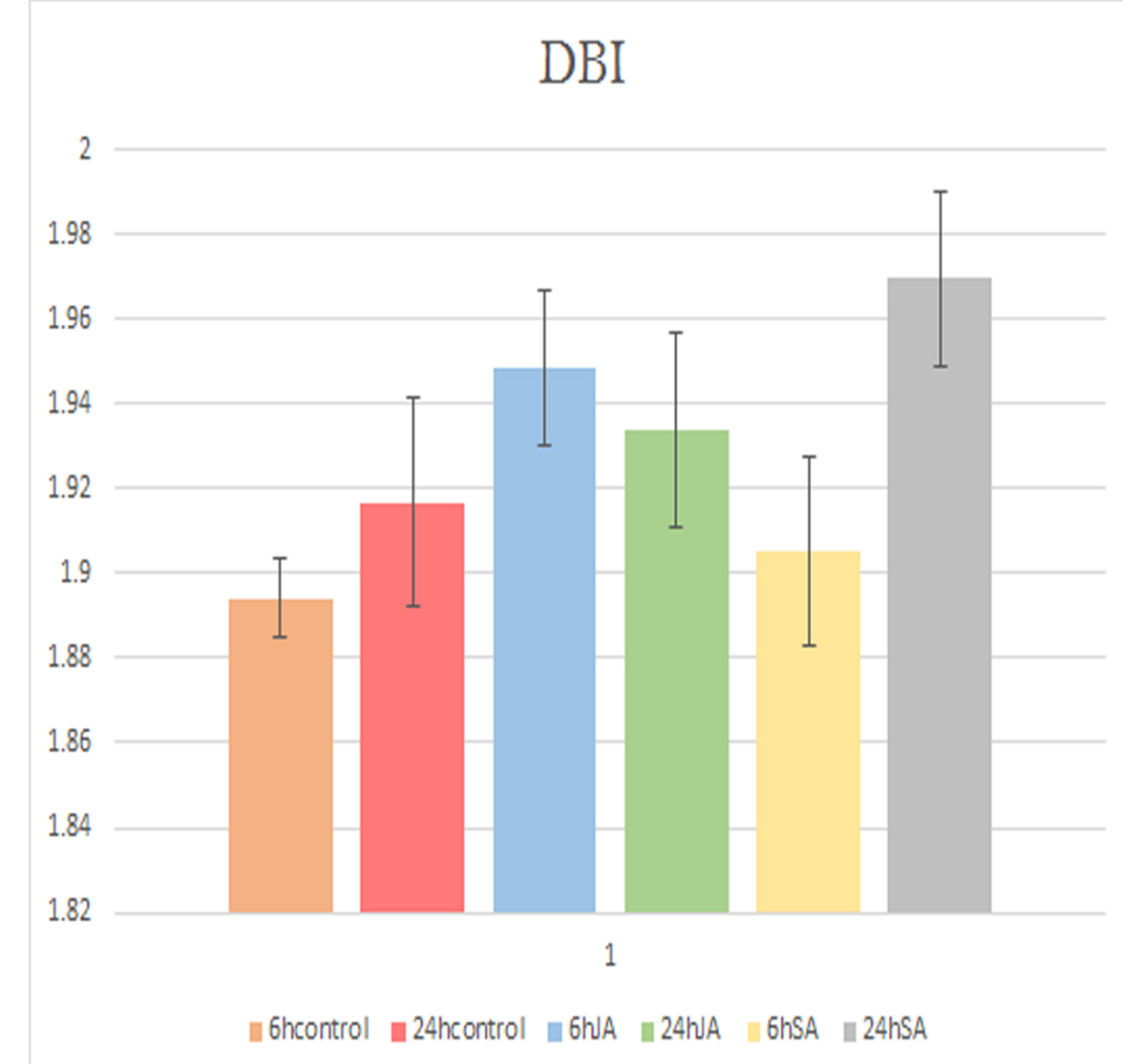
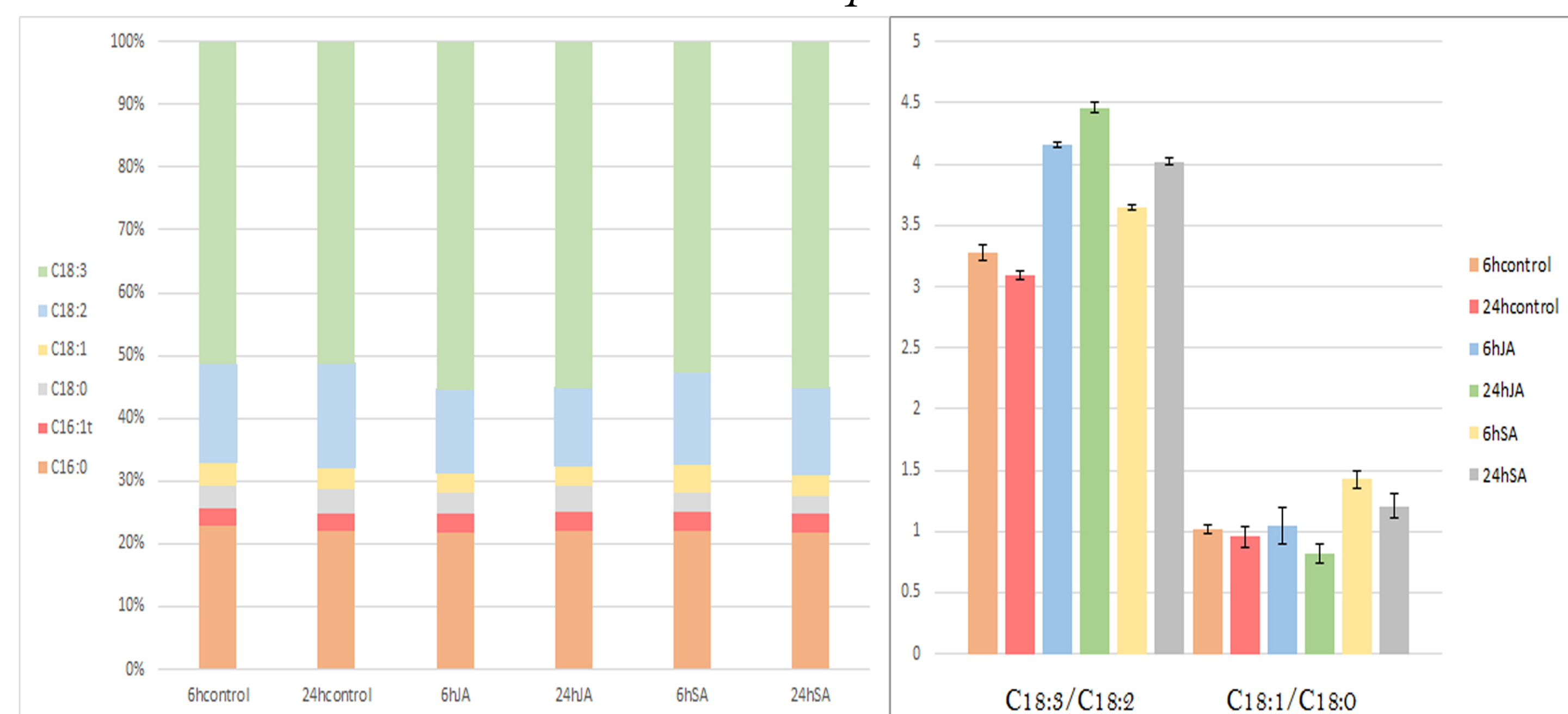


Fig. 3 - Total leaf lipid composition in *Vitis Riparia*: a) Fatty acids profile; b) C18:3/C18:2 and C18:1/C18:0 ratios; c) Double bound index.

Conclusions

Fatty acid profile allowed the discrimination between both species prior and post-elicitation and might, thus be considered as a valuable tool for plant resistance phenotyping;

After elicitation an increase of C18:3 occurs. C18:3 is related to oxylipin based signaling namely to the biosynthesis of JA, even when elicited with SA. Our result reinforce the hypothesis that both JA and SA are acting synergistically on the first hours after pathogen attack.

Acknowledgements

This work was supported by the project UID/MULTI/04046/2013, Investigator FCT program IF/00819/2015 from Fundação para a Ciência e Tecnologia (Portugal). The authors also wish to thank to Ana Rita Cavaco, Bernardo Duarte and Rui Nascimento for all the help and Manuela Lucas for technical assistance. This work is under the scope of Gonçalo Laureano (2017) master thesis, entitled "Fatty acids and lipid signaling in grapevine resistance to *Plasmopara viticola*".

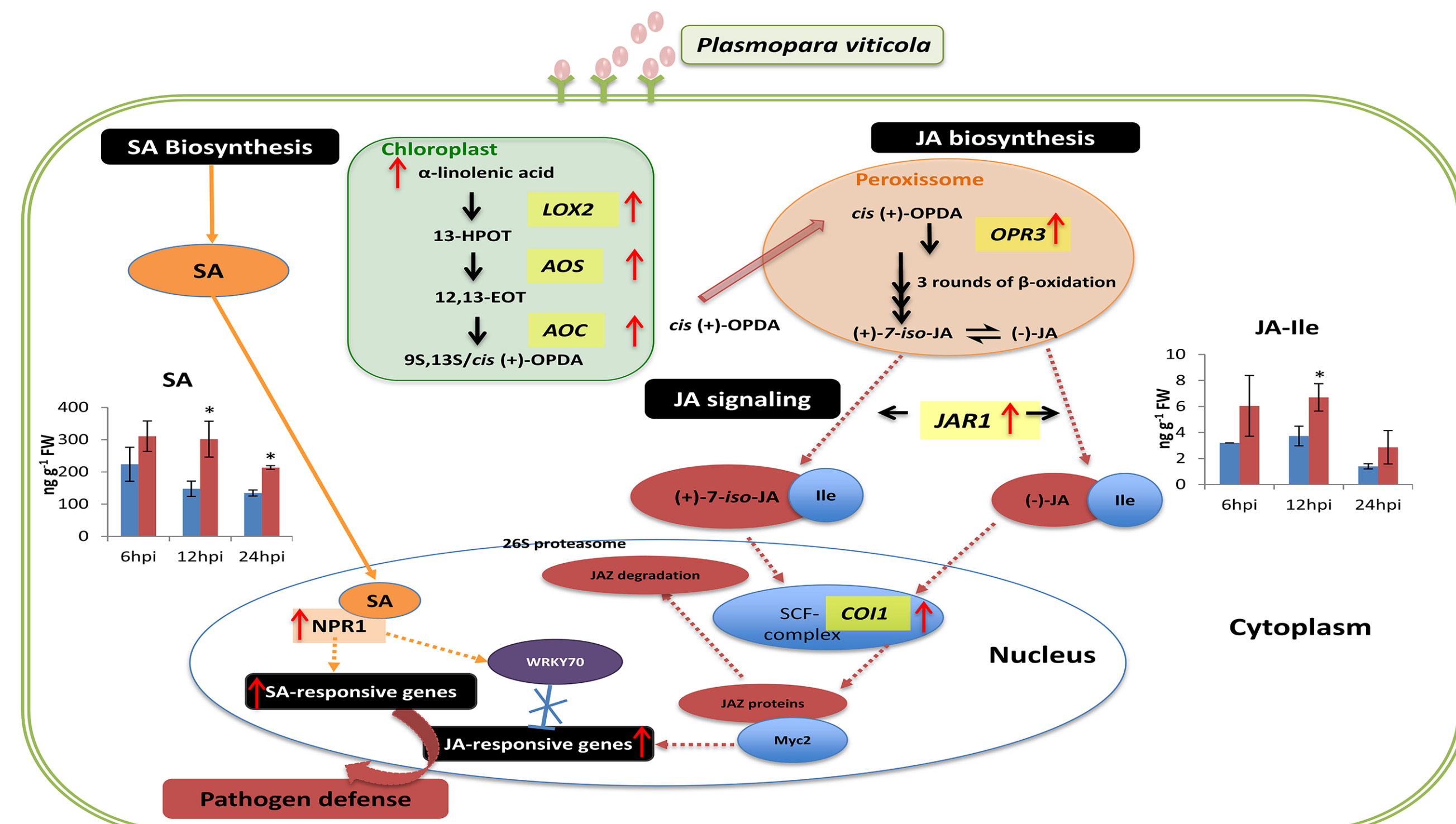


Fig. 1- Salicylic acid (SA) and jasmonic acid (JA) signaling pathways. The graphs represents the SA and JA-Ile concentrations in *Vitis vinifera* control (blue) and inoculated (red) at 6, 12 and 24 hours post-infection with *Plasmopara viticola*.

Objectives

Characterization of the fatty acids profile of two grapevine species with different resistance background towards fungal diseases (particularly downy mildew) after elicitation with both SA and JA.

Results

Fatty acid composition may vary environmental conditions, particularly after pathogen attack.

We have previously shown that major alterations occur in grapevine after *Plasmopara viticola* inoculation, namely on C18:3 content.

Here, we have analysed the fatty acid composition by Gas Chromatography of two *Vitis* species, *Vitis Riparia* and *Vitis vinifera* cv Pinot noir (resistant and susceptible to downy mildew) after elicitation with both SA and JA.

Vitis vinifera cv Pinot noir

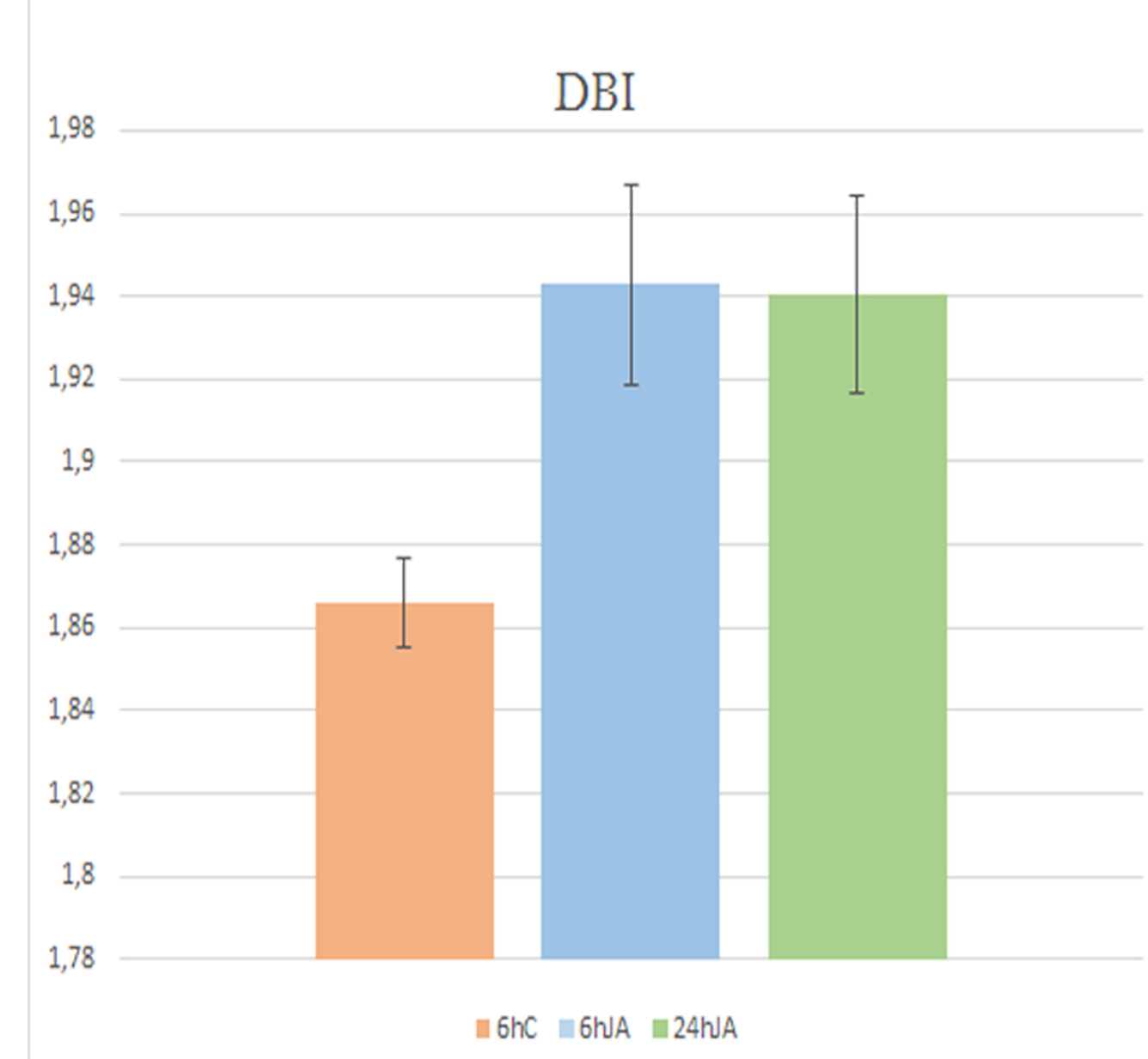
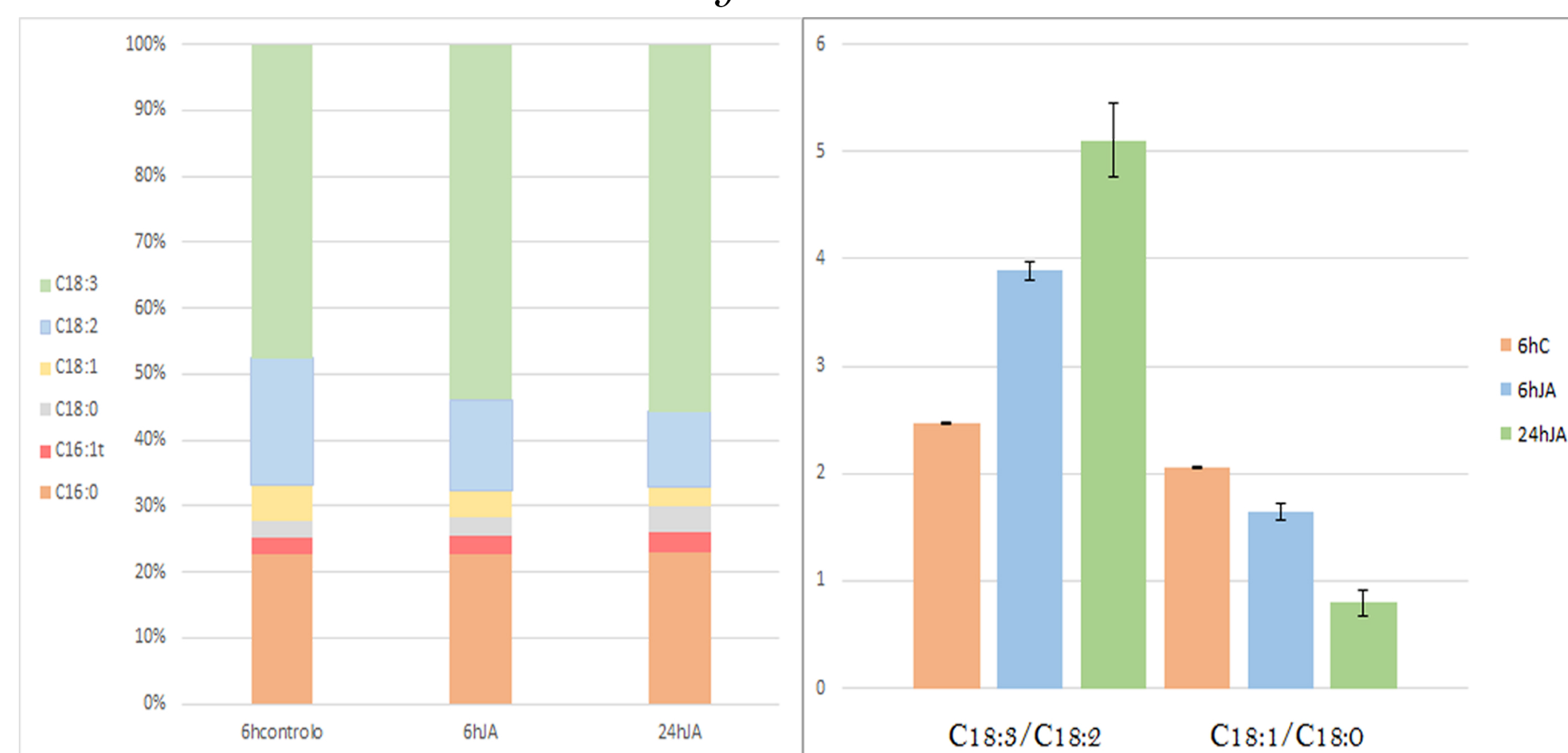


Fig. 4 - Total leaf lipid composition in *Vitis vinifera* cv Pinot noir: a) Fatty acids profile; b) C18:3/C18:2 and C18:1/C18:0 ratios; c) Double bound index.

Future Perspectives

Use several *Vitis* genotypes (species and cultivars) to access if lipid composition may be used as a biomarker to distinguish resistance from susceptibility.

Bibliography

- (1) Figueiredo, A., Monteiro, F., Sebastiana, M., 2015. First clues on a jasmonic acid role in grapevine resistance against the biotrophic fungus *Plasmopara viticola*. Eur. J. Plant Pathol. 142, 645–652. doi:10.1007/s10658-015-0634-7
- (2) Guerreiro, A., Figueiredo, J., Sousa Silva, M., Figueiredo, A., 2016. Linking Jasmonic Acid to Grapevine Resistance against the Biotrophic Oomycete *Plasmopara viticola*. Front. Plant Sci. 7. doi:10.3389/fpls.2016.00565
- (3) Figueiredo A, Martins J, Sebastiana M, Guerreiro A, Silva A, Matos AR, Monteiro F, Pais MS, Roepstorff P, Coelho AV, 2017, Specific adjustments in grapevine leaf proteome discriminating resistant and susceptible grapevine genotypes to *Plasmopara viticola*. Journal of Proteomics, 152: 48–57

Phenotypic characterization of *Chlamydomonas reinhardtii* mutants that perform a deficient CO₂ assimilation

Miguel C. Gaspar^{1,2}, Ana Rita Matos², Maria Glória Esquivel¹

¹Linking Landscape, Environment, Agriculture and Food (LEAF)

Instituto Superior de Agronomia (ISA) Universidade de Lisboa, Portugal, gesquivel@isa.utl.pt

²BioISI, Biosystems and Integrative Sciences Institute, Dep. de Biologia Vegetal, Universidade de Lisboa, Portugal, armatos@fc.ul.pt

Introduction

Ribulose-1,5-bisphosphate carboxylase/oxygenase (rubisco) is an enzyme responsible for atmospheric CO₂ assimilation. In this study we are performing a phenotypic characterization of the I58W3 *Chlamydomonas reinhardtii* mutant that has three Trp residues close to the entrance of the central channel of the rubisco enzyme. It was previously found that this mutation caused a deficient CO₂ assimilation due to a decrease in the carboxylation rate of rubisco compared with the control strain [1]. *C. reinhardtii* is able to accumulate significant amounts of storage lipids, particularly under nitrogen deprivation. In this study we have been looking for phenotypic alterations of this I58W3 mutated cells that are detected by changes in terms of growth, pigment levels and protein, lipid concentration and composition.

Objectives: Evaluate the impacts of the rubisco mutation in gas exchange parameters (photosynthesis and respiration) and lipid and photosynthetic pigments contents and fatty acids composition.

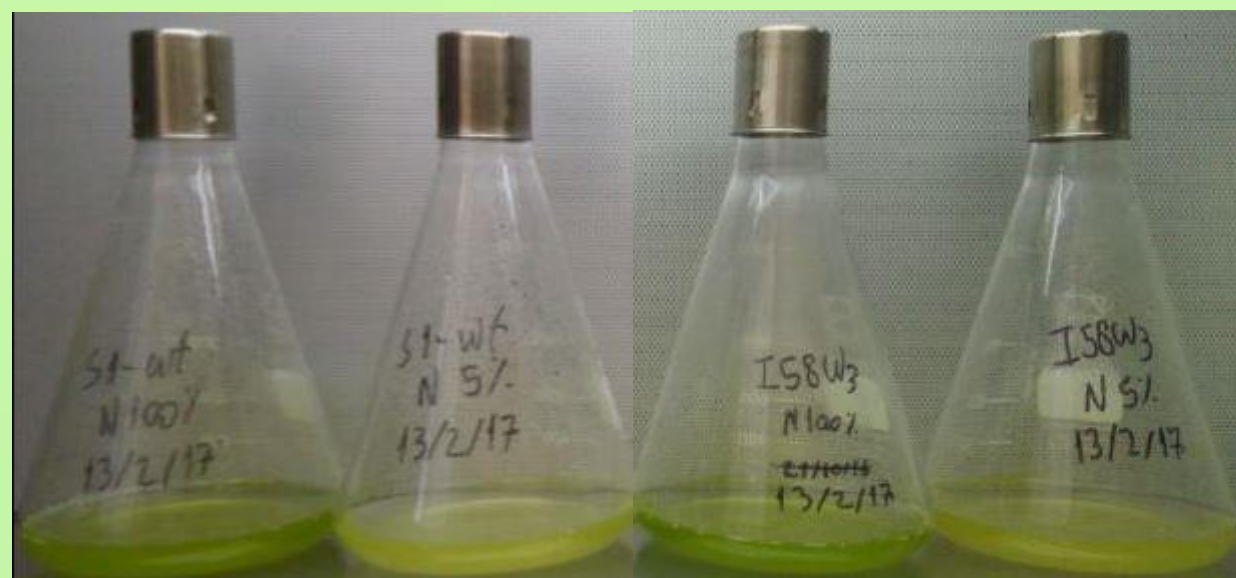


Fig. 1 - Liquid cultures of *Chlamydomonas reinhardtii*. Culture appearance under different growth conditions. Control strain (S1-Wt) and mutant strain (I58W3) in normal TAP medium (100% N) and with deficient nitrogen regime (5% N).

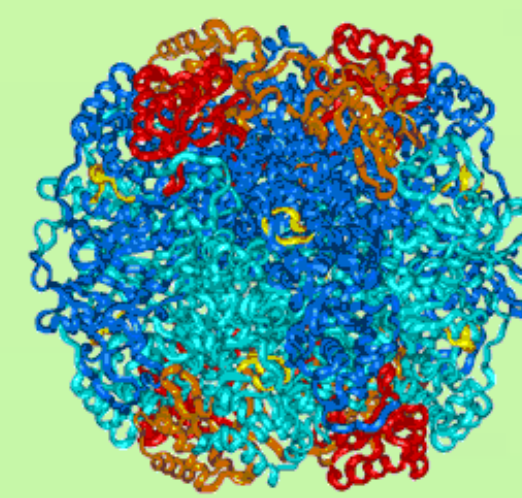


Figure 2 - Crystal structure of Rubisco. The 8 large subunits are colored blue and the 8 small subunits are colored red and orange. The I58W3 mutation is situated in the small-subunit that defines the narrowest diameter of the central solvent channel of the holoenzyme.

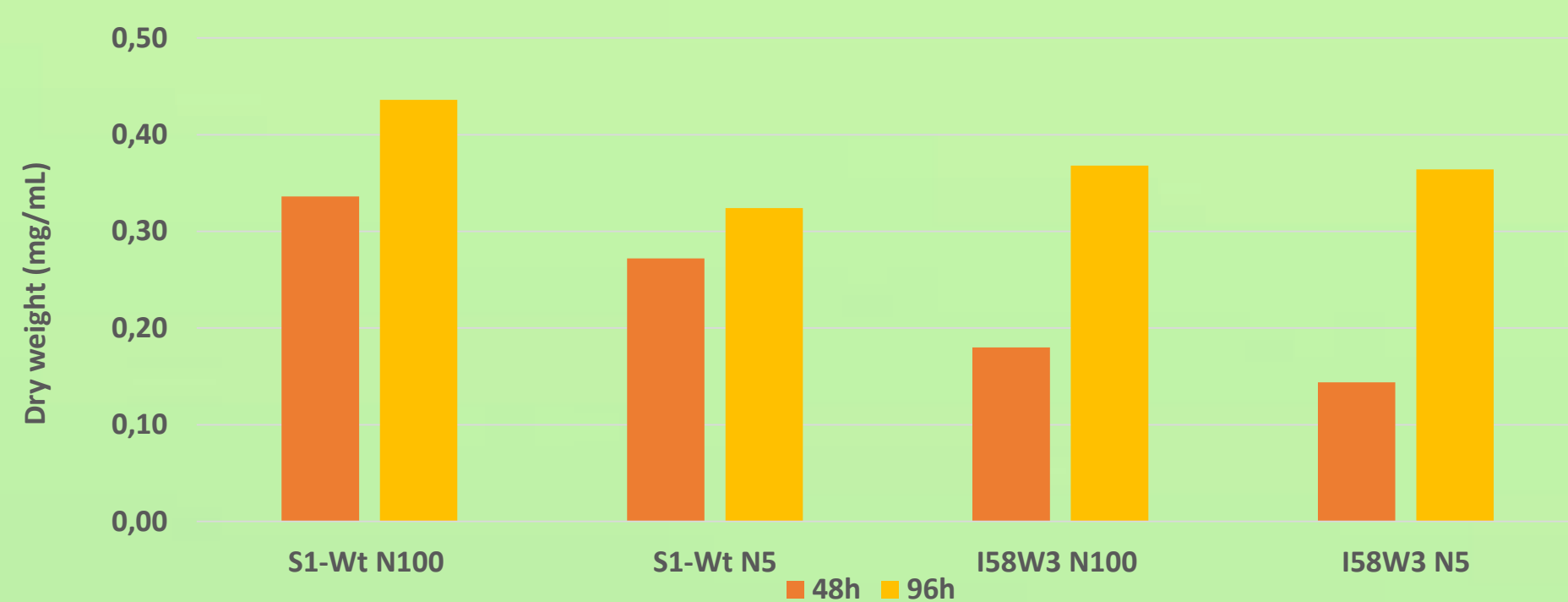


Fig. 3. Cultures dry weight (DW) at 48 and 96 hours. Control strain (S1-Wt) and mutant strain (I58W3) in normal TAP medium (100% N) and with deficient nitrogen regime (5% N).

Materials and methods: Cells were grown under continuous low light in culture containing acetate (TAP medium). Chlorophyll contents were analysed by spectrophotometry and measured throughout 5 days. Protein levels were measured by Lowry protein assay. Oxygen evolution rates were measured using a Clark-type O₂ electrode. Fatty acid compositions in both N-depletion and repletion were monitored by gas chromatography. Cell staining with Nile Red and further analysis by spectrophotometry allowed for a comparison between storage lipid content in N-depleted and repleted cells [2].

Results

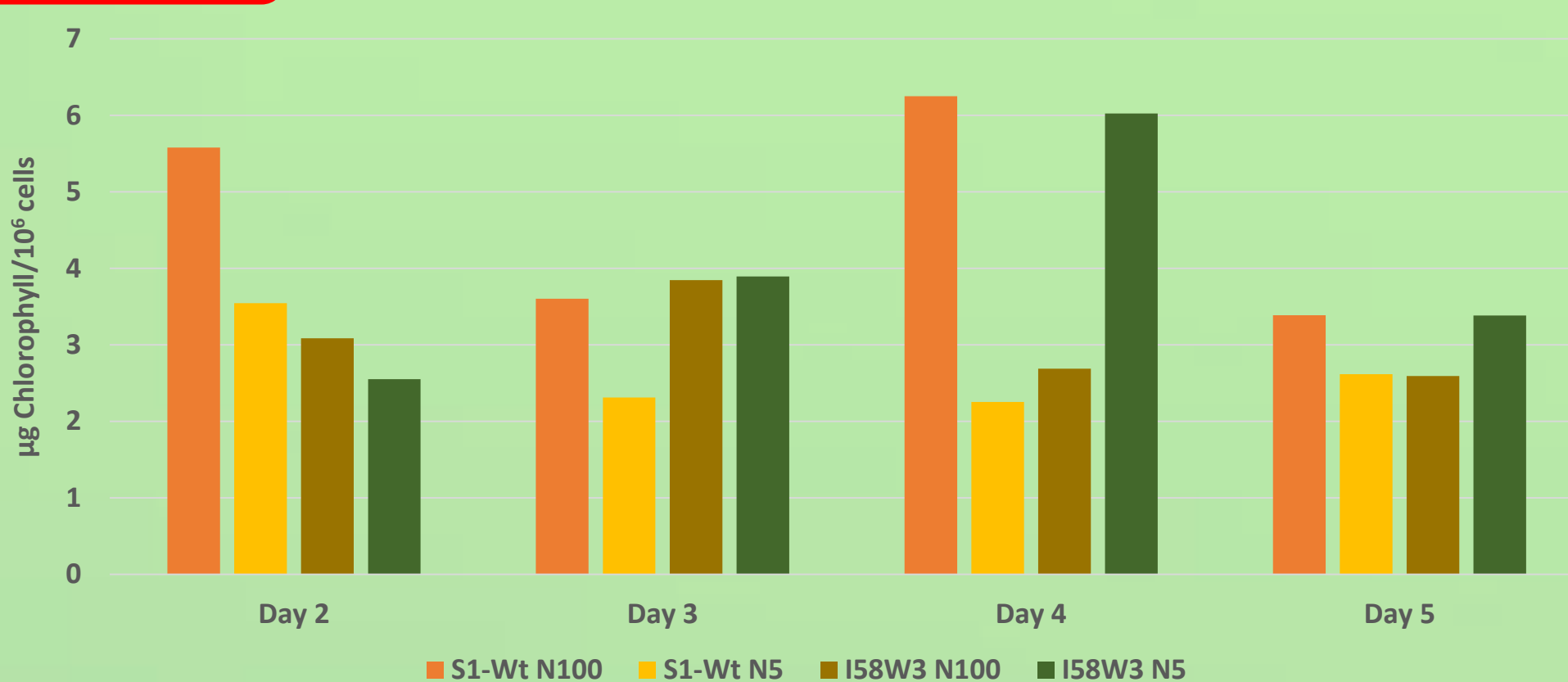


Figure 4 - Evolution of chlorophyll content per million cells in cultures of S1-Wt and I58W3 in normal TAP medium (100% N) and with deficient nitrogen regime (5% N).



Figure 7 - Fatty acid composition of S1-Wt and I58W3 in normal TAP medium (100% N) and with deficient nitrogen regime (5% N).

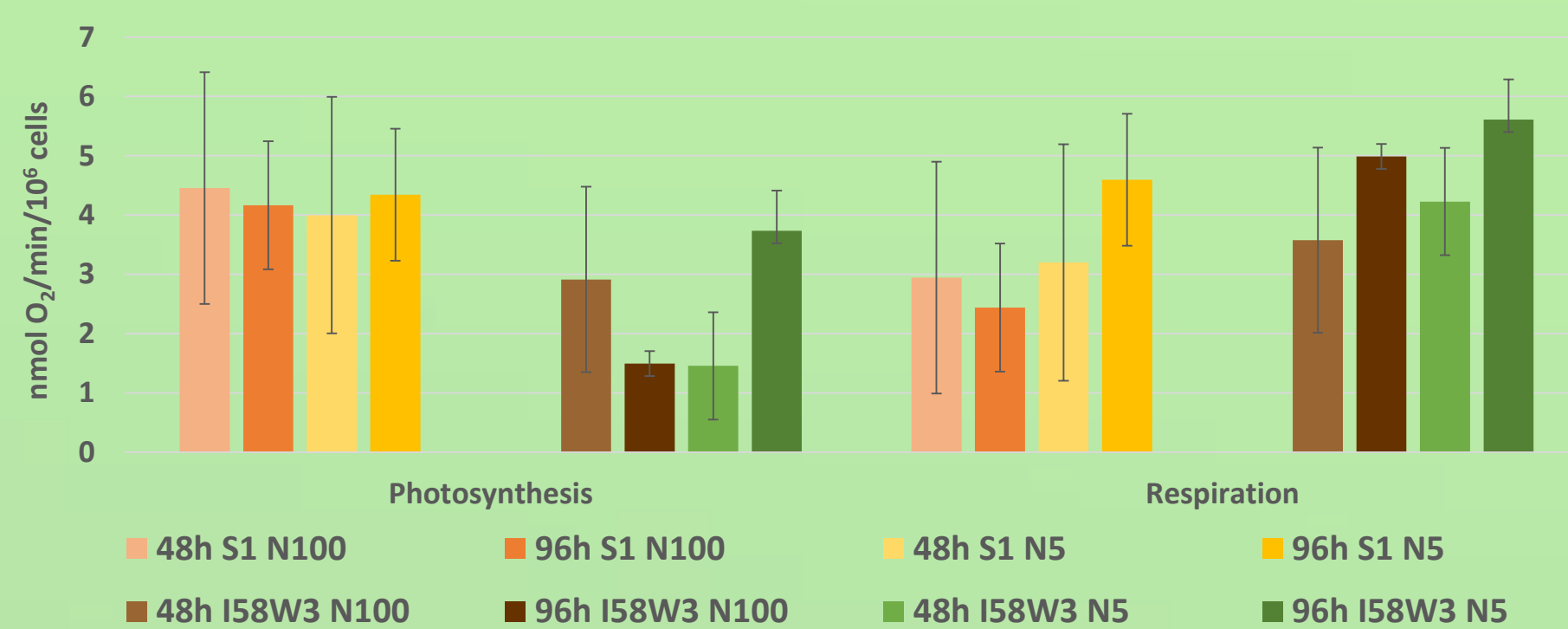


Figure 5 - Photosynthetic (left) and respiratory (right) rate at 48h and 96h of *C. reinhardtii* control strain (S1-Wt) and mutant strain (I58W3) in normal TAP medium (100% N) and with deficient nitrogen regime (5% N).

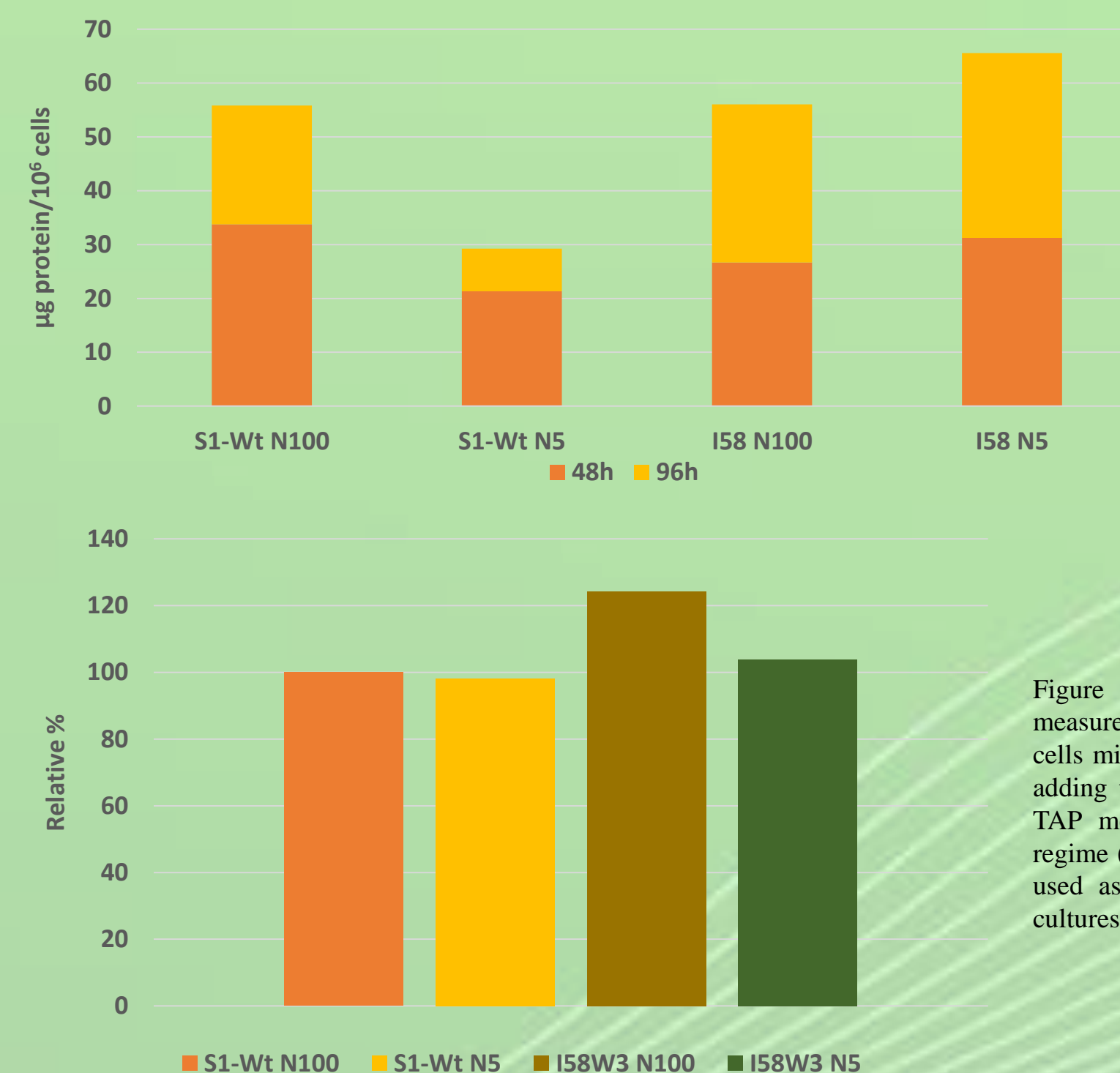


Figure 6 - Protein levels per million cells at 48h and 96h. Control strain (S1-Wt) and mutant strain (I58W3) in normal TAP medium (100% N) and with deficient nitrogen regime (5% N).

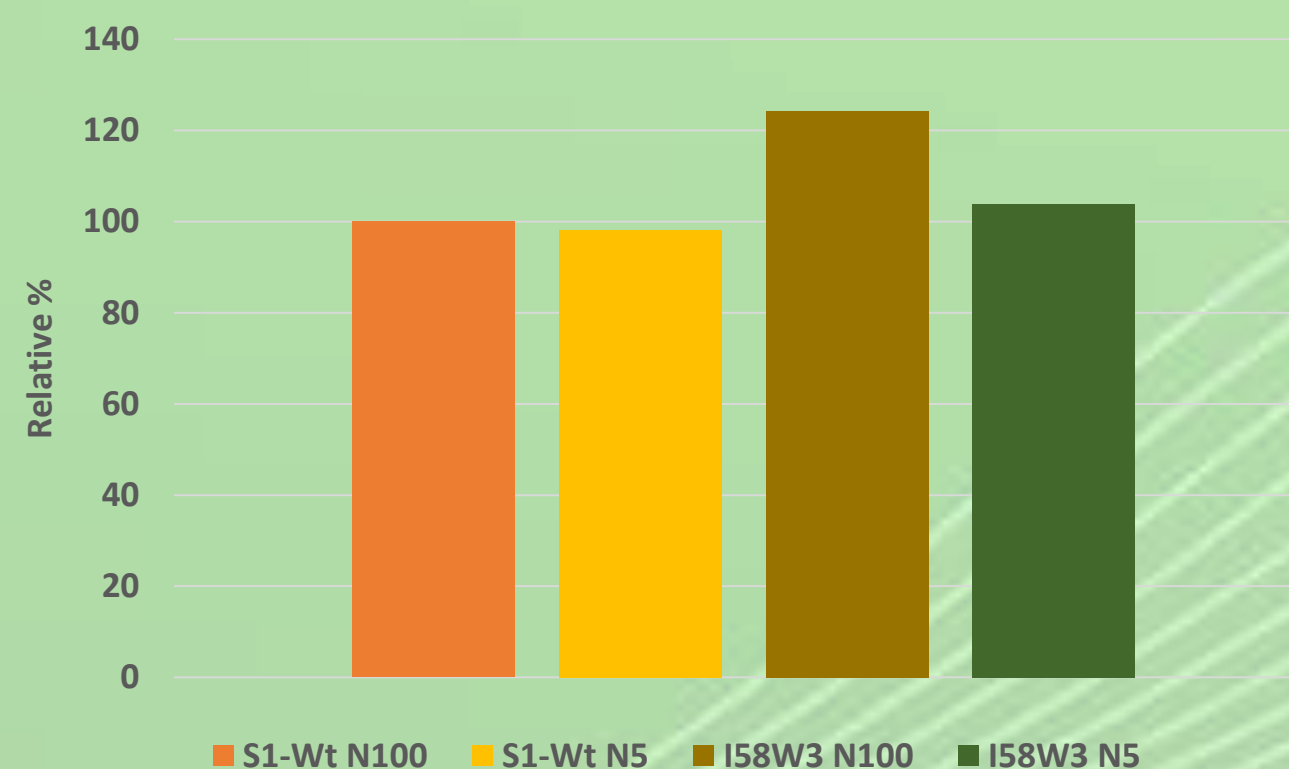


Figure 8 - Relative lipid levels in *C. reinhardtii* measured by fluorescence intensity of Nile red stained cells minus fluorescence intensity of chlorophyll (before adding the Nile red dye). S1-Wt and I58W3 in normal TAP medium (100% N) and with deficient nitrogen regime (5% N). The S1-Wt 100% N measurements were used as the baseline for comparison with other cells cultures.

Conclusions: In mixotrophic conditions Rubisco mutants had biomass below the control (fig.3) as well as lower chlorophyll content (fig.4). Photosynthetic rates were lower in mutant cells, but respiratory rates were higher (fig.5) indicating that the rubisco mutation has an impact in O₂ management by the cell. Protein levels show that wild-type control cells are more affected by N-deprivation than I58W3 cells (fig.6). Fatty acid analysis indicate differences between S1-Wt and I58W under N repletion, although N-depletion-induced changes are globally similar for both lines (fig.7). Storage lipid content in mutant cells was higher than in control (fig.8). The lower photosynthetic CO₂ assimilation, caused by the mutation appears to adjust the metabolism towards the accumulation of storage lipids. From the data gathered it appears that I58W3 cells have an altered photosynthetic performance, related to the closure of the solvent channel of rubisco. These mutants are however capable of accumulating increased amounts of storage lipids, which can be an advantage for biotechnological purposes.

Acknowledgments

The authors would like to thank the “Fundação para a Ciência e Tecnologia (FCT)”. Gonçalo Laureano for gas chromatography assistance. Eduardo Feijão for helping in cell culture maintenance and storage. João D. Arrabaça for the help with the oxygen electrode. Manuela Lucas and Maria João Fernandes for technical assistance.

References

- [1] Esquivel, M.G., Genkov, T., Nogueira, A.S. *et al.* (2013) “Substitutions at the opening of the Rubisco central solvent channel affect holoenzyme stability and CO₂/O₂ specificity but not activation by Rubisco activase” *Photosynth Res* 118: 209.
- [2] Alemán-Nava, G.S., Cuellar-Bermudez S.P *et al.* (2016) “How to use Nile Red, a selective fluorescent stain for microalgal neutral lipids” *J. Microbiol Methods* 128:74-9.

Quantification and identification of allele specific proteins for polyploid non-model crops:

Proof of principle for 3 banana (*Musa* spp.) genotypes/phenotypes.

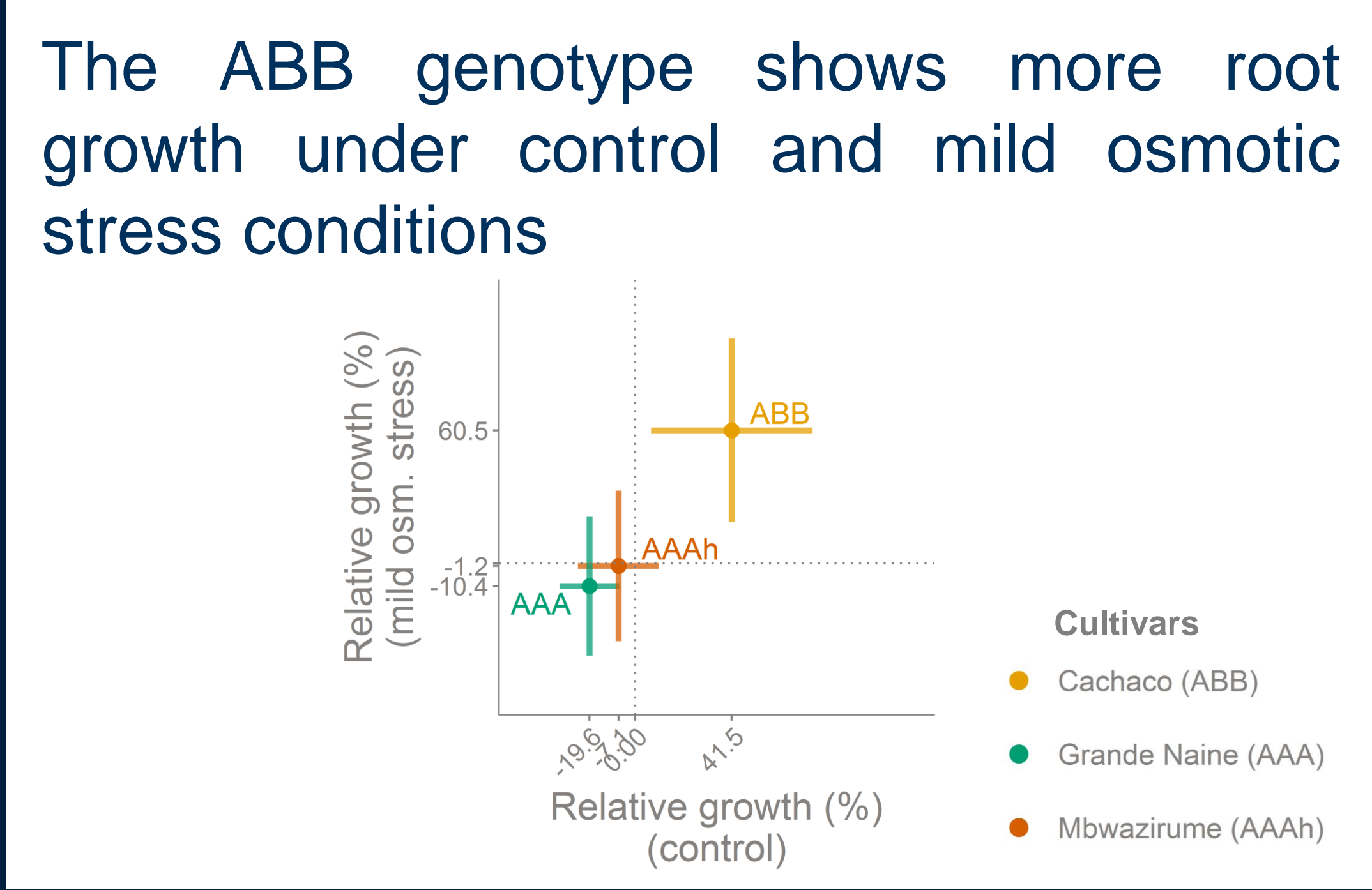


Jelle van Wesemael¹, Yann Hueber², Ewaut Kissel¹, Nadia Campos¹, Rony Swennen^{1,3,4}, Sebastien Carpentier^{1,5}

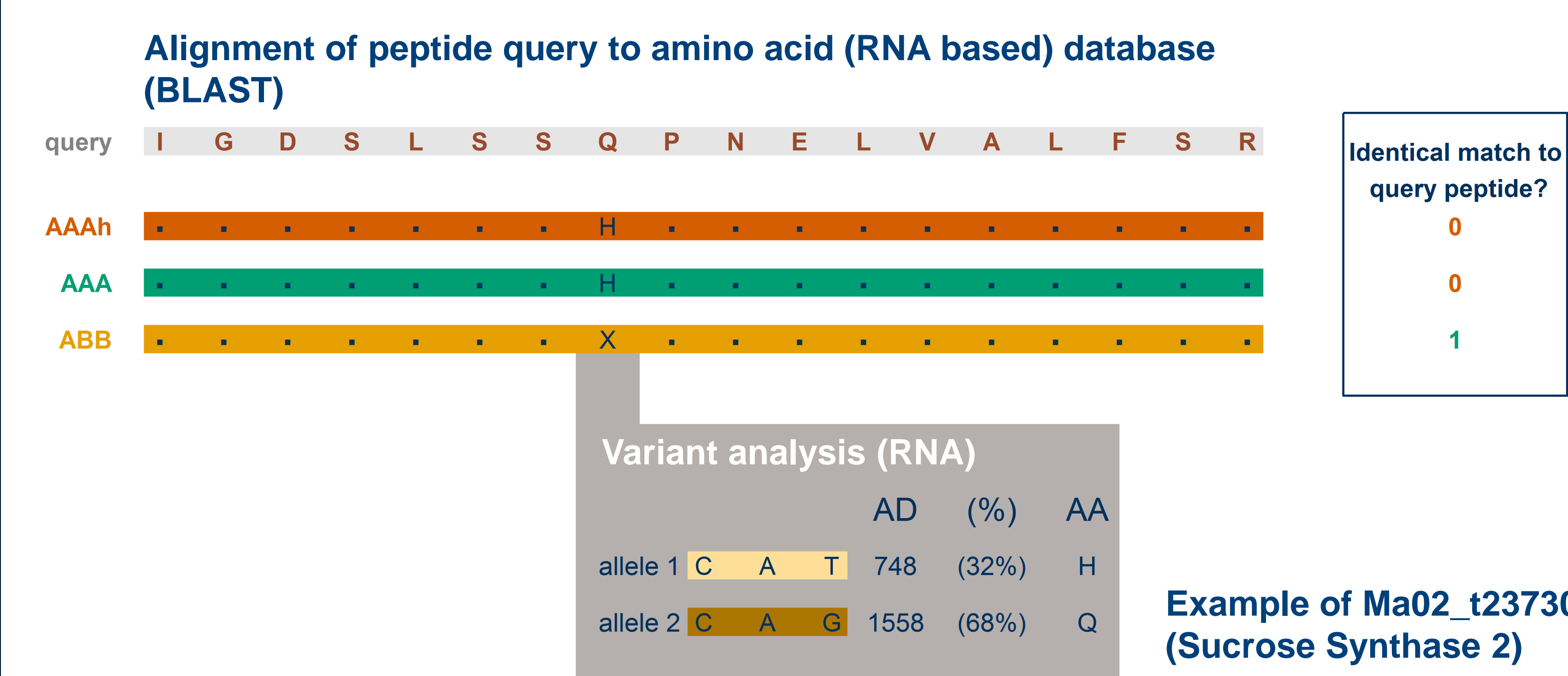
Banana is the most important fruit crop in the world.
Cultivars are triploid, hybrid crosses of *M. acuminata* (A) and *M. balbisiana* (B)
Vulnerable to drought

Polyploidy results in a plethora of genomic, transcriptomic, and proteomic products controlling the phenotype.
Allelic variants are of interest for climate smart agriculture : flexibility towards the environment

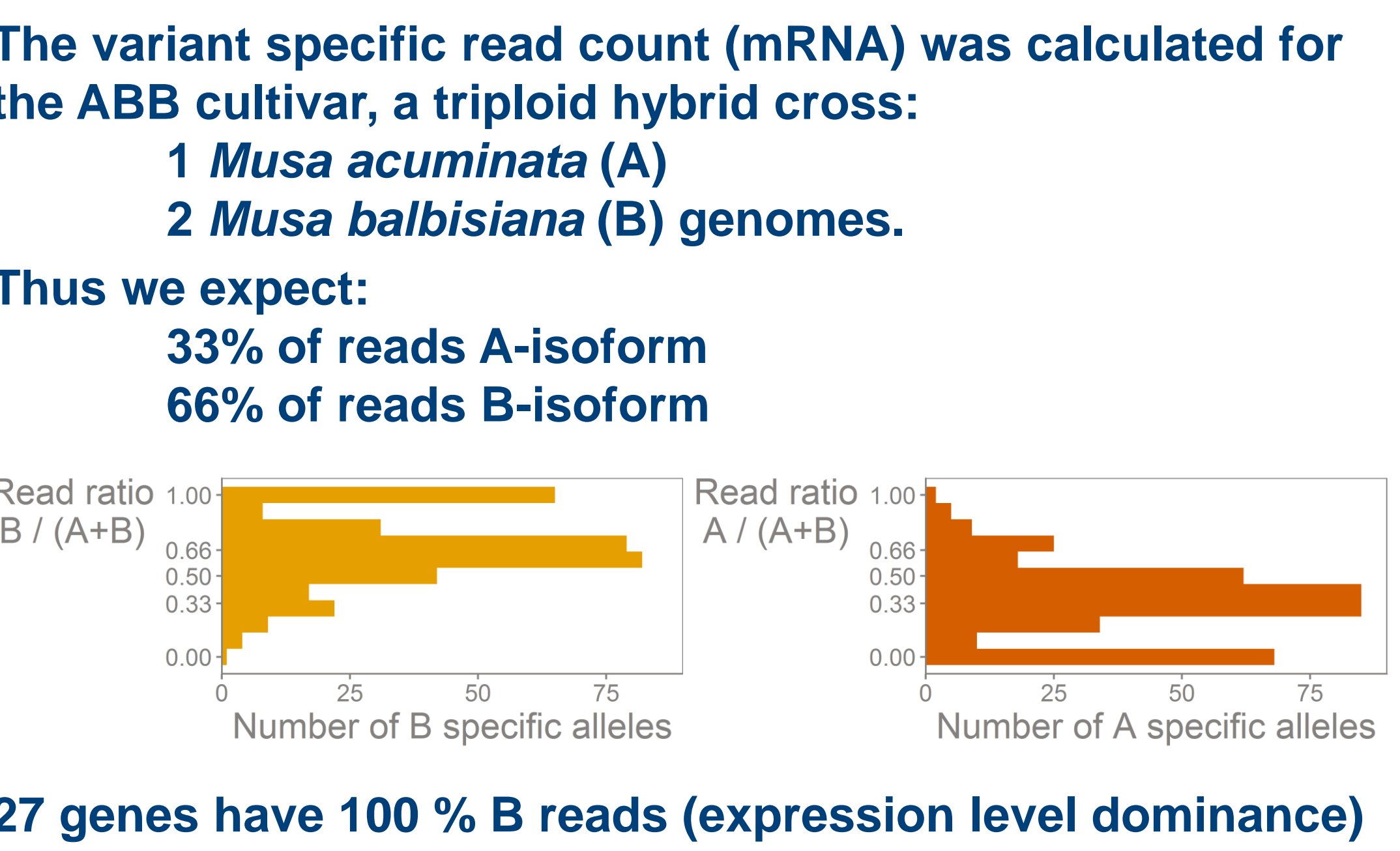
Our goal: Mining the *Musa* biodiversity for drought tolerance:
Select allele specific proteins linked to the observed phenotypic differences among three contrasting genotypes by integration of transcriptomics and proteomics.



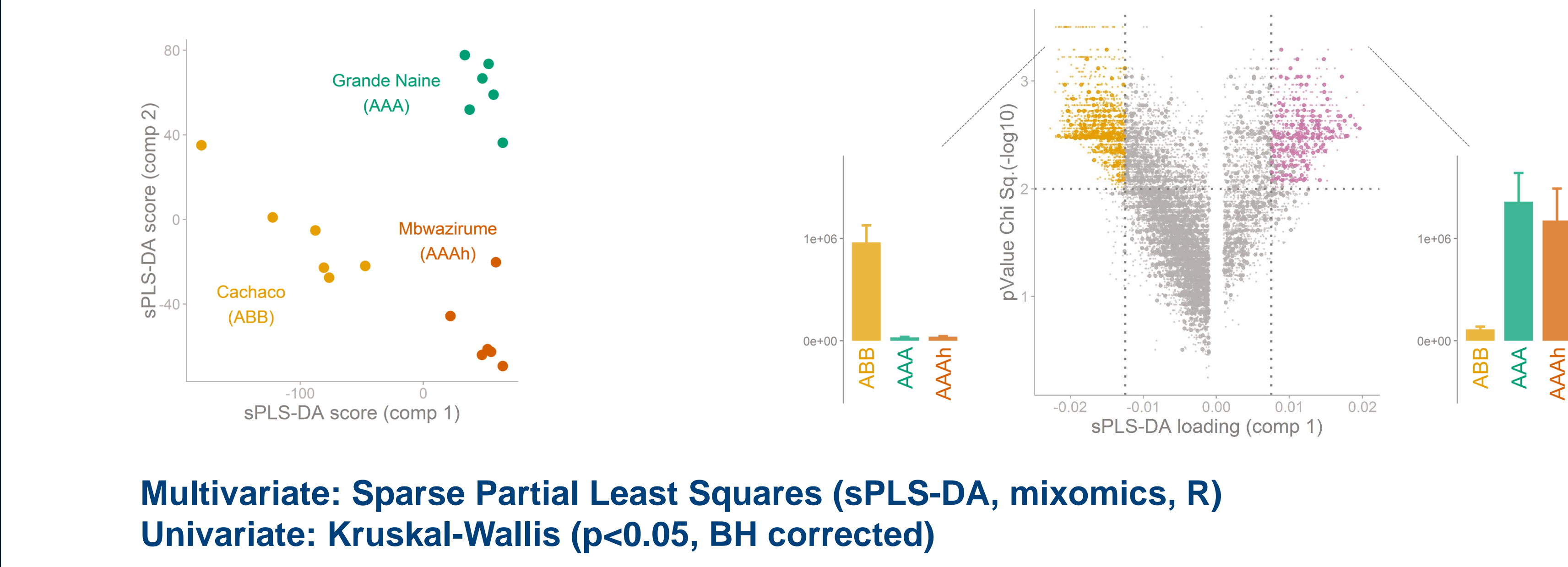
260 amino acid polymorphisms (SAAP) are identified by alignment of the peptide sequences to each cultivar specific database



Some polymorphisms in the drought tolerant phenotype (ABB) display homeolog expression bias



130 additional allele specific genes are selected through combination of univariate and multivariate statistics based on the peptide abundance



Cultivar specific genes are involved in general osmotic stress responses

Drought tolerant phenotype (ABB) invests in root growth with minimal setback under osmotic stress

The functions of identified alleles are enriched in general osmotic stress responses

GO-term	Description	p (Fisher)
GO:0006096	Glycolytic process	0.003
GO:0006457	Protein folding	0.015
GO:0006950	Response to stress	0.018

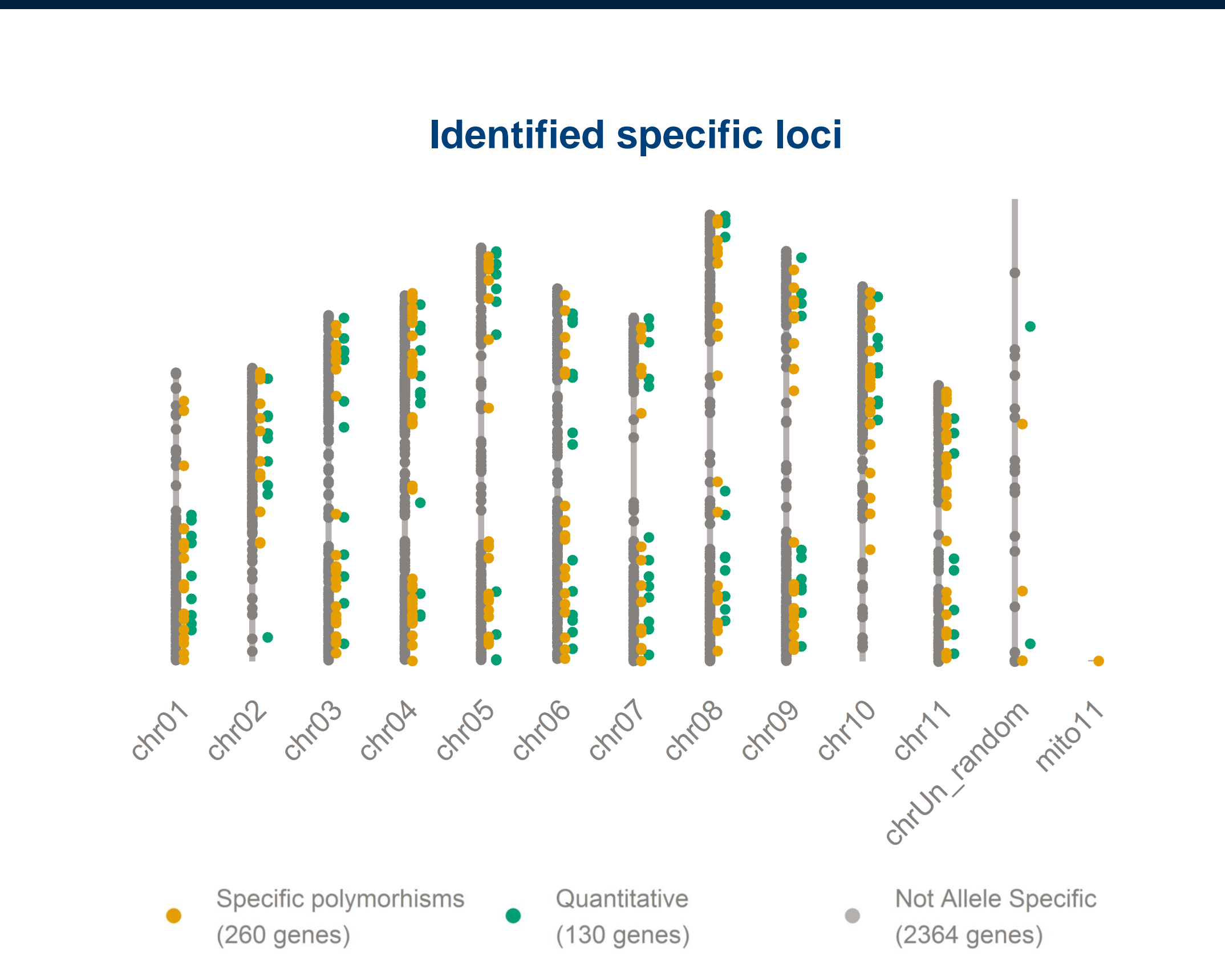
Mining the *Musa* genome by integration of transcriptomics with proteomics identifies 390 genes with allele specificity linked to the differential phenotype

The phenotype is controlled by different protein isoform(s) / transcript(s) / gene copy(s). This integrative workflow allows to unravel genetic diversity in polyploid (non-) model crops at the gene variant level.

We identified 2754 proteins
260 identified SAAP
130 with differential peptide abundance

Some of the allele specific transcript levels show deviations from what is expected based on the genomic constitution
27 identified polymorphisms show 100% biased expression levels.

Specific alleles are enriched in genes related to general osmotic stress responses, respiration, ROS scavenging, and HSP.



Analysis of the lipid content and photosynthesis in *Glycine max* under drought stress

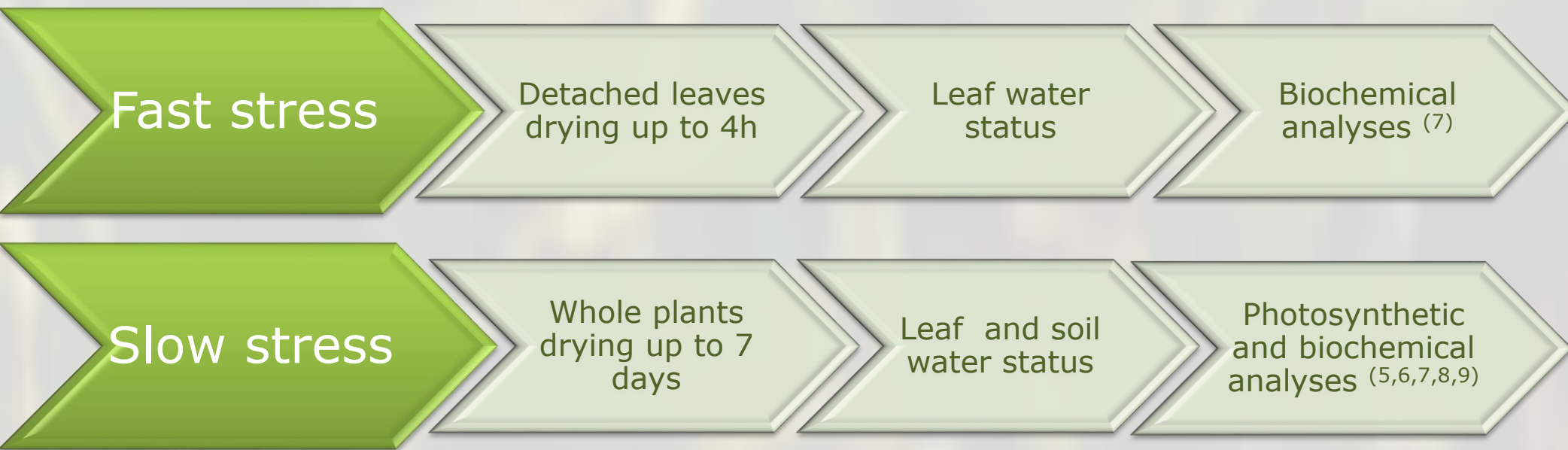


Daniela Ferreira¹, Bernardo Duarte², Isabel Caçador², Carla Gameiro², Andrei Utkin³ Andreia Figueiredo¹, Ana Rita Matos^{1*}
¹ Biosystems & Integrative Sciences Institute (BioISI), FCUL, Portugal; ²Marine and Environmental Sciences Centre (MARE), FCUL, Portugal; ³INOV—INESC Inovation, Portugal
* Corresponding author: armatos@fc.ul.pt

INTRODUCTION

United Nations claim that by 2030 half of the world's population will be living in desertified areas (1). Understanding how crops respond to water stress is crucial to maintain production yields. Cell membranes are major targets of drought and changes in their lipid composition affect photosynthesis and growth (2,3). The major thylakoid lipids monogalactosyldiacylglycerol (MGDG) and digalactosyldiacylglycerol (DGDG) are associated to photosystems and therefore are important in photosynthetic processes (4). Soybean, besides being a major crop with worldwide importance, is also a model legume. In this work soybean (*Glycine max* cv. Williams 82) plants were subjected to drought, by fast desiccation of detached leaves and by slow dehydration, by withholding irrigation of potted plants. Leaf glycerolipid composition was studied by thin layer- and gas chromatography (5). Photosynthetic pigments and lipid peroxidation products were analysed spectrophotometrically (6,7). Chlorophyll fluorescence was measured by Pulse Amplitude Modulation- and Laser Induced Chlorophyll Fluorescence (8,9).

METHODS



RESULTS

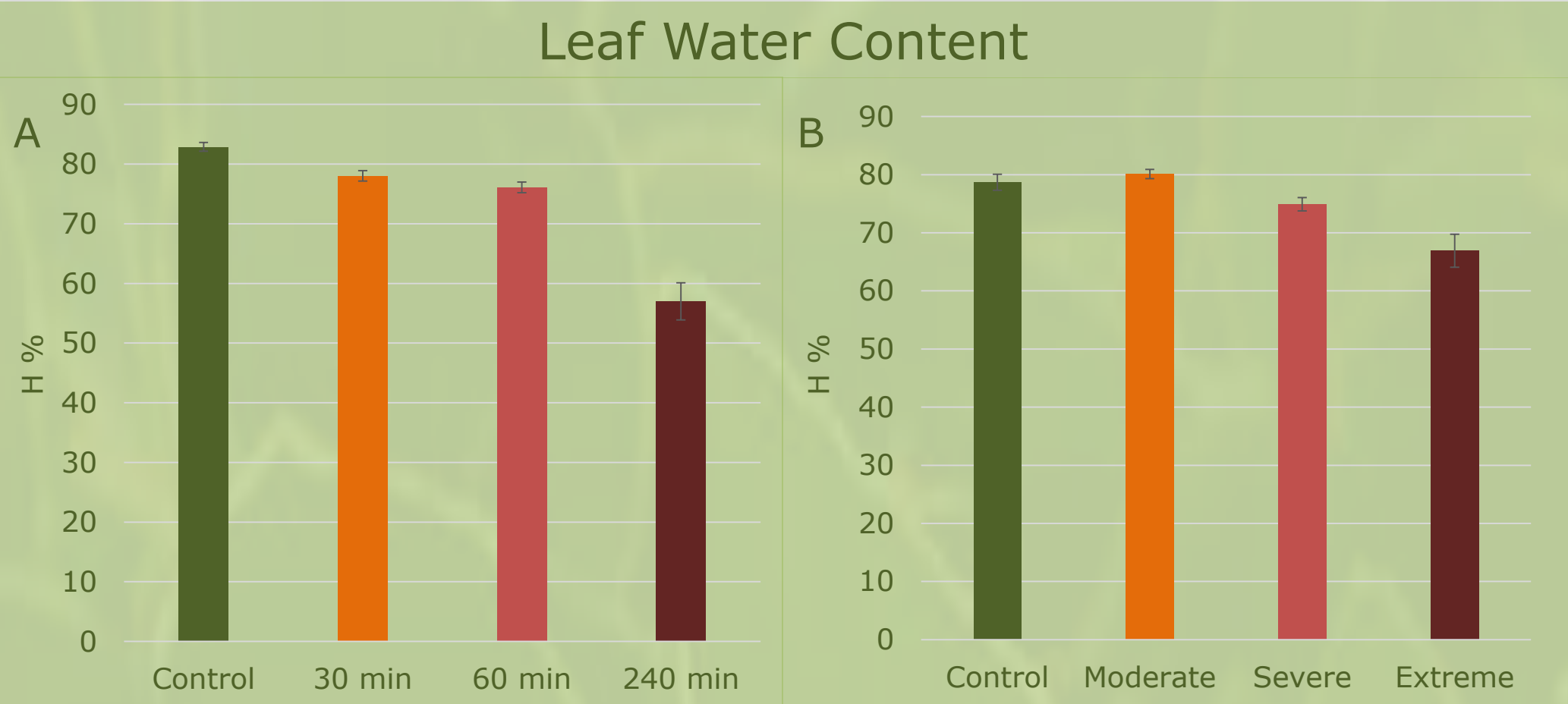


Figure 1: Leaf water content (H %) under fast (A) and slow stress (B)

Decrease in leaf water content

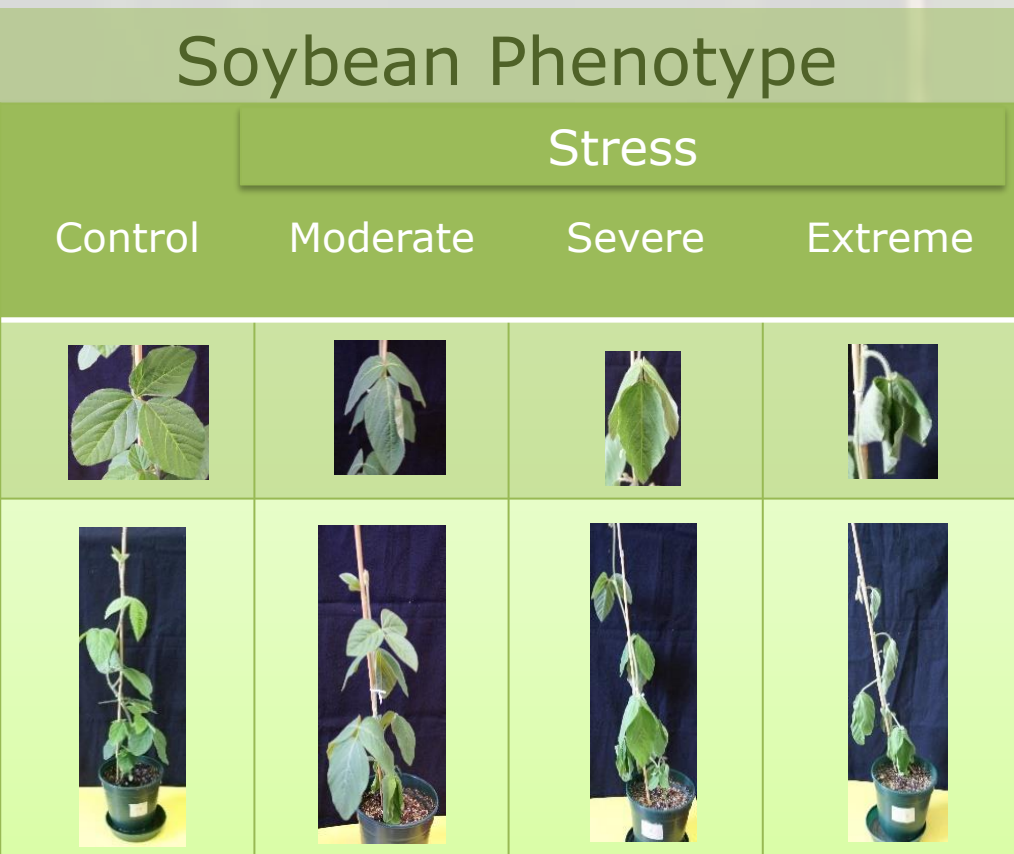


Figure 2: Soybean plants under slow stress

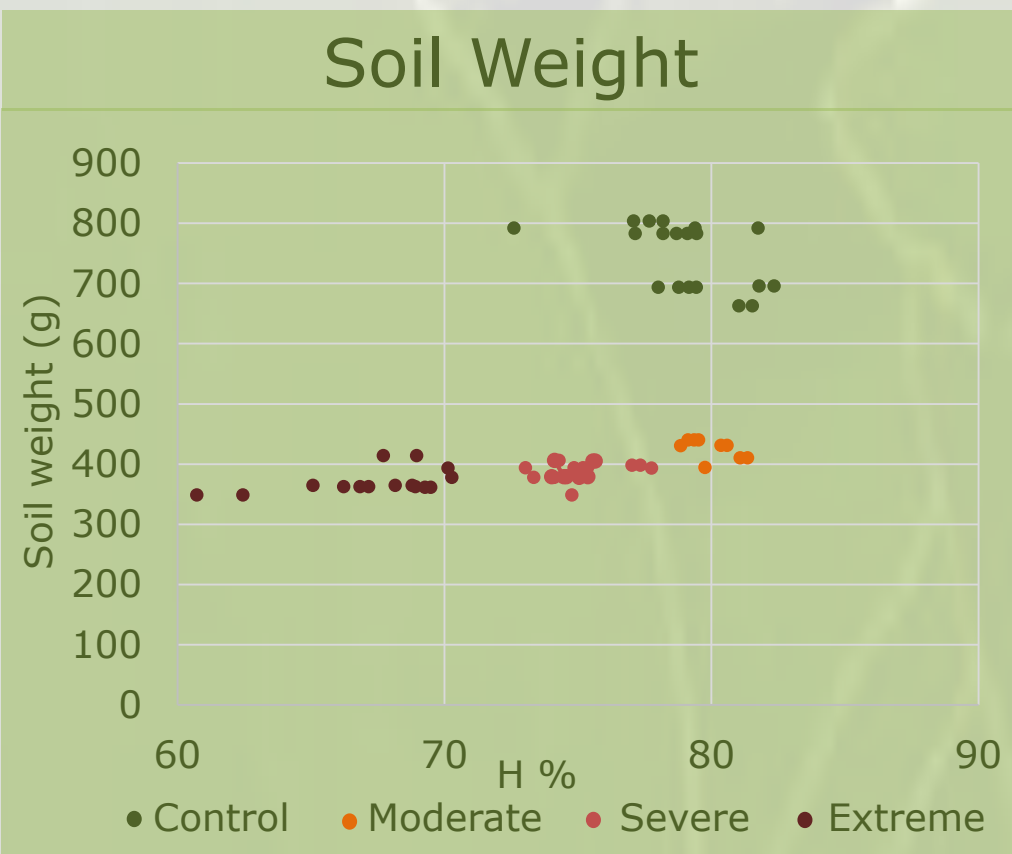


Figure 3: Leaf water content (H %) vs soil weight under slow stress

Control: H% ≥ 78 ; soil weight > 650 g
Moderate Stress: H% ≥ 78 %; soil weight = 394-400 g
Severe Stress: H% = 70-77%, soil weight = 405-366 g
Extreme Stress: H% =60-69; soil weight ≤ 365 g

RESULTS

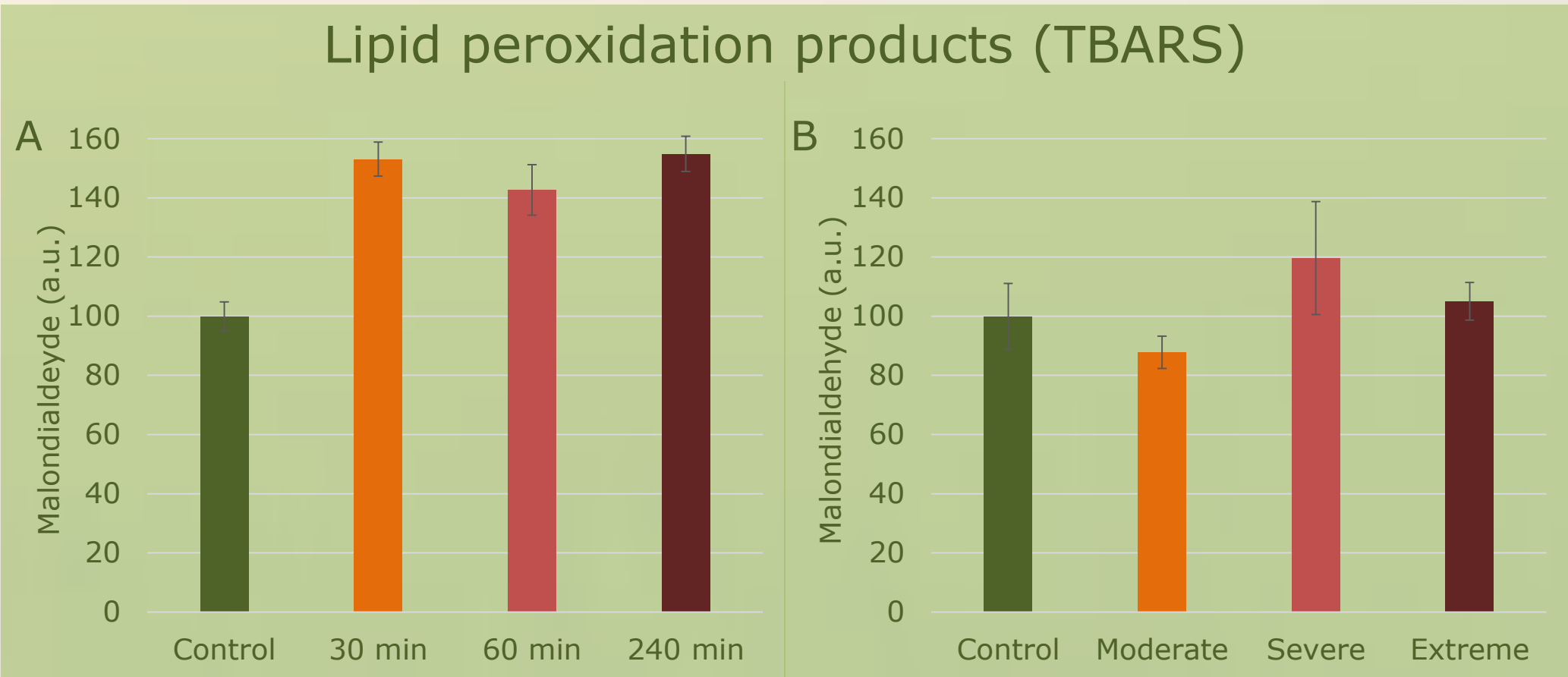


Figure 4: TBARS under fast (A) and slow (B) stresses

Lipid peroxidation products accumulation

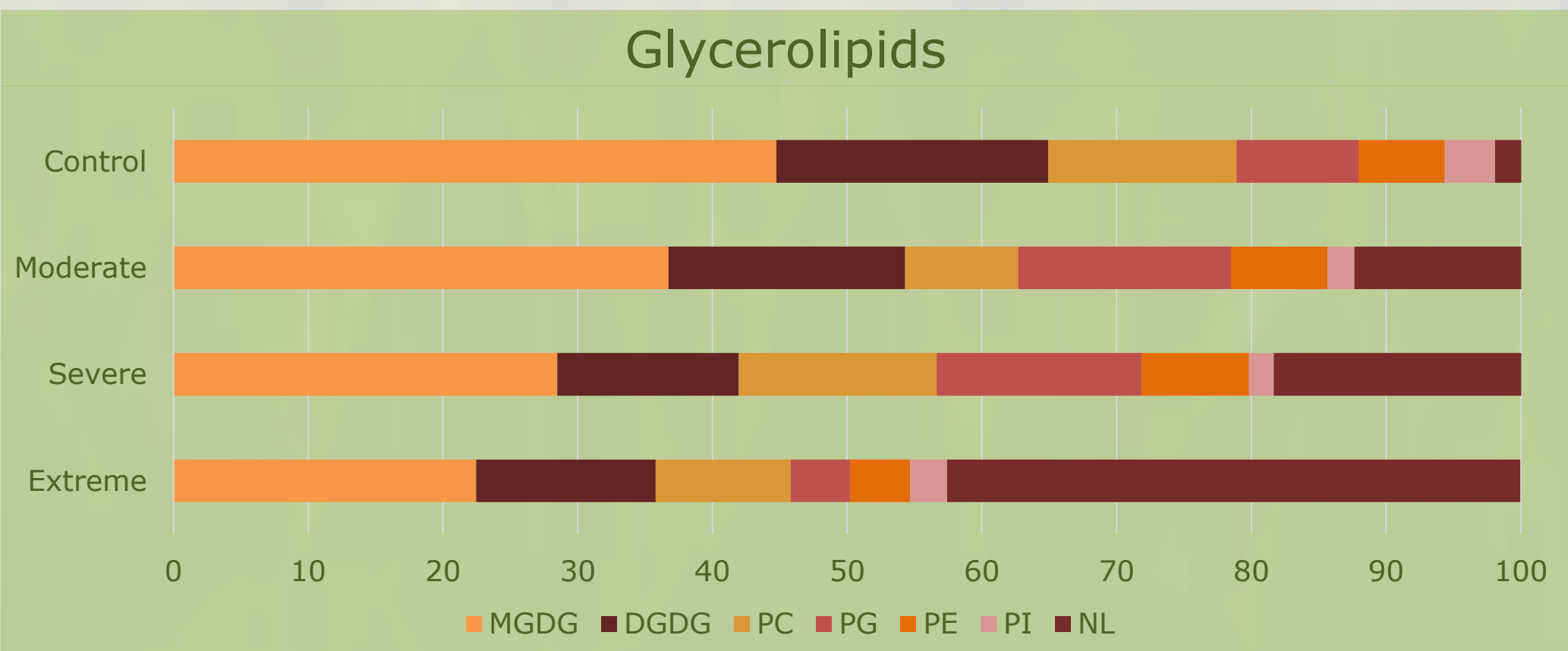


Figure 5: Relative amounts (%) of each leaf lipid class under slow stress. MGDG (monogalactosyldiacylglycerol), DGDG (digalactosyldiacylglycerol), PC (phosphatidylcholine), PG (phosphatidylglycerol), PE (phosphatidylethanolamine), PI (phosphatidylinositol) NL (neutral lipids)

Decrease in plastidial lipids

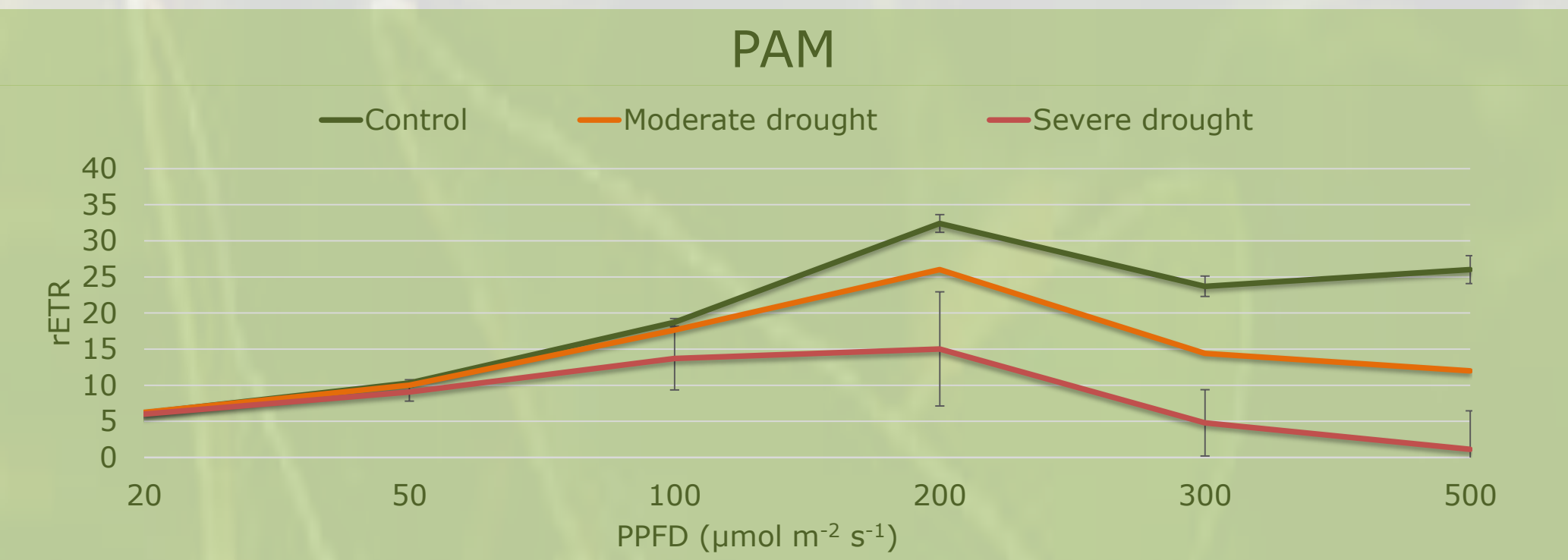


Figure 6: Rapid Light Curves under slow stress (ETR, relative electron transport rate)

Decrease in the electron transport rate

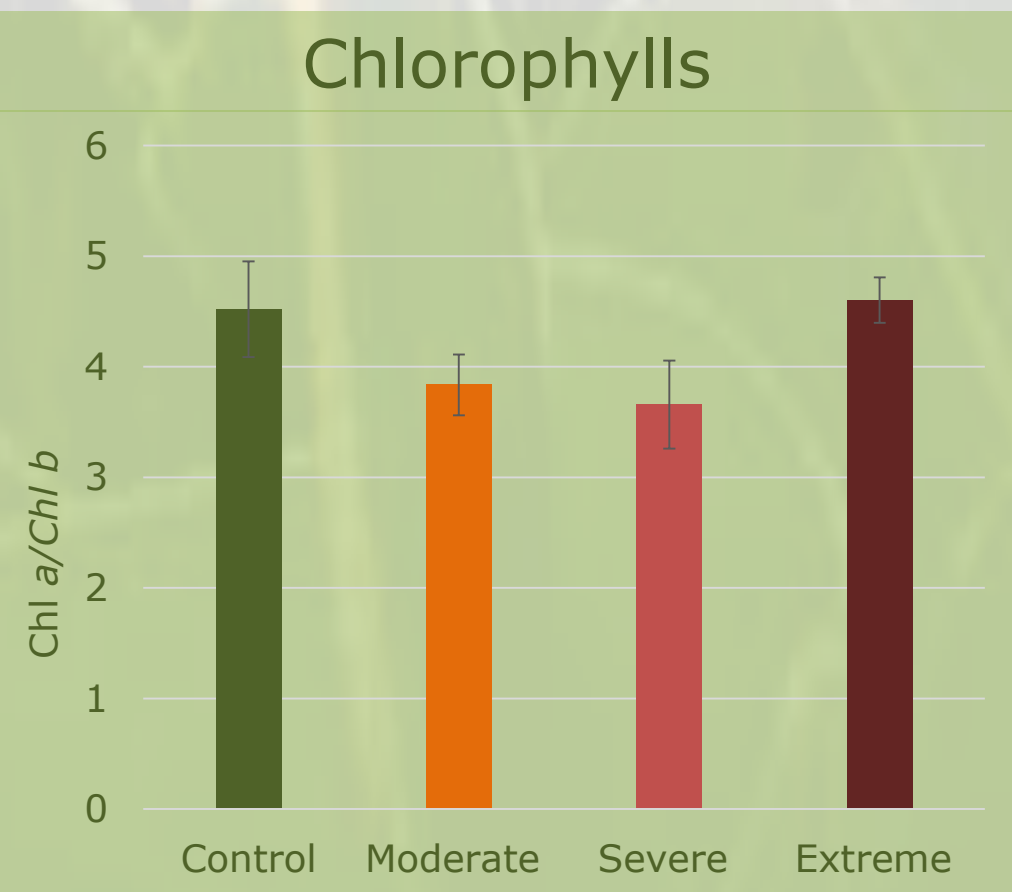


Figure 7: Chl a/Chl b ratios under slow stress

Changes in Chl a / Chl b ratio

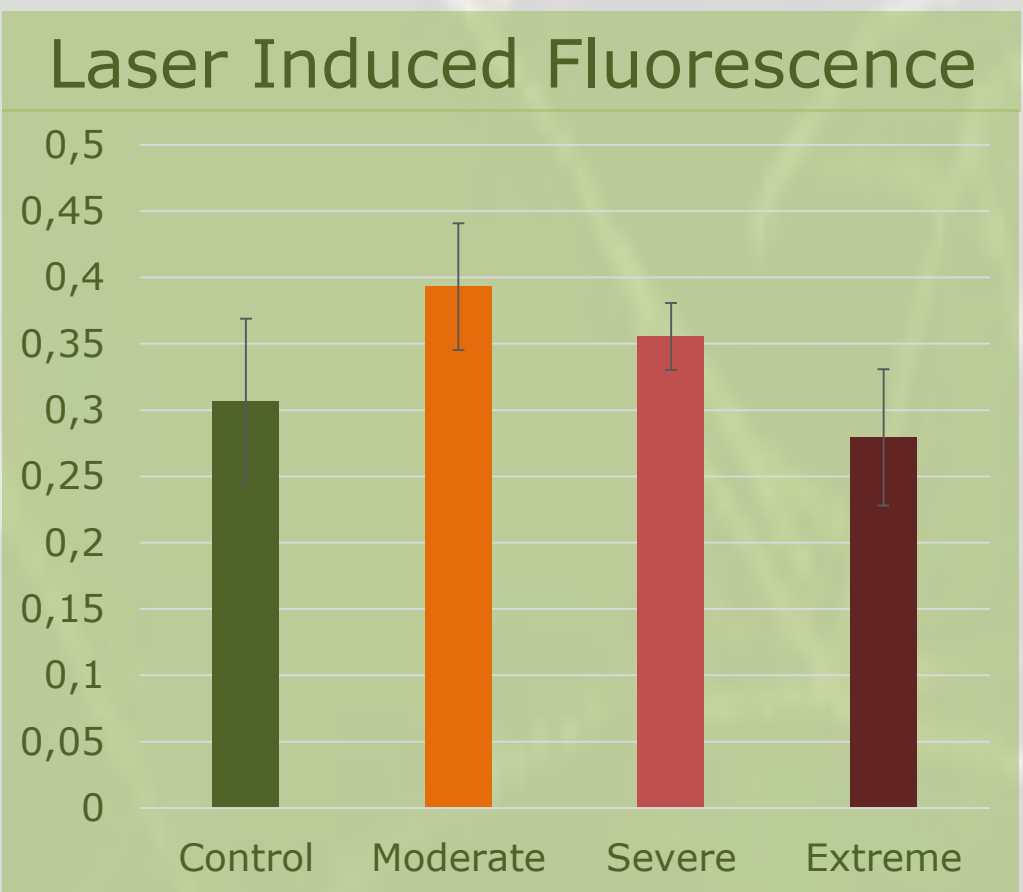


Figure 8: Ratio A₆₈₅/A₇₄₀ under slow stress

Changes in chlorophyll fluorescence ratio A₆₈₅/A₇₄₀

CONCLUSIONS

Lipid peroxidation products accumulate under fast stress

Decreases in the thylakoid lipids MGDG and DGDG and changes in chlorophylls profiles, under slow stress, are related to decreases in photosynthesis

Glycerolipid profiling and photosynthesis analyses of fast-stressed leaves are underway

ACKNOWLEDGEMENTS The authors would like to thank to the "Fundação para a Ciência e Tecnologia (FCT)" for funding the research in the Biosystems and Integrative Sciences Institute (BioISI) throughout the project UID/MULTI/04046/2013 and IF/00819/2015 and the research and the Marine and Environmental Sciences Centre (MARE) throughout the project UID/MAR/04292/2013. The authors also thank to Eduardo Feijão for helpful discussions and Manuela Lucas for technical assistance.

REFERENCES (1) United Nations (2010). United Nations Decade 2010 –2020 for deserts and the fight against desertification. (2) Matos, A.R. and Pham-Thi, A.-T. (2009). Plant Physiol. Biochem., 7(6):491-503. (3) Gigon, A., et al. (2004). Ann Bot, 94(3):345-51. (4) Boudière, L. et al. (2013). Biochim. Biophys. Acta, 1837(4):470-80. (5) Monteiro de Paula et al. (1989). Plant Sci., 66 (1990) 185-193; (6) Lichtenthaler, H. (1987). Methods Enzymol, 148: 350-382; (7) Heath, R., et al (1968). Arch. Biochem. Biophys., 125, 189-197; (8) Gameiro, C., et al. (2016) Agric. Water Manage., ; (9) Duarte, B., et al. (2014) AoB Plants.

Consequences of global warming and metal pollution on the metabolism of omega-3 and -6 fatty acids of *Phaeodactylum tricornutum*



Eduardo Feijão¹, Carla Gameiro², Bernardo Duarte², Isabel Caçador², Maria Teresa Cabrita³, Ana Rita Matos¹
¹ Biosystems & Integrative Sciences Institute (BioISI) and Plant Biology Department, FCUL, Portugal ²Marine Environmental Sciences Centre (MARE), FCUL, Portugal
³Centre for Geographical Studies, IGOT, UL, Portugal



Introduction

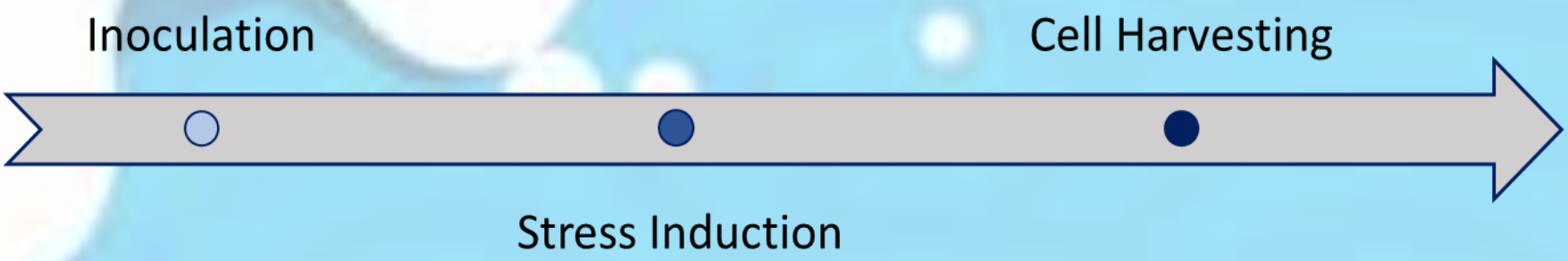
Global warming and metal pollution impact marine ecosystems^{1,2} and interactions between living organisms. Temperature changes and metal overload can modify the lipid composition of primary producers³, which will influence the energy and matter that reach higher trophic levels of marine food chains. The model diatom *Phaeodactylum tricornutum*, particularly rich in long chain polyunsaturated fatty acid eicosapentaenoic acid (C20:5, EPA), and able to accumulate substantial amounts of storage lipids, has been widely be used to assess impacts of various environmental stressors to the phytoplankton community^{2,4,5}.

Objective: This study aims to find changes caused by temperature increase and nickel (Ni) on growth rate, fatty acid composition, more specifically EPA, photosynthetic parameters, and pigment composition of the diatom *P. tricornutum*.



Figure 1— Different morphotypes of *P. tricornutum*; Fusiform (left); Oval (upper right); Triradiate (lower right).

Materials and Methods



INOCULATION (light blue) — Initial *P. tricornutum*⁴ cell concentration of 2.7x10⁵ cells mL⁻¹; growth in f/2 medium, at 18±1 °C, constant aeration, and 12-h light: 12-h dark photoperiod provided by a cool white fluorescent light source (80 μmol photons m⁻² s⁻¹).

STRESS INDUCTION (blue) — Cell exposure to Ni concentrations of 1, 2 and 5 μg/L, at either 18 or 26 °C at the beginning of the exponential phase (48 hours after inoculation).

CELL HARVESTING (dark blue) — Samples (three biological replicates) collected 72 hours after stress induction for analyses.

ANALYSES

Respiration and photosynthesis: oxygen evolution measurements with a Clark-type electrode to assess respiration and photosynthetic rates⁶.

Photosynthetic parameters: non-destructive Pulse Amplitude Modulated (PAM) fluorometry performed daily with a FlourPen to obtain Rapid Light Curves (RLC)³.

Pigment composition: pigments extracted with acetone and analysed spectrophotometrically. Data analysed with the GPS algorithm³.

Fatty acid profile: gas chromatography of fatty acid methyl esters^{4,5,6}; Pentadecanoic acid (C15:0) used as internal standard.

Results

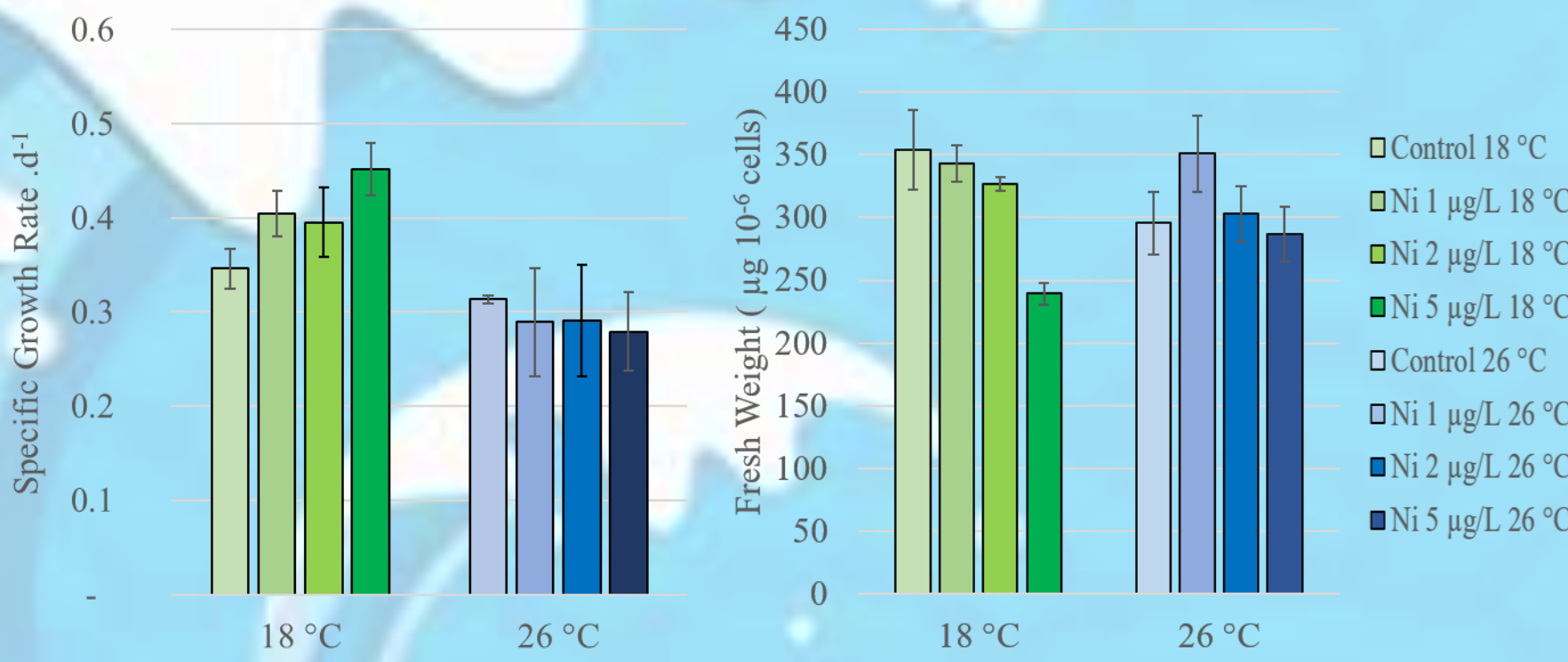


Figure 2 — Specific growth rate (left) and fresh weight (right) of *P. tricornutum* exposed to increasing concentrations of Ni at growth temperatures of 18 °C (green) and 26 °C (blue).

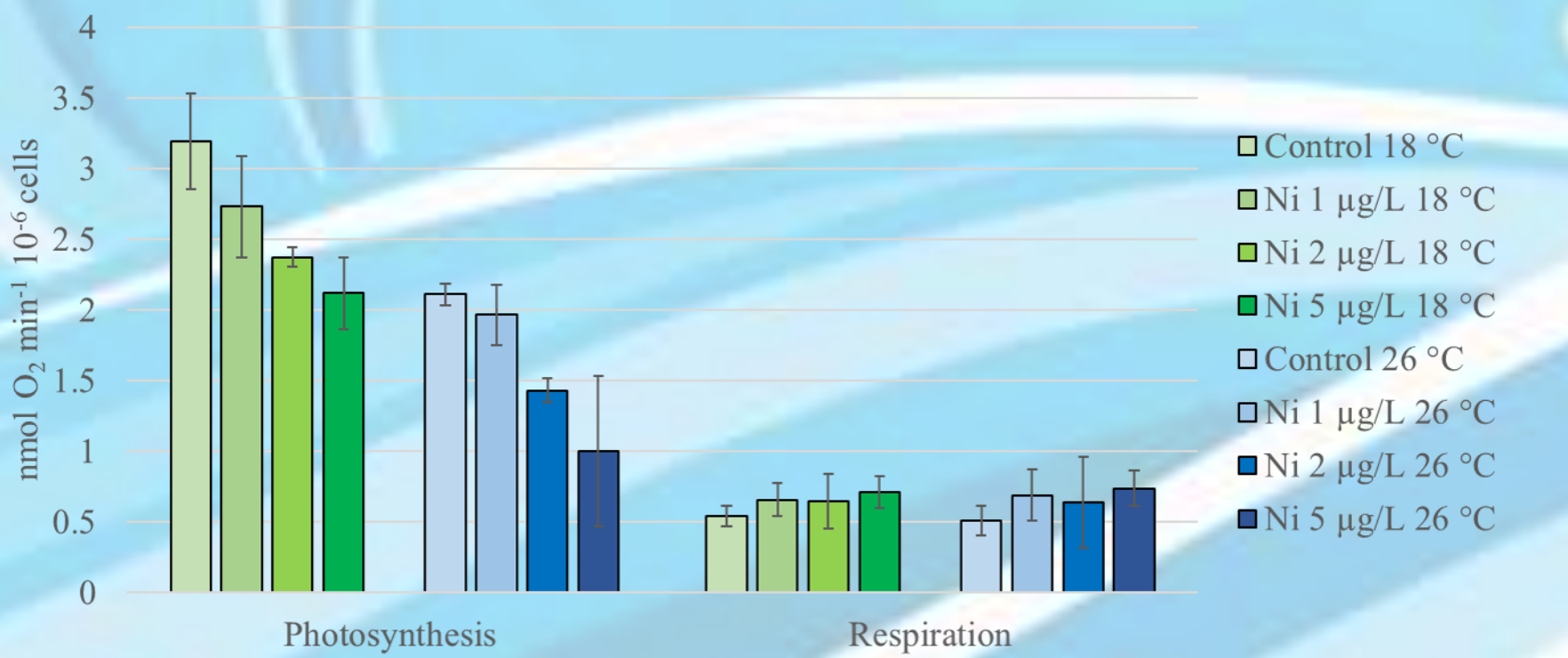


Figure 3 — Photosynthesis (left) and respiration rates (right) of *P. tricornutum* exposed to increasing concentrations of Ni at growth temperatures of 18 °C (green) and 26 °C (blue).

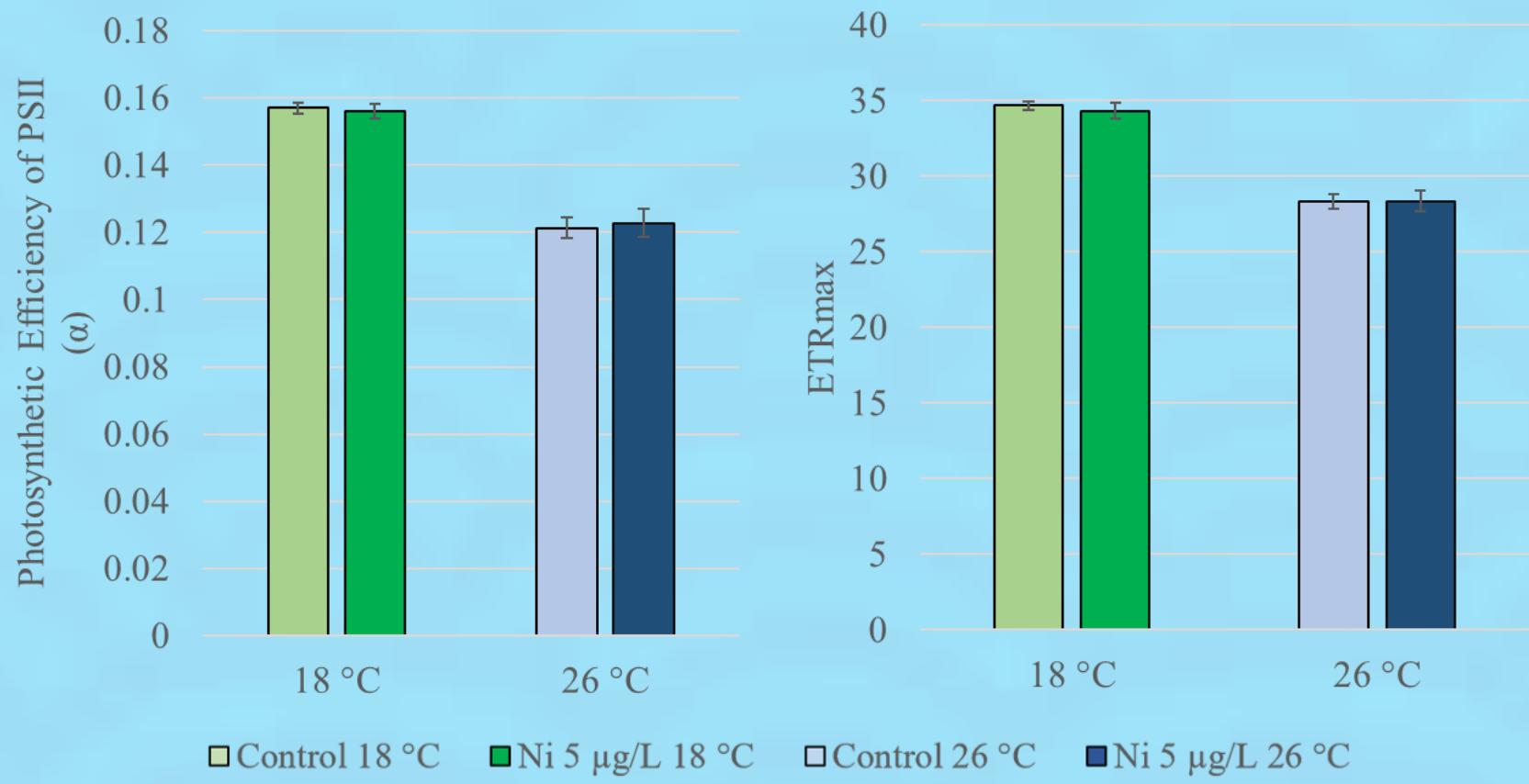


Figure 4 — Rapid Light Curve (RLC) derived parameters of *P. tricornutum* exposed to Ni 5μg/L, at growth temperatures of 18 °C (green) and 26 °C (blue). Maximum electron transport rate (ETRmax) (left); photosynthetic efficiency of Photosystem II (α) (right).

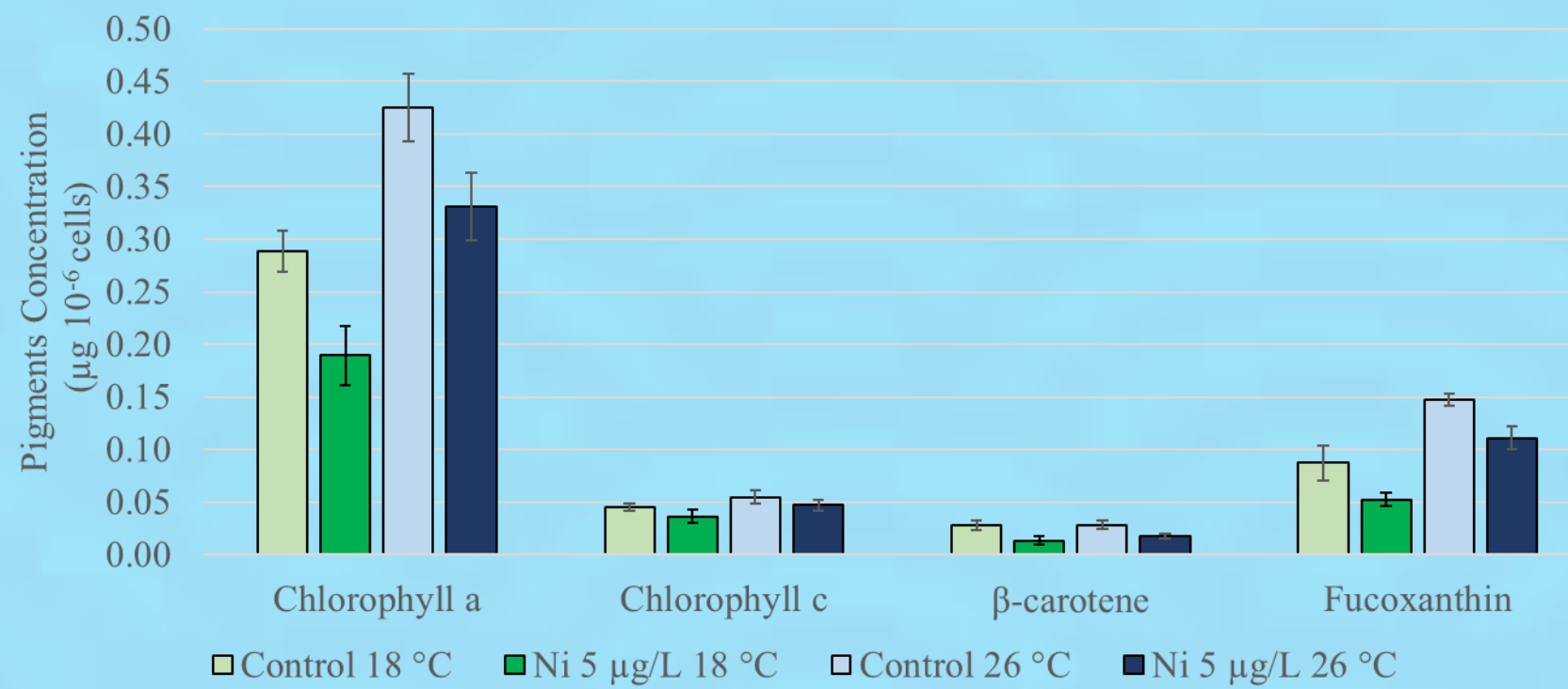


Figure 5 — Pigments concentration of *P. tricornutum* exposed to Ni 5μg/L, at growth temperatures of 18 °C (green) and 26 °C (blue).

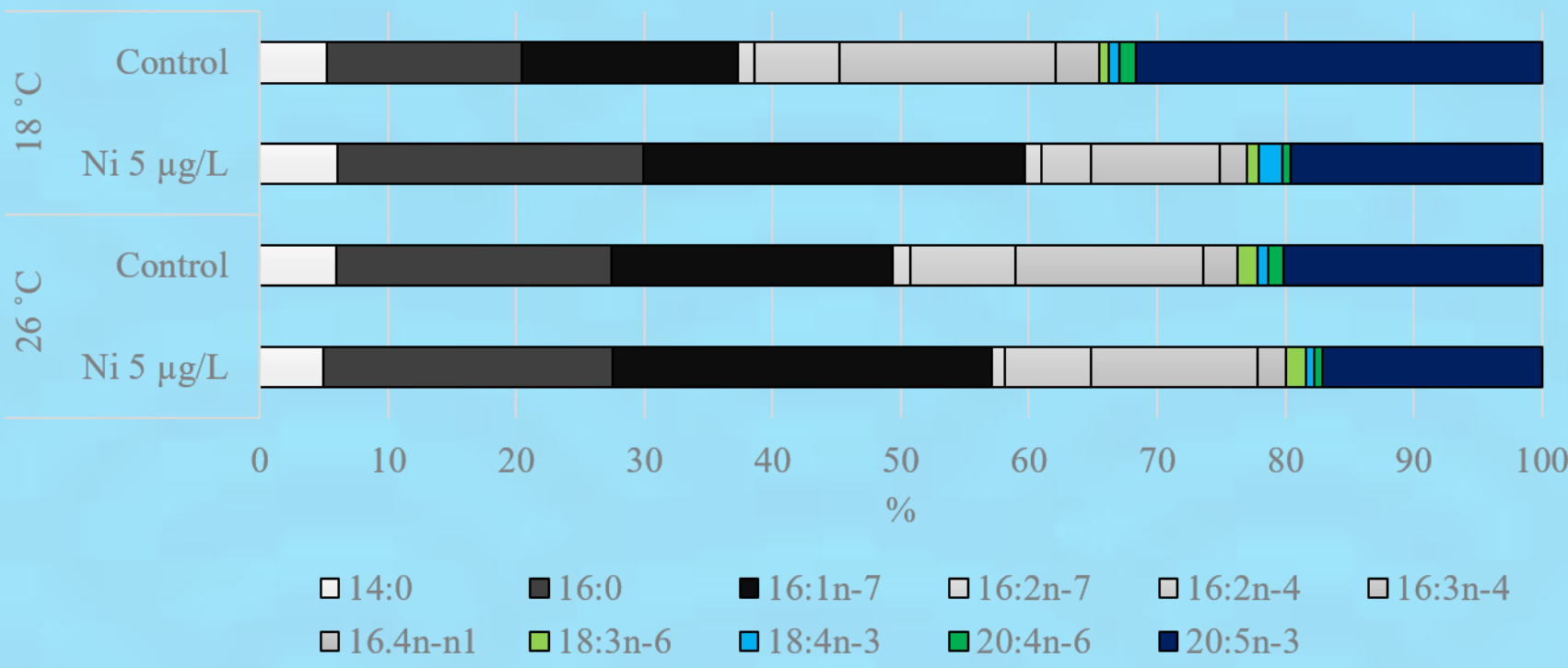


Figure 6 — Relative abundance of fatty acids of *P. tricornutum* exposed to Ni 5μg/L, at growth temperatures of 18 °C and 26 °C. Saturated and mono-unsaturated fatty acids (white, dark grey and black); Plastidial fatty acids (light grey); Omega-6 fatty acids (green); Omega-3 fatty acids (blue).

Major findings

- Nickel and temperature reduce biomass accumulation.
- Nickel and temperature decrease photosynthesis but not respiration.
- Impairment of the efficiency of PSII and electron transport is observed for high temperature but not for Ni.
- Temperature-induced pigment accumulation levels is reversed by Ni.
- Both Ni and high temperature reduce EPA percentage.

Conclusions

- Increases of temperature and Ni concentrations negatively affect biomass, photosynthesis and omega-3 content of *P. tricornutum*.
- Both stresses have ecological implications, namely by reducing nutritional value of phytoplankton and water oxygenation.

Acknowledgements

The authors would like to thank to the "Fundação para a Ciência e Tecnologia (FCT)" for funding the research in the Marine and Environmental Sciences Centre (MARE) throughout the project UID/MAR/04292/2013 and the Biosystems and Integrative Sciences Institute (BioISI) throughout the project UID/MULTI/04046/2013. B. Duarte and M.T. Cabrita investigation was supported by FCT throughout Post-doctoral grants (SPRH/BPD/115162/2016 and SPRH/BPD/50348/2009, respectively). The authors thank Rui Malhão for the help with microscopy, João D. Arraújo and Miguel Gaspar for the help with the oxygen electrode and Manuela Lucas for technical assistance.

References

- Gameiro, C., Cartaxana, P. & Brotas, V. Environmental drivers of phytoplankton distribution and composition in Tagus Estuary, Portugal. *Estuar. Coast. Shelf Sci.* 75, 21–34 (2007).
- Cabrita, M.T. et al. Photosynthetic pigment laser-induced fluorescence indicators for the detection of changes associated with trace element stress in the diatom model species *Phaeodactylum tricornutum*. *Environ. Monit. Assess.* 188, (2016).
- Duarte, B. et al. Disentangling the photochemical salinity tolerance in *Aster tripolium* L.: connecting biophysical traits with changes in fatty acid composition. *Plant Biol.* 19, (2017).
- Domingues, N., Matos, A. R., da Silva, J. M. & Cartaxana, P. Response of the Diatom *Phaeodactylum tricornutum* to photooxidative stress resulting from high light exposure. *PLoS One* 7, 1–6 (2012).
- Matos, A.R. et al. Effects of nickel on the fatty acid composition of the diatom *Phaeodactylum tricornutum*. *Front. Mar. Sci. Conference Abstracts: IMMIR International Meeting on Marine Research* (2016).
- Matos, A.R. et al. Alternative oxidase involvement in cold stress response of *Arabidopsis thaliana* fa2 and FAD3+ cell suspensions altered in membrane lipid composition. *Plant and Cell Physiology* 48, 856–865.

Metabolic characterization of *V. vinifera* cv. Trincadeira in response to *Plasmopara viticola*

Rui Nascimento^{1,2}, Marisa Maia^{1,2,3}, António Ferreira^{2,3}, Ana P. Marques^{2,3}, Ana Ponces², Carlos Cordeiro^{2,3}, Marta Sousa Silva^{2,3*}, Andreia Figueiredo^{1*}

¹ Biosystems & Integrative Sciences Institute (BioISI), FCUL, Portugal

² Centro de Química e Bioquímica, FCUL, Portugal

³ Laboratório de FTICR e Espectrometria de Massa Estrutural, FCUL, Portugal

*co-senior authors

Introduction

Grapevine (*Vitis vinifera* L.) is the most widely cultivated and economically important fruit crops in the world, mainly due to the wine industry(1). In Portugal, one of the most important cultivar in wine making is *V. vinifera* cv. Trincadeira. However, it is susceptible to fungal infections, namely to *Plasmopara viticola*, the causing agent of downy mildew(2). Fungicides are applied as the main method of downy mildew prevention, treatment levels are high and reach up to one spraying per week during the periods of agro-meteorological conditions suitable for the pathogen development. As an alternative to fungicide application, interspecific hybrids resistant to *P. viticola* have been produced, but more work is needed to combine resistance traits with the excellent organoleptic quality of *V. vinifera* cultivars. The infection process in susceptible genotypes is poorly characterized, although transcriptome and proteome studies have been conducted, few comparable data for changes at metabolome level exist (3). This complementary approach would be valuable as it would help to identify specific metabolites and processes involved in the progress and outcome of an infection.

We have carried out a comparative metabolomic analysis of grapevine leaves by Fourier Transform Ion Cyclotron Resonance MS (FTICR-MS), from the susceptible cultivar Trincadeira, at different time points following inoculation with *P. viticola*. Our data allows the identification of metabolites and pathways that reflect the establishment of a compatible interaction.

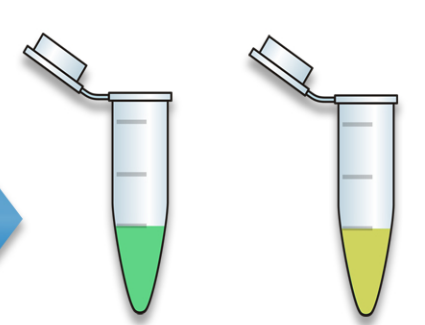
Materials and Methods

Grapevine inoculation experiments



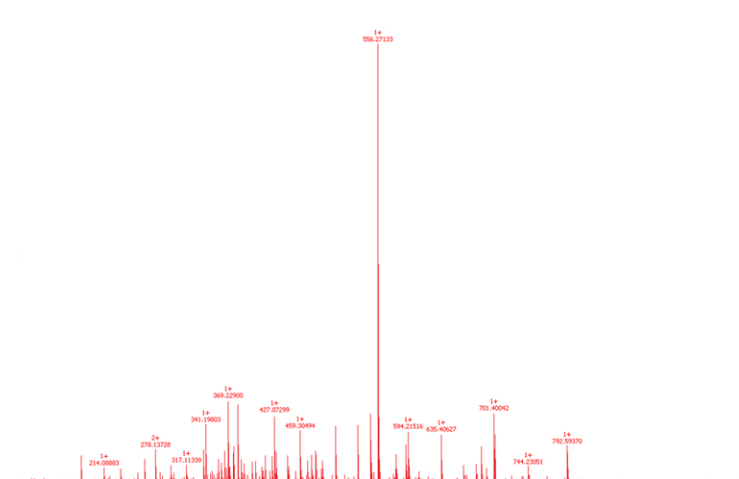
Solvent addition
(MeOH / H₂O);
Shaking;
Centrifugation;
Phase separation;
Based on (4)

Methanol extraction



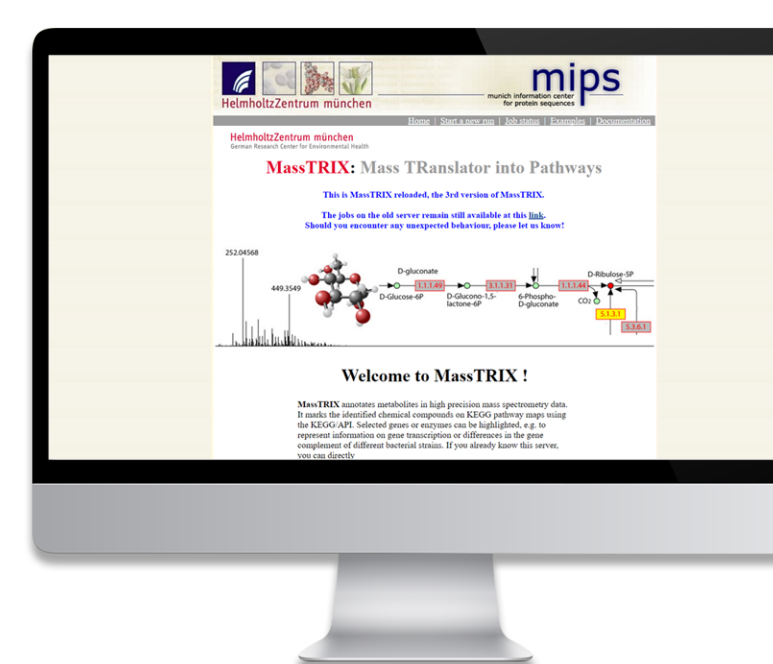
ESI Positive and Negative
FT-ICR-MS direct infusion

FT-ICR-MS Analysis



Biological samples aligned
with in-house build
python software

MassTRIX



Metabolic entities detected
by MassTRIX were analyzed
by MetaboAnalyst

MetaboAnalyst



Results & Conclusions

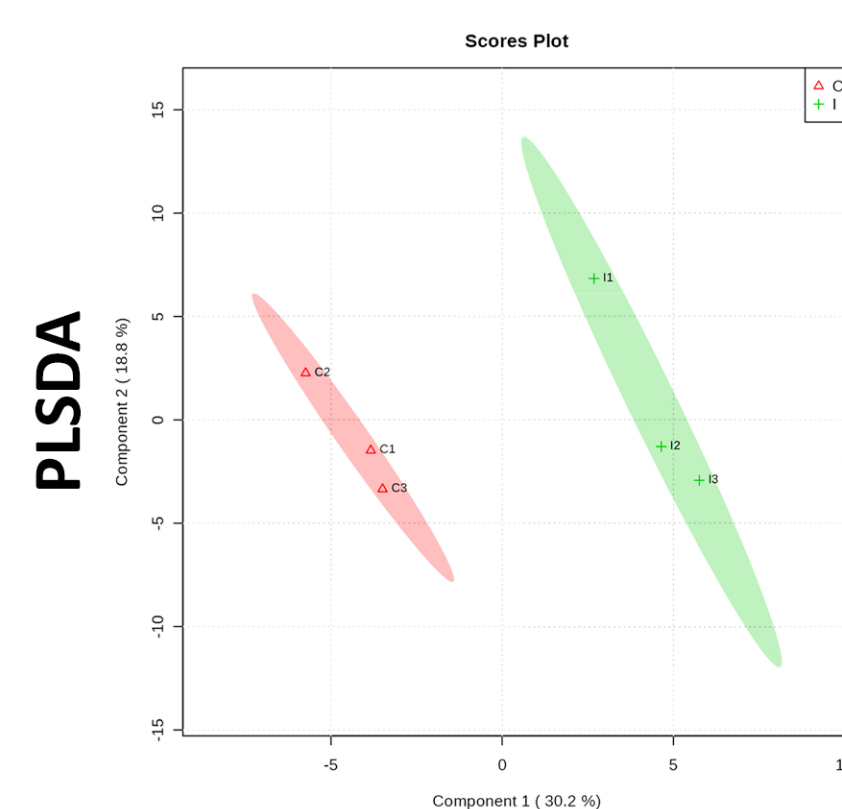
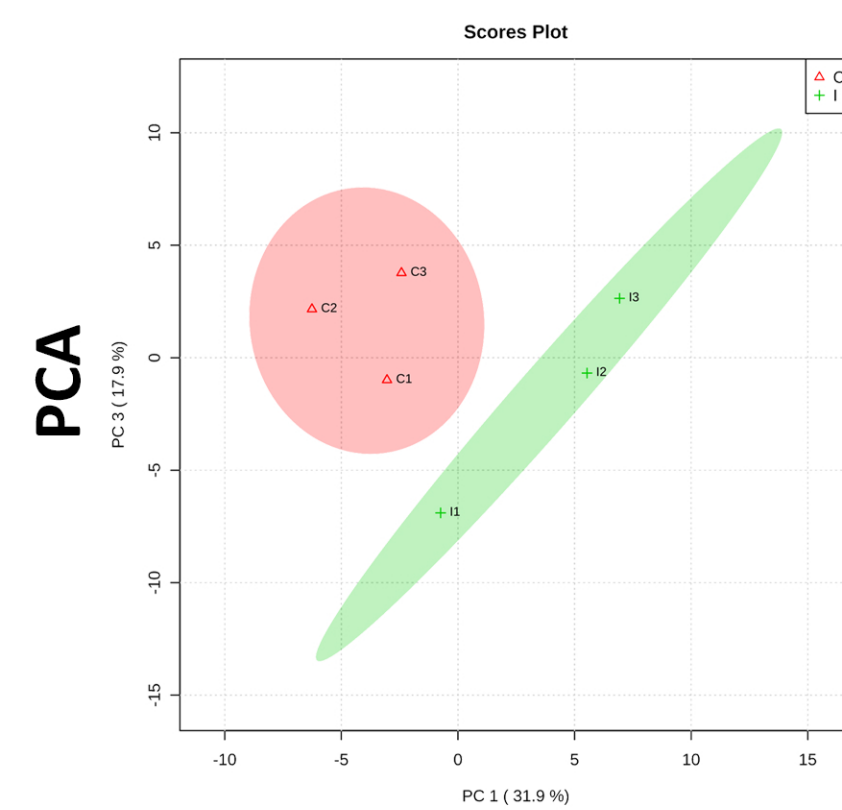
	Fold change > 2	p < 0.05
6h	91	11
12h	76	27
24h	95	19
	262	57

This analysis allows an high throughput metabolic discrimination of different experimental conditions (control and inoculated) with a direct infusion FT-ICR-MS experiment

Fold change analysis allowed the discrimination of differently accumulated metabolites

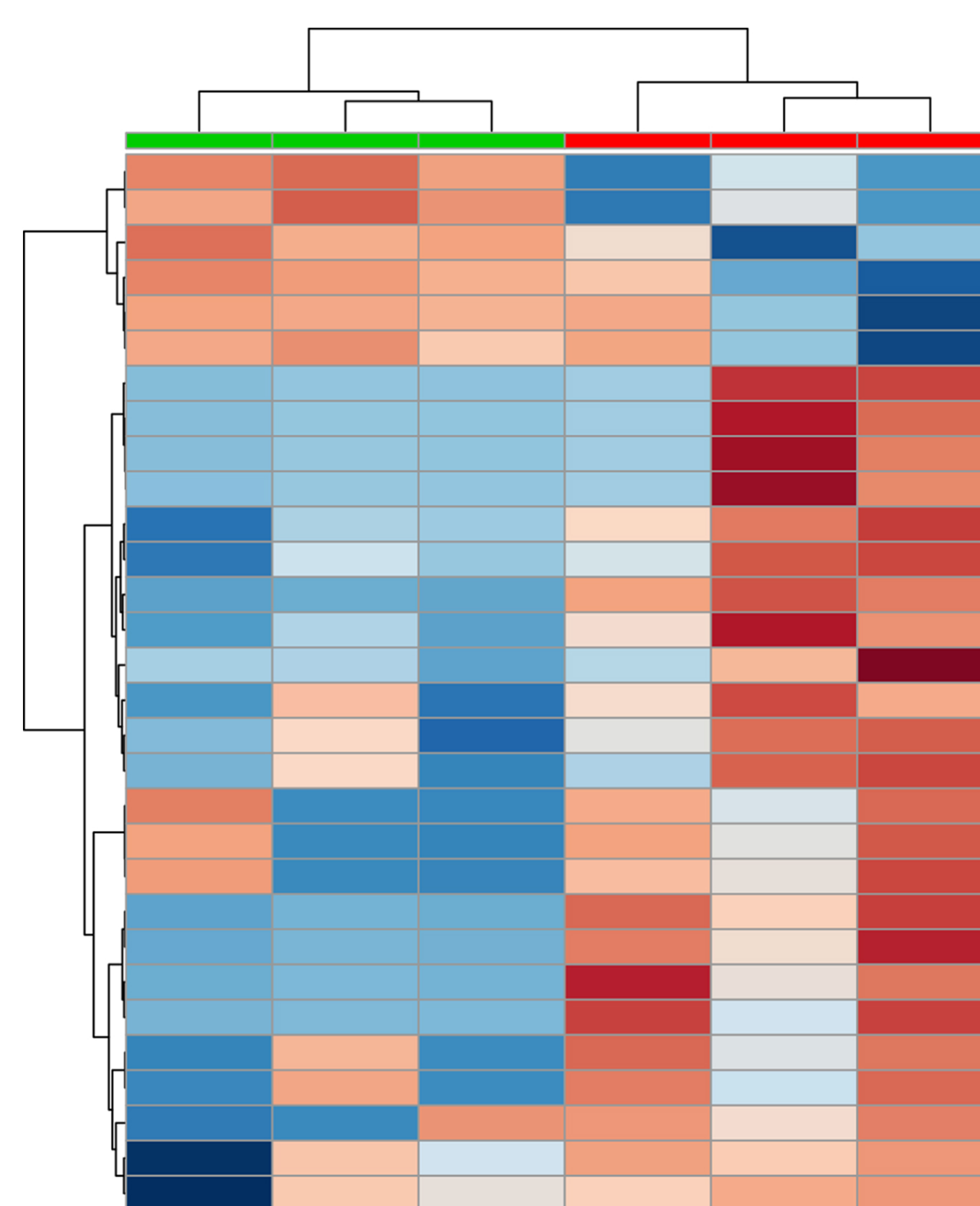
From all the experimental conditions, 24h allowed the better metabolic discrimination between groups

Sample Separation

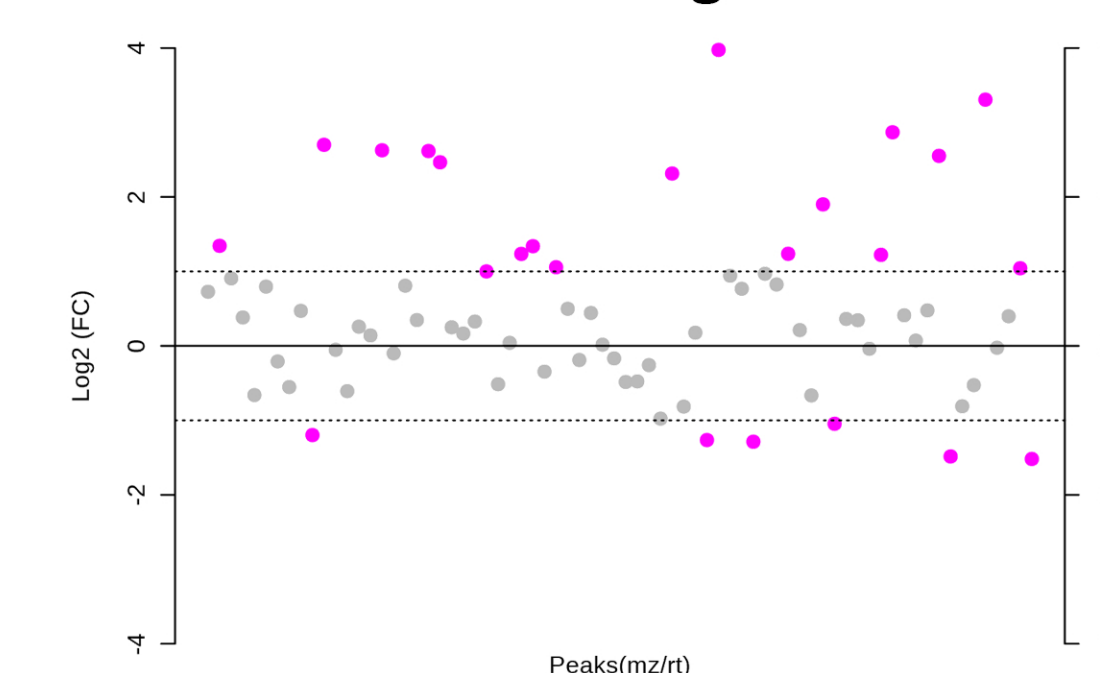


24hpi ESI⁺ Analysis

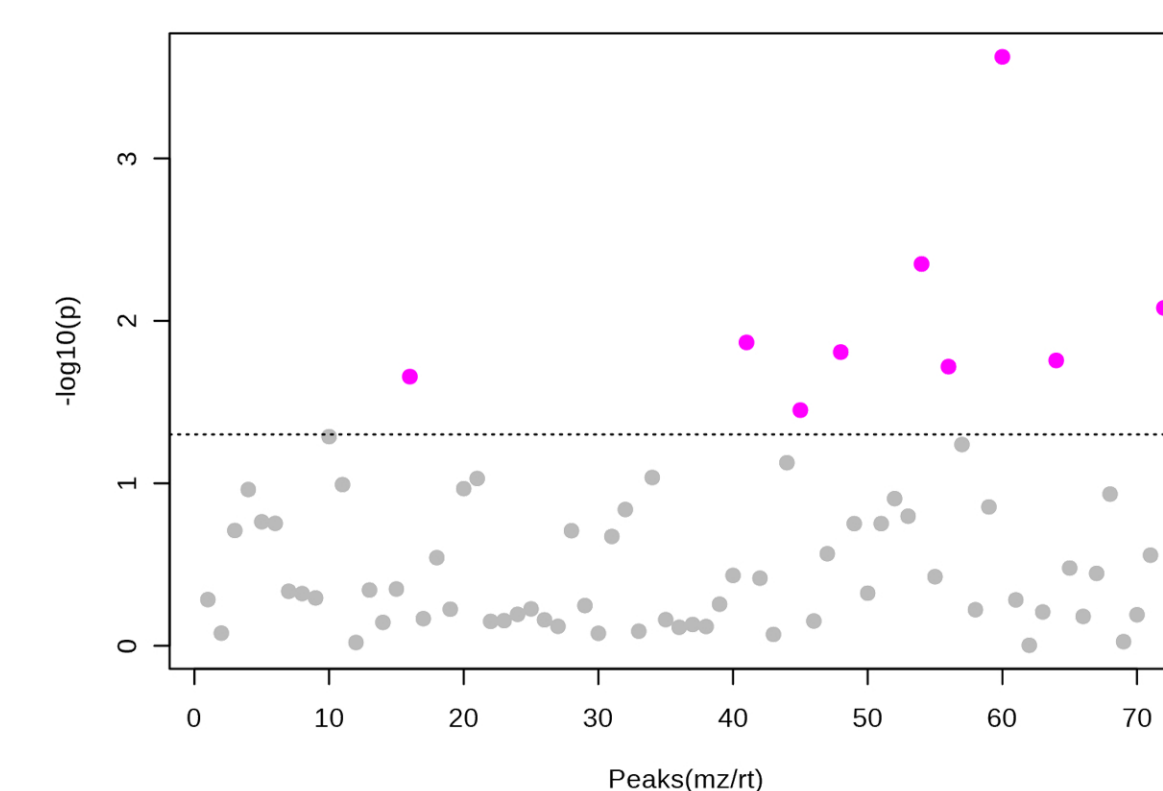
Fold Change & Statistical Analysis



Fold Change



T-test



Future Perspectives

Metabolic pathway search in order to identify coding enzymes

Gene expression analysis of each chosen enzyme by qPCR

Acknowledgements

FCT Fundação para a Ciência e a Tecnologia
MINISTÉRIO DA CIÊNCIA, TECNOLOGIA E ENSINO SUPERIOR

This work was supported by projects EXPL/BBB-BIO/0439/2013, REDE/1501/REM/2005, UID-/MULTI/00612/2013, PEst-OE/QUI/UI0612/2013, PEst-OE/BIA/UI4046/2014, by the investigator FCT program IF-/00819/2015 and grant SFRH/BD/116900/2016 from Fundação para a Ciência e Tecnologia (Portugal). We also had support from the Portuguese Mass Spectrometry Network, integrated in the National Roadmap of Research Infrastructures of Strategic Relevance (ROTEIRO/0028/2013; LISBOA-01-0145-FEDER-022125). This work is part of RN master thesis, entitled "Metabolic pathway characterization of *V. vinifera* to *Plasmopara viticola* infection" (2017).

References

1. Organisation of Vine and Wine. 2016. 2016 OIV Statistical Report on World Vitiviniculture,.
2. Gessler, C., I. Pertot, and M. Perazzolli. 2011. *Plasmopara viticola*: a review of knowledge on downy mildew of grapevine and effective disease management. *Phytopathol. Mediterr.* 50: 3–44.
3. Ali, K., F. Maltese, A. Figueiredo, M. Rex, A. M. Fortes, E. Zyprian, M. S. Pais, R. Verpoorte, and Y. H. Choi. 2012. Alterations in grapevine leaf metabolism upon inoculation with *Plasmopara viticola* in different time-points. *Plant Sci.* 191–192: 100–107
4. Maia, M., F. Monteiro, M. Sebastiana, A. P. Marques, A. E. N. Ferreira, A. P. Freire, C. Cordeiro, A. Figueiredo, and M. Sousa Silva. 2016. Metabolite extraction for high-throughput FTICR-MS-based metabolomics of grapevine leaves. *EuPA Open Proteomics* 12: 4–9.

Phenotyping the Disease Progress of Fusarium Head Blight (FHB) in Summer Wheat Using Hyperspectral Imaging

Elias Alisaac, Jan Behmann, Heinz-W. Dehne, Anne-K. Mahlein

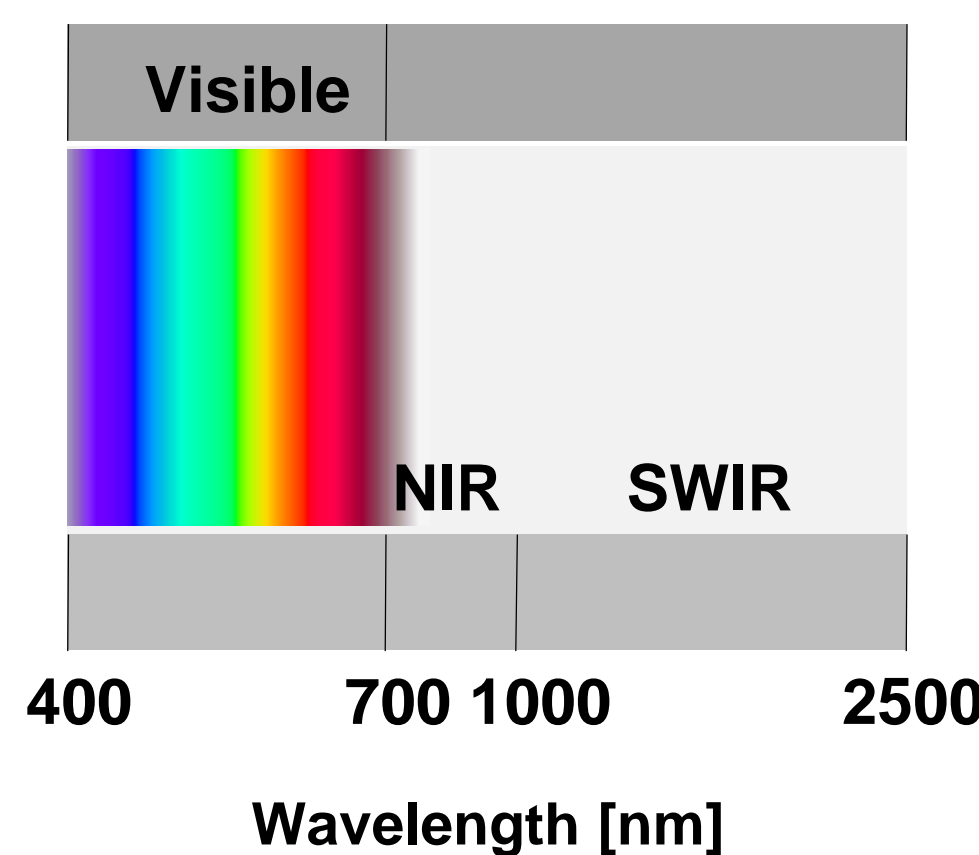
Institute of Crop Science and Resource Conservation (INRES), Department of Plant Diseases and Plant Protection, University of Bonn, Nussallee 9, 53115 Bonn, Germany

INTRODUCTION

- Fusarium* Head Blight (FHB), pose a serious threat to food safety and animal health.
- Resistant cultivars are effective tools to avoid quantitative and qualitative losses caused by FHB.
- Achieving resistant cultivars requires precise and innovative methods to phenotype genotype-environment interaction, disease symptoms and host-pathogen interaction.
- Proximal sensing techniques are promising methods to automate resistance phenotyping under controlled conditions.
- Aim: Phenotyping susceptibility of wheat cultivars non-invasively by hyperspectral imaging.

MATERIAL AND METHODS

- Seven summer wheat cultivars (Chamsin, Passat, Scirocco, Sonett, Taifun, Thasos and Triso) with different degrees of susceptibility (5, 4, 5, 6, 6, 3 and 4 respectively BSL) were used.
- Wheat ears were inoculated at anthesis with *F. graminearum*, *F. culmorum* (10^5 conidia/mL) and water, respectively.
- HyperSpectral Imaging (HSI) measurements were started four days after inoculation (dai) in time series 4, 6, 8 and 13 dai.
- Six ears of each treatment were measured.
- HSI cameras:**
 - VISible-Near InfraRed camera (400-1000 nm)
 - ShortWave InfraRed camera (1000-2500 nm)
- Spectral vegetation indices:**
 - Normalized Differences Vegetation Index, $NDVI = (R_{800} - R_{670}) / (R_{800} + R_{670})$
 - Biomass and vitality
 - Pigment Specific Simple Ratio a, $PSSRa = R_{800} / R_{680}$
 - Chlorophyll a
 - Water Index, $WI = R_{900} / R_{970}$
 - Water content



SPECTRAL VEGETATION INDICES

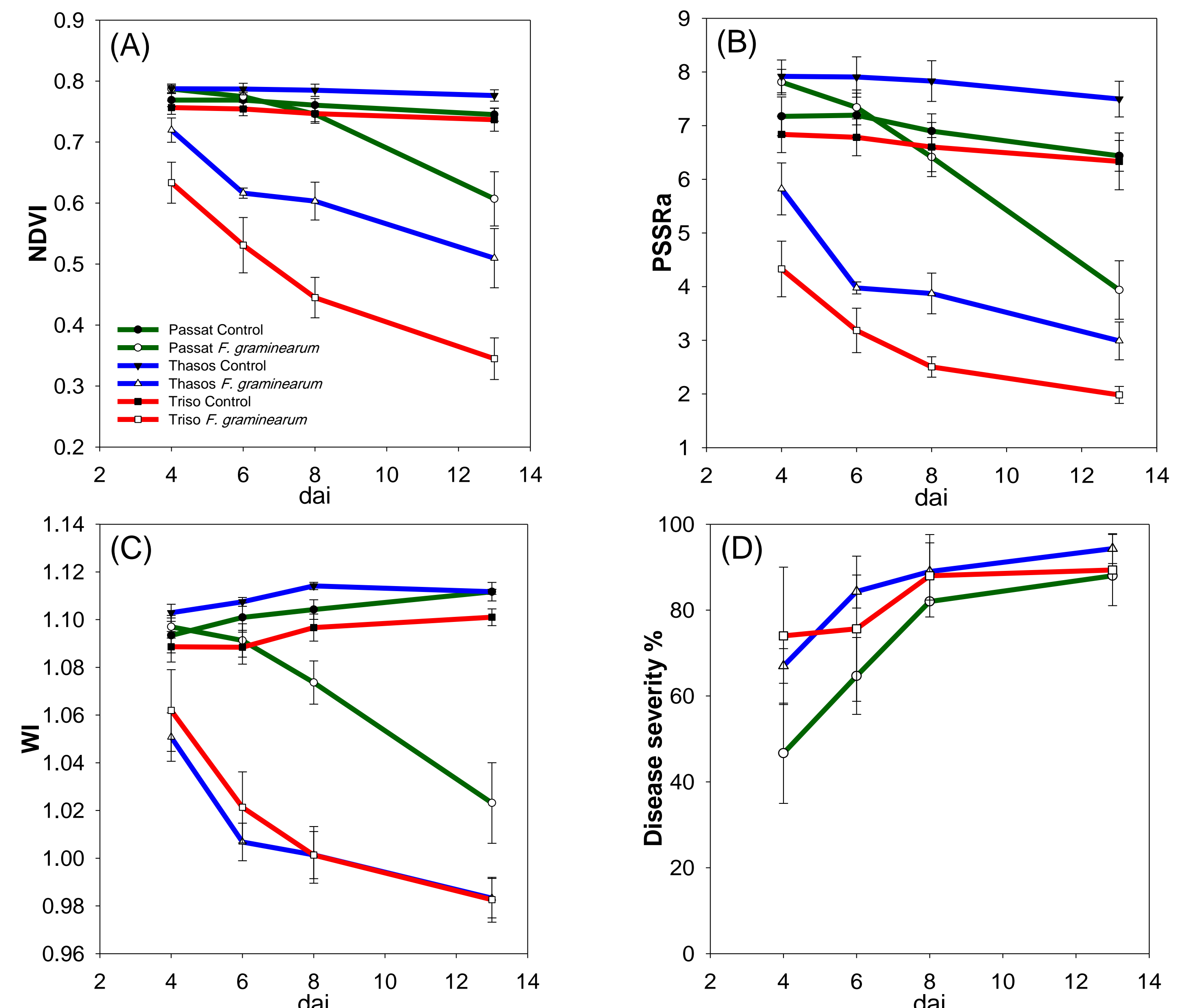


Fig. 1 Effect of FHB on normalized differences vegetation index (NDVI) (A) as indicator of biomass and vitality, pigment specific simple ratio a (PSSRa) (B) as indicator of chlorophyll a, water index (WI) (C) as indicator of the water content in the ear tissue and visually assessed disease severity (D) in comparison to non-inoculated control in three wheat cultivars with different degrees of susceptibility to FHB. Disease severity = ([Number of infected spikelets per ear/Total number of spikelets per ear]x100).

THRESHOLD-BASED CLASSIFICATION

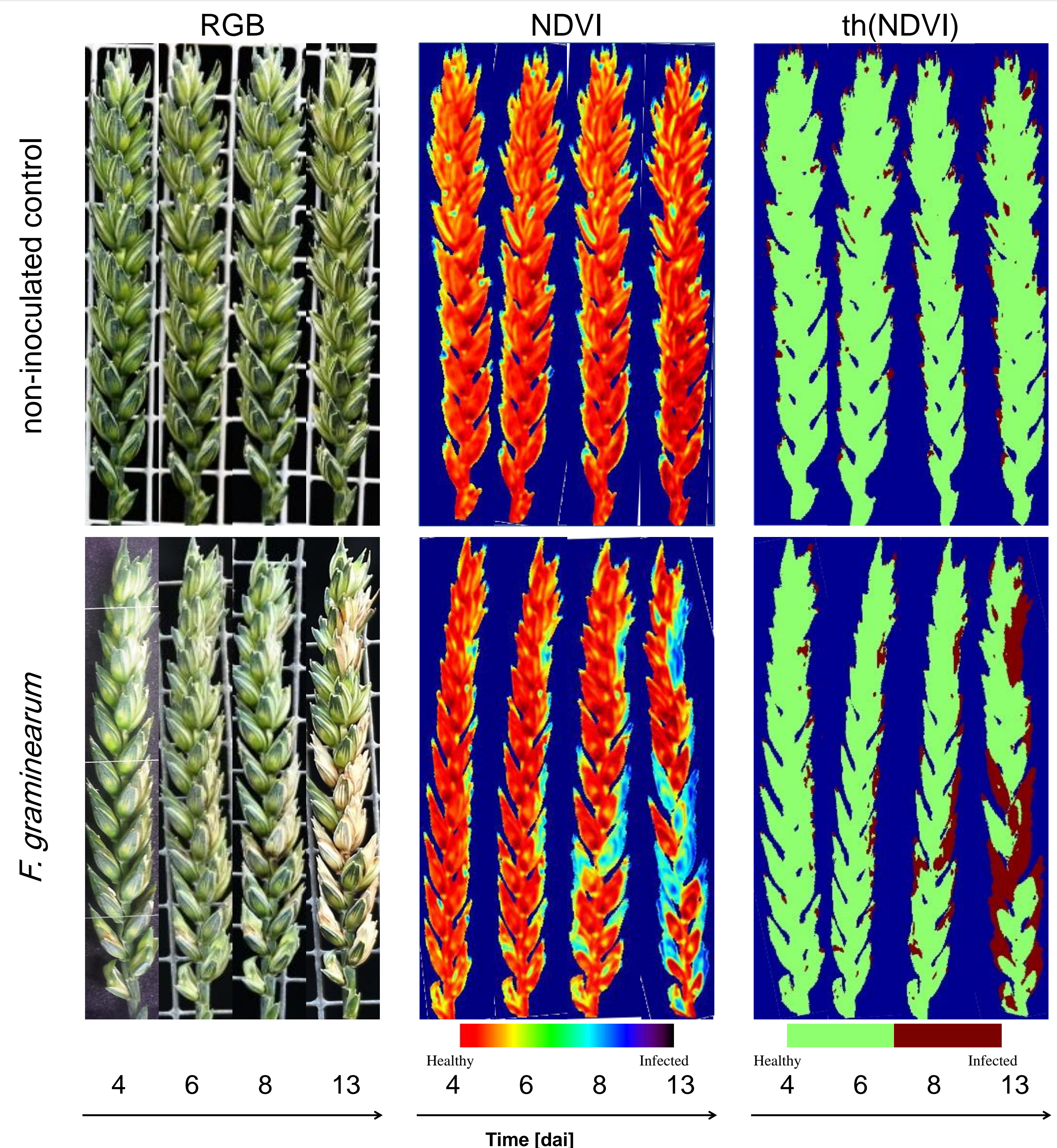


Fig. 2 RGB image (left), visualized NDVI (middle) and threshold based classification th(NDVI) (right) of non-inoculated control (above) and *F. graminearum* infected ears (below) in summer wheat (Passat) 4, 6, 8 and 13 dai.

RESULTS

- HSI proved ability to differentiate between cultivars with different degrees of susceptibility already 4 dai based on the applied vegetation indices NDVI, PSSRa and WI (Fig. 1 A, B and C).
- No significant differences in disease severity assessed visually along the time of the experiment (Fig. 1 D).
- Cultivars with different degrees of susceptibility differed significantly in spectral vegetation indices at early stage of infection 4 dai (Fig. 1).
- Differences between cultivars were more pronounced based on PSSRa starting 4 dai (Fig. 1 B).
- Precise phenotyping of FHB using NDVI threshold classification th(NDVI) (Fig. 2).

CONCLUSION

- Threshold-based classification is a reliable tool to automate FHB phenotyping based on NDVI.
- HSI is a promising method to phenotype FHB under controlled conditions.
- But its application under field conditions still needs further investigations.

Effect of meteorological factors on percentage of linalool in *Thymus pulegioides* growing in same field conditions

Kristina Ložienė, Vaida Vaičiulytė

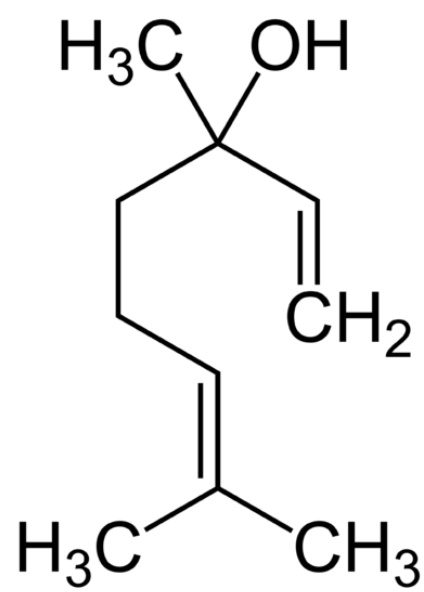
Nature Research Centre, Institute of Botany, Žaliojių Ežerų g. 49, LT-08406, Vilnius, Lithuania

E-mails: kristina.loziene@gmail.com, vaiciulyte.vaida@gmail.com

INTRODUCTION

Chemical polymorphism is characteristic of essential oil bearing medicinal and aromatic species *Thymus pulegioides* (Lamiaceae). Linalool, the main chemical compound of linalool chemotype, can reach up to 80% in *Thymus pulegioides* linalool chemotype and determine possibilities of use of this chemotype in cosmetic products, food and pharmaceutical industry. *Thymus pulegioides* is suitable for cultivation in Baltic States region, therefore, is actually as same meteorological factors can influence on composition of essential oils of linalool chemotype.

The aim of this work was to establish the effect of some meteorological factors on percentage of linalool in essential oil of *Thymus pulegioides* linalool chemotype growing under the same field conditions.



linalool

MATERIAL and METHODS



Thymus pulegioides

The parent plant of *Thymus pulegioides*, belonged to linalool chemotype, was vegetatively propagated and grown in the field collection of the Nature Research Centre (Vilnius, Lithuania) six year in an open ground under the same micro-edaphoclimatic environmental conditions. The aerial parts were annually collected at the full flowering stage and dried at room temperature. The essential oils of leaves-inflorescences (free from stems) were isolated by hydrodistillation in the European Pharmacopoeia apparatus during two hours. The metabolomic analysis carried out by gas chromatography and mass spectrometry. The meteorological data (temperature, precipitation, photosynthetically active solar radiation and sunshine duration) were obtained from the meteorological bulletins of the closest station of meteorology of Lithuanian Hydrometeorological Service under the Ministry of Environment..

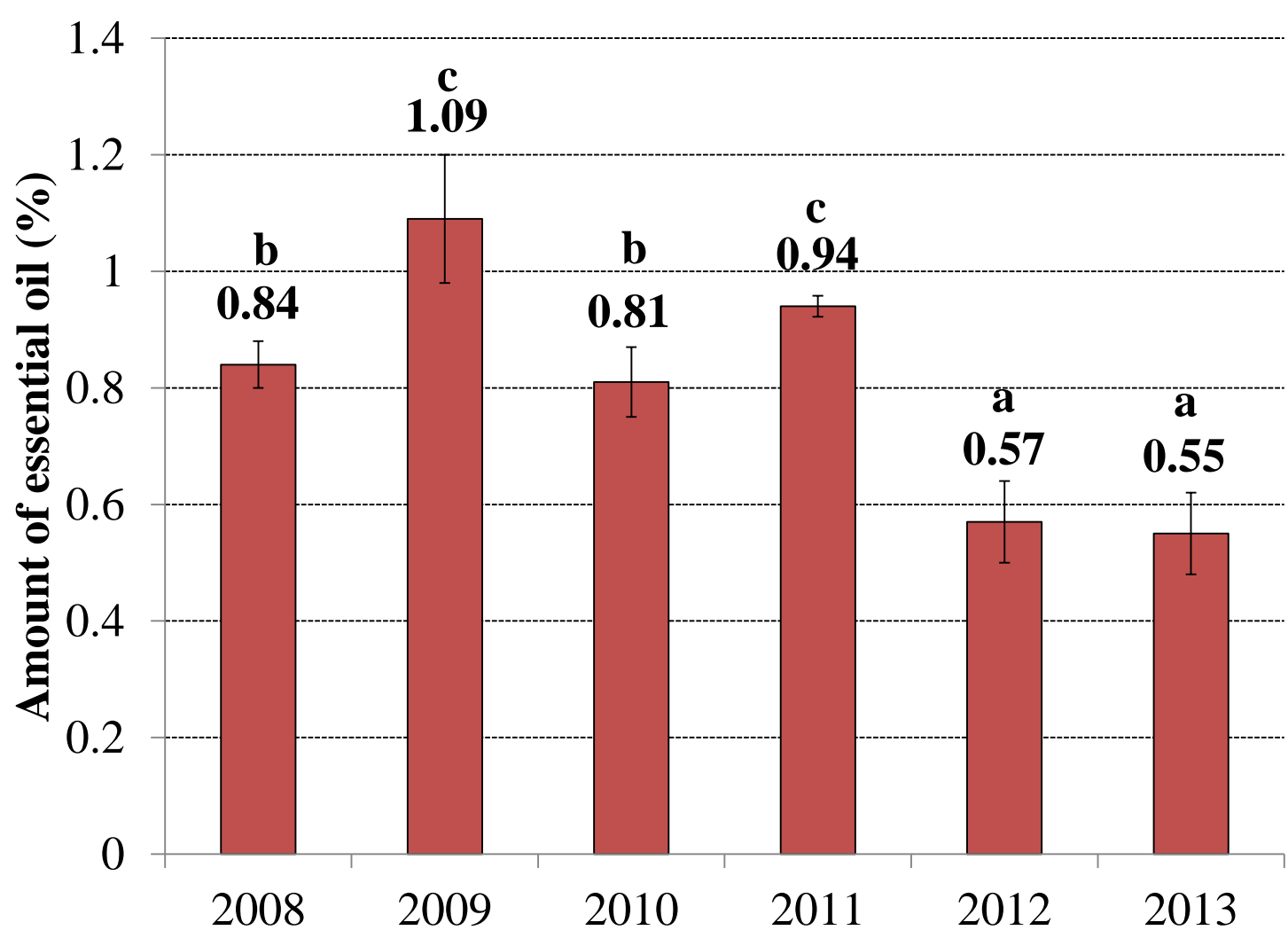
RESULTS

1. Variation of meteorological conditions in cultivation locality of *Thymus pulegioides*

Thymus pulegioides is the perennial plant: there its vegetation starts in April annually and plants flower in July in Lithuania. Therefore both the meteorological conditions in July and the sums of averages of monthly temperature (T), rainfall (R), sunshine duration (Sd) and photosynthetically (PAR) active solar radiation from April to July (Σ April–July) were analysed. Our analysis of meteorological data showed, that meteorological conditions varied during investigation period.

	Year						Period 2008–2013	
	2008	2009	2010	2011	2012	2013	Average \pm SD	CV (%)
Rainfall (mm)								
July	58	107	208	155	81	109	120 \pm 54	45
R Σ April–July	293	287	500	306	286	291	327 \pm 85	26
Temperature (°C)								
July	17.8	18	21.8	19.6	19.5	18	19.1 \pm 1.5	8
T Σ April–July	53.9	54.0	60.1	59.5	55.8	58.0	56.9 \pm 2.7	5
Photosynthetically active solar radiation (Mj/m ²)								
July	340	320	330	285	258	295	305 \pm 31	10
PAR Σ April–July	1210	1203	1085	1115	1093	1110	1136 \pm 56	5
Sunshine duration (h)								
July	305	295	300	220	280	220	270 \pm 40	15
Sd Σ April–July	1124	1379	1150	1288	1033	940	1152 \pm 161	14

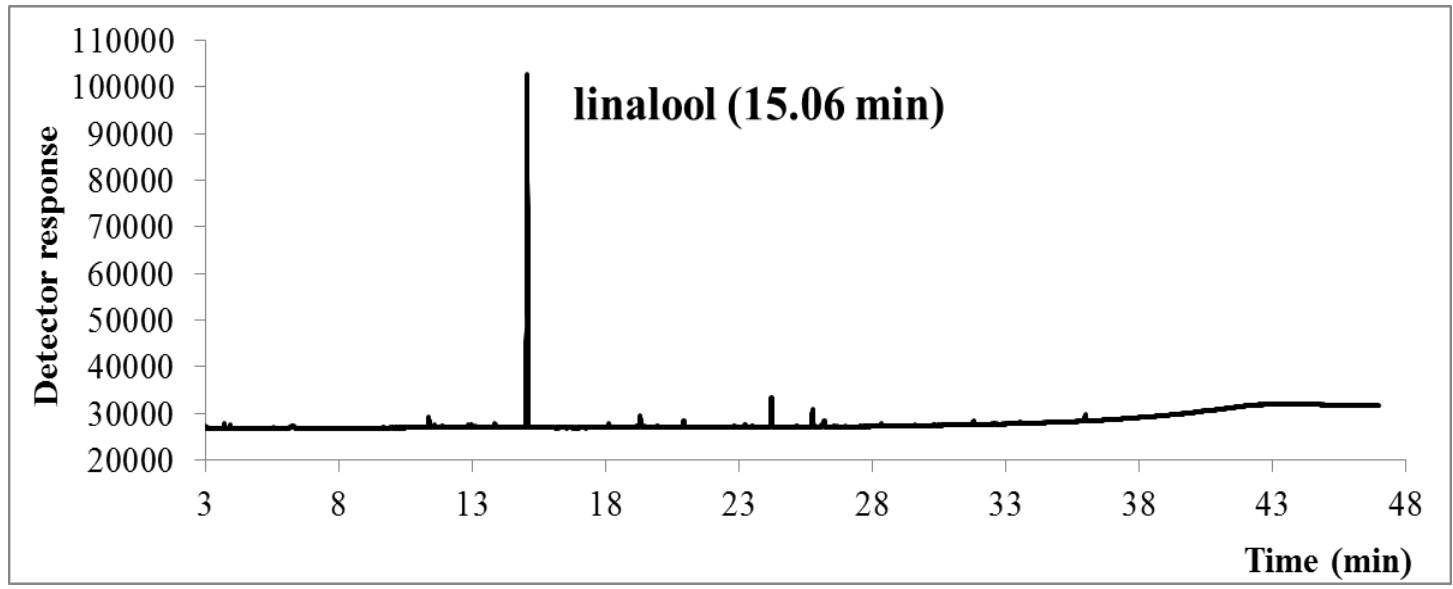
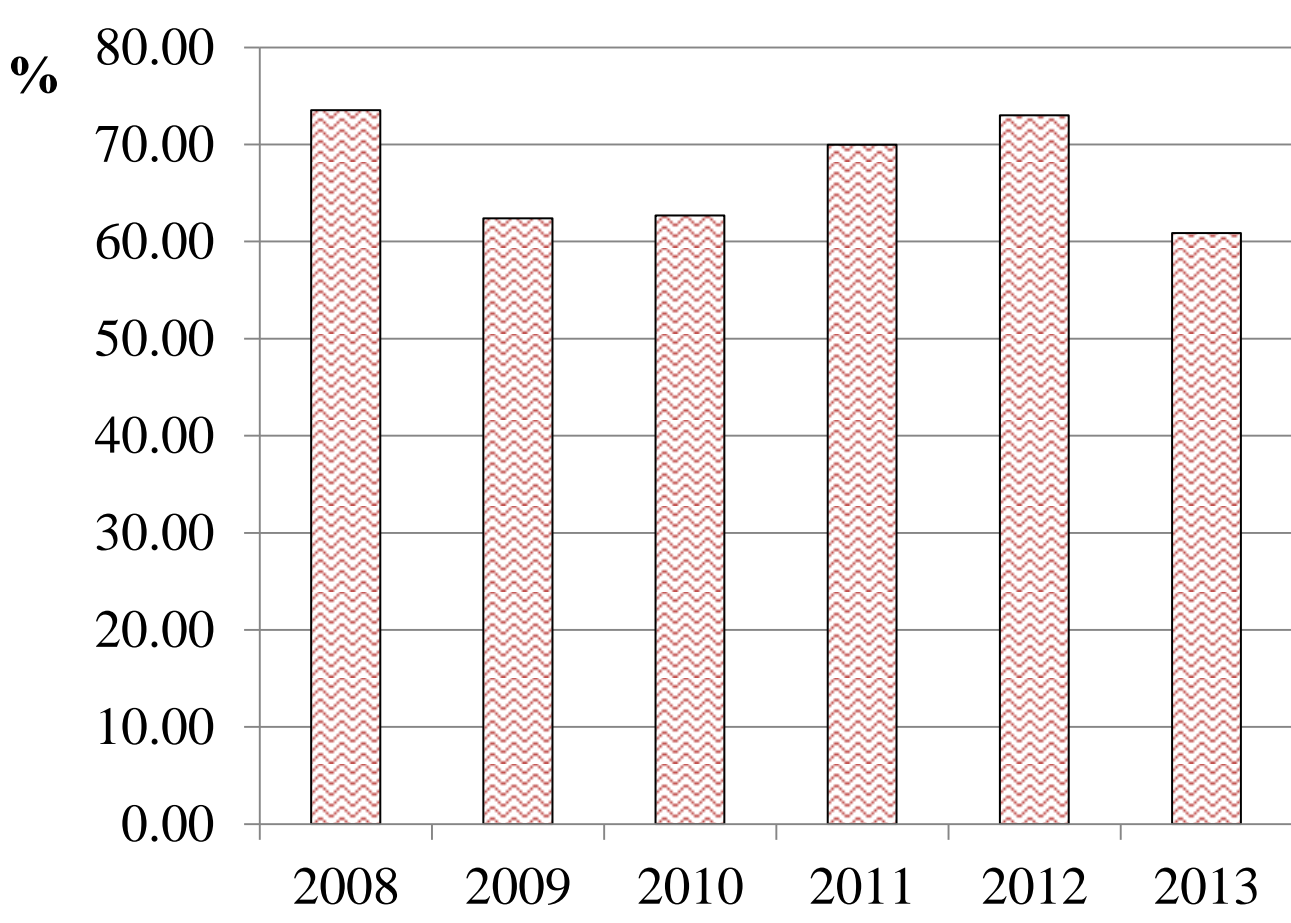
2. Effect of meteorological conditions on amount of essential oil in *Thymus pulegioides* linalool chemotype



2008 – 2013	Amount of essential oil (%)
Average \pm SD	0.77 \pm 0.08
Variation coefficient (%)	24

The correlation analysis showed that the amount of essential oil of *Thymus pulegioides* linalool chemotype significantly positively correlated with sum of sunshine duration from April to July ($r = 0.83$, $p < 0.05$)

3. Effect of meteorological conditions on percentage of linalool in essential oil of *Thymus pulegioides* linalool chemotype



2008–2013	Amount of essential oil (%)
Average \pm SD	67.08 \pm 5.74
Variation coefficient (%)	9

The significant correlations between yield of linalool and meteorological factors were not detected.

The six-year-long monitoring of linalool yield in linalool chemotype of *Thymus pulegioides* showed that the amount of this compound is very stable, and temperature, precipitation, photosynthetically active solar radiation and sunshine duration do not have significant effect on it. Therefore, the growing of linalool chemotype of *Thymus pulegioides* as the monoculture could enable to collect the raw material with fairly stable amount of linalool annually.

Plant phenotyping at the Central European Institute of Technology (CEITEC)

Natallia Valasevich

Mendel Centre for Plant Genomics and Proteomics, CEITEC – Central European Institute of Technology, Masaryk University, Kamenice 625 00 Brno, Czech Republic



Fig. 1. Walk-in phytotron growth chambers (PSI) enable researchers to maintain controlled growing conditions with independent selection of photoperiods for plant physiology applications.

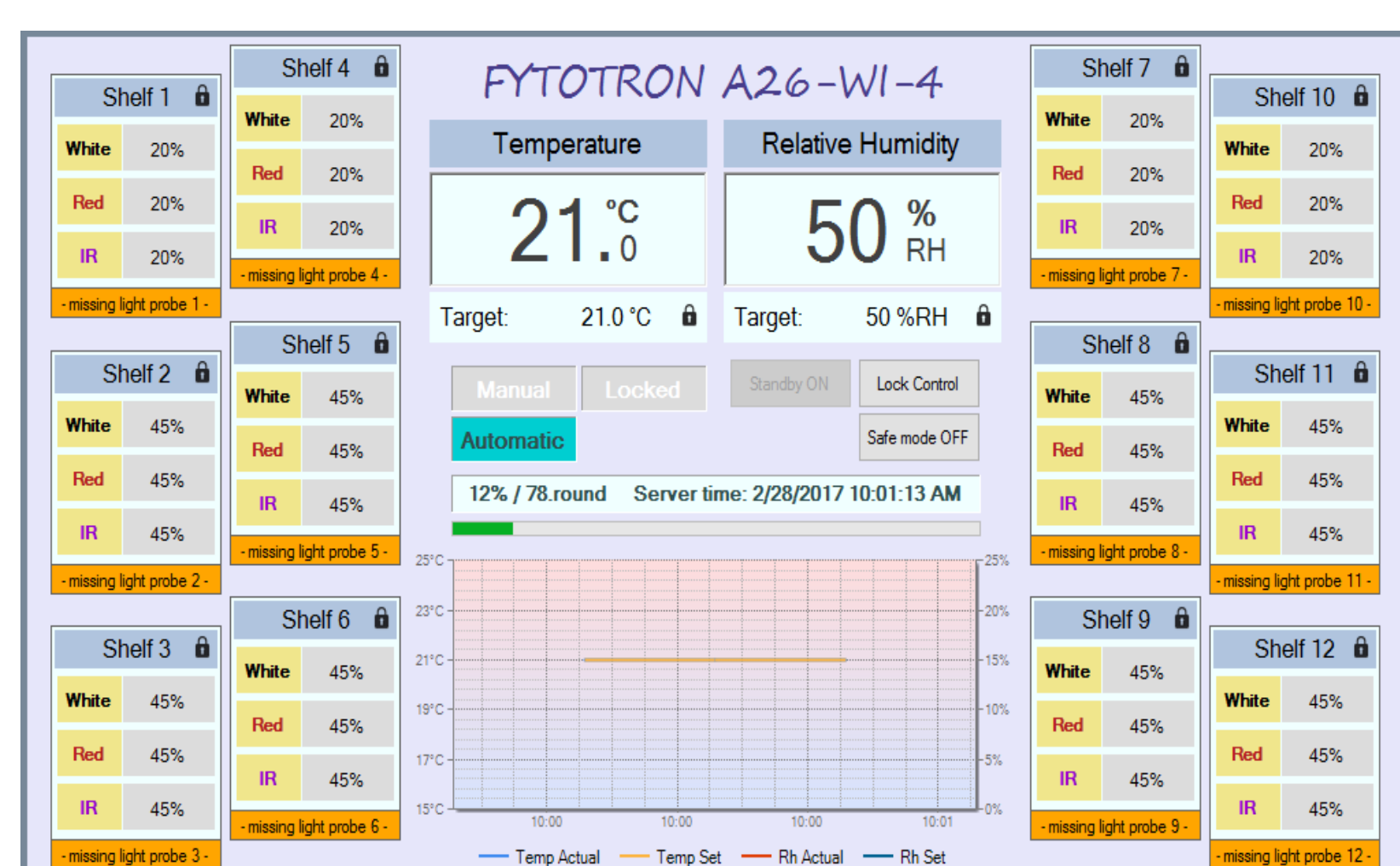


Fig. 2. Main tab of the client program (PSI) displays current and target values for the following parameters: temperature, relative humidity and lights in individual banks.

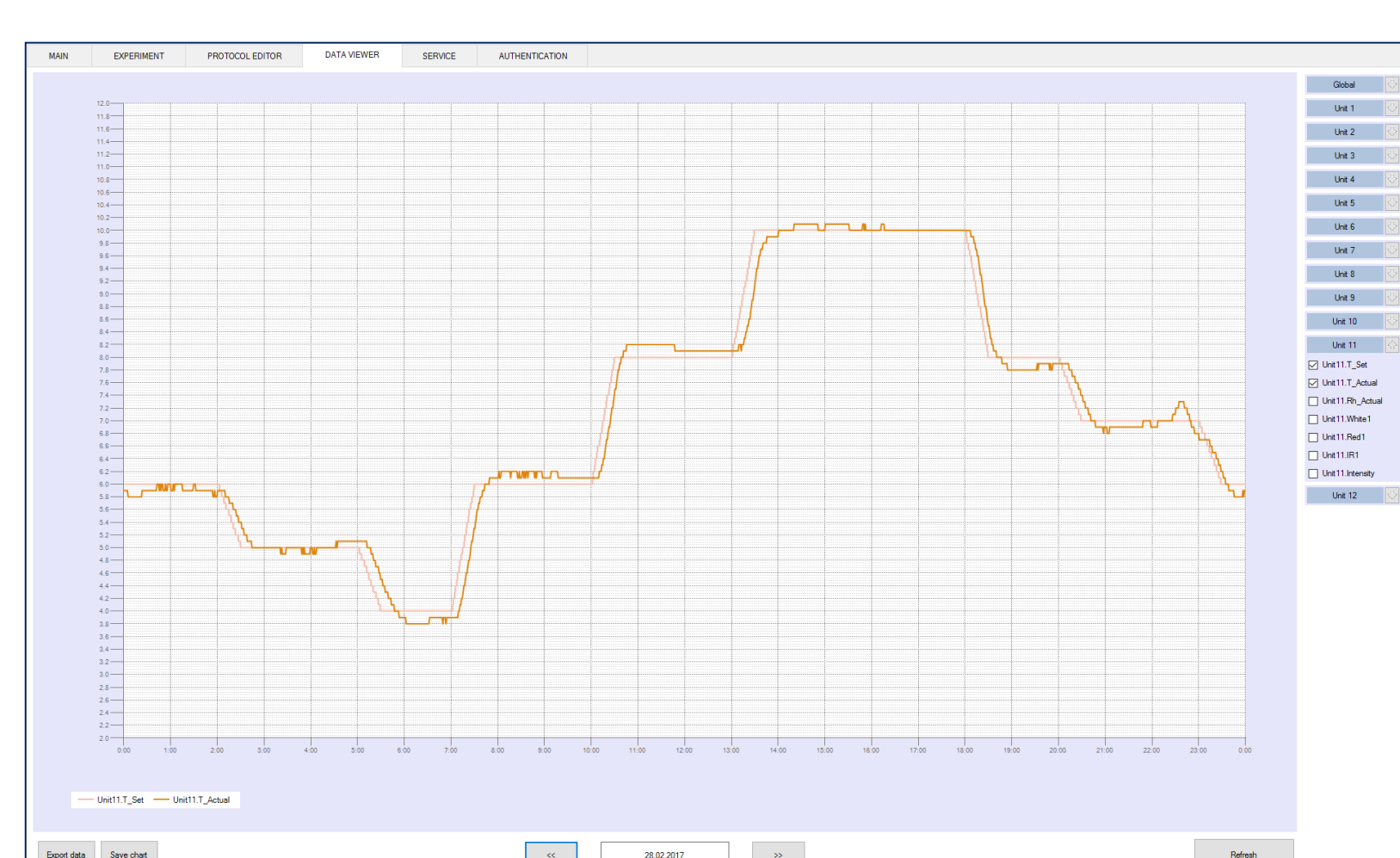


Fig. 3. Shows an example of cold stress protocol and illustrates the highly precise technical performance.

Plant Sciences Core Facility (Plant Sciences CF) of the CEITEC is a newly established facility which offers scientific services and access to the research infrastructure for phenotyping analyses. It serves as a focal point for broad-based cutting-edge biological research.

The core facility operates 16 computer assisted plant growth chambers (phytotrons) and provides defined environment for controlled plant growing. Controlled parameters are: temperature (+4 to +40°C), humidity (30 to 80%), light intensity (up to 250 $\mu\text{mol (photon)} \cdot \text{m}^{-2} \cdot \text{s}^{-1}$) with independent selection of photoperiods.

For optimum plant growth Light Emitting Diodes (LEDs) as a sole light source are used. This provides excellent spectral quality with high irradiance for plant physiology applications. The following light wavelengths are possible to be combined: UV_{365,385}, blue_{400,450}, green₅₂₅, amber₅₉₀, red₆₆₅ and far-red₇₃₀.

A full range of "day/night" cycles with "dawn/dusk" and "cloudy sky" effects can be programmed. In some chambers different gas conditions (e.g. ethylene and CO₂) can be adjusted. This allows simulation of various environmental stress conditions (drought stress, light stress, cold and heat stress).

Beside the environmental simulation the following services provided by the Core Facility are available: low-throughput screening for phenotyping of several crops, phenotyping of roots and seedlings on agar plates and phenotyping of seeds.

Collaboration with the Photon Systems Instruments (PSI) company makes it possible to test and implement innovative technologies in plant cultivation, imaging and phenotyping.

Thanks to the in house Cellular Imaging CF (CEITEC) documentation of plant phenotype may be supplemented by detailed analysis at cellular and subcellular levels.

Collaboration with Vienna BioCenter Core Facilities (VBCF) supported by the program INTERREG V-A Austria-Czech Republic (2014-2020) allows to share best practices in managing core facilities, and to share knowledge and expertise leading to improvement of the provided services.



Fig. 4. White LED illumination with supplementary RED and FAR-RED LEDs (PSI) for excellent plant growth.

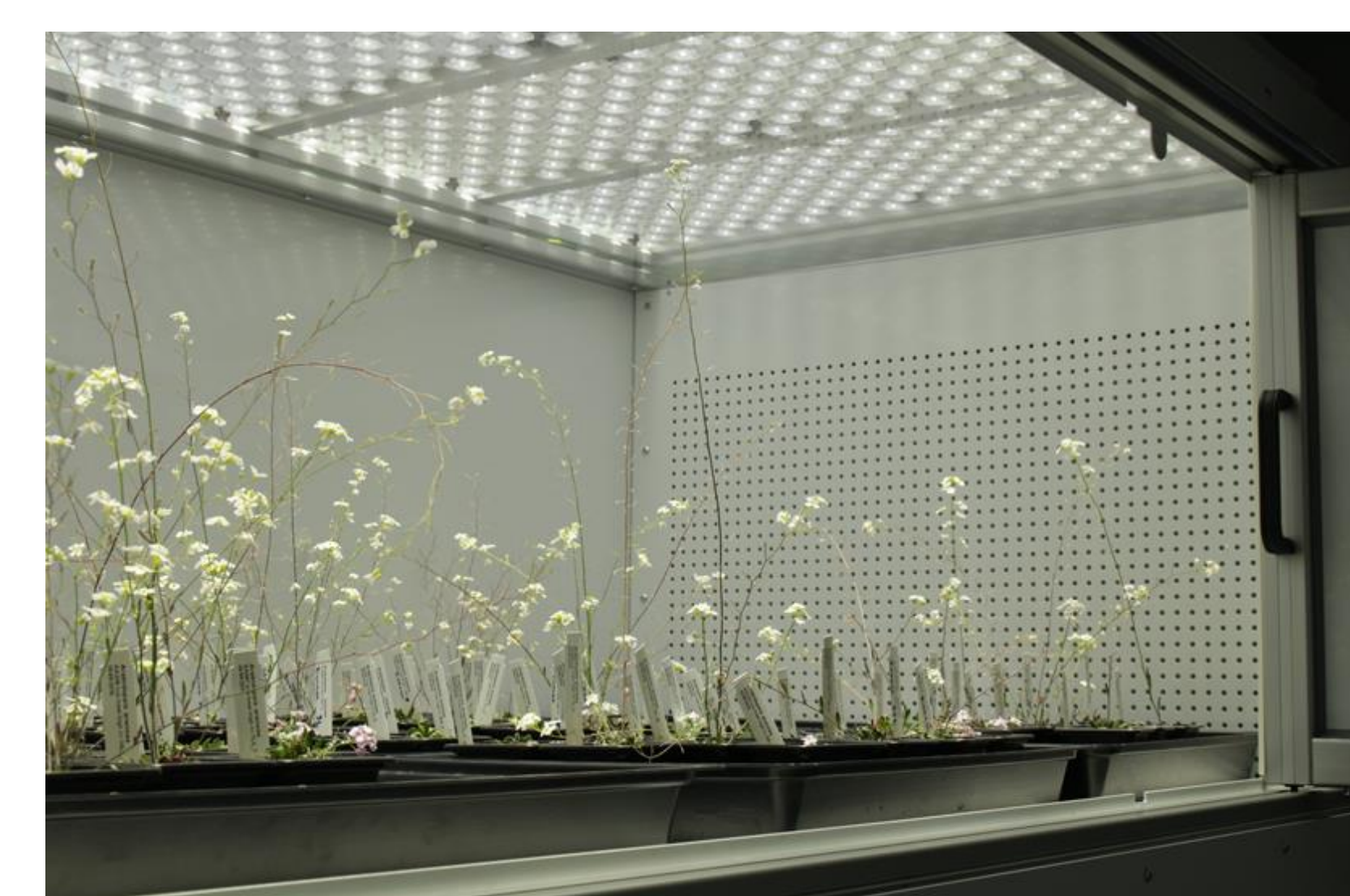


Fig. 5. Plants under the high light stress.

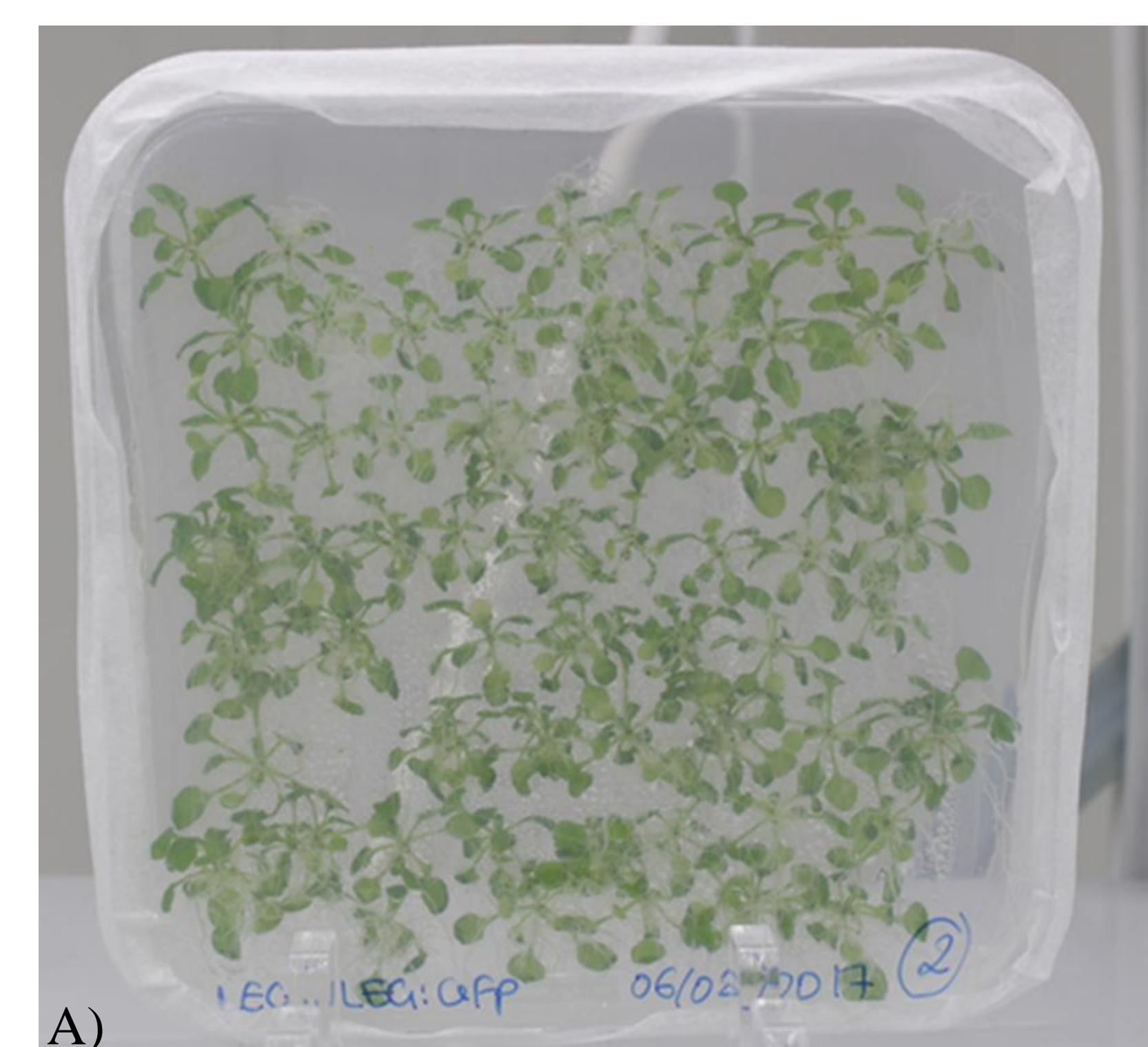


Fig. 6. Screening for phenotyping of roots and seedlings on agar plates and phenotyping of plants in pots are available in CEITEC.

JASMONIC ACID AND ETHYLENE-RELATED GENES RETRIEVED FROM TRANSCRIPTOMIC DATA SHOW DIFFERENTIAL EXPRESSION DURING COFFEE – COLLETOTRICHUM KAHAWAE INTERACTIONS



Inês Diniz^{1,2}, Andreia Figueiredo³, Andreia Loureiro², Dora Batista^{1,2,4}, Helena Azinheira^{1,2}, Vitor Várzea^{1,2}, Ana Paula Pereira¹, Elijah Gichuru⁵, Pilar Moncada⁶, Leonor Guerra-Guimarães^{1,2}, Helena Oliveira², Maria do Céu Silva^{1,2}



¹Centro de Investigação das Ferrugens do Cafeeiro (CIFIC), Instituto Superior de Agronomia (ISA), Universidade de Lisboa, PT. ² Linking Landscape, Environment, Agriculture and Food (LEAF), ISA, Universidade de Lisboa, PT. ³Biosystems and Integrative Sciences Institute (BioISI), Faculdade de Ciências, Universidade de Lisboa, PT. ⁴ Centre for Ecology, Evolution and Environmental Changes (Ce3c), Faculdade de Ciências, Universidade de Lisboa, PT. ⁵ Coffee Research Institute, (KALRO),KEN. ⁶Cenicafe, COL.

Introduction

Coffee Berry Disease (CBD) caused by the hemibiotrophic fungus *Colletotrichum kahawae* (Ck) (Fig. 1) is a major constraint for Arabica coffee production at high altitudes in Africa [1,2,3,4]. Although plant breeding is an important strategy to produce coffee cultivars resistant to CBD, the molecular basis of this resistance is still poorly understood. A high throughput RNA sequencing approach was used to identify the transcriptional profile during key steps of Ck’s infection process in the variety Catimor (which exhibits field resistance to Ck in Kenya) and the susceptible variety Caturra. From this dataset, key genes of the salicylic acid (SA), jasmonic acid (JA) and ethylene (ET) pathways were selected and analysed by qPCR aiming to elucidate the phytohormone involvement in coffee-Ck interactions.

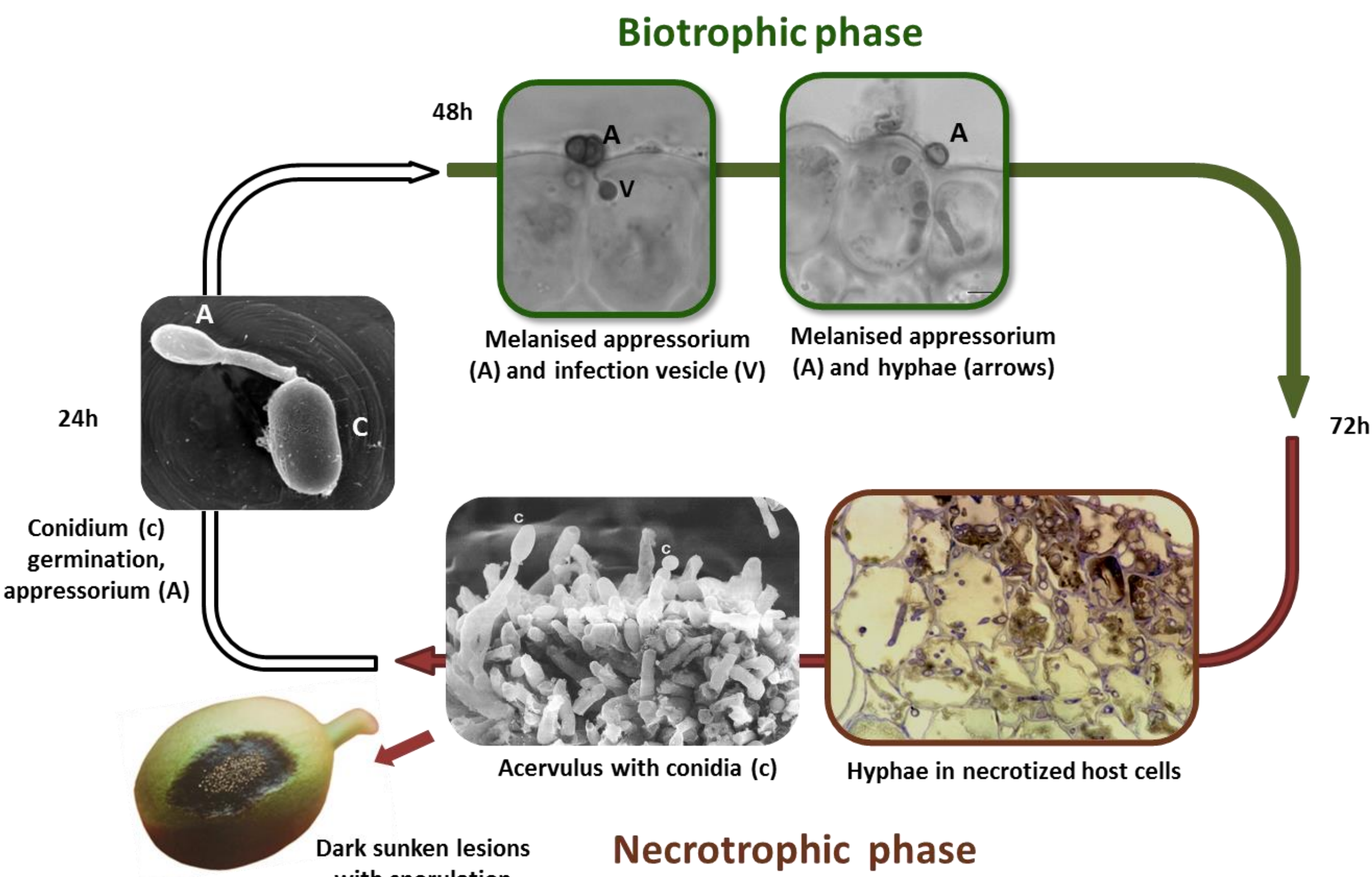


Fig. 1 - Time-course of Ck infection in coffee tissues

Results

- A global perspective of the relative expression levels of SA, JA and ET pathway-related genes in the resistant and susceptible varieties suggest a **more relevant role of JA and ET than SA** in this pathosystem (Fig. 2).
- On the contrary, the expression level of genes from JA and ET pathways showed differences between the two varieties.

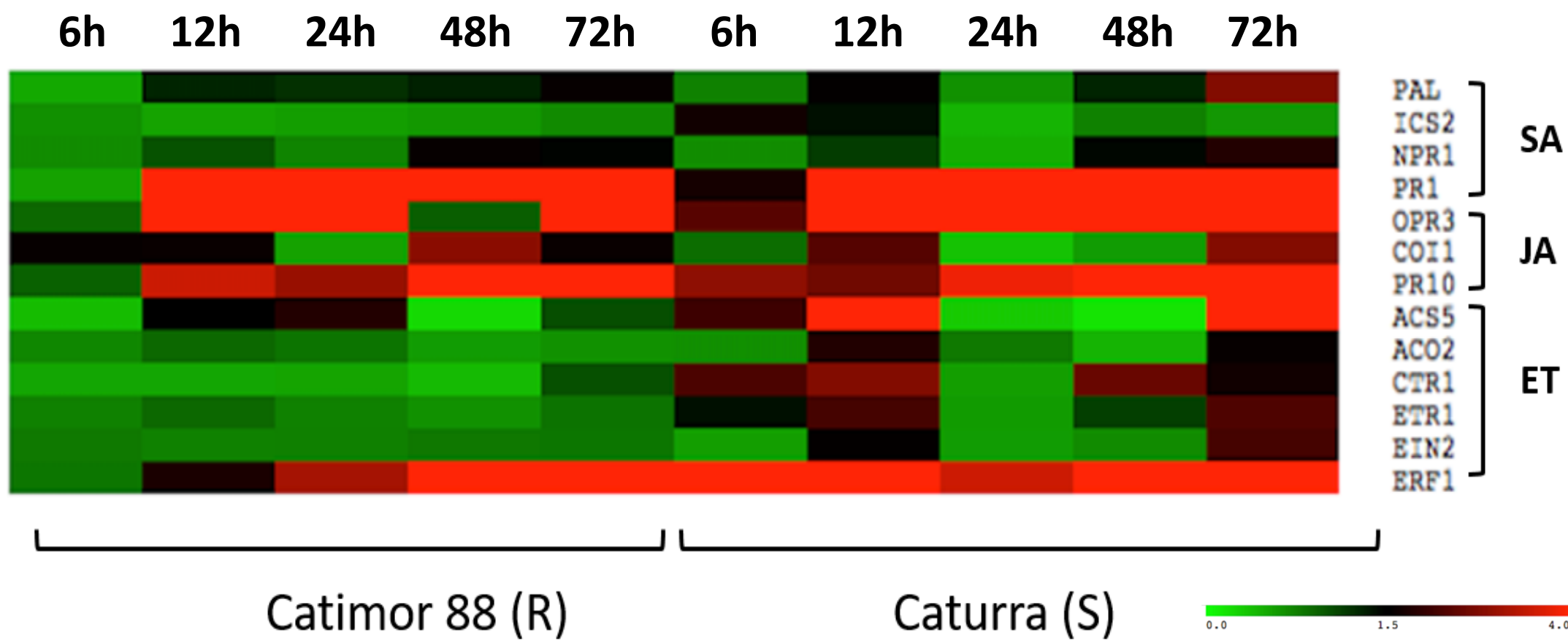


Fig. 2 - Expression analysis of SA, JA and ET pathway related genes in resistant and susceptible varieties inoculated with Ck.

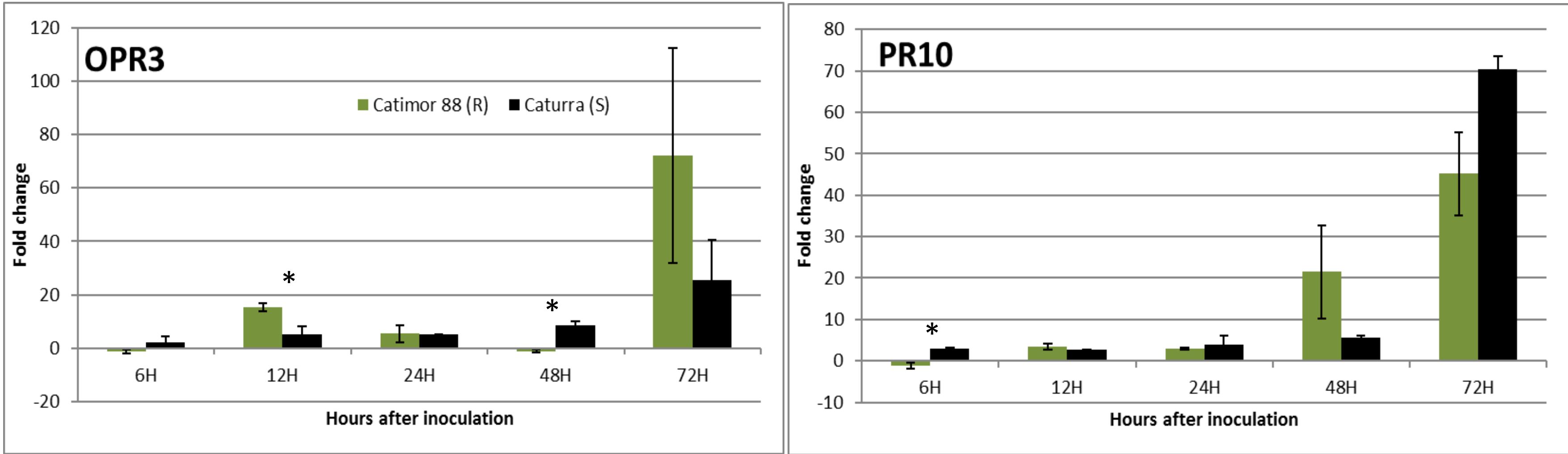


Fig. 3 - qPCR expression analysis of JA pathway related genes (OPR3-biosynthesis and PR10-hormone responsive).
* - statistical significance ($p \leq 0.05$) of gene expression between the two coffee varieties by the non-parametric Mann-Whitney U test

- An earlier and stronger induction of the JA pathway (OPR3-biosynthesis and PR10-hormone responsive related genes) was only observed in the resistant genotype suggesting that JA maybe responsible for the successful activation of defense responses (Fig. 3).

- In the susceptible genotype, ET seems to be involved in the tissue senescence observed at the beginning of the necrotrophic fungal growth (ACS5-biosynthesis and ERF1-hormone responsive related genes) (Fig. 4).

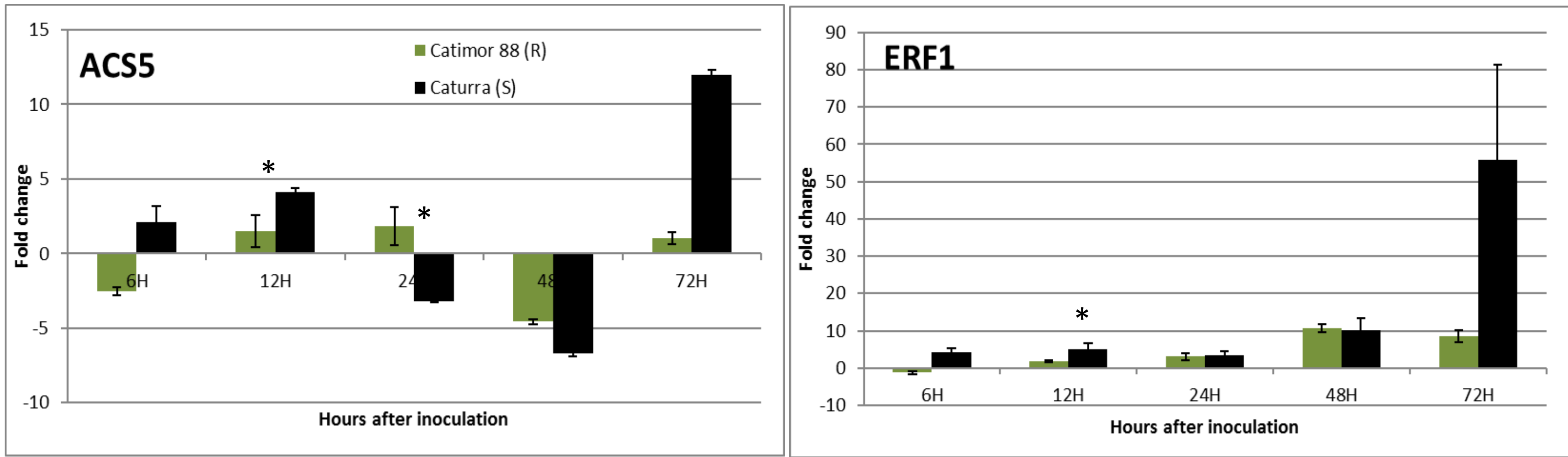


Fig. 4 - qPCR expression analysis of ET pathway related genes (ACS5-biosynthesis and ERF1-hormone responsive).
* - statistical significance ($p \leq 0.05$) of gene expression between the two coffee varieties by the non-parametric Mann-Whitney U test

Conclusions

Our results revealed a differential activation of the JA and ET phytohormone pathways in the coffee-Ck pathosystem. As far as we know, this is the first attempt to unveil the role of phytohormones in coffee responses to Ck infection, thus contributing to deepen our knowledge on the complex mechanisms of plant signaling and defense, and for future phenotyping approaches of coffee resistance.



To learn more about CIFIC

REFERENCES

[1] Gichuru EK, et al. (2008). *Plant Pathology* **57**:1117-1124, [2] Silva MC, et al. (2006). *Brazilian Journal of Plant Physiology* **18**:119-147, [3] Van der Vossen HAM, Walyaro DJ (2009). *Euphytica* **165**:105-116. [4] Loureiro et al. (2012). *Physiol Mol Plant Pathol* **77**: 23-32

ACKNOWLEDGMENTS

This work was funded by Portuguese national funds through Fundação para a Ciência e a Tecnologia (PTDC/AGR-GPL/112217/2009, LEAF (UI/AGR/04129/2013) and grants LEAF-AGR/04129/BPD/2015, SFRH/BPD/63641/2009, SFRH/BPD/104629/2014, SFRH/BD/84188/2012, SFRH/BPD/88994/2012.



Effect of $G \times E$ interaction on oil and protein content in wheat (*Triticum aestivum*, L.)

Ankica Kondić-Špika¹, Novica Mladenov¹, Ana Marjanović-Jeromela¹, Nada Grahovac¹, Sanja Mikić¹, Dragana Trkulja¹, Nikola Hristov²

¹*Institute of Field and Vegetable Crops, Novi Sad, Serbia*

²*Chemical Agrosava, Novi Beograd, Serbia*

Oil and protein content in wheat grain are quality indicators important for food processing, cosmetics and pharmaceutical industries. These and many other quality parameters could be significantly influenced by genotype, growing conditions and cultivation practices, especially fertilization. The objective of this study was to investigate effects of genotype, growing season, nitrogen (N) fertilization and their interactions on the oil and protein content in 24 varieties of winter wheat (*Triticum aestivum*, L.). Field trials with two N rates (low nitrogen N₄₅ and high nitrogen N₁₁₀) were conducted at the location of Rimski Šančevi, Serbia, during two growing seasons (2007 and 2008). The oil was extracted from wheat bran obtained by laboratory mill MLU 202. Classical Rushkovsky method was used to determine oil content, while protein content was determined by the ICC 105/2 method. Significant variability was found among the genotypes for both analysed traits. In two growing seasons and at different N rates, the oil content varied from 2.02% to 5.58%, with the average value of 3.96% and coefficient of variation (CV) 9.2%. The protein content ranged from 10.7% to 17.7% with the CV of 3.1%. All sources of variation (genotype - G, year - Y and N fertilization - F) and their interactions had significant effects on oil and protein content, except the Y \times F interaction on the latter. Regarding the oil content, the effect of the year was stronger than the effect of nitrogen (Figure 1). In contrast, protein content was more affected by the N fertilization than by the year (Figure 2). Principal component analysis was used for grouping genotypes according to their stability and reaction to different growing environments. Cvs. Cipovka, Dragana and Simonida were identified as very stable with high oil content in different growing conditions (Figure 3), while cvs. Bankut 1205 and Banatka were identified as potential sources of high protein content (Figure 4). The identified genotypes can serve as parents in wheat breeding for higher oil and protein content.

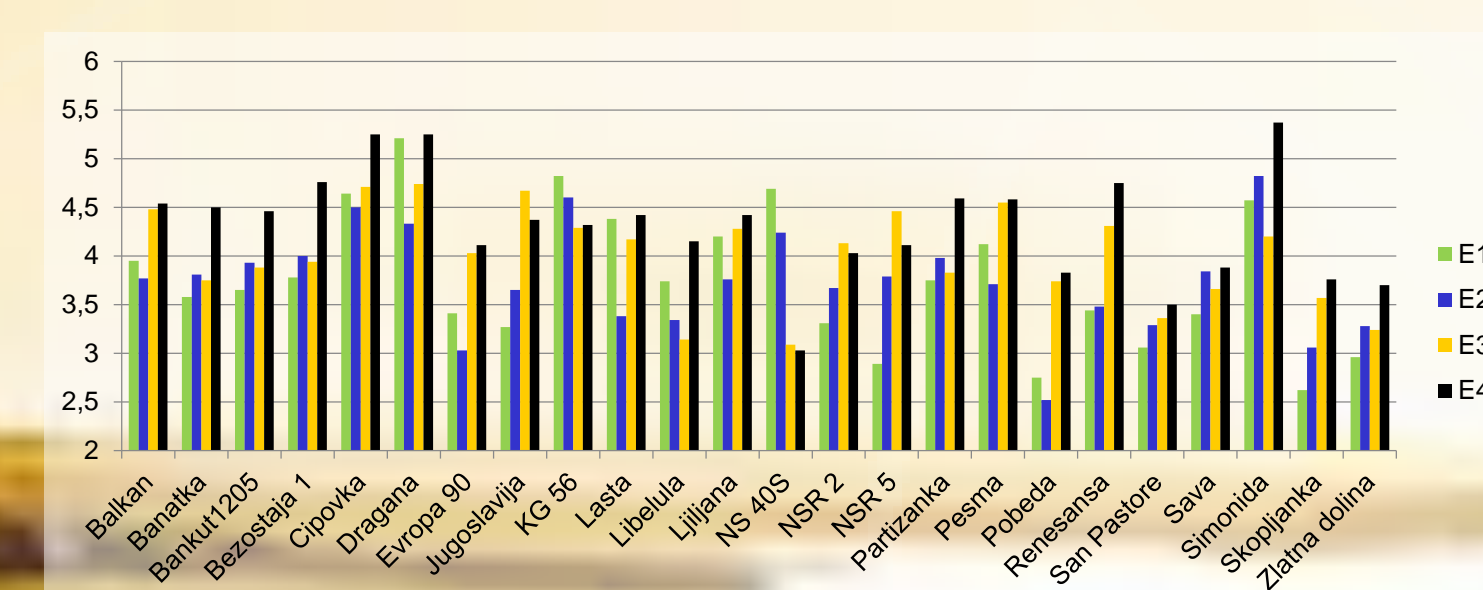


Figure 1. Effect of growing environments on oil content of 24 wheat genotypes: E1-2007, low N; E2-2007, high N; E3-2008, low N; E4-2008, high N.

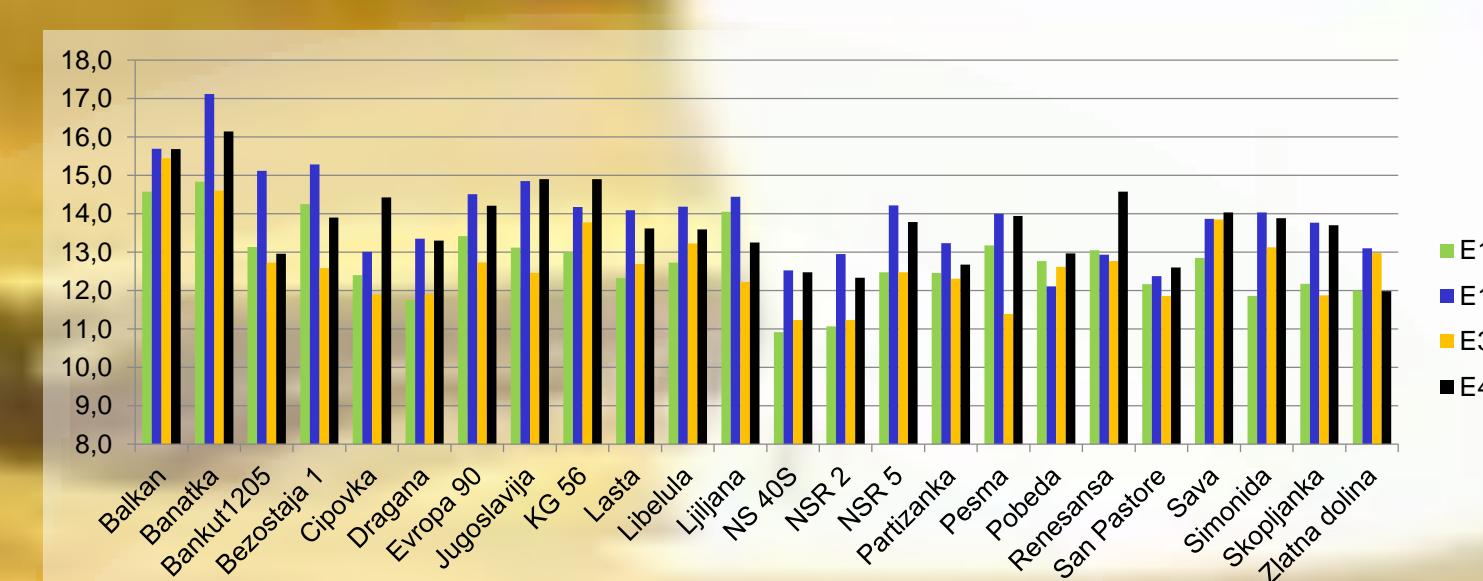


Figure 2. Effect of growing environments on protein content of 24 wheat genotypes: E1-2007, low N; E2-2007, high N; E3-2008, low N; E4-2008, high N.

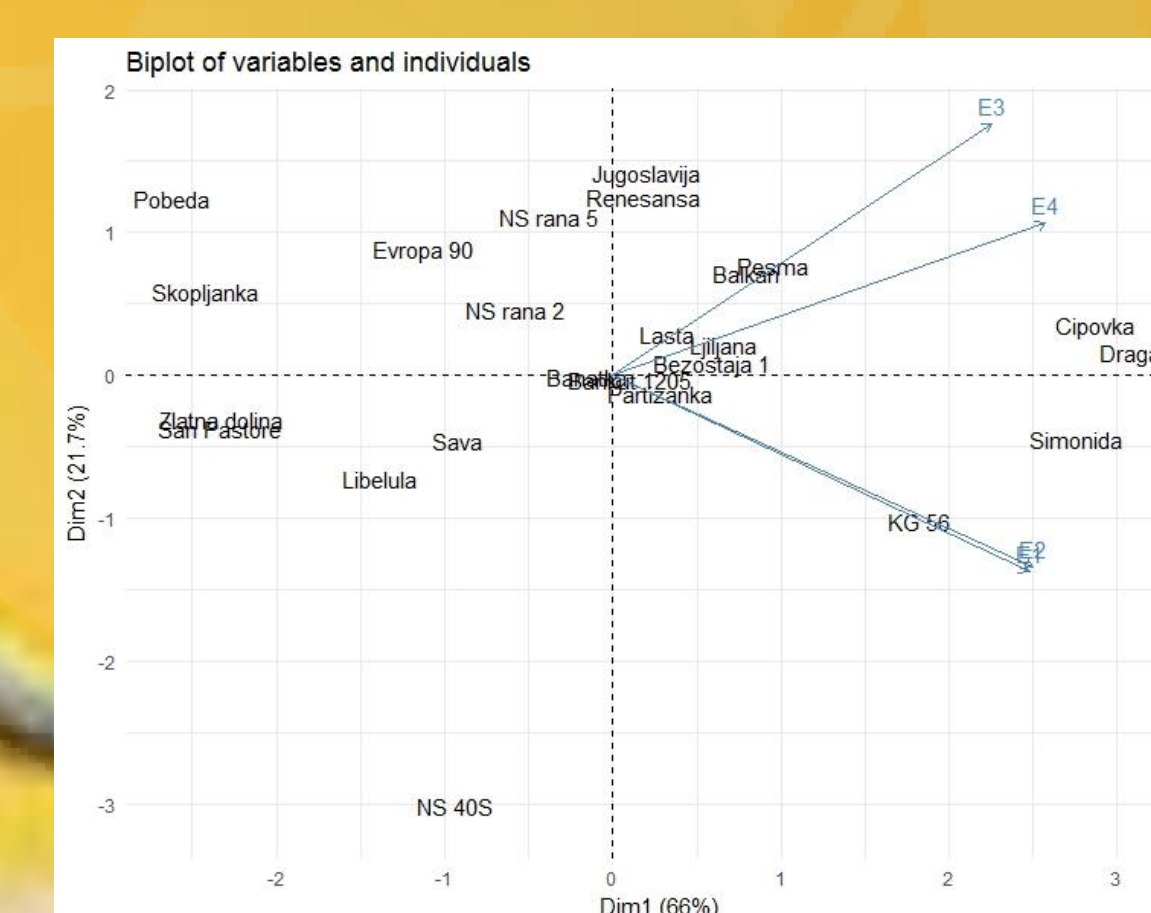


Figure 3. Principal component analysis (PCA) for oil content of 24 wheat genotypes in four growing environments: E1-2007, low N; E2-2007, high N; E3-2008, low N; E4-2008, high N.

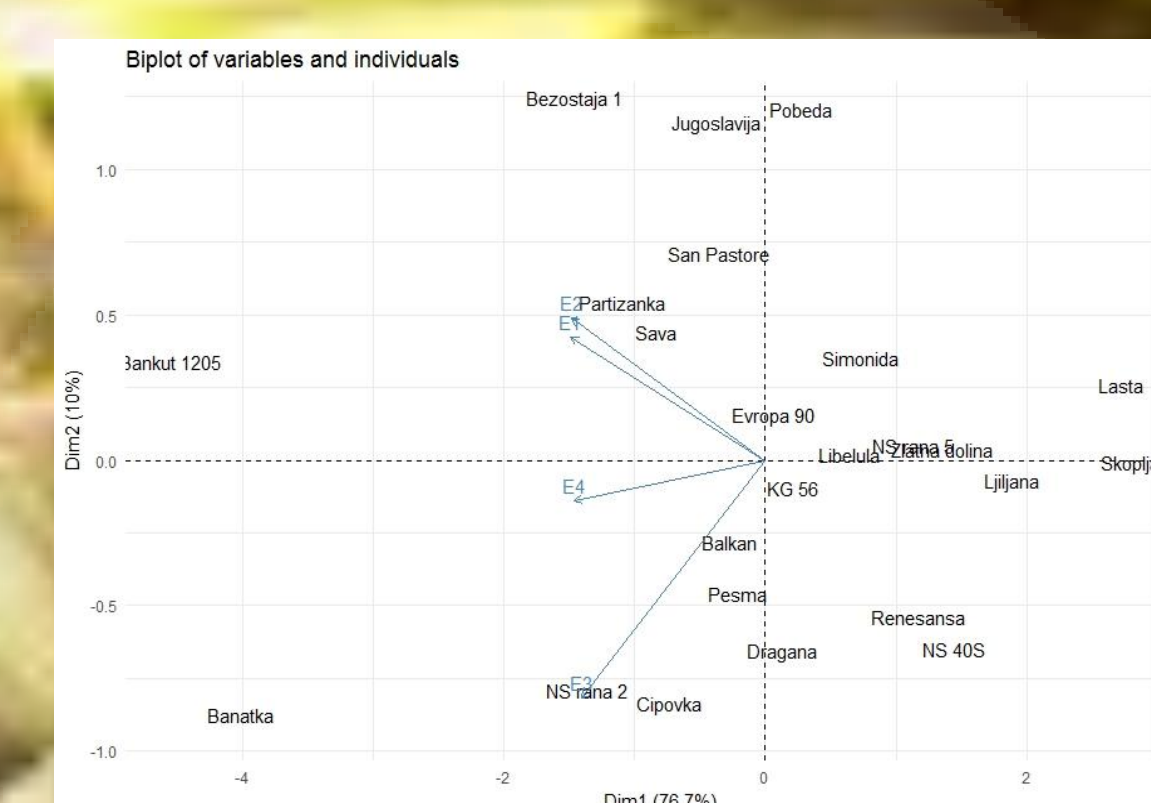


Figure 4. Principal component analysis (PCA) for protein content of 24 wheat genotypes in four growing environments: E1-2007, low N; E2-2007, high N; E3-2008, low N; E4-2008, high N.

ACKNOWLEDGMENT

This study was supported by the Ministry of Education, Science and Technological Development of the Republic of Serbia and by the COST Action FA 1306.

STUDY OF CMS STABILITY IN NS RAPESEED LINE

Ana Marjanović Jeromela, Aleksandra Dimitrijević, Jovanka Atlagić, Sreten Terzić, Ankica Kondić-Špika, Dragana Miladinović
Institute of Field and Vegetable Crops, Novi Sad, Serbia

Using stable cytoplasmic male sterility (cms) systems in rapeseed is essential in hybrid creation. This task is challenging since during conversion to sterile form some fertile individuals can be found in cms lines that can be determined by flower observation in the field. Improving the process of identifying atypical plant individuals is essential in both breeding and seed production. Obtaining accurate phenotypic evaluation is crucial in development of easy and quick laboratory tools for early detection of *cms* and (fertility restoration) *Rf* genes.

We examined rapeseed lines which are a part of Novi Sad breeding program and in which Ogu INRA cms was introduced. We analyzed anther development and microsporogenesis on cytological level and observed rudimentary developed anthers in 16 cms lines.

Interruption in microsporogenesis occurred most often after the phase of tetrads. Additionally, we used cms-p molecular marker (Sigareva and Earle 1997) for evaluation of the presence/absence of *cms* gene in 12 experimental cms lines (15 individuals per line). Marker cms-p amplified a single band approximately 500 bp in all tested cms individuals (Figure 1), while this band was absent in fertile individuals.

By performing accurate field phenotyping and developing quick methods, such as cytogenetic and molecular markers for gene identification, obtaining rapeseed cms lines for hybrid creation can be significantly accelerated. However, for identification of the best suited molecular markers for marker assisted selection, reliable and time-efficient phenotyping is imperative.

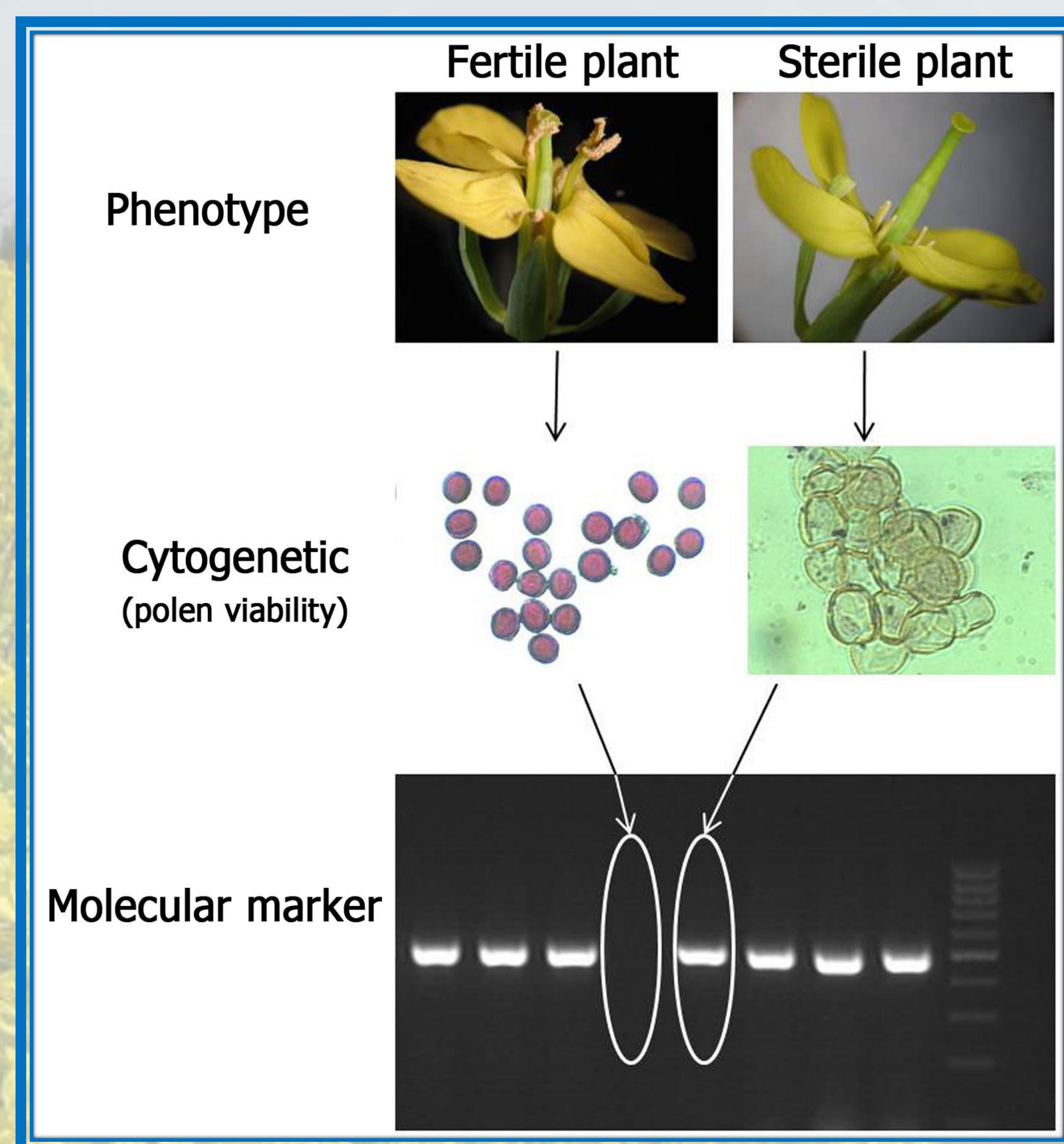


Figure 1. Discrimination between fertile and sterile rapeseed genotypes based on their phenotype and cytogenetic and molecular profiles

ACKNOWLEDGMENT

This study was supported by the Ministry of Education, Science and Technological Development of the Republic of Serbia and by the COST Action FA 1306.

REFERENCE

Sigareva, M. A. and Earle, E. D. 1997. Theor Appl Genet 94: 213-220.

Ana Marjanović Jeromela
ana.jeromela@ifvcns.ns.ac.rs

Aleksandra Dimitrijević
aleksandra.dimitrijevic@ifvcns.ns.ac.rs

Jovanka Atlagić
jovanka.atlagic@ifvcns.ns.ac.rs

Sreten Terzić
sreten.terzic@ifvcns.ns.ac.rs

Ankica Kondić-Špika
ankica.spika@ifvcns.ns.ac.rs

Dragana Miladinović
dragana.miladinovic@ifvcns.ns.ac.rs

SOURCES OF RESISTANCE TO DOWNY MILDEW DISEASE IN WILD ROCKET CROP

Paula S. Coelho^{a,b}, Luísa Valério^b, and António A. Monteiro^b

^a INIAV, National Institute for Agrarian and Veterinarian Research, Quinta do Marquês, Av. da República, 2784-505 Oeiras, Portugal

^b LEAF, Linking Landscape, Environment, Agriculture and Food, ISA, Universidade de Lisboa, Tapada da Ajuda 1349-017 Lisboa, Portugal

Introduction

Wild (*Diplotaxis tenuifolia*) and cultivated (*Eruca sativa*) rocket varieties are used in Mediterranean cuisine in fresh cut salads, being part of packaged ready-to-eat products and garnish for food.

Rocket downy mildew (DM), caused by the oomycete from the genus *Hyaloperonospora*, is a severe leaf disease that attacks all plant stages and is particularly adverse in packed baby leaf salads, because apparently-healthy leaves can sporulate inside the bags.

Due to restrictions in the use of chemicals, resistant genotypes are an important tool for disease control. The main objectives of this study were: (1) to develop a method for cotyledon and leaf DM evaluation in controlled conditions, and (2) to screen different genotypes for sources of resistance.



Cotyledons and leaves of 21 days rocket plants sporulated with downy mildew.

Material and Methods

Plant material: Seeds of 10 commercial wild rocket lines were germinated in multi-cell trays (4x4x5 cm) filled with a peat-based substrate (*Traysubstrat*) and maintained in a controlled growth chamber at day/night 23/21°C and 19/5h photoperiod under cool white fluorescent light for 14d. A total of 96 plants from each accession were tested in three replications.

Inoculum preparation: Rocket leaves infected with *Hyaloperonospora* were collected in the field and maintained in the laboratory. Sporulating leaves were dipped in distilled water and gently agitated to dislodge conidia and the resulting inoculum was diluted to 2.5×10^4 spores.ml⁻¹.

Laboratory testing: Plants at two-leaf stage were inoculated by pulverization with the conidial suspension. The plants were incubated at 16°C (RH=100% in the dark) for 24h and return to the growth chamber under the conditions described for seedlings production. Six days after inoculation, the plants were lightly sprayed with distilled water and re-incubated (16°C in the dark) for 24h. Each cotyledon and the first two leaves were visually assessed at 21d, using a six-class scale of increasing susceptibility (Coelho *et al.*, 2012).

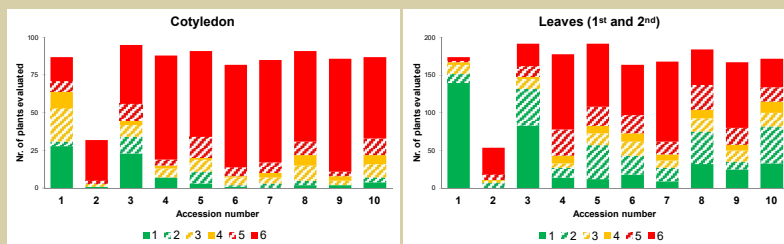
Data analysis: The data were averaged and the standard errors were calculated. The accessions were classified in three resistant groups according to cotyledon and leaves disease index: resistant (DI≤2.5); intermediate resistant (2.5<DI<4.5) and susceptible (DI≥4.5).

Conclusion

- The methodology is adequate for screening rocket plants for downy mildew resistance.
- A good correlation ($r = 0.927^{***}$) was observed between resistance to DM at cotyledon and true-leaf stages.
- Clear differences in DM susceptibility on wild rocket leaves were identified ranging from susceptibility to resistance. Varietal resistance has potential to provide good downy mildew control, which encourages further testing of material from different origin.

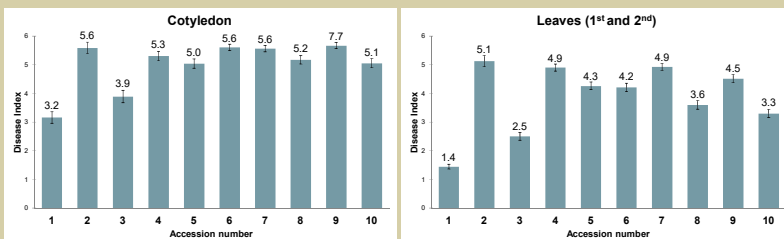
Results and Discussion

Number of plants per six-class of resistance of cotyledon and leaves



- All wild rockets lines were heterogeneous for resistance showing plants in every class of resistance. The interaction phenotype ranged between dark necrosis without sporulation (classes 1-2) to heavy sporulation (class 6).

Disease index of cotyledon and leaves (mean±S.E.) of ten wild rocket



- Cotyledons of rocket plants were more susceptible to DM than first two leaves.
- At cotyledon stage there were no resistant accessions, only two accessions showed intermediate resistance (Nr. 1 and 3) and the remaining eight were susceptible (DI higher than 5.1).
- At leaf stage wide differences in DM susceptibility were identified. Two accessions were resistance (Nr. 1 and 3), four accessions were intermediate (Nr. 5, 6, 8 and 10) and four accessions were susceptible (Nr. 2, 4, 7 and 9).

Reference

Coelho P.S., Vicente J.G., Monteiro A.A. and Holub E.B. 2012. Pathotypic diversity of *Hyaloperonospora brassicae* collected from *Brassica oleracea*. *Eur. J. Plant Pathol.* 134: 763-771.

Acknowledgement This research was supported by Radialis project.



The **Advanced Microscopy Facility** (AdvMicro) maintains and develops cutting-edge and custom-designed optical microscopy solutions, and provides associated assistance to researchers at the VBC and beyond.

Core Team:



Lijuan Zhang
Marek Suplata
Edmundo Sanchez Guajardo
Kareem Elsayad (Facility Head)

If you are interested in using one of our microscopes or collaborating on a project you can contact us at:
info@am.vbcf.ac.at

For more info (and wiki on available techniques) see:
www.vbcf.ac.at/am

The **Vienna Biocenter Core Facilities GmbH** (VBCF) is a public funded non-profit research institute, situated at the Vienna Biocenter. We offer access to state of the art research infrastructure and scientific services.

VBCF is organized in **11 scientific core facilities** equipped with cutting edge instruments and highly skilled technical and scientific personnel.

We acknowledge funding from:

Brillouin Light Scattering (BLS) Spectroscopy and correlative Fluorescence Brillouin imaging (FBI) based non-invasive Mechanical Phenotyping of *Arabidopsis* Mutants

Lijuan Zhang¹, Stephanie Werner², Marçal Gallemí², Jixiang Kong², Edmundo R. Sánchez Guajardo¹, Yvon Jaillais³, Thomas Greb², Youssef Belkadir², Kareem Elsayad¹

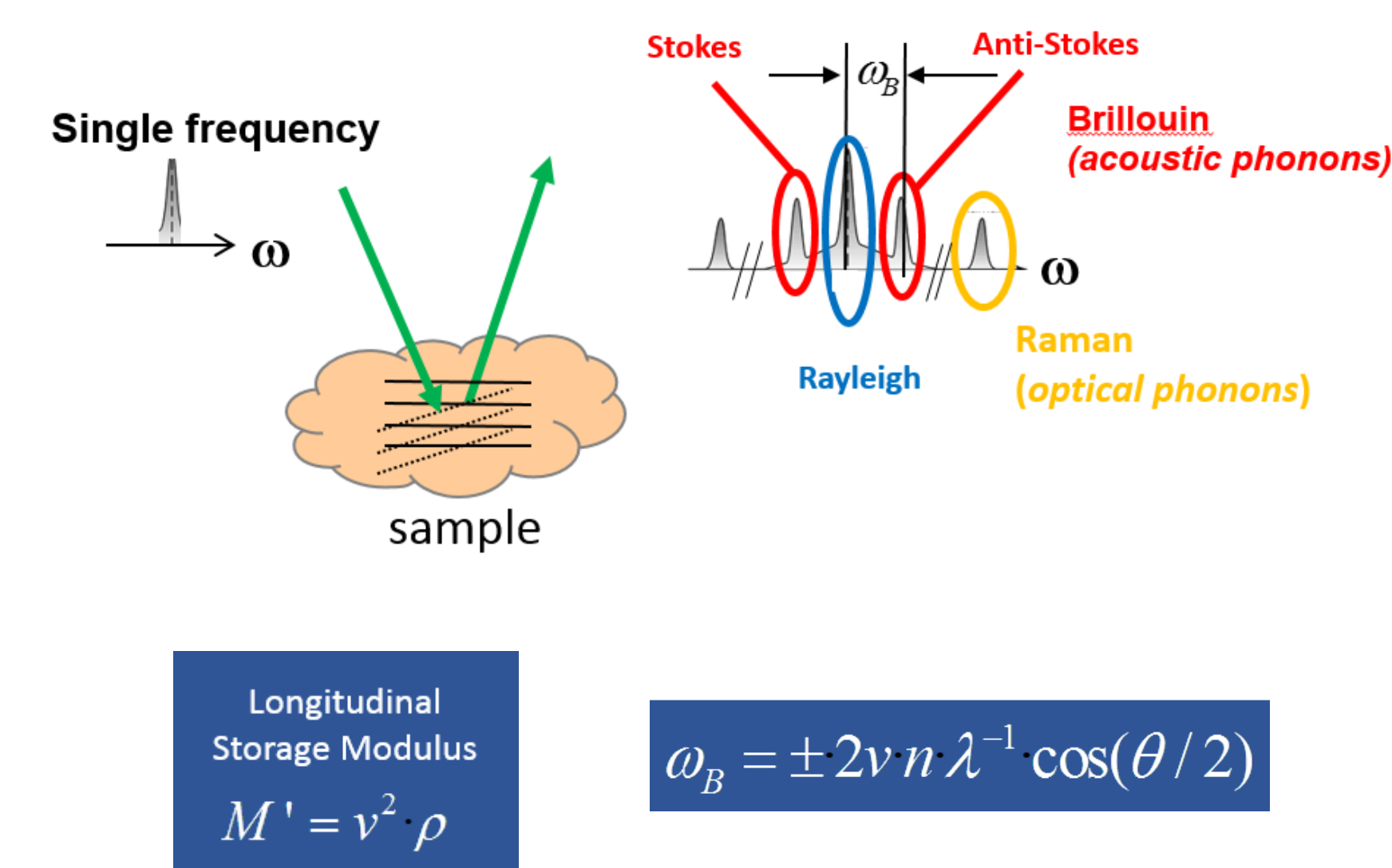
¹ Advanced Microscopy Facility, Vienna Biocenter Core Facilities, A-1030 Vienna, Austria

² Gregor Mendel Institute, Austrian Academy of Sciences, Vienna Biocenter, A-1030 Vienna, Austria

³ Laboratoire Reproduction et Développement des Plantes, Univ Lyon, ENS de Lyon, UCB Lyon 1, CNRS, INRA, F-69342 Lyon, France

THE PRINCIPLES OF BLS MICROSCOPY

FBI measures viscoelasticity at high frequencies

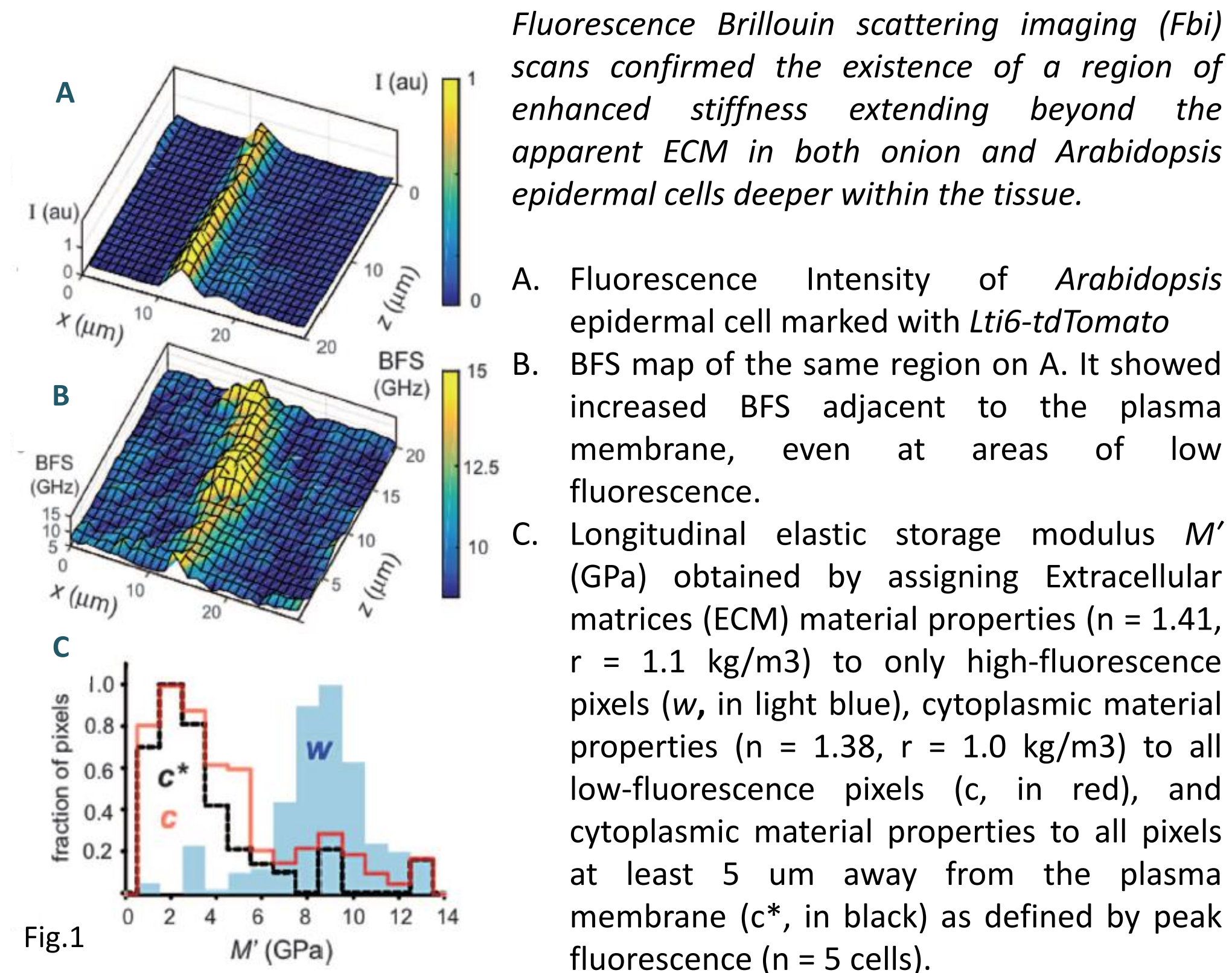


Brillouin light-scattering microscopy relies on the interaction of light with inherent thermal vibrations (acoustic phonons) in the sample. When probing a sample with a single-frequency laser source, this interaction will result in a small component of the backscattered light that is spectrally shifted by several gigahertz relative to the wavelength of the probing laser. This spectral shift is referred to as the Brillouin frequency shift (BFS) and is proportional to the speed of sound waves in the sample, V . V can be used to calculate the longitudinal elastic storage modulus M' at the probed region via $V = \sqrt{M'/\rho}$, where ρ is the sample density.

Qualitatively, the Brillouin Scattering signal can be thought of as the result of very small red- and blue- shifts (Stokes and anti-Stokes Brillouin peaks in figure) in the scattered light from moving density fluctuations— the optical equivalent to the famous Doppler effect. The mechanical properties determine the dynamics of these fluctuations and hence also the measured amount of red & blue shift of the Brillouin peaks.

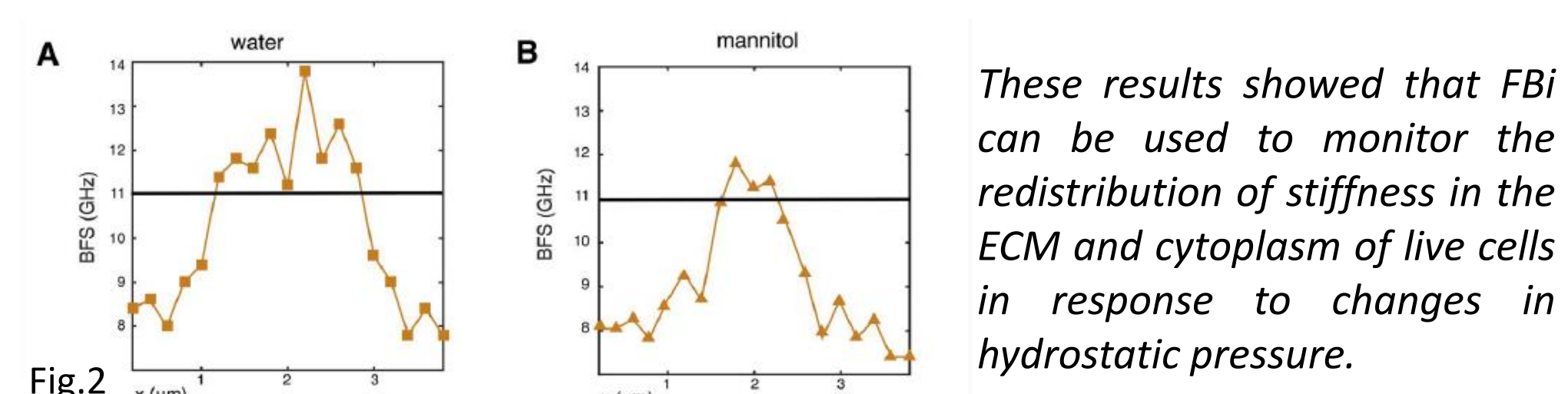
OBTAINED RESULTS AND SCHEME OF THE SETUP

I. *Arabidopsis* epidermal cells, where the plasma membrane is marked with *Lti6-ttdTomato*



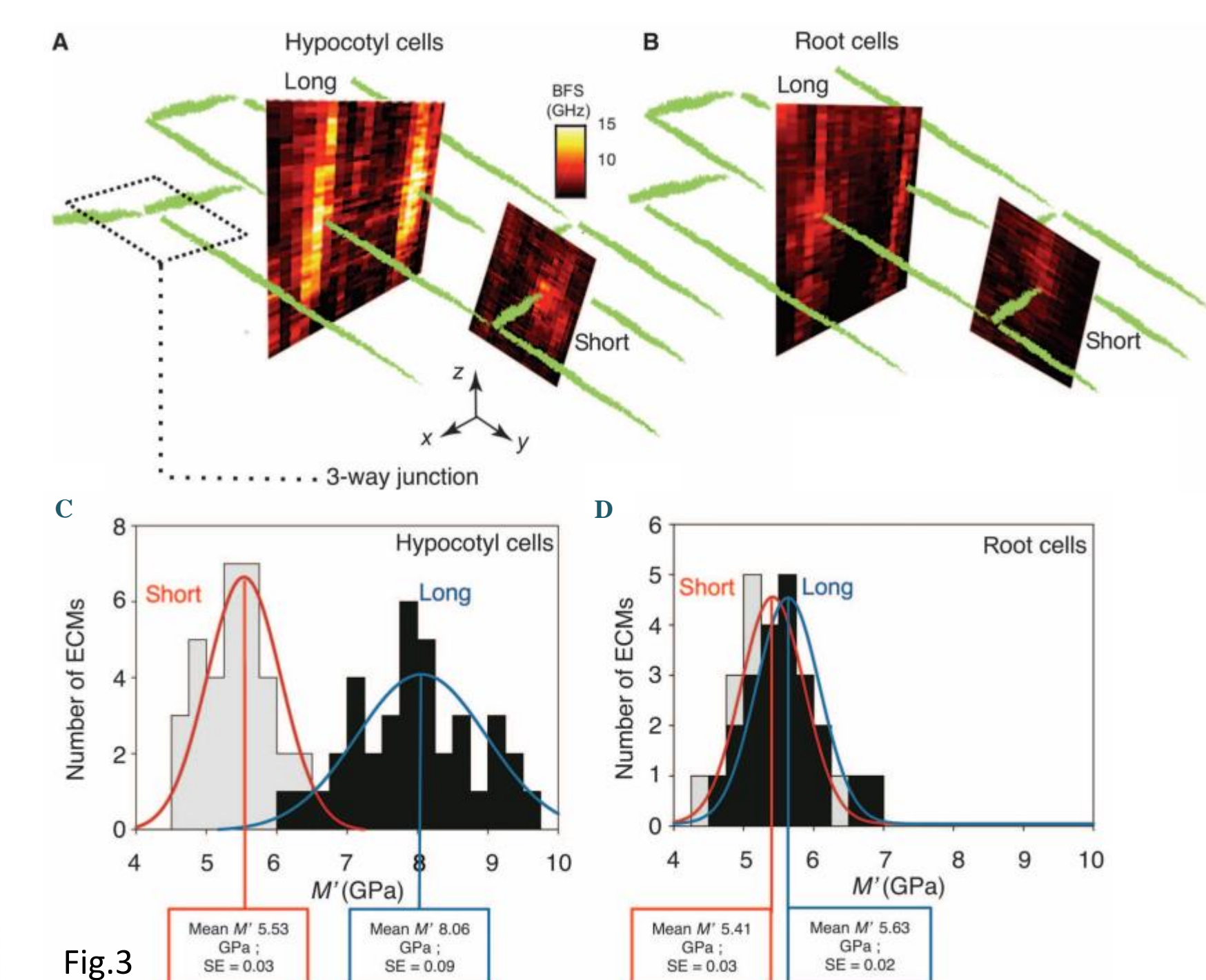
II. We hypothesize that the internal turgor pressure could modulate the stiffness of cytosolic regions surrounding the plasma membrane.

To test this hypothesis, we subjected the hypocotyls of *Lti6-ttdTomato* transgenic *Arabidopsis* seedlings to a hypertonic solution containing 0.8 M mannitol, which causes shrinkage of the cell (plasmolysis), and performed FBI scans before (Fig. 2A) and after (Fig. 2B). Within 10 min of plasmolysis, we observed a drop and a redistribution of the BFS over an area of ~ 1 μ m, approximately corresponding to the ECMs.



III. We measured the BFS of the long (parallel to the axis of growth) and short (perpendicular to the axis of growth) sides of the growing cells in the hypocotyls and roots of live *Arabidopsis* seedlings. Our measurements show that the ECM located on the long sides of hypocotyls cells is significantly stiffer than the ECM on the short sides (Fig. 3, A and B).

To confirm the difference was a universal property, we analyzed the stiffness of the ECMs in matching long and short sides of cells of numerous independently grown hypocotyls and roots (Fig. 3, C and D). This revealed a statistically significant difference in M' of the ECM of the long and short sides. In contrast, the elongating root cells had similar ECM stiffness on the long and short sides (Fig. 3B).



SCHEME OF THE FBI SETUP

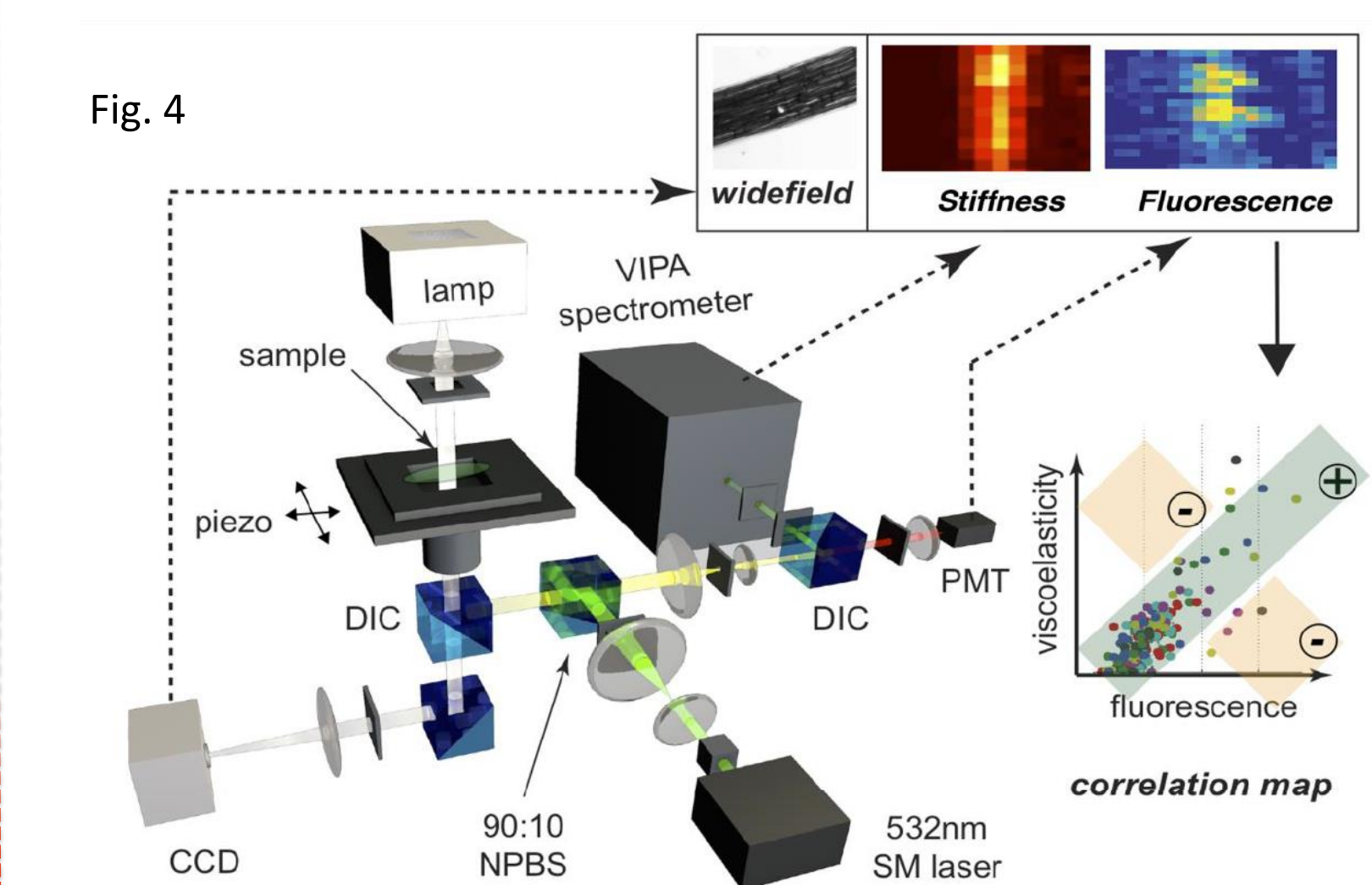
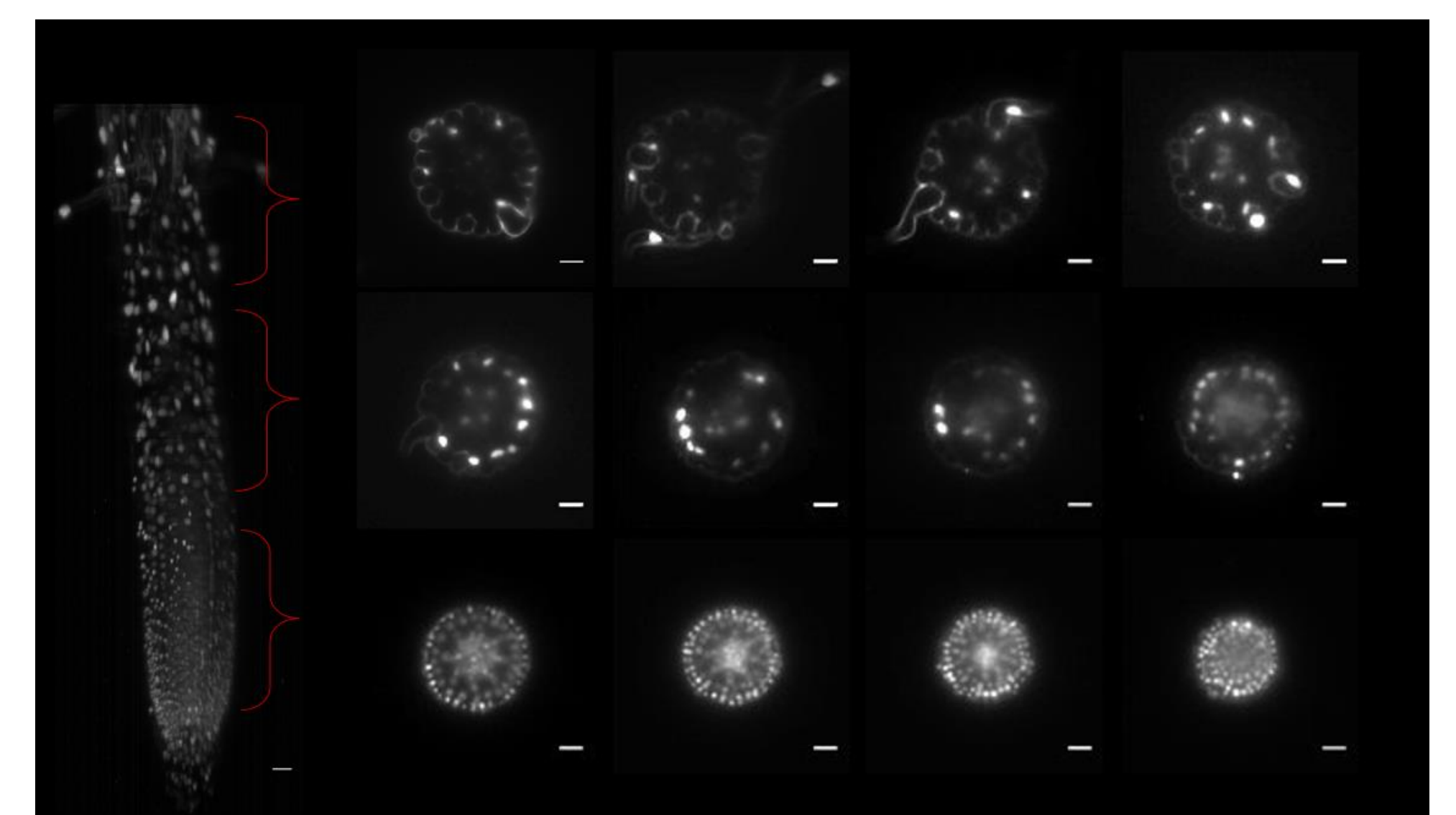
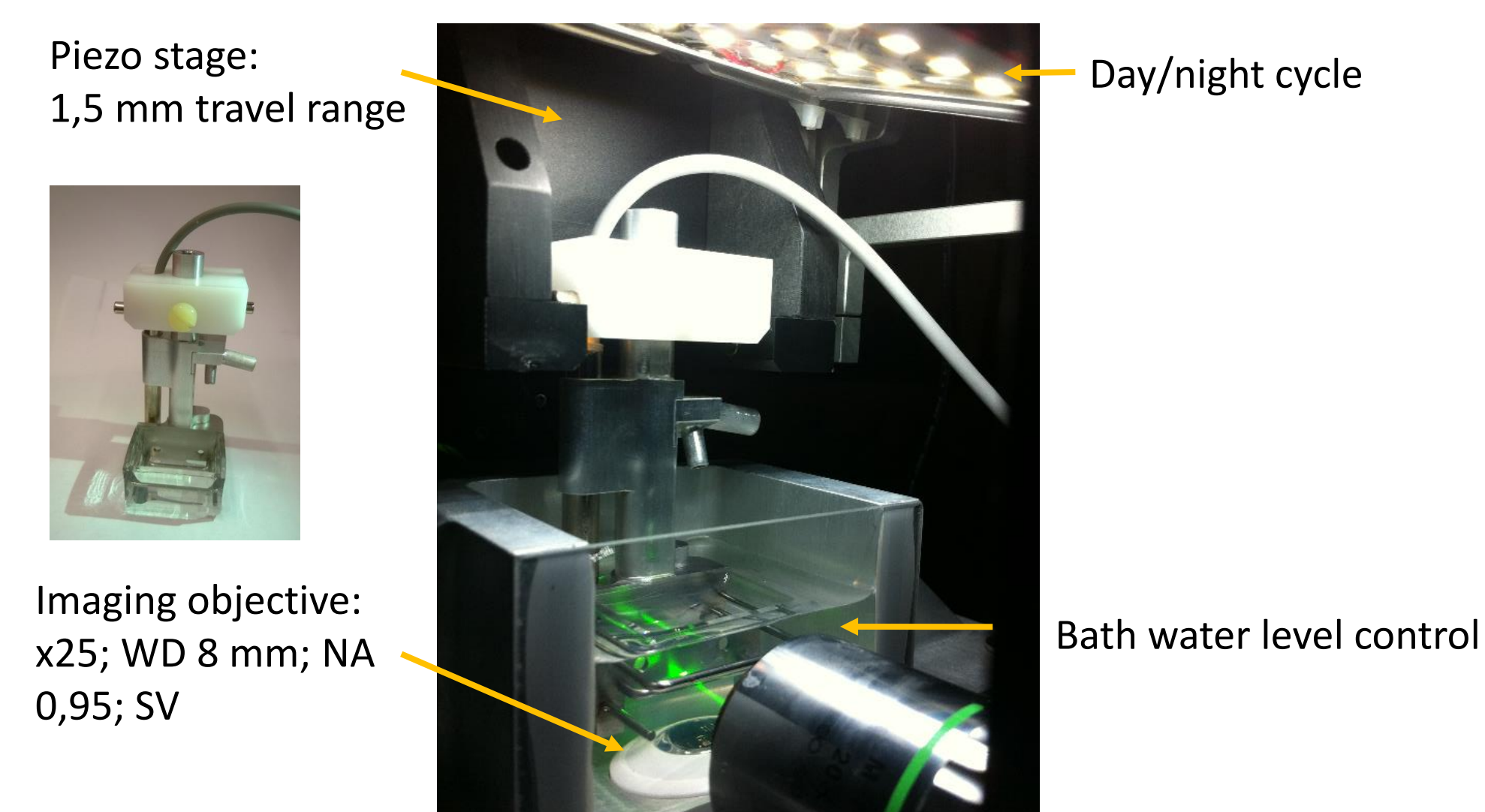
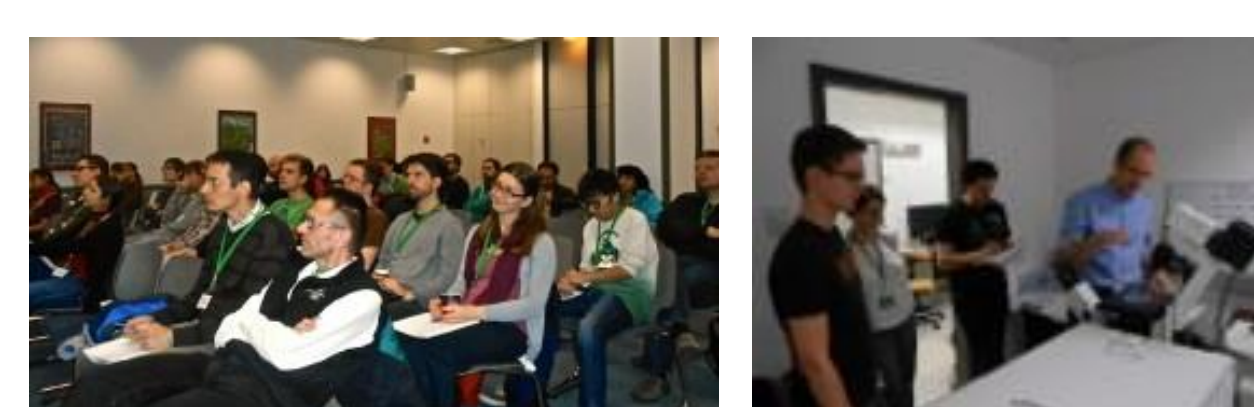


Fig. 4 DIC = Dichroic Mirror, PMT = Photo-Multiplier Tube, NPB S= non-polarizing beam splitter, CCD = Charge-Coupled Device, VIPA = Virtually-Imaged Phased Array. Top Insets: transmitted light picture, viscoelasticity scans (red-black), FBI scans (blue-yellow).

LIGHT SHEET MICROSCOPY FOR PHENOTYPING



Workshops on available techniques



“Frontiers in Optic & Microscopy Lecture Series”

Guiliano Scarcelli (Harvard)
Alberto Diaspro (Genoa)
Tony Wilson (Oxford)
Hari Shroff (NIH/NIBB)
Eric Betzig (Janelia Farm)
Peter Torok (Imperial College)
Pavel Tomancak (MPI,Dresden)
Joerg Enderlein (Goettingen)

Mini Projects

Custom microscope upgrades & modifications for specific experiments



STRESS TOLERANCE IN PRE-CONDITIONED PLANT POPULATIONS THROUGH PULSE AMPLITUDE MODULATED (PAM).

JOÃO CARREIRAS^{1*}, CARLA GAMEIRO¹, ANA RITA MATOS², JOÃO CARLOS MARQUES³, BERNARDO DUARTE¹, ISABEL CAÇADOR¹

* CORRESPONDING AUTHOR: JOÃO CARREIRAS, EMAIL: JOAOALBUQUERQUECARREIRAS@GMAIL.COM

¹ MARE – MARINE AND ENVIRONMENTAL SCIENCES CENTRE, FACULTY OF SCIENCES OF THE UNIVERSITY OF LISBON, CAMPO GRANDE 1749-016 LISBON, PORTUGAL.
² BIOISI—BIOSYSTEMS AND INTEGRATIVE SCIENCES INSTITUTE, PLANT FUNCTIONAL GENOMICS GROUP, PLANT PHYSIOLOGY DEPARTMENT, FACULTY OF SCIENCES OF THE UNIVERSITY OF LISBON, CAMPO GRANDE 1749-016 LISBON, PORTUGAL.
³ MARE – MARINE AND ENVIRONMENTAL SCIENCES CENTRE, C/O DEPARTMENT OF ZOOLOGY, FACULTY OF SCIENCES AND TECHNOLOGY, UNIVERSITY OF COIMBRA, 3000 COIMBRA, PORTUGAL.



Introduction

Different plant populations of the same species can be exposed to different environmental stresses which can precondition plant tolerance and resistance responses to other stresses. Thus, it is important to identify and assess functional traits in which environmental variability has a significant role in how the species respond to global and local change. The effects of abiotic and biotic stresses in plants are generally revealed by chlorophyll fluorescence analysis, a non-invasive measurement of photosystem II (PSII) activity. Pulse-amplitude modulated (PAM) fluorometry is one of the most common techniques used to study the induction and quenching of chlorophyll fluorescence in physiological studies. Using PAM to measure heat-stress induced changes in two halophytes populations with different pre-conditioning histories (heavy metal contaminated are versus non-contaminated environment) showed significant physiological variances in the PSII photochemistry regarding response and resistance to the same stress which shows intraspecific variation probably due to environmental variation. The findings were supported by biochemical analysis of the leaf fatty acid composition presenting a significant variance in linoleic acid (18:2), linolenic acid (18:3) and palmitic acid (16:0) concentrations and between the ratio of linoleic acid to linolenic acid, which expresses the same variability between populations. In the near future, it will be important to increase long-term studies on natural populations in order to understand plant response to environmental factor including climate change.

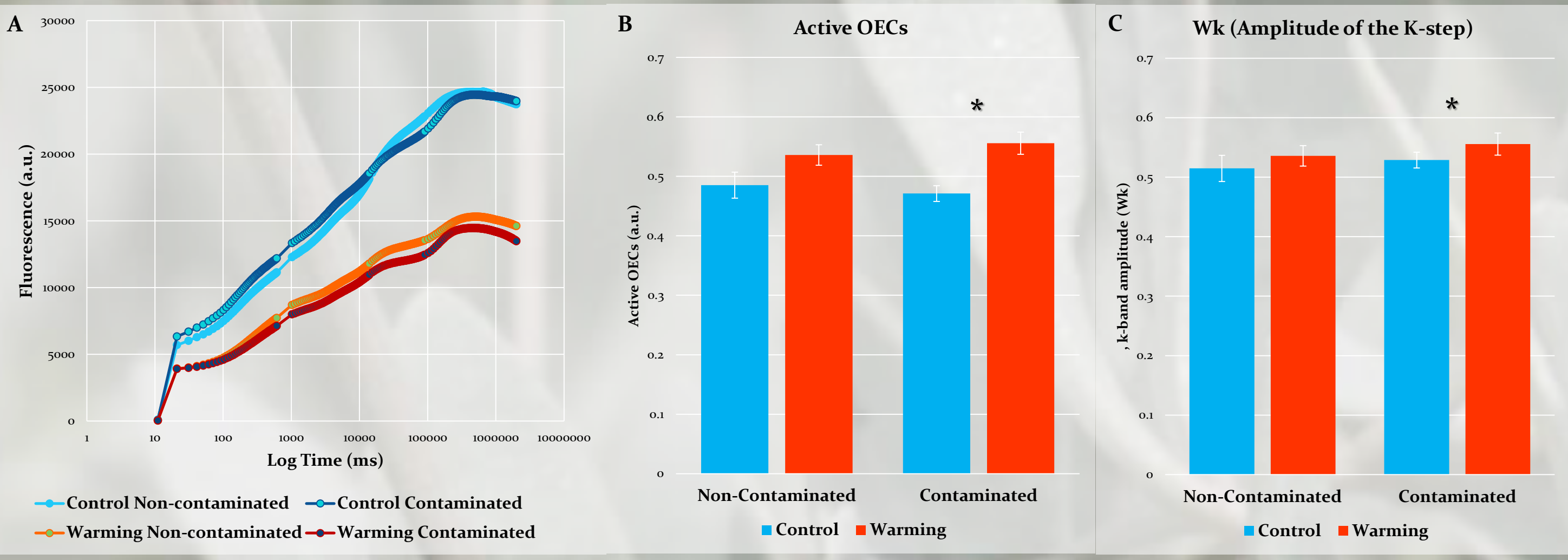


Figure 1: Kautsky curves obtained from chlorophyll fast-induction curves (A) and kautsky curves derived parameters: Active oxygen-evolving complexes (OECs; B) and Wk, k-band amplitude (C) in *H. portulacoides* (average \pm SE, N=5, asterisk marks significant differences between treatments at $p<0.05$).

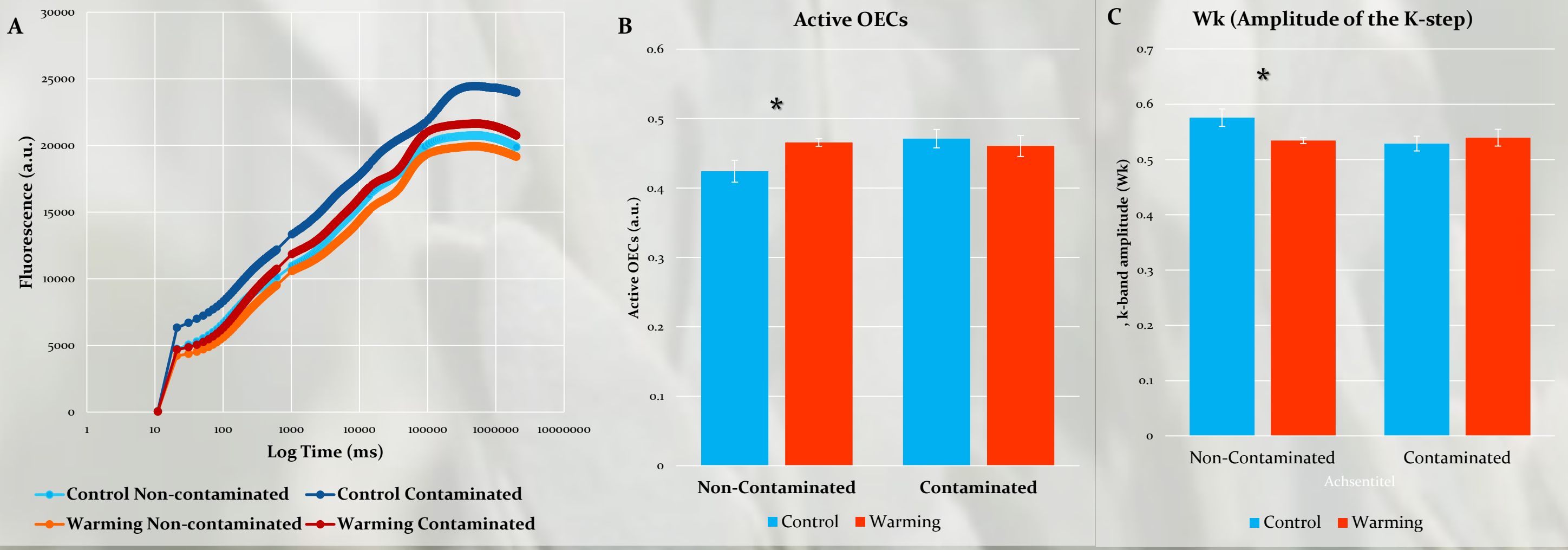


Figure 2: Kautsky curves obtained from chlorophyll fast-induction curves (A) and kautsky curves derived parameters: Active oxygen-evolving complexes (OECs; B) and Wk, k-band amplitude (C) in *S. patens* (average \pm SE, N=5, asterisk marks significant differences between treatments at $p<0.05$).

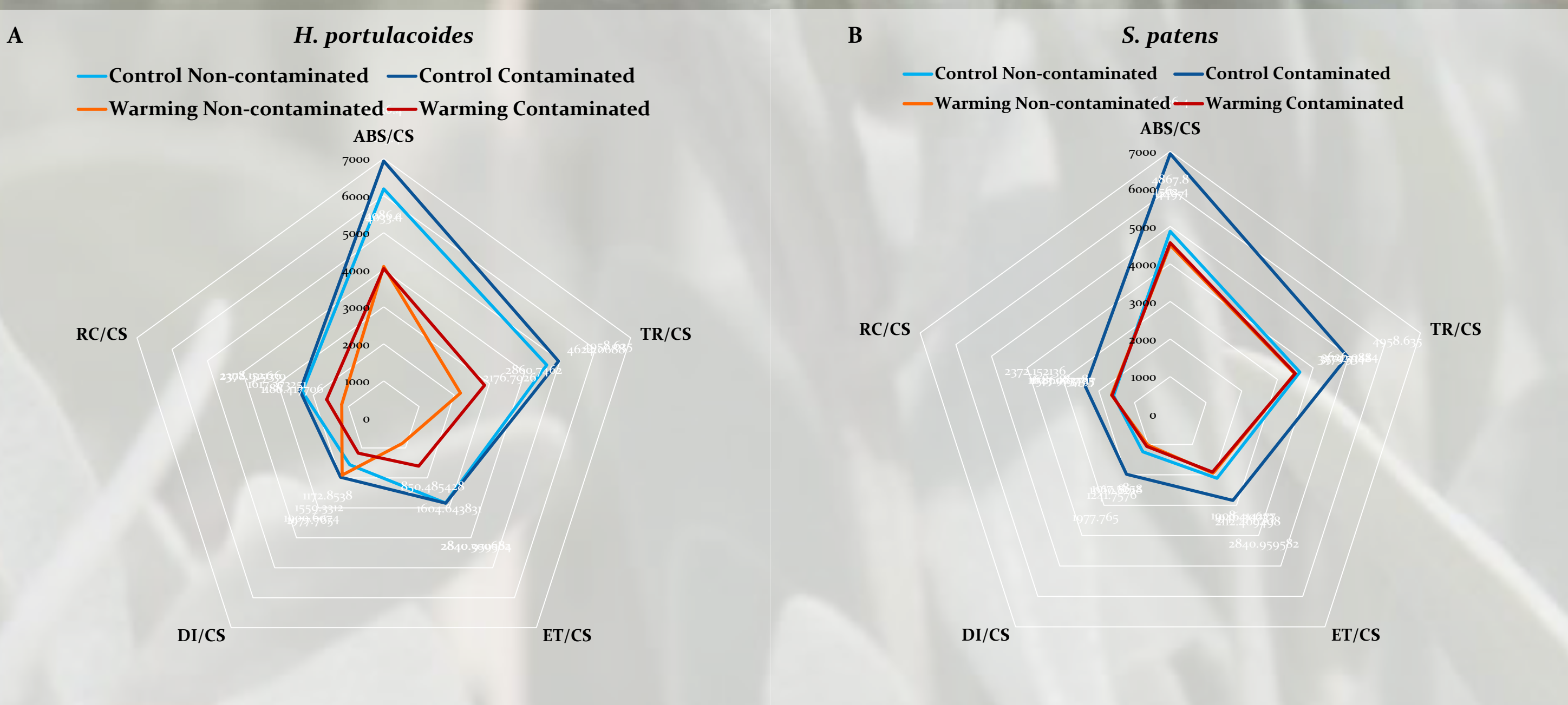


Figure 3: Phenomenological fluxes: Absorbed (ABS/RC), Trapped (TR/CS), Transported (ET/CS) and Dissipated (DI/CS) energy fluxes and PSII Reaction Center density (RC/CS) in *H. portulacoides* (A) and *S. patens* (B).

References
• Reborela R., Caçador I. (2007) Halophyte vegetation influences in salt marsh retention capacity for heavy metals. *Environmental Pollution*, **146**, 1 147-157
• Duarte B., Goessling J.W., Marques J.C., Caçador I., (2015b) Ecophysiological constraints of *Aster tripolium* under extreme thermal events impacts: merging biophysical, biochemical and genetic insights. *Plant Physiology and Biochemistry*, **97**, 217-228.
• Matos A.R., Hourton-cabassa C., Cicek D., Rezé N., Alternative oxidase involvement in cold stress response of *Arabidopsis thaliana* fad2 and FAD3+ cell suspensions altered in membrane lipid composition. *Plant and Cell Physiology*, **48**, 856-865.

Acknowledgments
The authors would like to thank to the "Fundação para a Ciência e Tecnologia (FCT)" for funding the research in the Marine and Environmental Sciences Centre (MARE) throughout the project UID/MAR/04292/2013 and the Biosystems and Integrative Sciences Institute (BioISI) throughout the project UID/MULTI/04046/2013. B. Duarte investigation was supported by FCT throughout Post-doctoral grants (SFRH/BPD/115162/2016).

Methodology

Samples of two different populations of *Halimione portulacoides* and *Spartina patens* were collected in the Tagus estuary. The first population was collected in Alcochete salt marsh a non-contaminated environment belonging to the Tagus Estuary Natural Reserve. The second was collected in Rosário salt marsh that is contaminated by heavy metal (Reborela *et al.*, 2007). The plants were irrigated with 1/4 Hoagland solution and kept under the control environmental conditions (16/8h:day/night rhythm; day temperature $20 \pm 0.5^\circ\text{C}$, night temperature $18 \pm 0.5^\circ\text{C}$). The plants from both locations (Contaminated and non-contaminated) were separated into 2 groups (N=5) and subjected to different thermal treatments (day/night) during one week:

- Control 20/18°C
- Warming 35/30°C

Pulse amplitude modulated (PAM) fluorometry

Using a FluorPen FP100 (Photon System Instruments) pulse amplitude modulated chlorophyll fluorescence measures were performed at the end of the experiment on 30-min. dark-adapted attached leaves as previously described (Duarte *et al.* 2015b).

Leaf fatty acid composition

Immediately after the fluorescence analysis, leaf samples were weighed, flash-frozen in liquid N₂ and stored at -80 °C for fatty acid analysis. Leaf fatty composition was determined by direct acidic transesterification of leaf portions previously described (Matos *et al.*, 2007). Using a 3900 Gas Chromatograph (Varian) fatty acid methyl esters (FAME) were separated. Heptadecanoate (C17:0) was used as internal standard.

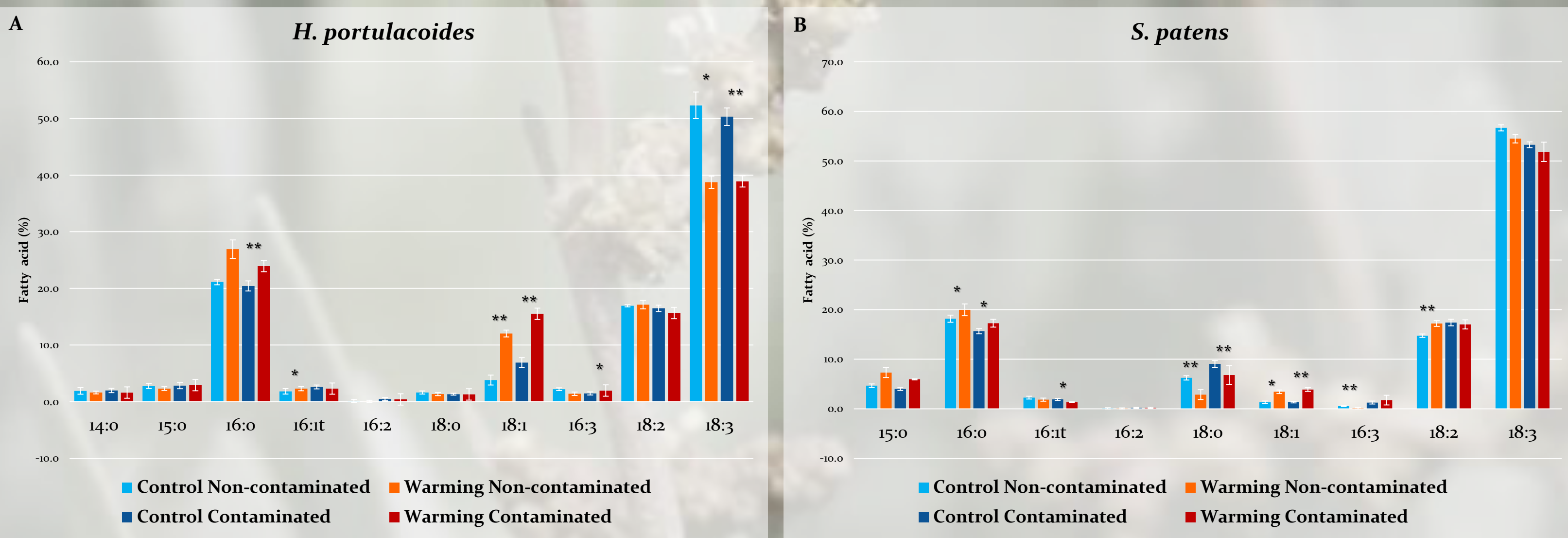


Figure 4: Fatty acid content (% average) in *H. portulacoides* (A) and *S. patens* (B) (average \pm SE, N=5, asterisk marks significant differences between treatments at $p<0.05$).

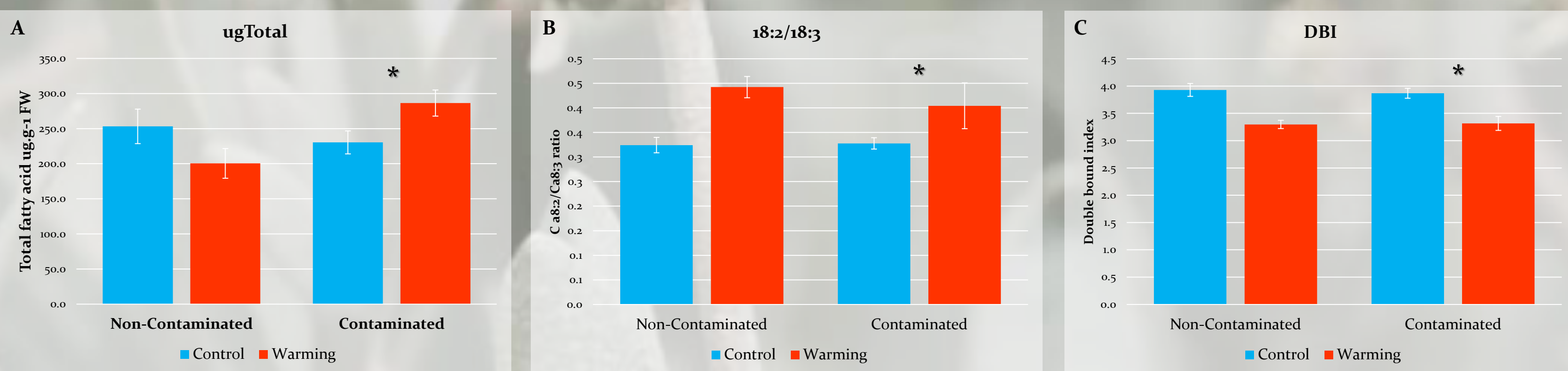


Figure 5: Total content (ug.g⁻¹ FW; A), C18:2/C18:3 ratio (B) and double bond index (DBI; C) in *H. portulacoides* (average \pm SE, N=5, asterisk marks significant differences between treatments at $p<0.05$).

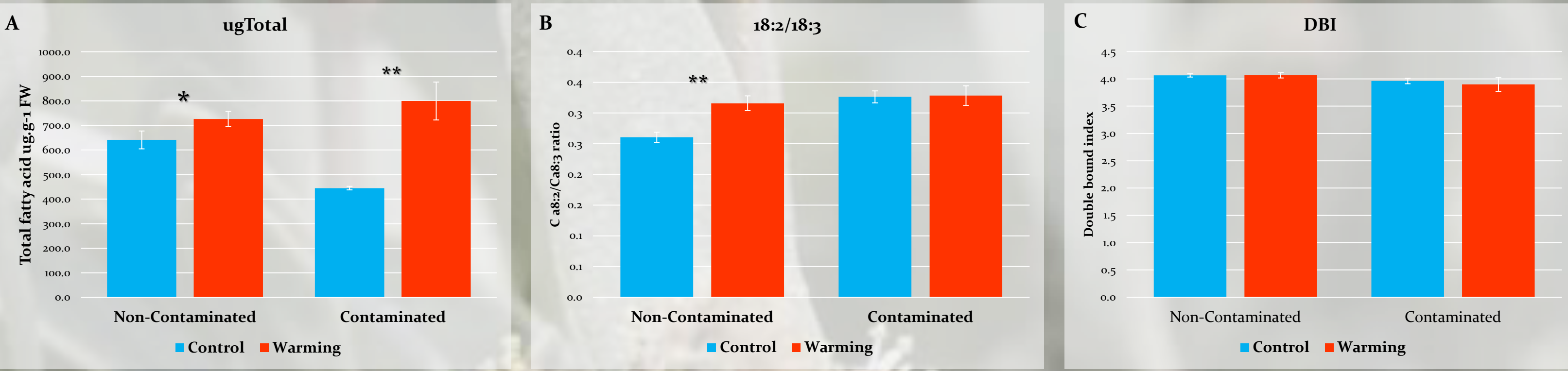


Figure 6: Total content (ug.g⁻¹ FW; A), C18:2/C18:3 ratio (B) and double bond index (DBI; C) in *S. patens* (average \pm SE, N=5, asterisk marks significant differences between treatments at $p<0.05$).

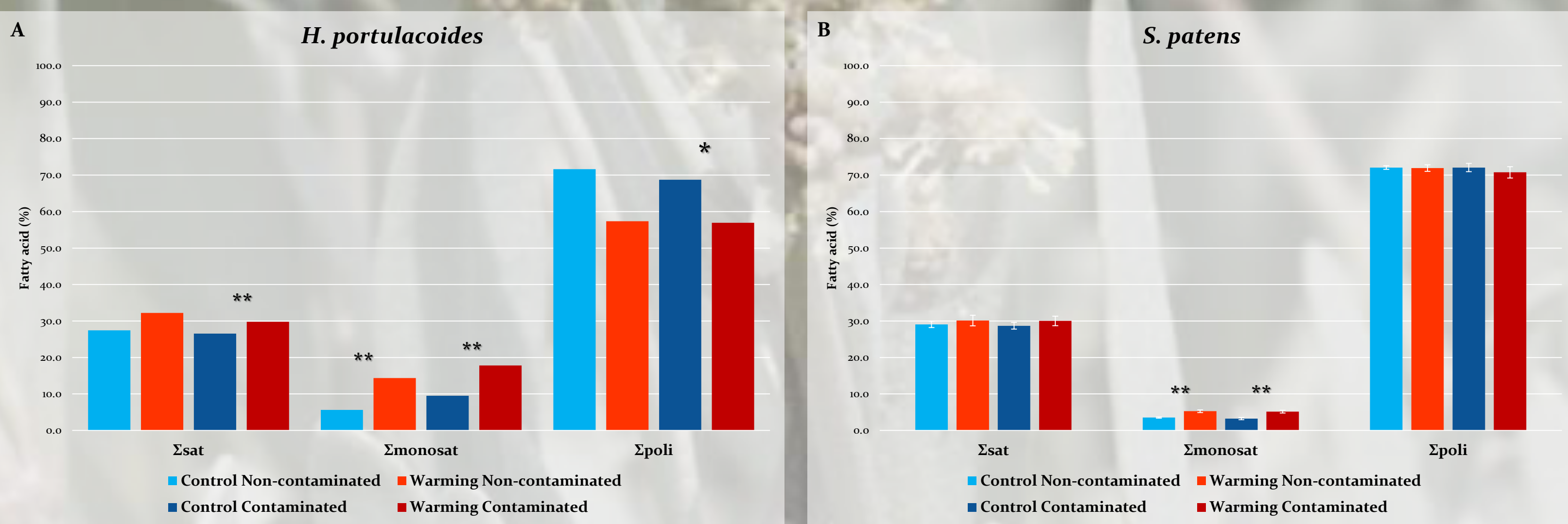


Figure 7: Saturation classes (% average) in *H. portulacoides* (A) and *S. patens* (B) (average \pm SE, N=5, asterisk marks significant differences between treatments at $p<0.05$).



Populations of both plants show warming-induced stress. The increase of the active OECs suggests damage in the PSII efficiency, which is supported by the increase in palmitic acid concentration.



The differences between the data obtained by PAM fluorometry and leaf fatty acid composition from the *Spartina Patens* populations can indicate a considerable different physiological response or resistance to warming-induced stress.



Unlike the *H. portulacoides* populations, control *S. patens* populations have significant differences in their physiology showing a visible pre-conditioning.



The data of this study suggests an apparent population pre-conditioning to the environment in *H. portulacoides* and *S. patens*.

The relationship between dehydrin accumulation and winter survival of winter wheat and barley

Pavel Vítámvás¹, Klára Kosová¹, Jana Musilová¹, Ludmila Holková², Pavlína Smutná², Pavel Mařík³ and Ilja T. Prášil¹

¹ Crop Research Institute, Prague, Czechia

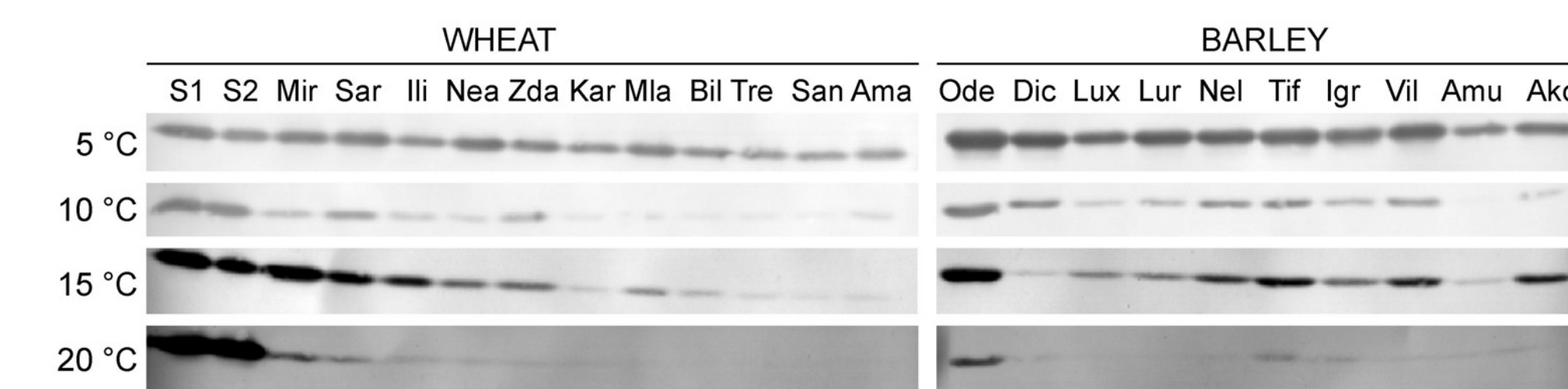
² Mendel University in Brno, Brno, Czechia

³ SELGEN, Lužany Plant Breeding Station, Czechia

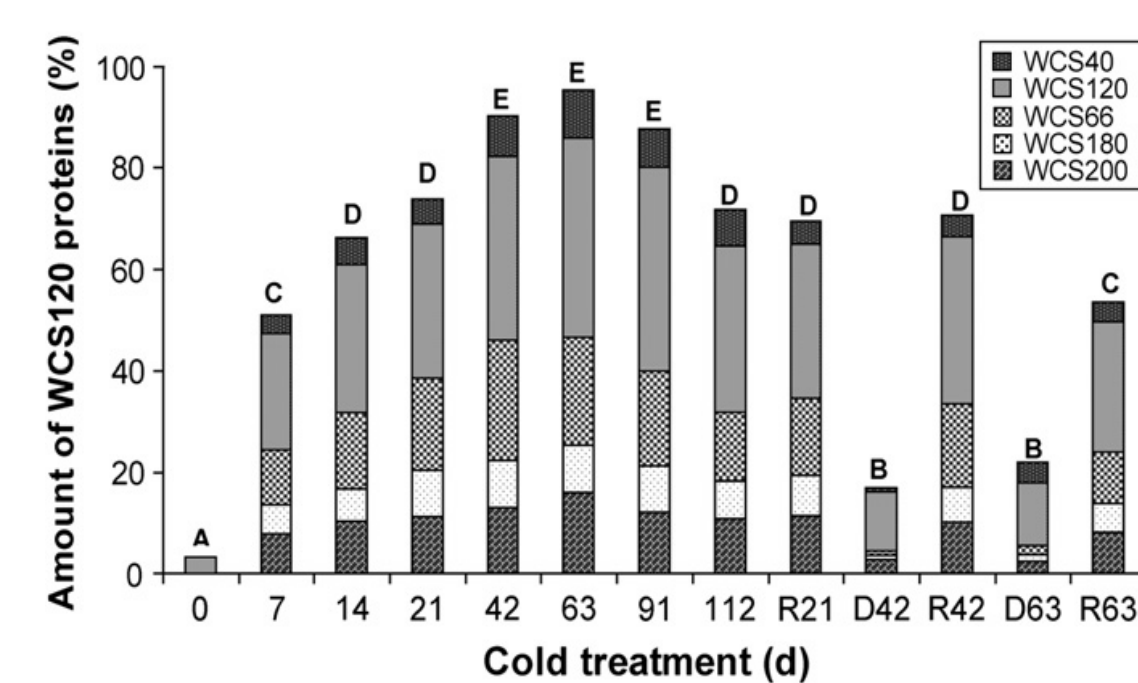
INTRODUCTION

Low temperatures induce an active plant acclimation response which is associated with enhanced accumulation of several stress-inducible proteins including dehydrins. Dehydrins present a distinct biochemical group of late embryogenesis abundant (LEA) proteins characterised by the presence of a lysine-rich amino acid motif, the K-segment. They are highly hydrophilic, soluble upon boiling, and rich in glycine and polar amino acids. In controlled conditions, a significant correlation between dehydrin protein or transcript relative accumulation and plant acquired frost tolerance (determined as LT50) was found (e.g., Kosová et al. 2013, Vítámvás et al. 2007, 2010). However, the accumulation of dehydrins in reacclimated plants after deacclimation is less correlated with LT50 especially after saturation of vernalization requirement (Vítámvás and Prášil 2008).

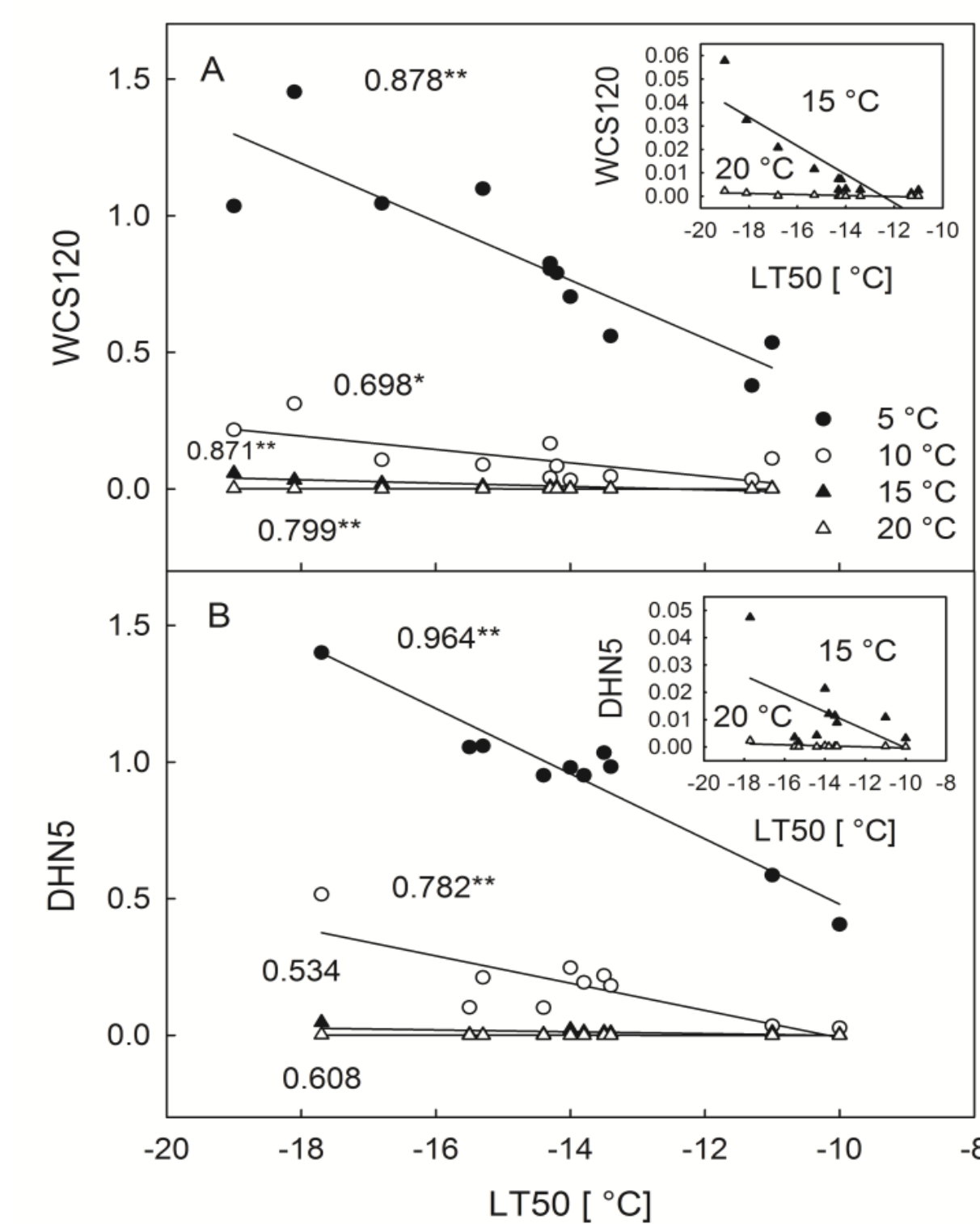
The aim of this study was found if dehydrins can be used as reliable marker of plant frost tolerance not only in controlled growth conditions, but also in field conditions.



Representative immunoblot sections showing accumulation of WCS120 in wheats and DHN5 in barleys grown at 5, 10, 15, and 20 °C after 280 degree-days. Samples from the plants grown at 15 and 20 °C were 10 and 100 times more concentrated than samples from the plants grown at 5 and 10 °C. For comparison of band density on different 1-D gels, cv. Mir grown at 5 °C was used as an internal standard in two different sample concentrations (one sample revealing the same concentration as the samples grown at 5 °C and 10 °C – S1 and the other sample with a ten-times lower concentration - S2; Kosová et al. 2013).



Accumulation of WCS120 proteins in leaves during cold acclimation (0–112 days), deacclimation (D42; D63) and reacclimation (R21; R42; R63) of plants. Bars show the amount of each protein in the WCS120 family as a percentage of the highest sum of the density of all WCS120 protein bands. Values with the same letter (A–E) were not significantly different for the sum of the values for all proteins (Vítámvás and Prášil 2008).



Correlations between WCS120 (A) and DHN5 (B) relative accumulation in wheat and barley cultivars grown at 5, 10, 15, and 20 °C, and LT50. The values of correlation coefficients are shown for each sample set. *, ** - significant correlations at 0.05 and 0.01 levels, respectively (Kosová et al. 2013).

CONCLUSION

Our present study shows that cold-inducible dehydrin proteins as well as dehydrin transcripts can be correlated to plant winter survival, but only in non-vernalized winter cereals plants. Unlike in controlled conditions, rather a sum of all WCS120 proteins detected on the immunoblots than a single dehydrin protein (WCS120 alone) reveals a correlation with plant frost tolerance (winter survival) under field conditions. This finding may reflect a more complex nature of plant acquired frost tolerance under field conditions with respect to controlled conditions.

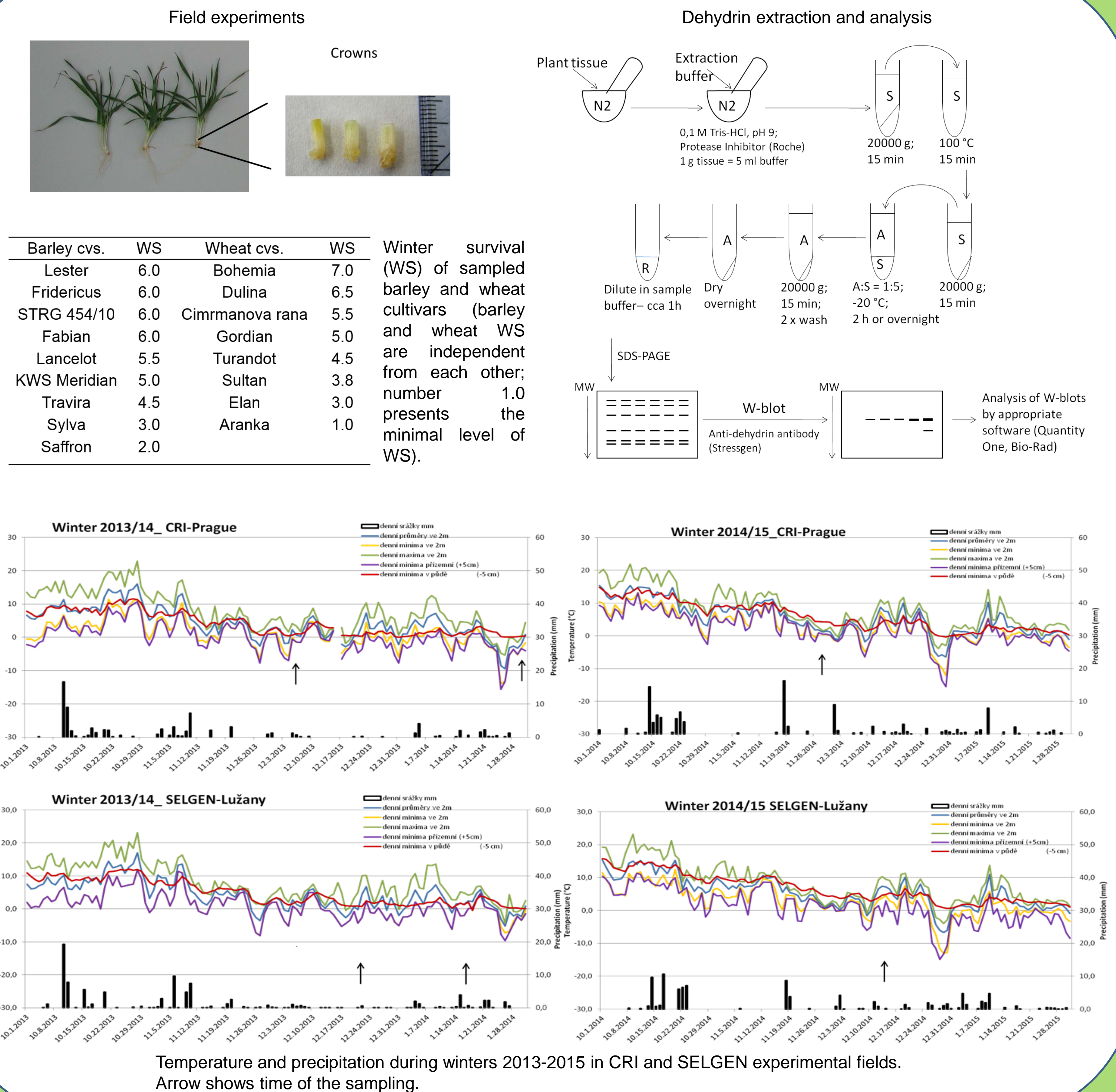
ACKNOWLEDGEMENTS

This work was supported by the Ministry of Agriculture of the Czech Republic (QJ1310055 and MZE RO0417) and by the Ministry of Education, Youth and Sports (LD15167 as parts of COST Actions FA1306).

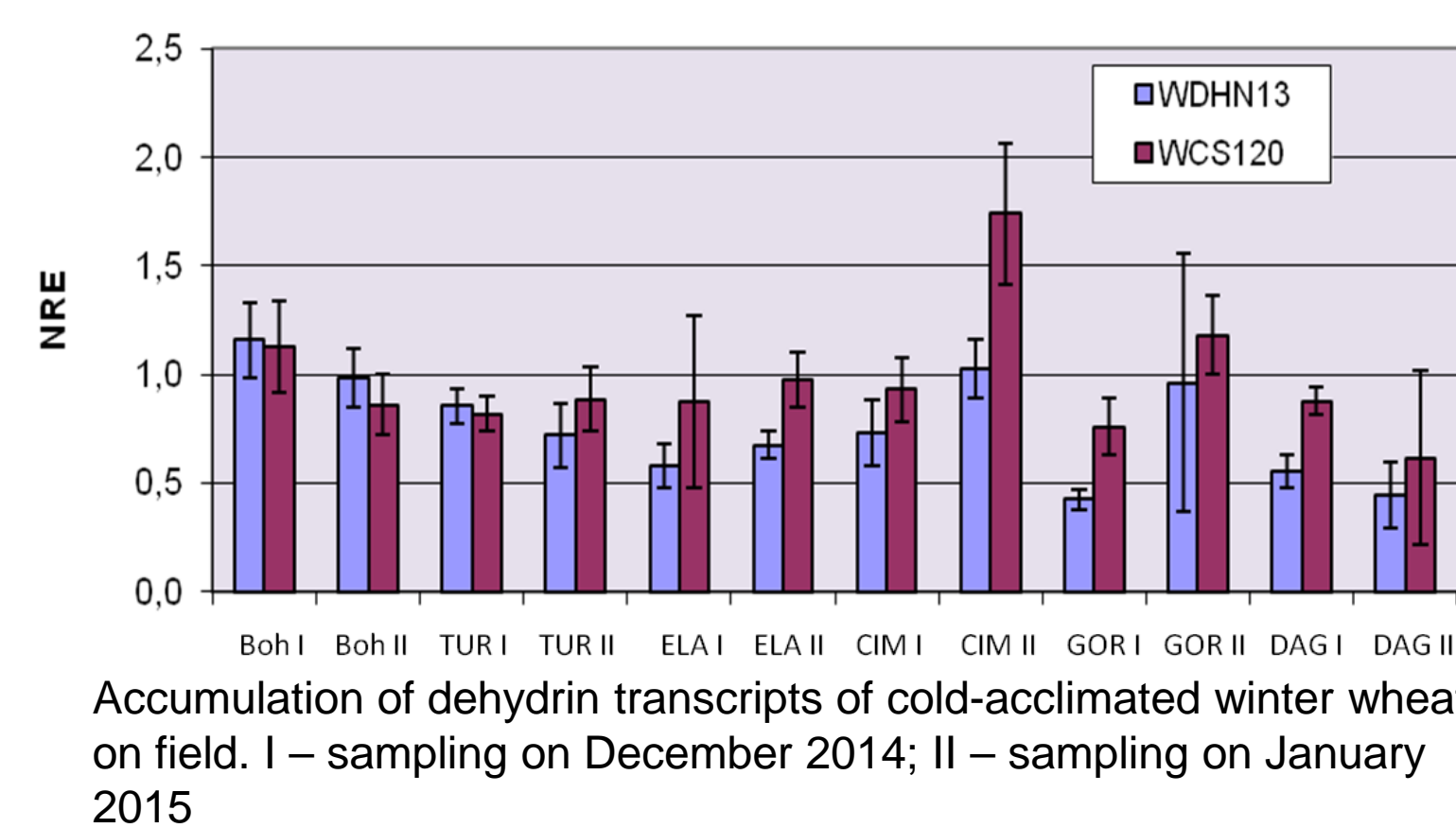
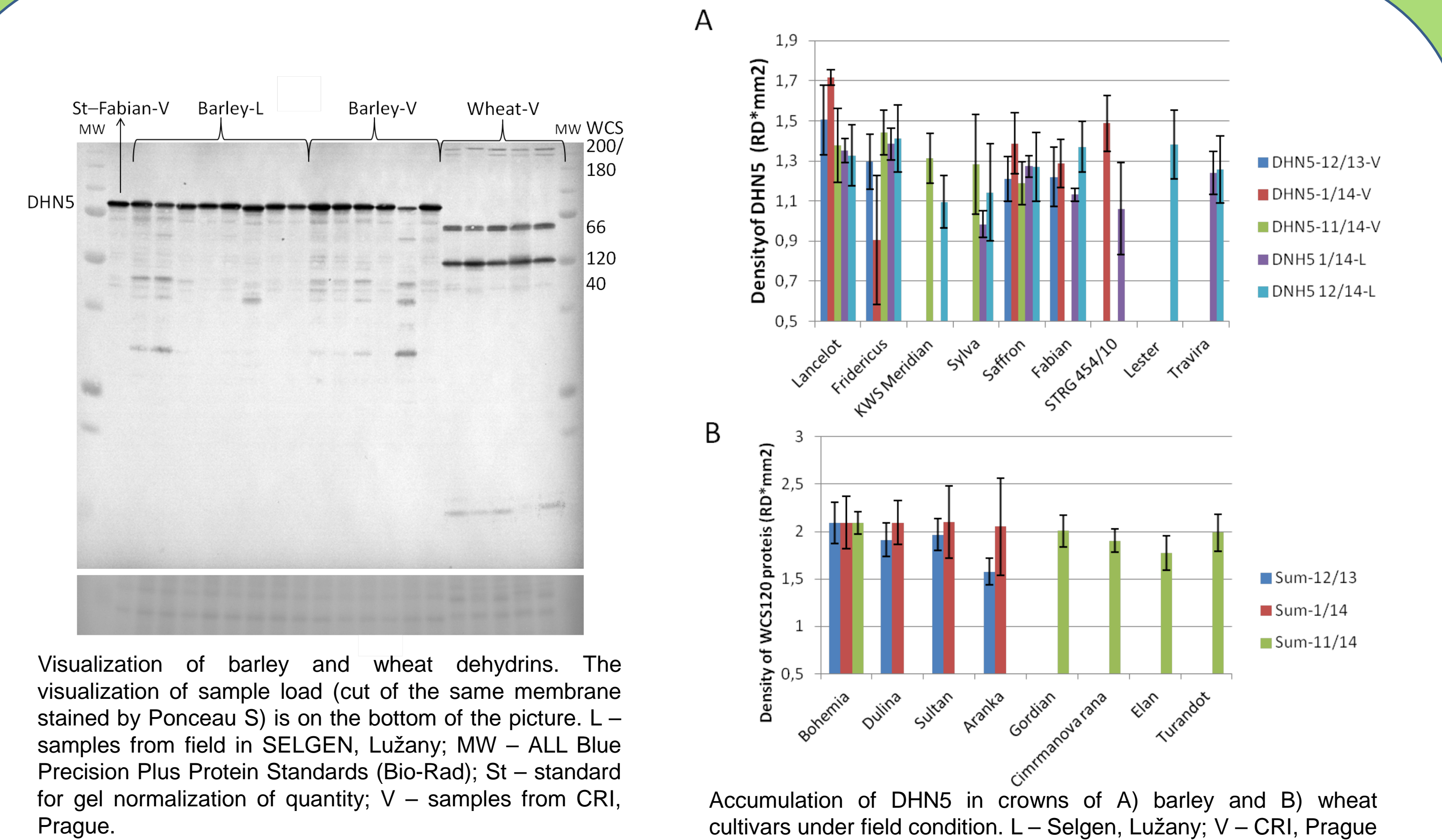
REFERENCES

- Vítámvás P., Saalbach G., Prášil I.T., Čapková V., Opatrná J. and Jahoor A. (2007): WCS120 protein family and proteins soluble upon boiling in cold-acclimated winter wheat. *Journal of Plant Physiology* 164: 1197-1207.
- Vítámvás P. and Prášil I.T. (2008): WCS120 protein family and frost tolerance during cold acclimation, deacclimation and reacclimation of winter wheat. *Plant Physiology and Biochemistry* 46: 970-976.
- Vítámvás P., Kosová K., Prášilová P. and Prášil I.T. (2010): Accumulation of WCS120 protein in wheat cultivars grown at 9 °C or 17 °C in relation to their winter survival. *Plant Breeding* 129: 611-616.
- Kosová K., Vítámvás P., Prášilová P. and Prášil I.T. (2013): Accumulation of WCS120 and DHN5 proteins in differently frost-tolerant wheat and barley cultivars grown under a broad temperature scale. *Biologia Plantarum* 57: 105-112.

MATERIALS AND METHODS



RESULTS



Correlation coefficient between barley (A) and wheat (B) dehydrins and winter survival (WS) of tested genotypes. Bold numbers means significant correlation coefficient ($P \leq 0.05$); L – Selgen, Lužany; V – CRI, Prague. Numbers in brackets means number of series n measurements.

Barley	12/13-V (4)	1/14-V (5)	11/14-V (5)	1/14-L (7)	12/14-L (8)	all 11+12 (8)	all 1 (7)	all DHN5 (9)
WS	0.362	-0.145	0.980	0.110	0.658	0.797	0.172	0.509

Wheat	12/13-V (4)	1/14-V (4)	11/14-V (5)	all 12+11 (8)	all DHN (8)
WS	0.853	0.747	0.883	0.846	0.720

Values of Pearson cor. coefficient (r) between levels of transcripts of WDHN13 and WCS120 genes and degrees of frost-tolerance (DFT). I – sampling on December 2014; II – sampling on January 2015

r (n=8)	DFT (CRI)
WDHN13 I	0.727 *
WDHN13 II	0.516
WCS120 I	0.505
WCS120 II	0.256

Introduction

Among the most abundant secondary metabolites accumulating in grape berry throughout development are flavonoids. The flavonoids pathway leads to the formation of anthocyanins which are the major contributors of red grape and wines and are the most abundant flavonoids in grape skin. Anthocyanin concentrations depend on the variety and are influenced by viticultural management and environmental stresses. Water and heat stresses modulated the ripening of grape berries and consequently the berry and wine quality. It is currently accepted that the ripening of the non climacteric grape berries is at least regulated by abscisic acid (ABA). ABA is also a signaling hormone that plays a key role on the perception of abiotic stress, namely water stress. However, ABA rapidly turns over in plants, thus the measurement of free ABA alone may give limited information on the total amount of ABA produced over time and potentially active products resulting from ABA catabolism within plant tissues. Irrigation is being used in vineyard in order to maintain vine growth and yield under drought conditions. However, effects of the irrigation system on ABA metabolism during ripening are still largely unknown.

In the present study we aimed at investigating the phenotypic plasticity of Aragonez (syn. Tempranillo) grape berries by comparing berry skin anthocyanin and ABA metabolism under two different irrigation regimes and two sides of the canopy.

Results

Vine water status and berry temperature

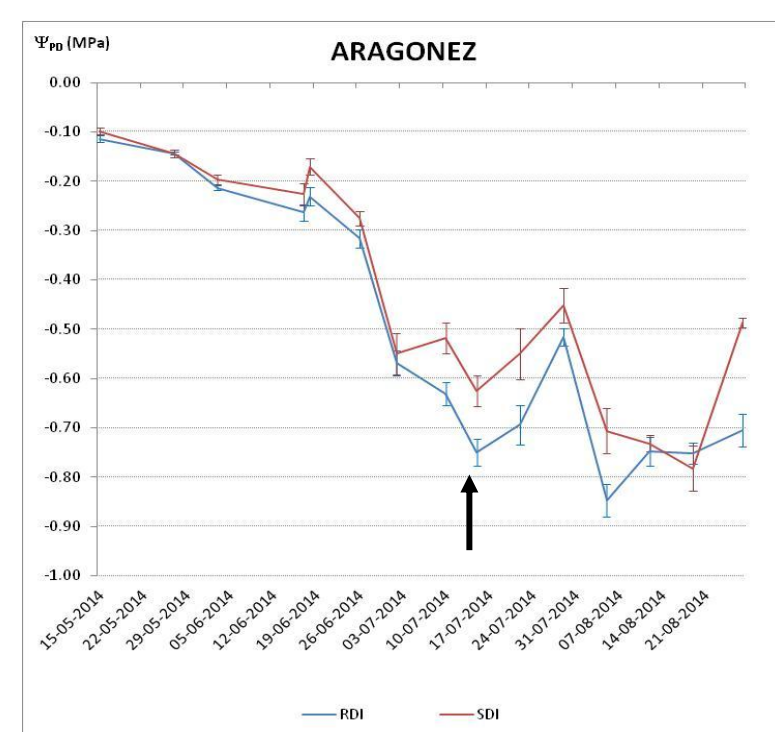


Fig 1. Pre-dawn leaf water potential (Ψ_{pd}) for Aragonez along vine growing season subjected to two different irrigation regimes (SDI and RDI). Arrow indicates *véraison*. Values are means \pm SE (n=4-6).

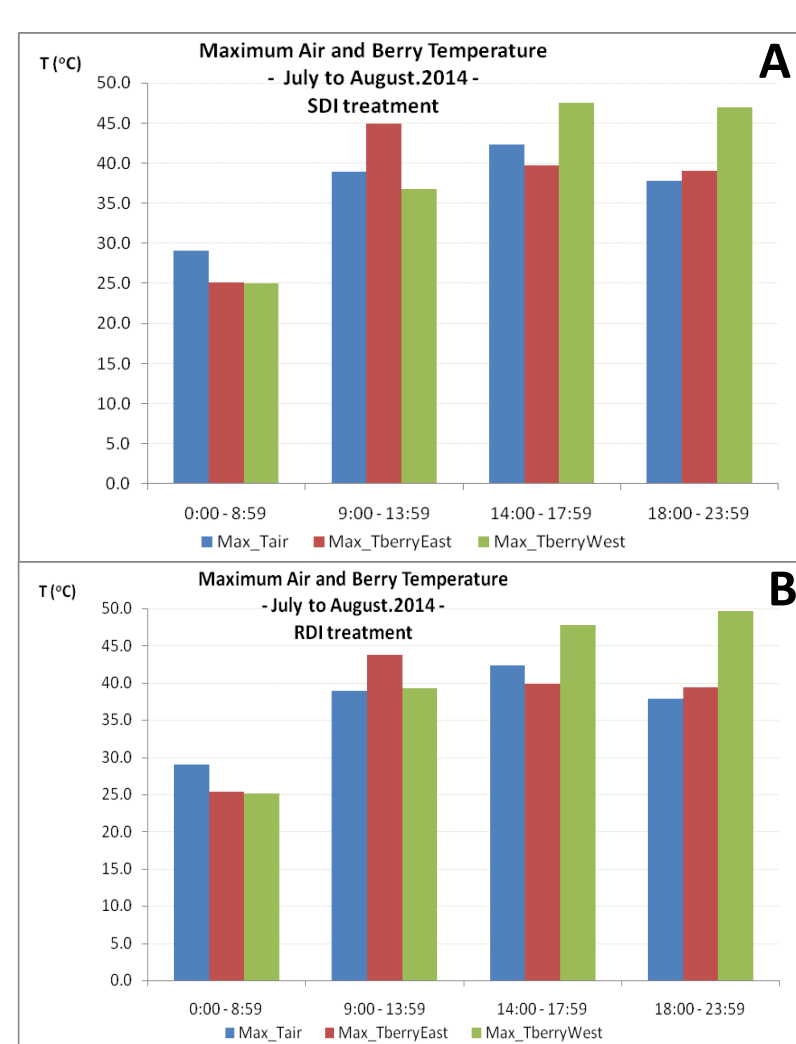


Fig 2. Maximum air and berry temperature on east and west sides of the vine canopy for SDI (A) and RDI (B) Treatments.

ABA, ABA-GE, PA and DPA concentrations

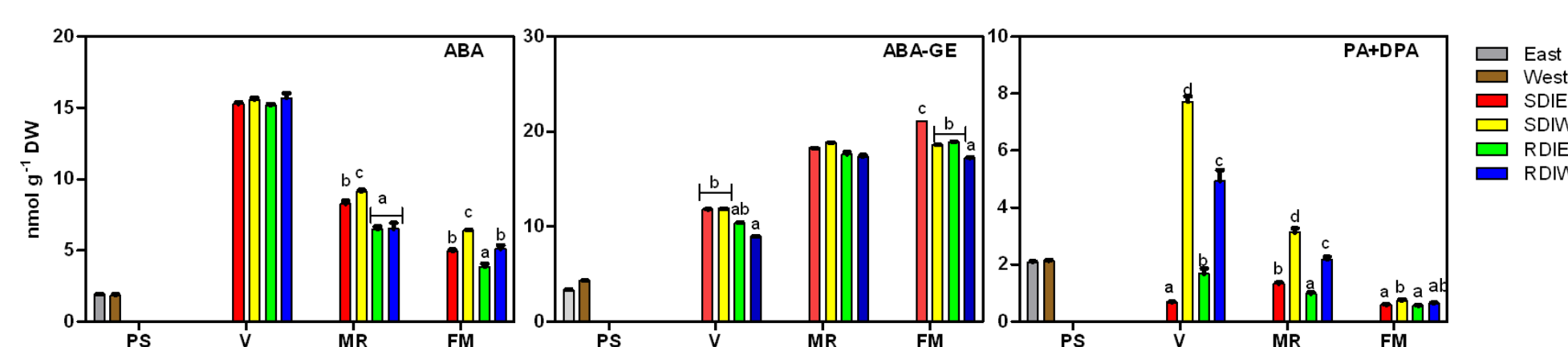


Fig 6. Concentration of ABA, ABA-GE, PA+DPA in berry skin of SDI and RDI vines and from east and west sides. Values are mean \pm SE (n=3). Different letters indicate significant differences using Duncan's test ($p \leq 0.05$).

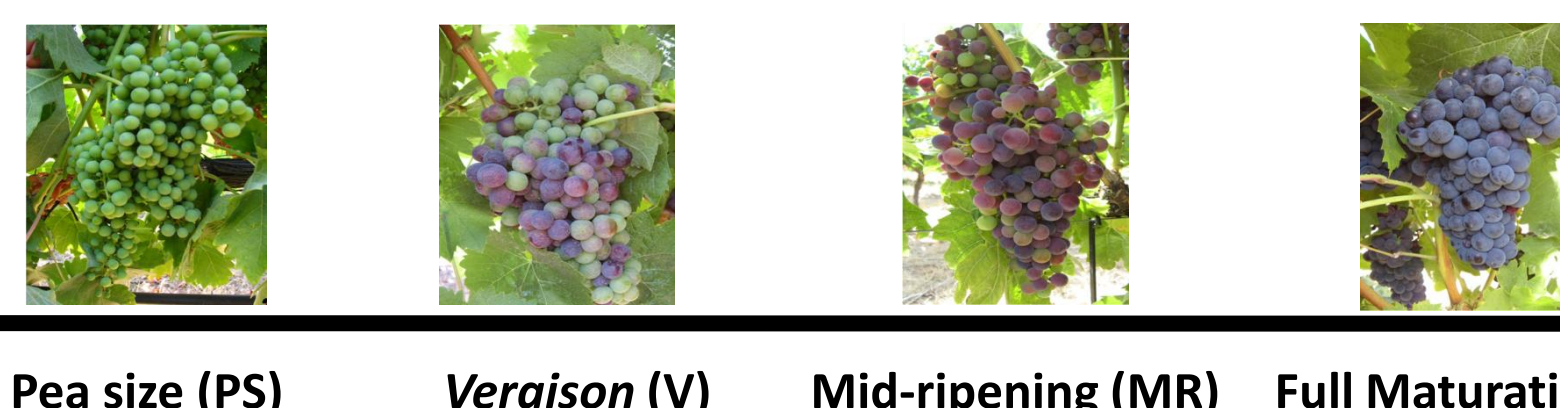
- * ABA and ABA-GE accumulation differ significantly between irrigation treatments.
- * PA and DPA were highest at west side of the canopy both in SDI and RDI, suggesting a highest rate of ABA degradation at west side of the canopy.

Conclusions

The canopy side -east vs west and the irrigation levels (SDI and RDI) affected berry ripening. The different irrigation strategies significantly altered the anthocyanin and ABA content of the berry skin. In our conditions, SDI seemed to yield berries with greater concentrations of anthocyanin than RDI, with the additional advantage of attenuate heat incidence at the west side of the canopy, which may be considered beneficial for wine production.

Material and Methods

The plant material analyzed was collected during the summer season of 2014 at the commercial vineyard Herdade do Esporão in Reguengos de Monsarraz (Alentejo region), Portugal. Berries from cv. Aragonez (syn. Tempranillo) were randomly sampled from both sides (East and West) at four developmental stages: pea size (PS), *véraison* (V), mid-ripening (MR) and full maturation (FM). Berries were collected from vines subjected to 2 different irrigation regimes: Sustained Deficit Irrigation (SDI, 20% Etc) and Regulated Deficit Irrigation (RDI, 14% Etc).



At each sample date, skins were removed and ground in liquid nitrogen to a fine powder and stored at -80°C until analysis.

Determination of Anthocyanin, ABA, ABA-GE, PA and DPA: anthocyanin and hormone extraction was performed in acidified methanol and stored at -80°C till analysis. Three biological replicates were considered. The analysis was performed using HPLC MS/MS. **RNA extraction and quantitative real-time PCR:** Total skin RNA extractions were performed using the method of Reid et al. (2006). qRT-PCR was performed in the iQ5 2.0 Standard Edition (Bio-Rad). Each PCR was run in triplicate. Primer pairs for *actin* was retrieved from Reid et al. (2006), *VviUFGT* from Castellarin et al (2007) and *VviNCED1* and *VviBG1* from Sun et al. (2010).

Data analysis: Results were examined by ANOVA with SPSS 12.0 (SPSS Inc, Chicago, USA). Means were separated by Duncan's multiple range test ($P \leq 0.05$).

Anthocyanin accumulation and degradation

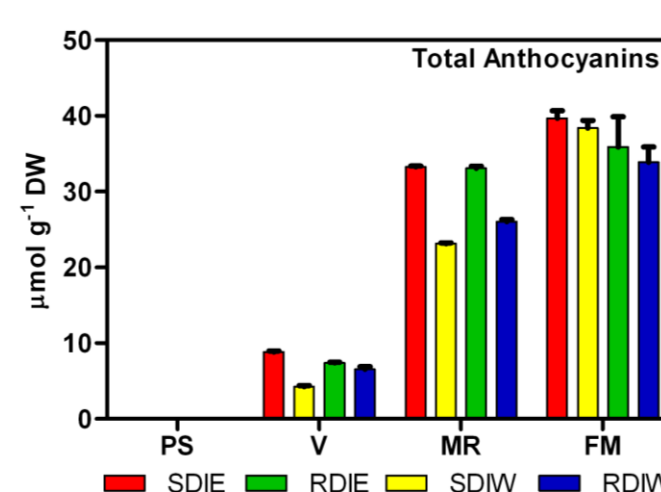


Fig 4. Total skin anthocyanin concentration along berry ripening belonging from two different irrigation regimes (SDI and RDI) and two sides of the canopy (E and W). Values are means \pm SE (n=3).

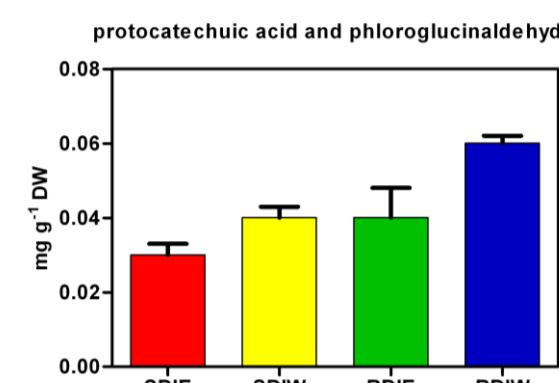


Fig 5. Effect of deficit irrigation and side of the canopy in flavonoid degradation products concentration in berry skin at full maturation stage. Values are means \pm SE (n=3).

- * At MR, anthocyanin concentration was higher at east side (E) of the canopy than the west side (W) independently from the irrigation regime.
- * Degradation products were only observed at FM and were highest at west side, in particular in RDI treatment.

Gene expression levels

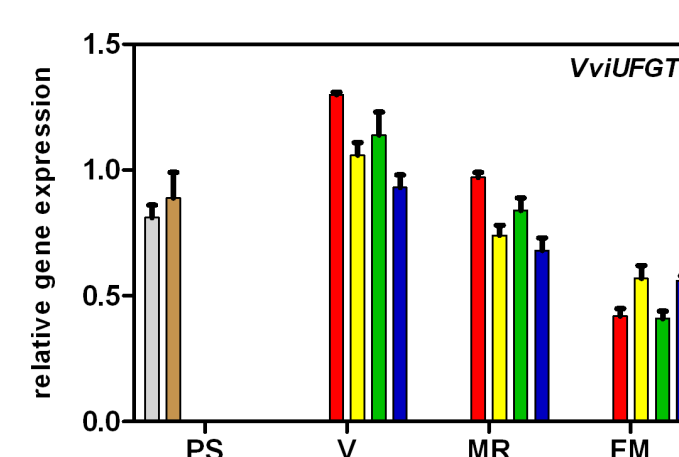


Fig 7. Transcript levels of *VviUFGT* in skins during berry development of SDI and RDI at E and W sides. Gene expression is expressed relative to *actin* in each sample. Values are mean \pm SE (n=3).

- * *VviUFGT* gene associated with anthocyanin biosynthesis, was down-regulated in RDI berries and at the west side of the canopy

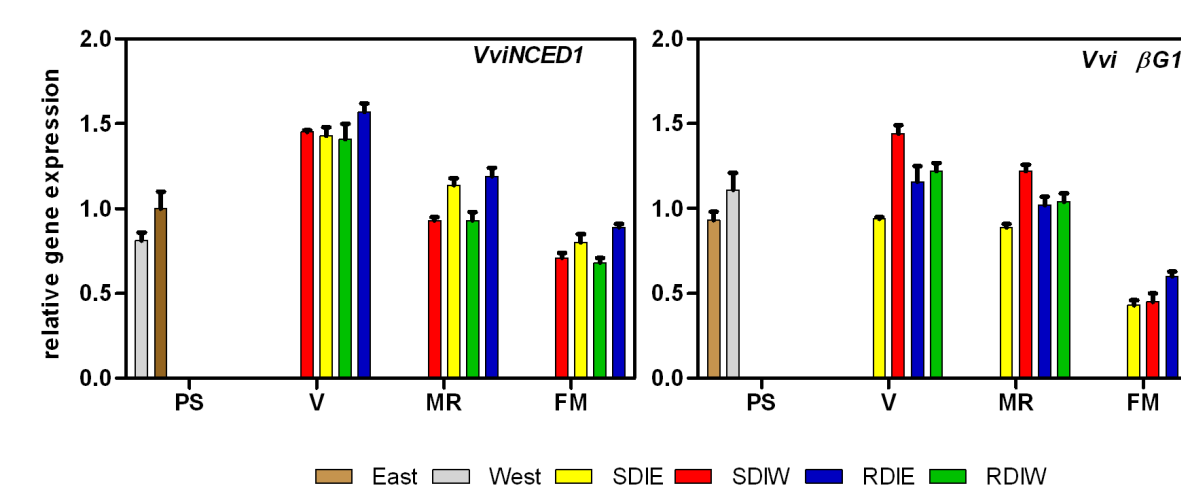


Fig 8. Transcript levels of *VviNCED1* and *VviBG1* in skins during berry development of SDI and RDI at E and W sides. Gene expression is expressed relative to *actin* in each sample. Values are mean \pm SE (n=3).

- * The trend of variation of *VviNCED1* in skin match with the change in ABA concentration in all treatments.
- * *VviBG1* was up-regulated in SDIW at *véraison* and MR in accordance with ABA concentration.

Acknowledgements

In vitro phenotyping of seminal root traits in wheat

Paula Scotti-Campos^{1,2}, Isabel P. Pais^{1,2}, Aladje Dabó³, José N. Semedo^{1,2}, José Coutinho² and Benvindo Maças²

¹Unidade de Biotecnologia e Recursos Genéticos, Instituto Nacional de Investigação Agrária e Veterinária, I.P.

Quinta do Marquês, Av. República, 2784-505 Oeiras / Apartado 6, 7350-591 Elvas, Portugal.

²GeoBioTec, Fac. Ciências Tecnologia, Univ. Nova Lisboa, 2829-516 Caparica, Portugal

³Escola Profissional Agrícola D. Dinis – Paiã, R. Pedro Álvares Cabral, 1675-076 Lisboa, Portugal



INTRODUCTION

Plants ability to efficiently capture water and nutrients from the soil strongly depends on its root system. Crop production is greatly affected by environmental stresses such as drought and waterlogging. Drought-resistant plants tend to develop a deeper root system, while shallow roots can be beneficial under waterlogging conditions. The root growth angle (RGA) is a principal component of root system architecture and determines direction of root elongation. It may be considered as a potential trait to improve crop production (Uga *et al.*, 2015). The aim of this work was to perform the screening of root traits at the seedling stage in a set of 72 genotypes of bread wheat (*Triticum aestivum* L.) divided in seven groups according to their origin. Evaluation of genetic variability in seedling root traits (RGA, seminal root and radicle) allows to take advantage of naturally occurring diversity to select for more adapted varieties as regards environmental constraints such as drought and waterlogging. Results are expected to contribute to Portuguese Wheat Breeding Program under Mediterranean climate conditions, where unpredictable heavy rainfall as well as drought episodes may increase in the context of climate changes.

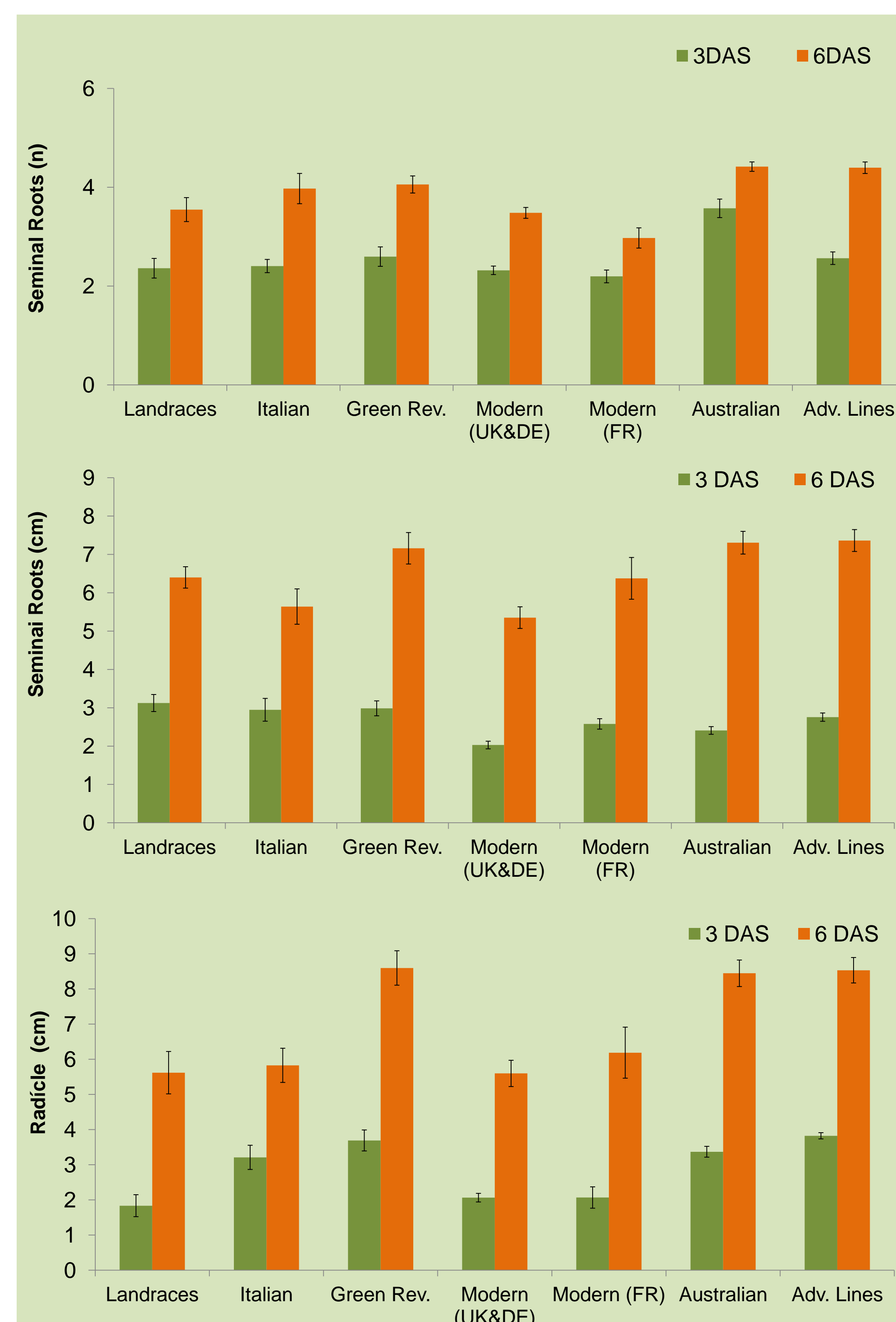
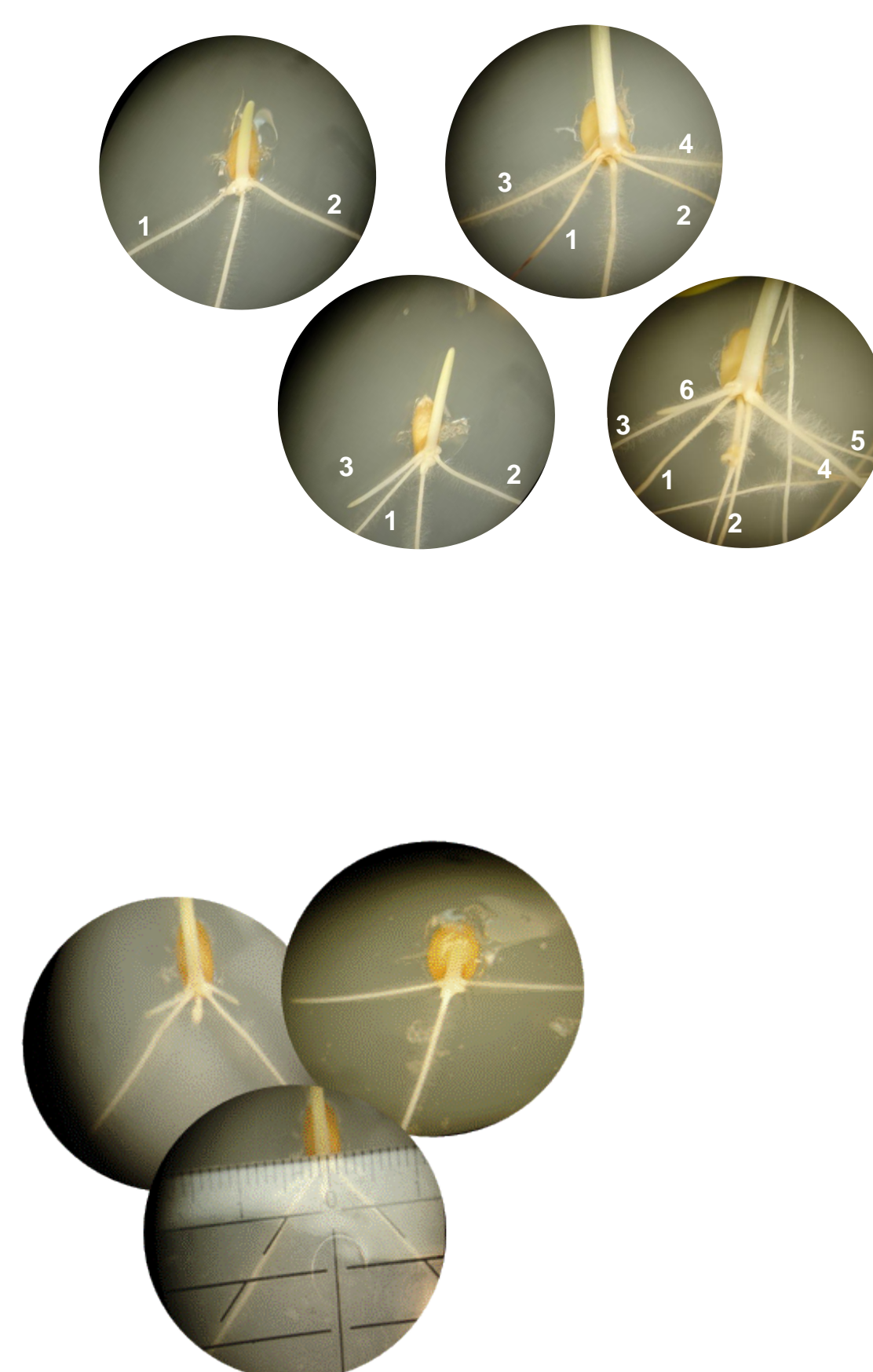
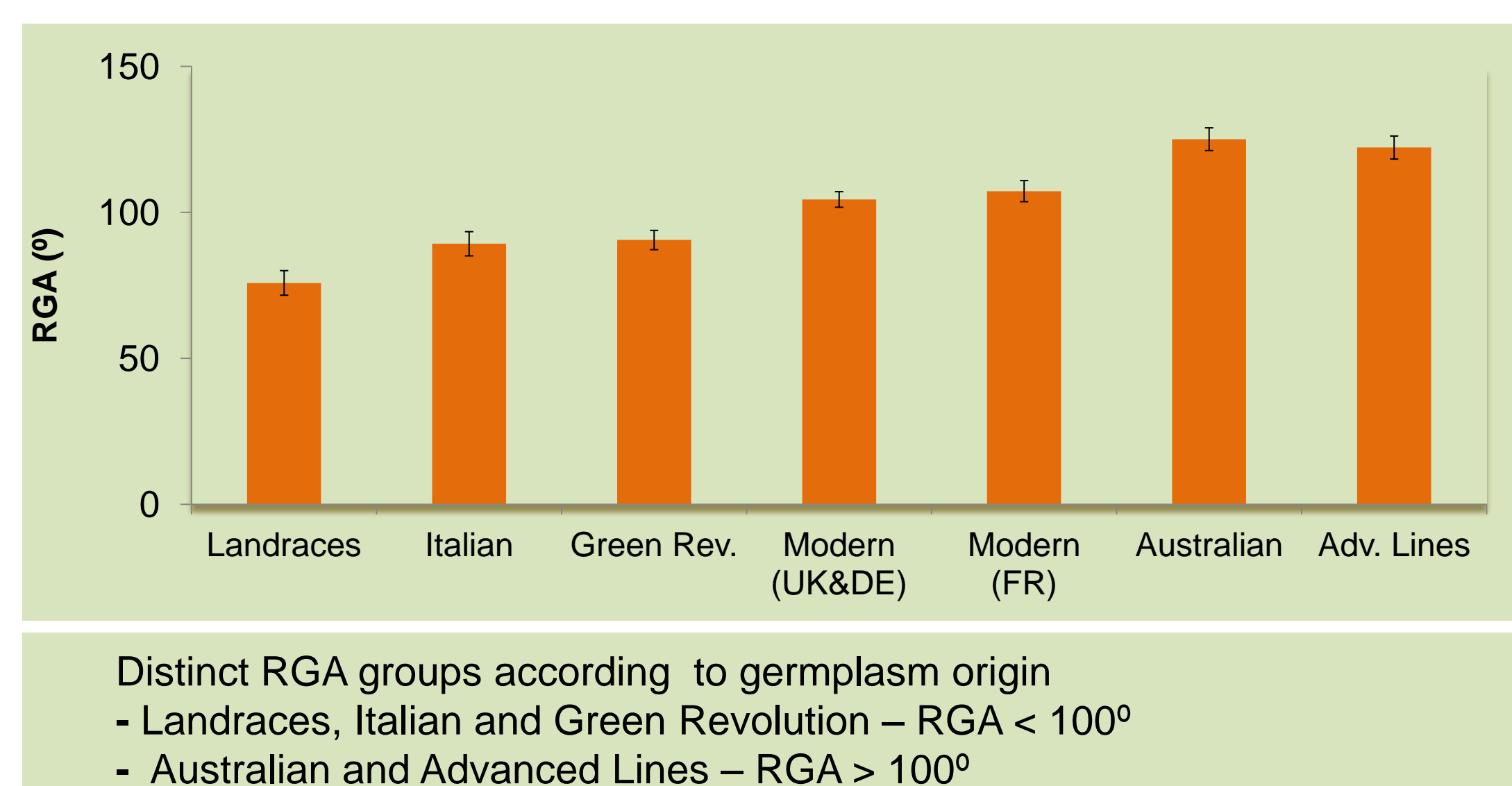
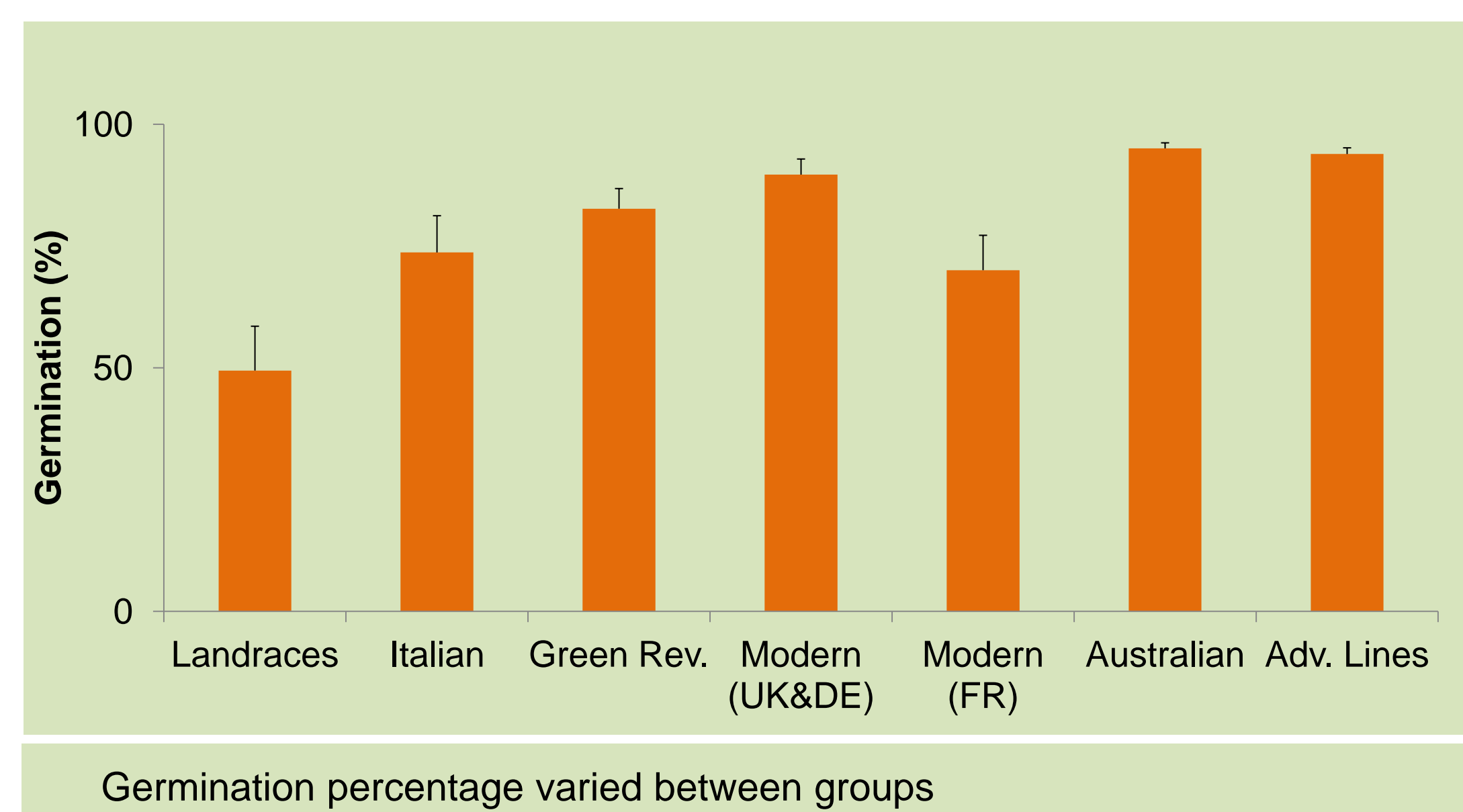
MATERIAL & METHODS

WHEAT GERMPLASM	
10	Landraces (Vasconcelos, 1933)
7	Italian var.
10	Green Revolution var.
10	Modern var. (UK & DE)
12	Modern var. (FR)
10	Australian var.
13	Advanced Lines (INIAV Breeding Program)

Seeds (18 for each variety) were first soaked in ethanol for 10 sec, and subsequently in sodium hypochlorite 2% for 1 min, according to Sauer and Burroughs (1986). They were finally rinsed twice with sterilized deionized water. Sowing was performed in square Petri dishes filled with agar (2%), under sterilized conditions. Seeds were incubated at 21°C in the dark and in vertical position. Visual assessment and biometrical features were performed at 3 and 6 days after sowing (DAS). Germination, RGA, seminal roots and radicle development were evaluated. Two experiments were done.



RESULTS



Variation was observed as regards:

- The number of seminal roots (2-6 roots at 6 DAS)
- The length of radicle and seminal roots (1st pair)

CONCLUSIONS

A large variability was found in RGA values, that ranged from 76° (Landraces) to 125° (Australian).

Germplasm diversity was observed among groups as concerns other seedling root features, and the work also highlighted genotypic variability within each group.

Genetic variability as regards this wheat seedling trait represents a useful breeding resource for selection at early growth stages.

REFERENCES

- Sauer, D.B. and Burroughs, R. 1986. Disinfection of seed surfaces with sodium hypochlorite. *Phytopathology* 76: 745-749.
- Uga, Y., Kitomi, Y., Ishikawa, S. and Yano, M., 2015. Genetic improvement for root growth angle to enhance crop production. *Breeding Science* 65: 111-119.
- Vasconcelos, J.C. 1933. Trigos portugueses ou de há muito cultivados no país. D.G.A.S. Agrária. Separata do Boletim de Agricultura, Ano I, 1/2, I Série, pp. 1-150

Using the chlorophyll fluorescence signal and machine learning techniques to automatically identify *Quercus* species: preliminary results

Tomás Ochôa Cruz,¹ Cíntia Macedo,¹ João Nunes Silva,¹ Nuno Burnay,¹ Pedro Mariano^{1,2} and Jorge Marques da Silva^{1,2}

¹University of Lisbon, Faculty of Science

²Biosystems and Integrative Sciences Institute

Introduction

- The genus *Quercus* is an important group of woody plants native to the Northern Hemisphere. It dominates temperate, subtropical and tropical regions.
- The rapid fluorescence induction curve (Kautsky Effect) has been proposed to be a fingerprint of plant species [1]. It allows the calculation of several parameters (e.g. Fv/Fm, the maximum quantum efficiency of photosystem II; PI, the integrated photochemical Performance Index; and C-Area, the complementary area above the induction curve) which are informative in plant stress physiology [2].
- Artificial intelligence is becoming an important tool in many human activities, including biology and agronomy, where it plays a growing role in high throughput plant phenotyping [3].
- In this work we aimed to automatically identify three different *Quercus* species using a machine learning technique applied to rapid fluorescence induction curves.

Results and Discussion

- Fv/Fm was statistically different (ANOVA, t-test, $p < 0.05$) for all species; for both C-area and PI, there was a statistically significant difference between *Q. suber* and *Q. rotundifolia*, and between *Q. suber* and *Q. canariensis* (Fig.1). When given only the three selected parameters, the algorithm had an identification success of 75% (Fig.2), much higher than the percentage of success expected for a random classification of the curves (circa 33%). When the entire data set of the curve was given the algorithm had a slightly higher identification success (80%) (Fig.3). This indicates that there is some information of the induction curves, relevant for the identification of the species, that is not reflected in the calculated parameters. The success of the automatic classification of the species was independent of the minimum number of samples in a leaf. It increased with the maximum tree depth and the maximum number of leaves, but only at low values, remaining unchanged after a threshold of approximately 5 for MaxDepth and 10 for MaxLeafNodes.

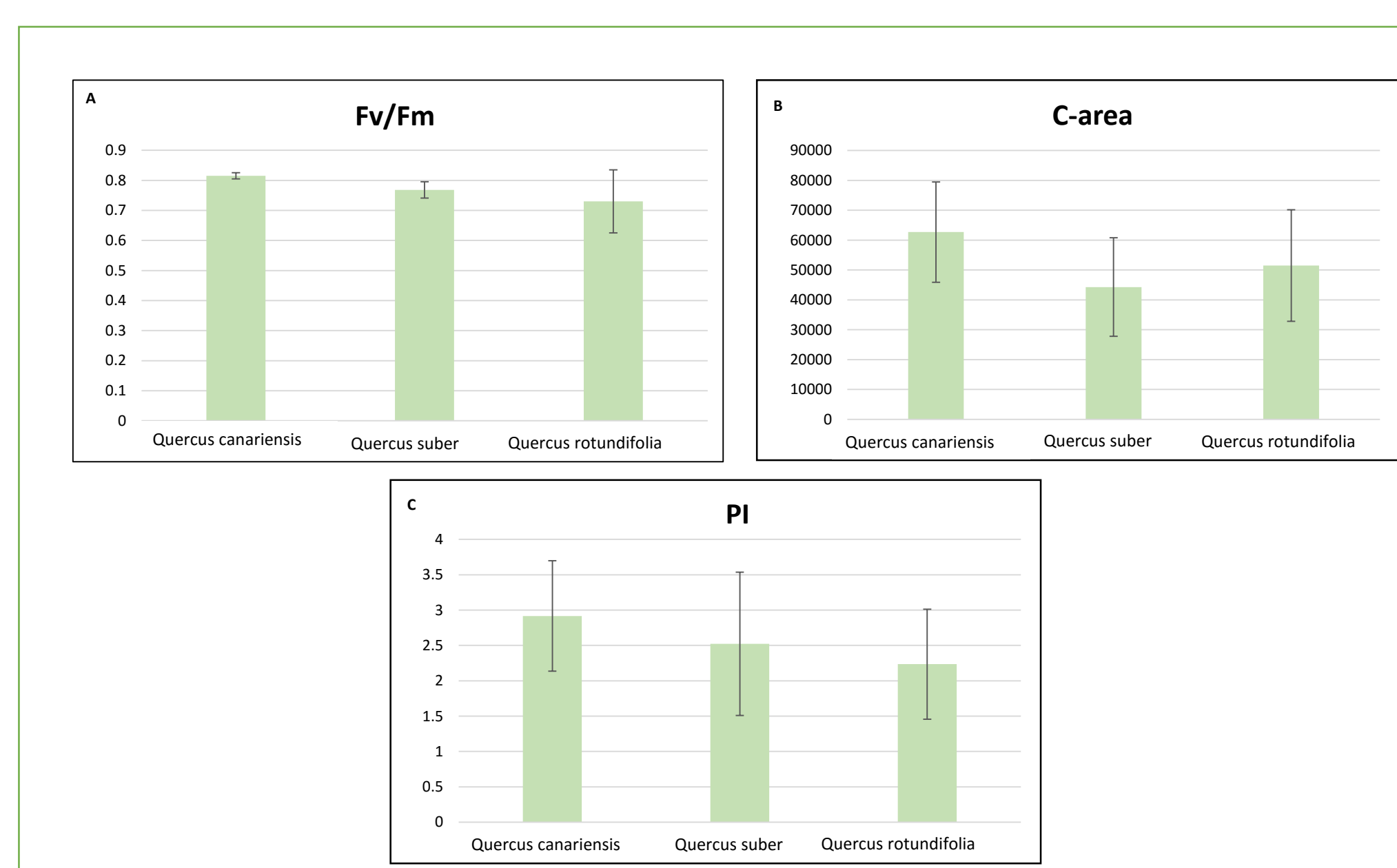


Fig.1 – Mean \pm S.D. of Fv/Fm (A), C-area (B), and PI (C) values from each of the three *Quercus* species studied.

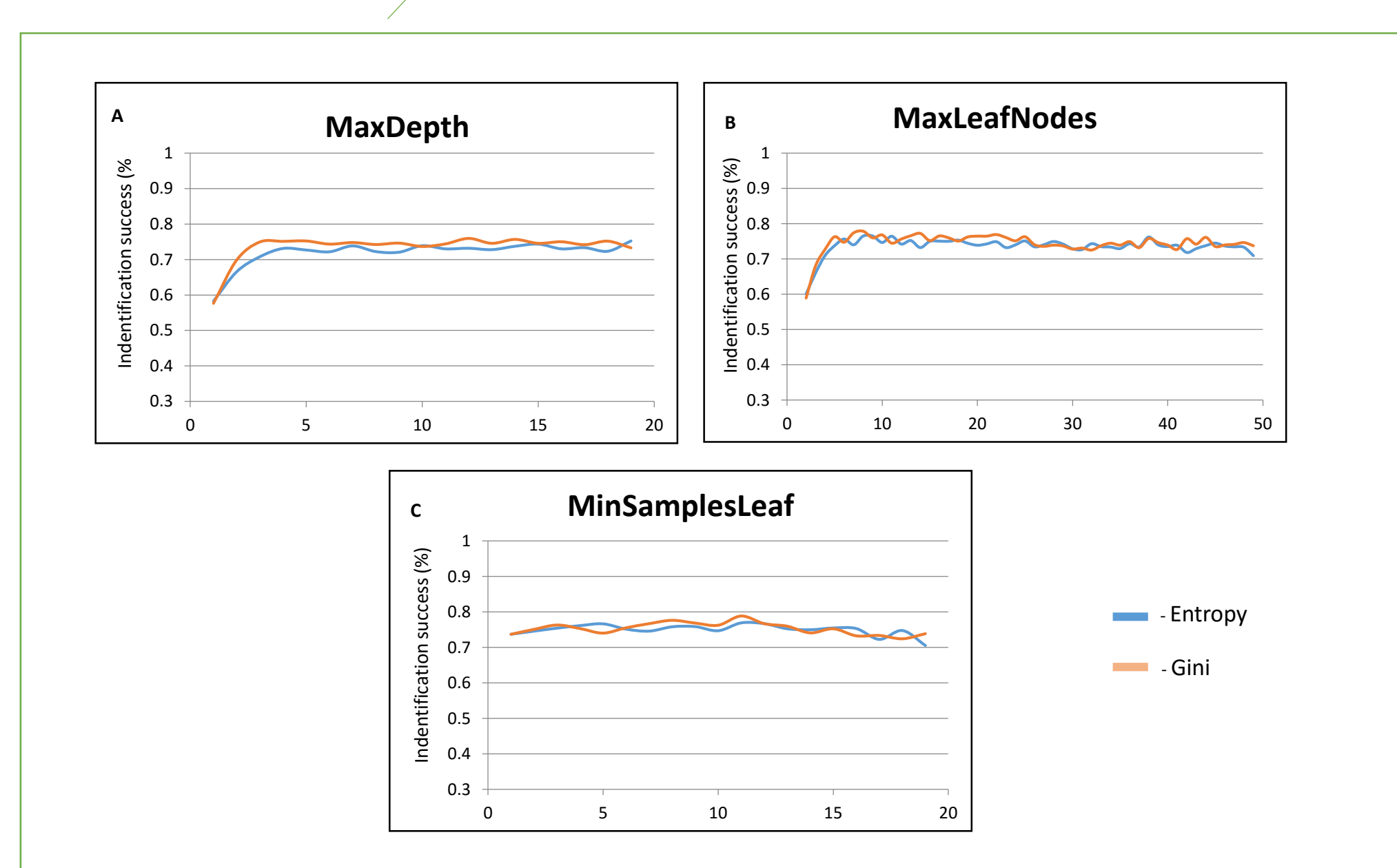


Fig. 2 – *Quercus* species identification success by two decision criteria (Entropy and Gini), when using the values obtained for Fv/Fm, C-area, and PI. A) Variation in the identification success by altering the maximum tree depth. B) Variation in the identification success by altering the maximum number of leaves. C) Variation in the identification success by altering the minimum number of samples in a leaf.

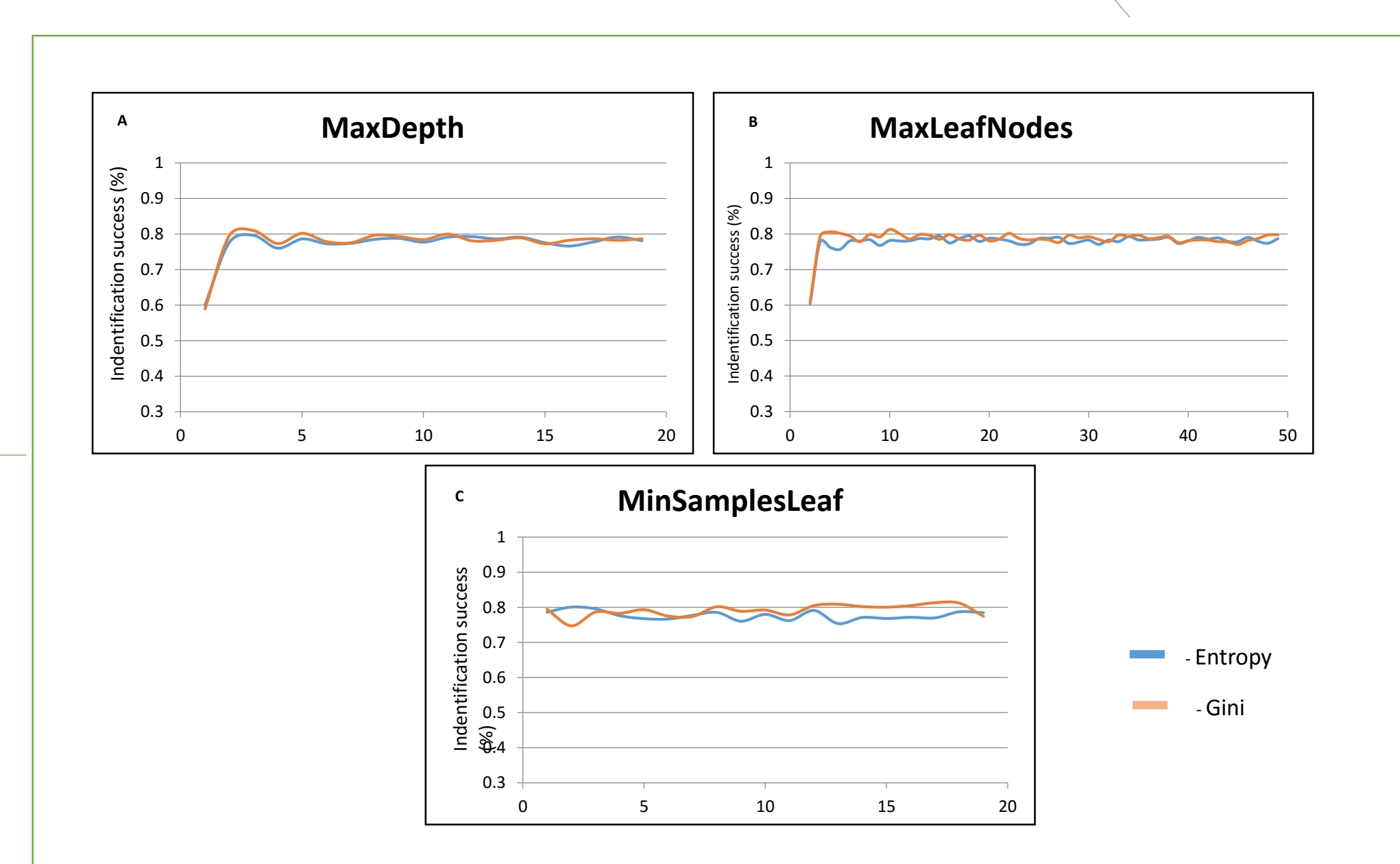


Fig.3 – *Quercus* species identification success by two decision criteria (Entropy and Gini), when using the entire dataset of points from the fluorescence curves. A) Variation in the identification success by altering the maximum tree depth. B) Variation in the identification success by altering the maximum number of leaves. C) Variation in the identification success by altering the minimum number of samples in a leaf.

Conclusions

Albeit the three species studied are closely phylogenetically related, belonging to the same genus, the analysis of their rapid fluorescence induction curves with decision trees was able to automatically distinguish between them with reasonable accuracy, suggesting that this approach may be suitable for high throughput plant phenotyping.

REFERENCES

- [1] Tyystjärvi E, Koski A, Keranen M, Nevalainen O (1999) The Kautsky Curve Is a Built-in Barcode. *Biophysical Journal* 77: 1159 – 1167.
- [2] Silvestre S, Araújo SS, Vaz Patto MC, Marques da Silva J (2014) Performance index: an expeditious tool to screen for improved drought resistance in the *Lathyrus* genus. *Journal of Integrative Plant Biology* 56 (7): 610–621.
- [3] Singh A, Ganapathysubramanian G, Singh AK, Sarkar S (2016) Machine Learning for High-Throughput Stress Phenotyping in Plants. *Trends in Plants Sciences* 21 (2): 110-124.
- [4] Strasser RJ, Srivastava A, Tsimilli-Michael M (2000) The Fluorescence Transient As a Tool to Characterize and Screen Photosynthetic Samples. In: Yunus M, Pathre U, Mohanty P (eds.), *Probing Photosynthesis: Mechanisms, Regulation and Adaptation*. Taylor & Francis: London, pp. 445- 483
- [5] Gameiro, C., Pereira S., Figueiredo, A., Bernardes da Silva, A., Matos, A.R., Pires, M.C., Teubig, P., Burnay, N., Moniz, L., Mariano, P., Marques da Silva, J. (2016). Preliminary results on the use of chlorophyll fluorescence and artificial intelligence techniques to automatically characterize plant water status. *Actas del XIII Simposio Hispano-Portugués de Relaciones Hídricas en las Plantas – Aprendiendo a optimizar el uso del agua en las plantas para hacer de nuestro entorno un ambiente más soastenable*. Pamplona, España, 18 - 20 octubre, pp 15 – 18.

ACKNOWLEDGMENTS

We would like to thank Dr. Carla Gameiro for the help provided during the experimental procedure; we would also like to thank Nelly Silva for her helpful assistance.

Are chlorophyll fluorescence and machine learning techniques able to automatically classify *Arabidopsis* water stress status?

Cíntia Macedo,¹ Tomás Ochôa Cruz,¹ João Nunes Silva,¹ Nuno Burnay,¹ Carla Gameiro,¹ Pedro Mariano^{1,2} and Jorge Marques da Silva^{1,2}

¹University of Lisbon, Faculty of Science

²Biosystems and Integrative Sciences Institute

Introduction

- ❖ Breeding plant varieties more resistant to water stress and more water use efficient is a major goal for plant breeders. The rapid and precise characterization of the phenotypes of the plants produced is crucial to attain this goal.
- ❖ Chlorophyll fluorescence provides non-invasive information on the functional photosynthetic status of plants and has been extensively used in low throughput plant phenotyping for water stress. In particular, the JIP test, based in the rapid fluorescence induction curve (Kautsky effect) allows the computation of several parameters physiologically relevant, such as the maximum photochemical efficiency of photosystem II (Fv/Fm), the integrated photochemical performance index (PI) and the complementary area above the fluorescence induction curve (C-area), a measure of the plastoquinone pool.
- ❖ In this work we introduced the data from the fluorescence induction curves (either the three abovementioned calculated parameters or the entire dataset of fluorescence vs time) in a machine learning algorithm in order to construct decision trees and test the ability to automatically classify *Arabidopsis* leaves according to their relative water content.

Materials & Methods

❖ Plant material and water stress conditions

Arabidopsis thaliana plants (n=60) were grown in a phytotron (25/18°C (day/night), RH 50%, photoperiod 16 hours and PAR approximately 250 µmol/m²s). Fully-expanded leaves (n=60, one per plant) were excised, immediately weighed, and a JIP test was performed. Leaves were floated in distilled water for 4 hours to obtain the fully-turgid weight and a JIP test was performed again. Excised leaves were then transferred to a phytotron at 25°C, RH of 40% and a PAR of 200 µmol/m²s in order to induce rapid water stress. Leaves were periodically weighed (twice during the experiment) and JIP tests performed. At the end leaves were oven dried, dry weight was obtained and the Relative Water Content (RWC) was calculated for each JIP test using the equation in Smart *et al.* (1974). We divided the samples in 4 classes according to their RWC: higher than 80% (class 1), between 50 and 80% (class 2), between 30 and 50% (class 3) and lower than 30% (class 4).

❖ Chlorophyll Fluorescence (JIP test)

Rapid induction curves (JIP test) were measured with a Handy PEA (Hansatech, U.K.) after 10 min leaf dark adaptation followed by the application of a saturating light pulse of 3500 µmol m⁻² s⁻¹ for 1 s (Strasser *et al.*, 2000).

❖ Machine learning program

Decision trees were built for the data collected with the fluorometer; the algorithm was applied either to the entire set of points of the curves or to the three selected parameters; two different decision criteria were used: Entropy and Gini. The influence of the Maximum tree Depth (MaxDepth), Maximum number of Leaves (MaxLeafNodes) and Minimum number of Samples in a Leaf (MinSamplesLeaf) on the success of the classification was studied.

Results and Discussion

- ❖ For Fv/Fm and PI, the differences observed were statistically significant (ANOVA, T-test, p<0.05) for all classes except between classes 2 and 3; For C-area, there was only a statistically significant difference between classes 1 and 3, 1 and 4, and 3 and 4 (Fig. 1). As expected, whereas Fv/Fm sharply decreased only at the extreme water stress level, PI showed an almost linear decrease with water stress.
- ❖ With only the three abovementioned parameters being fed into the machine learning algorithm, the success of classification reached approximately 85% (being the random classification success circa 25%), approximately the same score obtained when the entire set of the points of the curves (fluorescence F(time) was used (Fig. 2 A and B and Fig. 3 A and B). This suggests that the selected parameters (Fv/Fm, PI and C-area) contain all the relevant information present in the JIP curves, in what relates to the relation between fluorescence induction and the RWC of the leaves.
- ❖ The Maximum tree Depth (MaxDepth), Maximum number of Leaves (MaxLeafNodes) and Minimum number of Samples in a Leaf (MinSamplesLeaf) did not significantly affect the success of the classification.

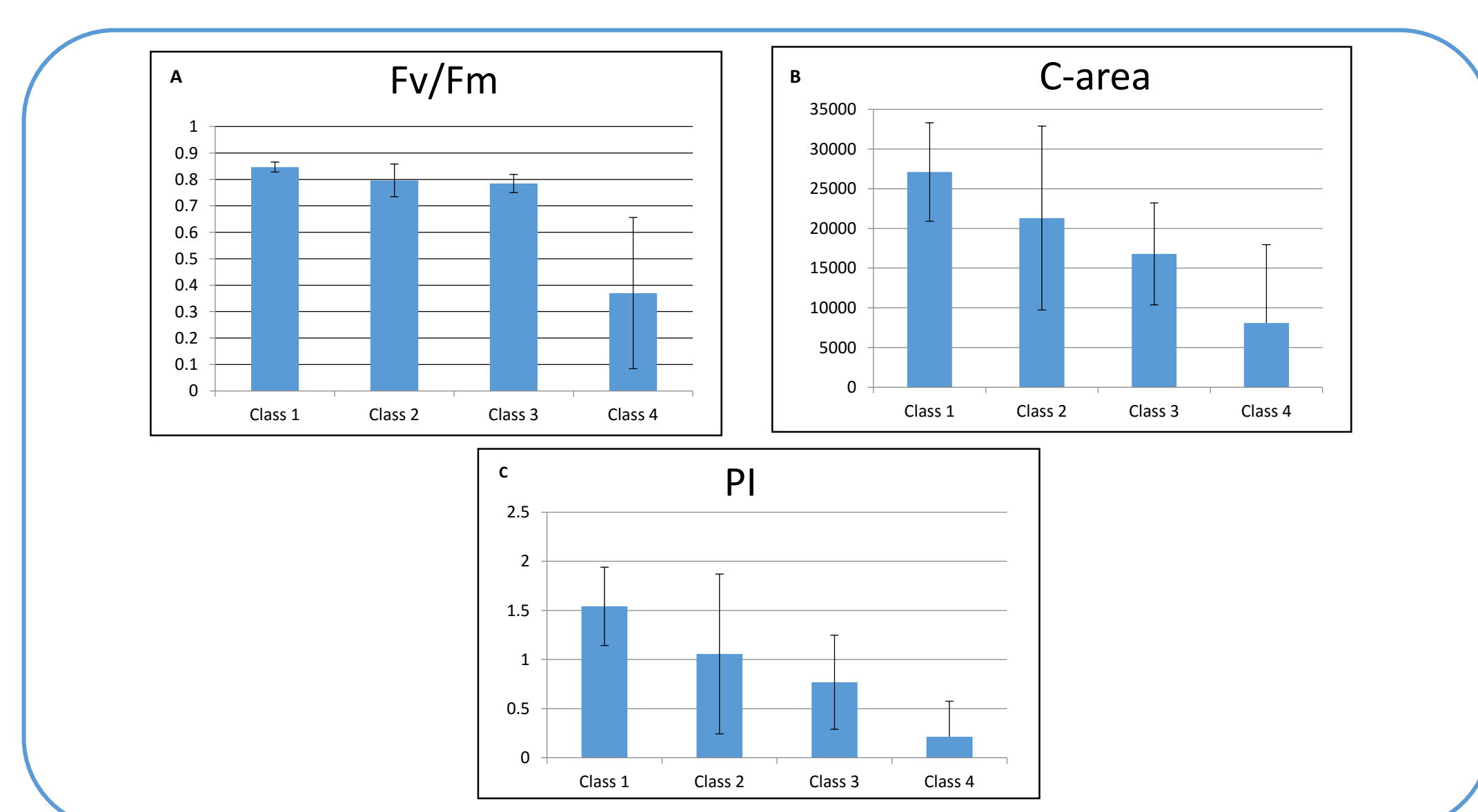


Fig.1 – Fv/Fm (A), C-area (B), and PI (C) values for each class of RWC of *Arabidopsis thaliana* (mean ± S.D.).

Conclusions

Decision trees applied to rapid fluorescence induction curves were able to automatically classify *Arabidopsis* leaves according to their RWC with satisfactory accuracy. Despite our initial predictions, using a specific subset of parameters did not decrease the probability of a correct identification, which may facilitate the use of this technique in high throughput plant phenotyping.

ACKNOWLEDGMENTS

We would like to thank Manuela Lucas for assistance in the lab. We acknowledge Nelly Silva for support in the poster production.

❖ REFERENCES

- ❖ Strasser RJ, Srivastava A, Tsimilli-Michael M (2000) The Fluorescence Transient As a Tool to Characterize and Screen Photosynthetic Samples. In: Yunus M, Pathre U, Mohanty P (eds.), Probing Photosynthesis: Mechanisms, Regulation and Adaptation. Taylor & Francis: London, pp. 445- 483
- ❖ Smart RE, Bingham GE (1974) Rapid Estimates of Relative Water Content. Plant Physiol. 53(2):258–60.

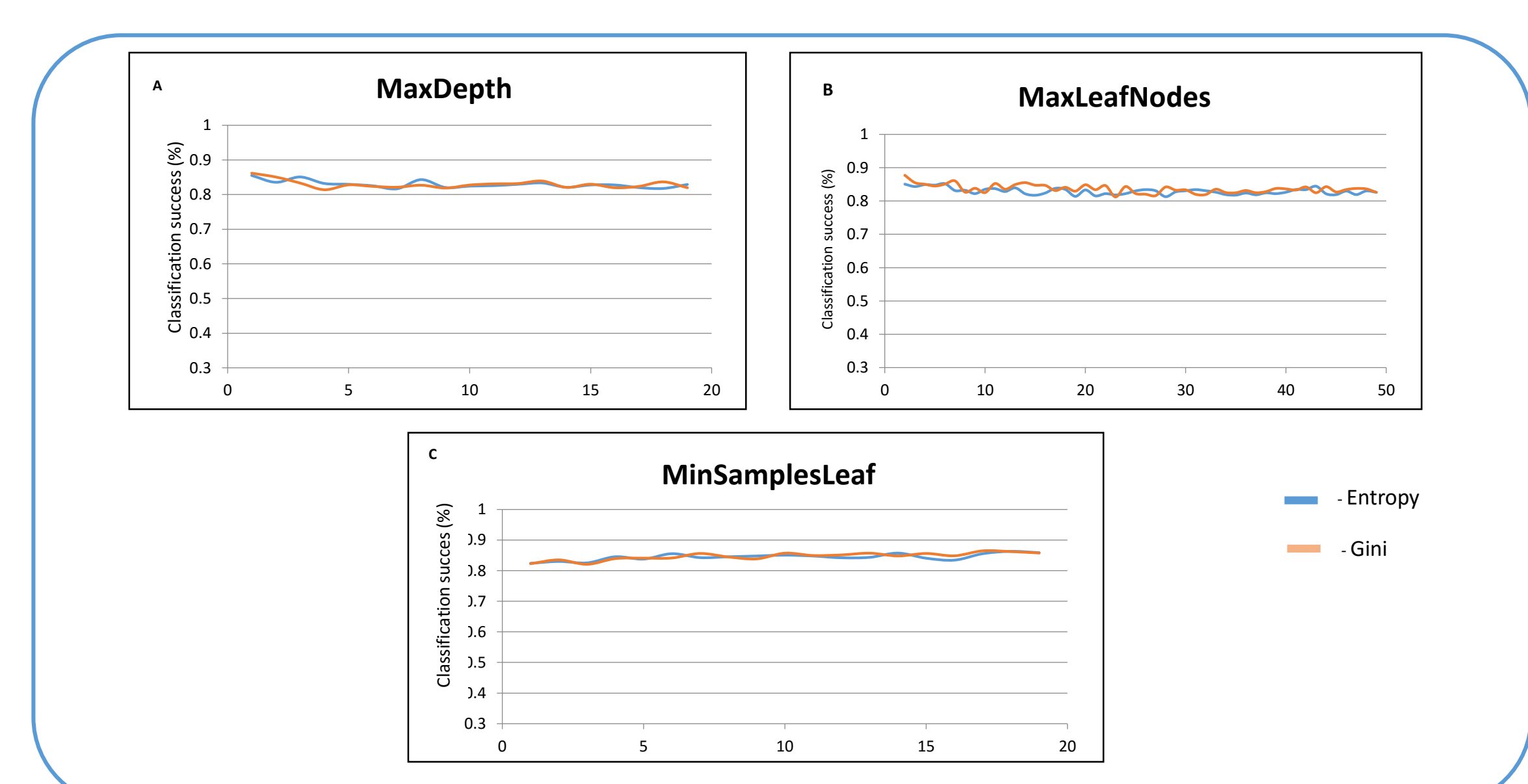


Fig. 2 – Classification success of the state of water stress (RWC class) in *Arabidopsis thaliana* by two decision criteria (Entropy and Gini), when using the values obtained for Fv/Fm, C-area, and PI. A) Variation in the classification success by altering the maximum tree depth. B) Variation in the classification success by altering the maximum number of leaves. C) Variation in the classification success by altering the minimum number of samples in a leaf.

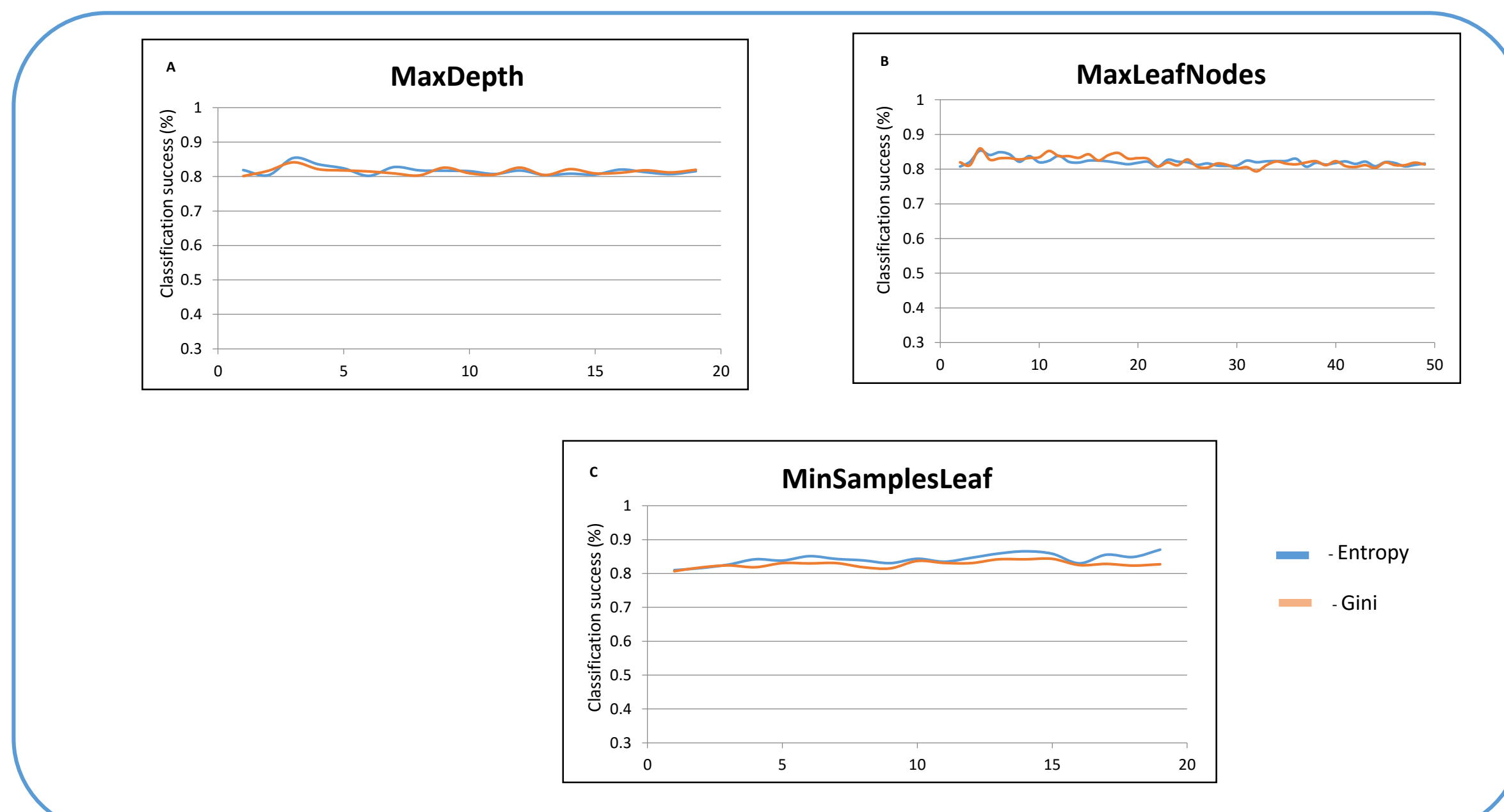


Fig.3 - Classification success of the state of water stress (RWC class) in *Arabidopsis thaliana* by two decision criteria (Entropy and Gini), when using all the data points of fluorescence induction curves. A) Variation in the classification success by altering the maximum tree depth. B) Variation in the classification success by altering the maximum number of leaves. C) Variation in the classification success by altering the minimum number of samples in a leaf.

Portuguese traditional olive tree (*Olea europaea* L.) identification using endocarp characteristics and SSR markers

Maria Manuela Veloso^{1,3}, M. Cristina Simões-Costa^{2,3}, Luís C. Carneiro¹, Pedro Fevreiro^{4,5}, Cândido Pinto-Ricardo⁴

¹Unidade de Investigação de Biotecnologia e Recursos Genéticos, Instituto Nacional de Investigação Agrária e Veterinária, Quinta do Marquês, 2784 – 505 Oeiras, Portugal

²Departamento de Recursos Naturais, Ambiente e Território, Instituto Superior de Agronomia, Universidade de Lisboa, Tapada da Ajuda, 1349-017 Lisboa, Portugal

³LEAF, Linking Landscape, Environment, Agriculture and Food, Instituto Superior de Agronomia, Universidade de Lisboa, Tapada da Ajuda, 1349-017 Lisboa, Portugal

⁴Instituto de Tecnologia Química e Biológica, Universidade Nova de Lisboa, Av. Da República, Apt 127, 2781-901 Oeiras, Portugal

⁵Universidade de Lisboa, Faculdade de Ciências, Dept. Biologia Vegetal, Campo Grande, 1749-016 Lisboa, Portugal

Background

Portugal has a large genetic patrimony of olive tree (*Olea europaea* L.) represented by many “old” local cultivars, some of restricted distribution. The olive tree crop represents 9.2% of the Utilized Agricultural Area (UAA) and the traditional orchards are 80% of the olive area in Portugal. About 60% of the national olive oil is produced in the Alentejo region by two quite different cultivation systems: the traditional farming system (85% of area and 35% of total olive oil production) and the semi intensive and intensive system (15% of area and 65% of the total olive oil production) (1). Dominant cultivars in the Alentejo traditional orchards are “Cordovil de Serpa” and “Verdeal Alentejana”, but other local cultivars are always present, although in small numbers (2).

Material and methods

Thirty two olive trees were studied from **seven traditional** olive orchards.

Morphological study: **40** fruits from each tree were collected during two seasons. **Five endocarp characters** were evaluated: weight, length, width, number and distribution of vascular bundles. Endocarp images were captured with a stereoscope Leica Wild MZ8 equipped with a Leica DC200 camera.

Microssatellites (SSR) study: **seven loci** were used based on the reproducibility, quality of scoring, information content and discriminative capacity.

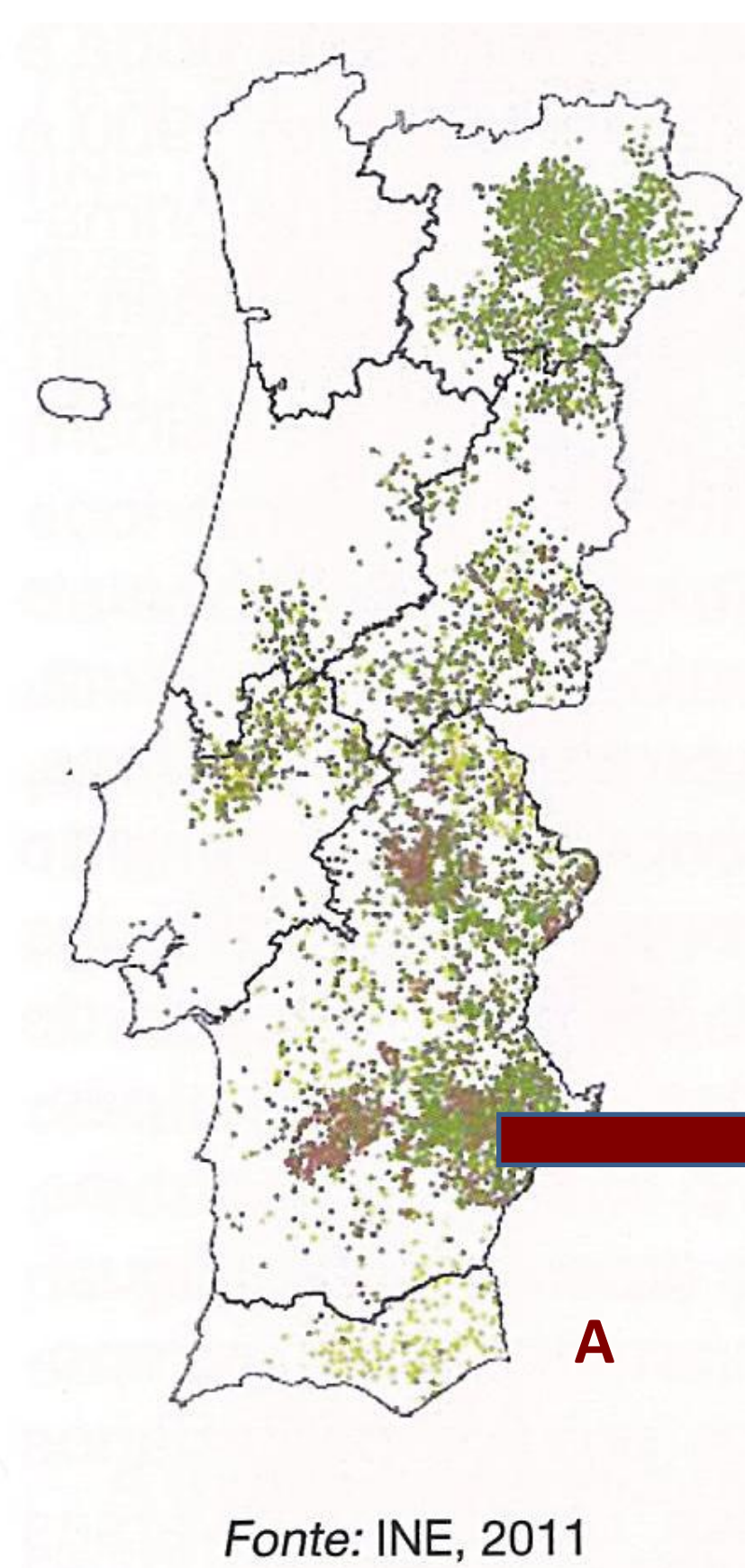
Data analysis:

PCA was performed using the program NTSYS-pc, version 2.1

IDENTITY and MICROSAT were used to study the genetic diversity. Neighbor-joining (weighted) algorithm as implemented in DARwin software package, version 6. 0. 12 (CIRAD, Montpellier, France) was performed to evaluate the relationships among olive trees.

Objectives

The objective of this work was: i) to identify the autochthonous olive trees present in traditional orchards of Vila Verde de Ficalho (Alentejo), using endocarp characteristics and SSR markers; ii) to investigate the genetic relationship between the studied olive trees; iii) to estimate the extent of olive tree genetic diversity.

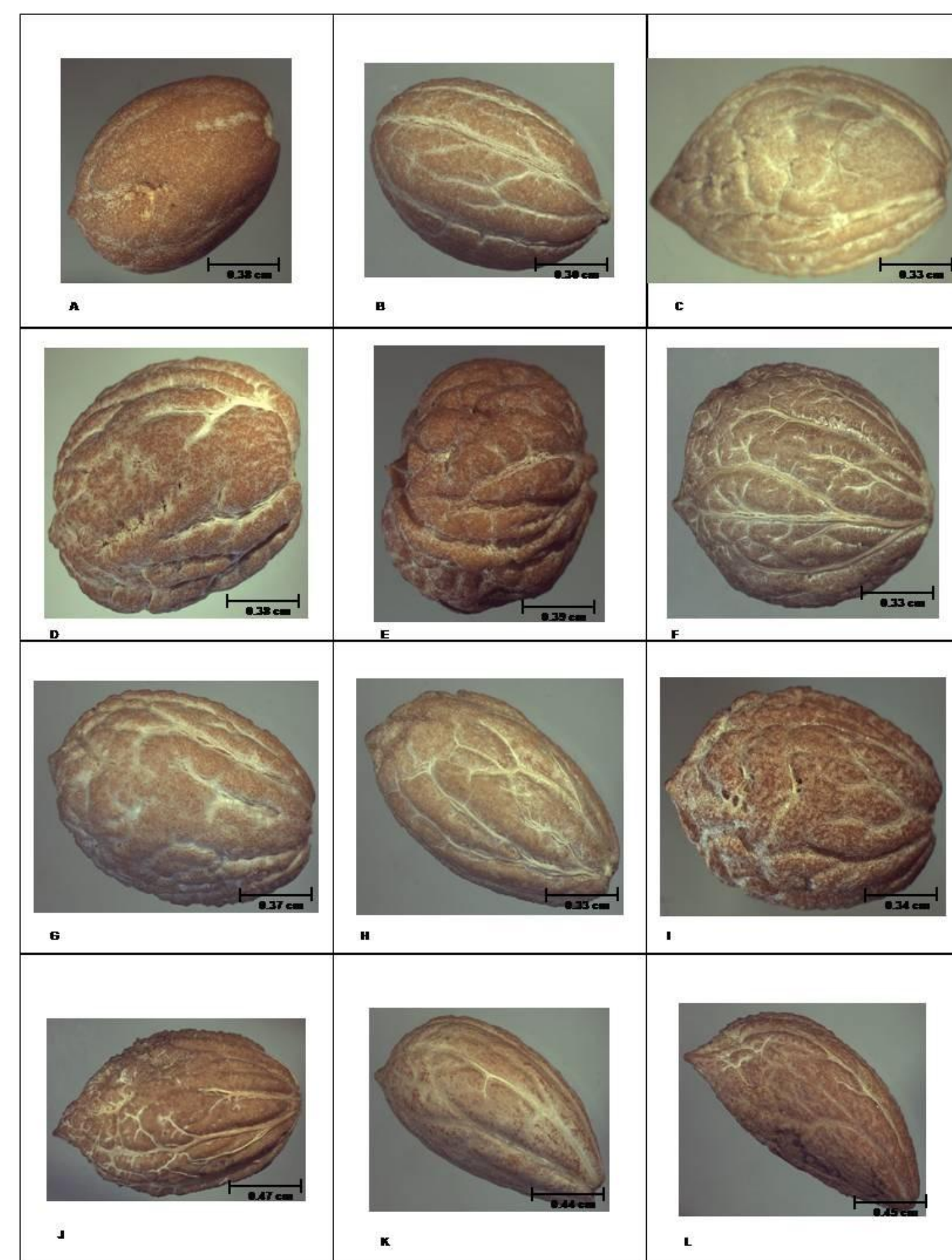


Olive tree distribution in Portugal (A) and traditional olive orchard at Vila Verde de Ficalho (B)

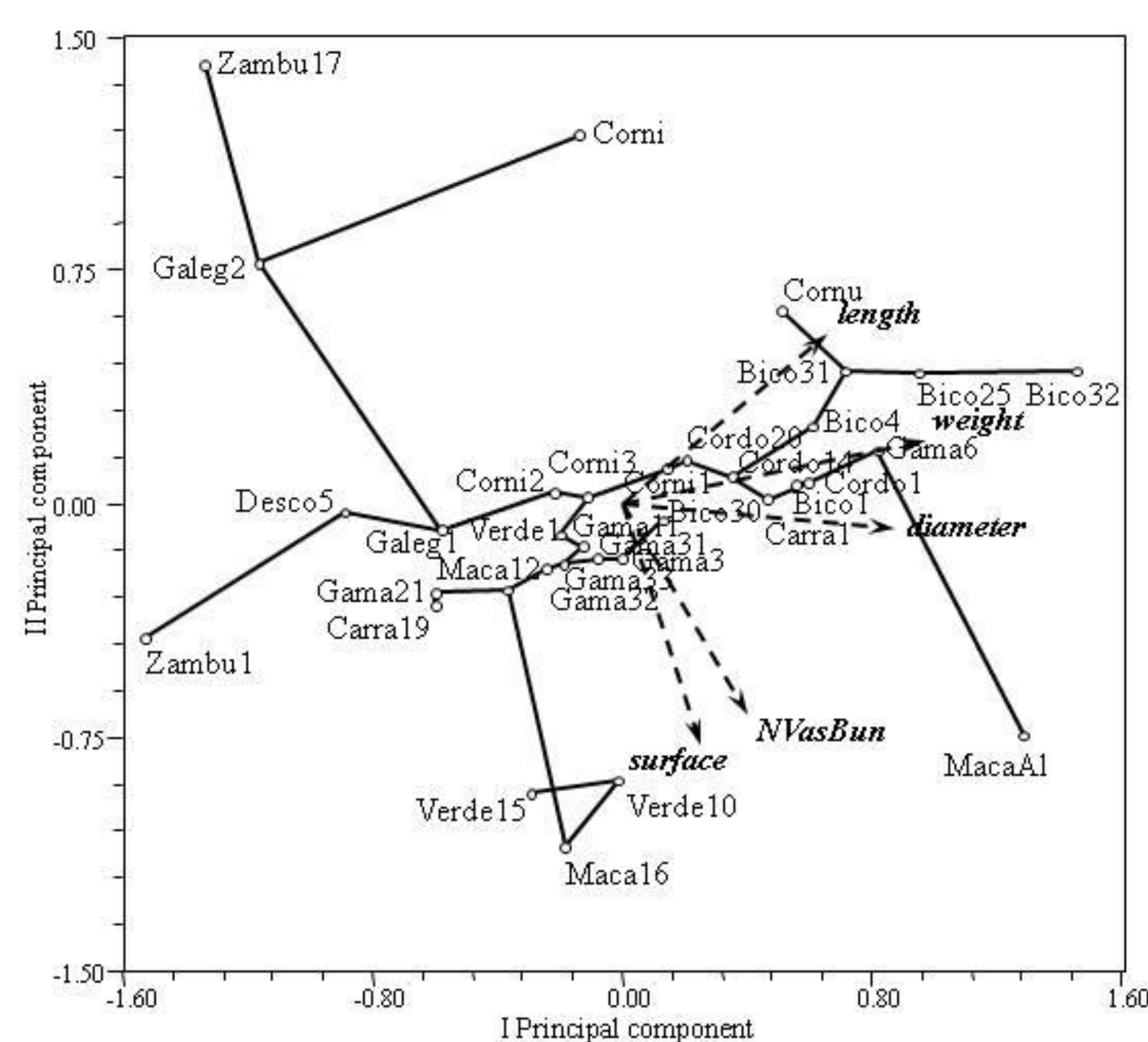
Findings

The endocarp images express important differences of shape and surface texture. PCA analysis allows the discrimination of all the olive trees on the basis of these two endocarp characters.

➤ Cases of farmers mislabelling were identified.



Endocarp images captured with a stereoscope Leica Wild. A – Zambu17; B – Zambu1; C – Galega1; D – MacaA1; E – Maca16; F – Gama32; G – Cordo1; H – Verde1; I – Verde15; J – Bico4; K – Cornic1; L – Cornic

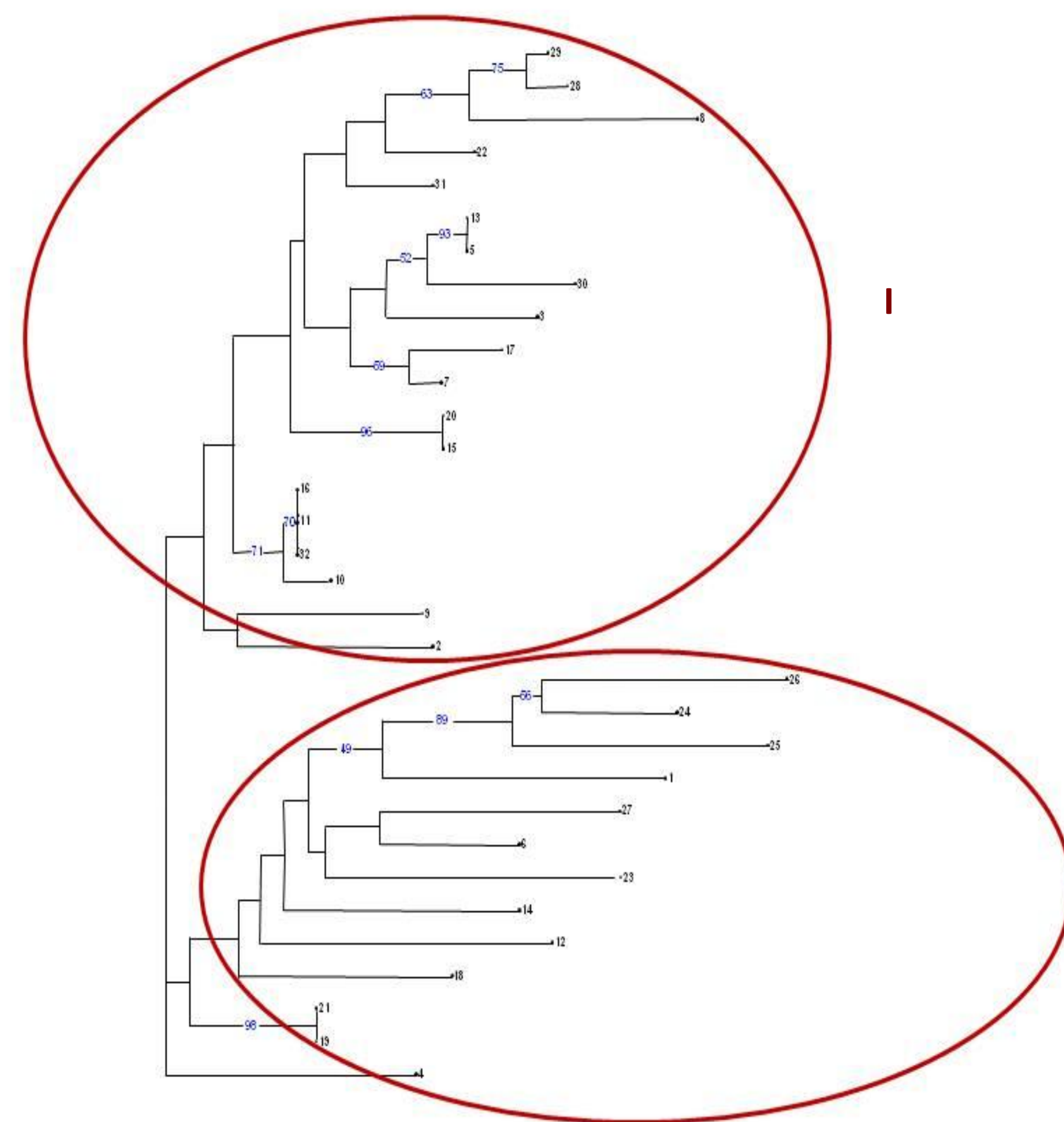


Projections of the olive trees onto the plane defined by the I (46.7%) and the II (27.7%) principal components with superimposition of the minimum spanning tree and eigenvectors. The variables correspond to weight, length, width, number and distribution of vascular bundles over the endocarps.

- Fifty six different alleles were scored with 7 SSR markers.
- An average of 8 alleles/SSR locus (range 5-14) were observed.
- Two main germplasm groups were detected in the traditional orchards:

- I – Autochthonous olive trees
- II – Mainly oleasters and unknown olive trees.

- Cases of farmers mislabelling were identified
- Cases of identical plants were identified



Neighbor-joining tree of 32 *Olea europaea* plants based on SSR analysis. Number at the branches correspond to bootstrap values (%) out of 1,000 replications

Conclusions

It is evident that both endocarp and SSR analyses separated the olive trees in two groups: I) autochthonous olive trees; II) wild and unknown olive trees. However, the relationships detected among the autochthonous trees varied with the analytical system used.

On the other hand, it was observed that olive trees genetic diversity is still existing in the Ficalho's orchards. However, it should be taken in consideration that the emergence of modern olive growing practices is endangering the traditional system which is a valuable repository of genetic variability. So, the conservation of autochthonous olive trees is a priority of great value for olive breeding, particularly important when considering tolerance and adaptation to biotic and abiotic stresses that are expected to be intensified by global climatic change.

References

- Matos M. 2014. As oliviculturas nacionais: uma nova realidade em Portugal. In: Olival Tradicional - Contextos, Realidades e Sustentabilidade. Rota do Guadiana Eds. pp. 47-53.
- Veloso MM. 2014. Os agroecossistemas tradicionais na conservação da diversidade genética da oliveira (*Olea europaea*) em Vila Verde de Ficalho. In: Olival Tradicional - Contextos, Realidades e Sustentabilidade. Rota do Guadiana Eds. pp. 147-153.

Looking at biochemical responses following cork harvesting in *Quercus suber* L.

Clara A. Pinto^{1,2}, Carla Pinheiro^{3,4}, Filipe Costa-e-Silva^{1,2}, Alexandra C. Correia², Teresa S. David^{1,2}, João S. Pereira²

¹ Instituto Nacional de Investigação Agrária e Veterinária I.P., Quinta do Marquês, Av. da República, 2780-159 Oeiras, Portugal; ² Centro de Estudos Florestais, Instituto Superior de Agronomia Universidade de Lisboa, Tapada da Ajuda, 1349-017 Lisboa, Portugal; ³ Instituto de Tecnologia Química e Biológica, Av. da República, EAN, 2780-157 Oeiras, Portugal; ⁴ Faculdade de Ciências e Tecnologia, Avenida da República, Universidade Nova de Lisboa, 2829-516 Caparica, Portugal. e-mail: clara.pinto@gmail.com

INTRODUCTION

Quercus suber L. (cork oak) woodlands occupy about 1.7 million ha in the western Mediterranean Basin, being the largest areas located in Portugal (over 700×10^3 ha). They are in the base of ecosystems with a high socio-economic and conservation value, hosting high levels of biodiversity, whilst supporting the cork industry and acting as a source of income for rural populations. Although it is generally assumed that *Q. suber* is well adapted to Mediterranean-type climate conditions, especially to high summer temperatures and recurrent droughts, a general trend of decline in the occupied area and in tree vitality has been observed during the last decades, threatening the long-term sustainability of these woodlands. In spite of its importance and the number of previous studies focusing the species, there are still knowledge gaps, especially in relation to the potential impacts of cork harvesting (the major economic activity related to these woodlands) for trees. As cork is harvested from late May to late August, usually coinciding with hot, dry periods, marked by water stress, trees might be subjected to an increased level of physiological stress after harvesting. To address this issue we set up an experiment aiming to reveal possible biochemical responses of trees to cork harvesting.

RESULTS

Preliminary results show that, after cork harvesting and as summer progressed, phenolic compounds in the phloem tissue increased more in cork stripped than in control trees (fig. 2a). This difference was higher when, in each group, the analysis was restricted to the trees that were experiencing higher levels of water stress and classified as producers of good quality cork (fig. 2b). Sucrose content in the phloem tissue of control trees increased steadily in the weeks after cork harvesting, being much higher than in treatment trees (fig. 3). Following the first sampling date, leaf galactose content was consistently higher in cork stripped than in control trees, peaking two weeks after cork harvesting (fig. 4). Glucose content in the leaves differs markedly when water stress is considered but not in function of cork harvesting (fig. 5).

MATERIAL AND METHODS

- 50-year-old *Q. suber* woodland (177 trees ha⁻¹) (fig. 1a and b).
- Two similar pairwise sets of cork stripped and unstripped (control) trees were monitored (fig. 1c).
- Physiological monitoring included tree water status (predawn and midday leaf water potentials and leaf gas exchange) and daily sap flow.
- After cork harvesting, leaves and phloem tissue (fig. 1d and e) of all trees were sampled at intervals with increasing duration for biochemical determinations (e.g. total phenolic compounds and sugars). The total phenolic content of the extracts was determined by the Folin-Ciocalteu method. Starch and sugars content was assessed using commercially available assay kits (fig. 1f).



Fig. 1: Location of the study site (a); perspective of study site (b); and studied trees (c); detail of phloem tissue sampling (d and e); example of raffinose determinations (f).

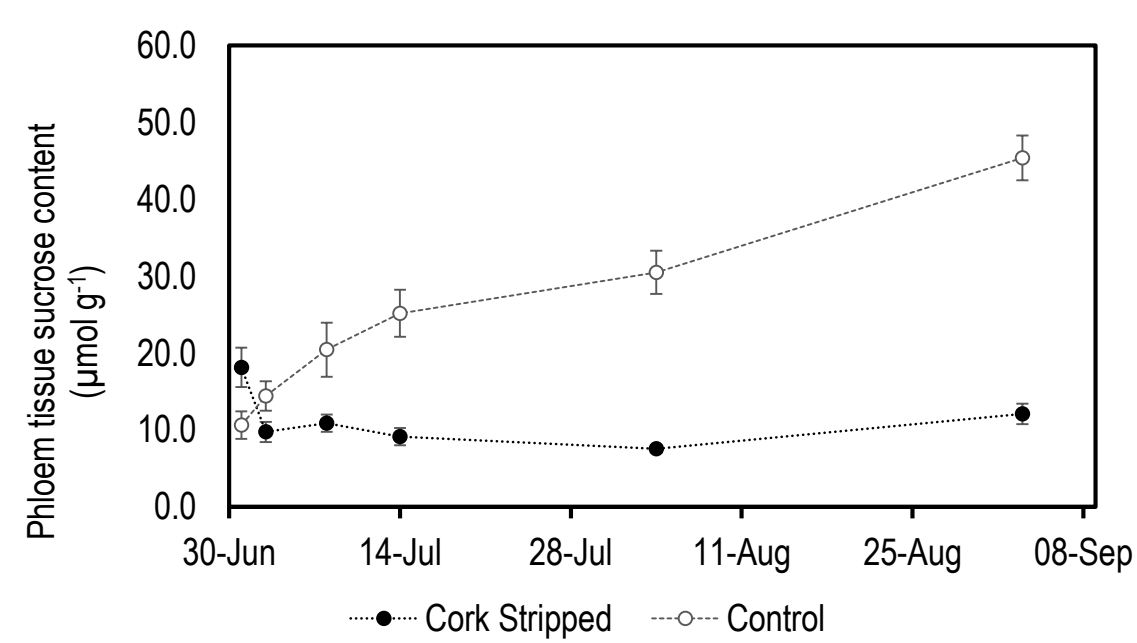


Fig. 3: Sucrose content in the phloem tissue of Cork Stripped and control trees. Error bars are standard errors.

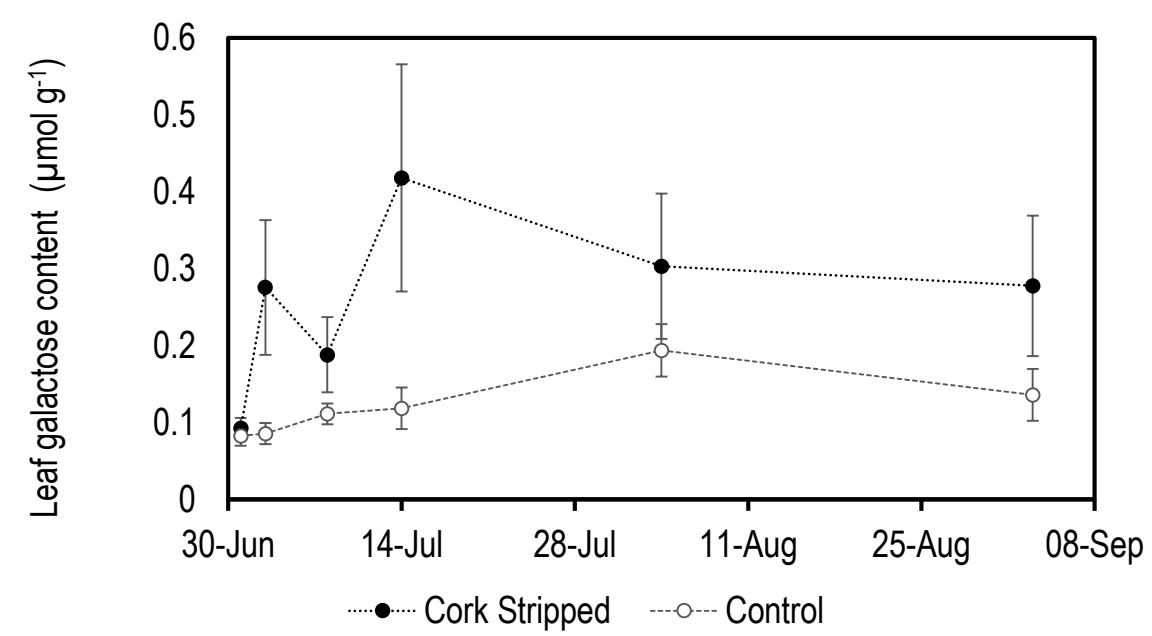


Fig. 4: Galactose content in leaves of Cork Stripped and control trees. Error bars are standard errors.

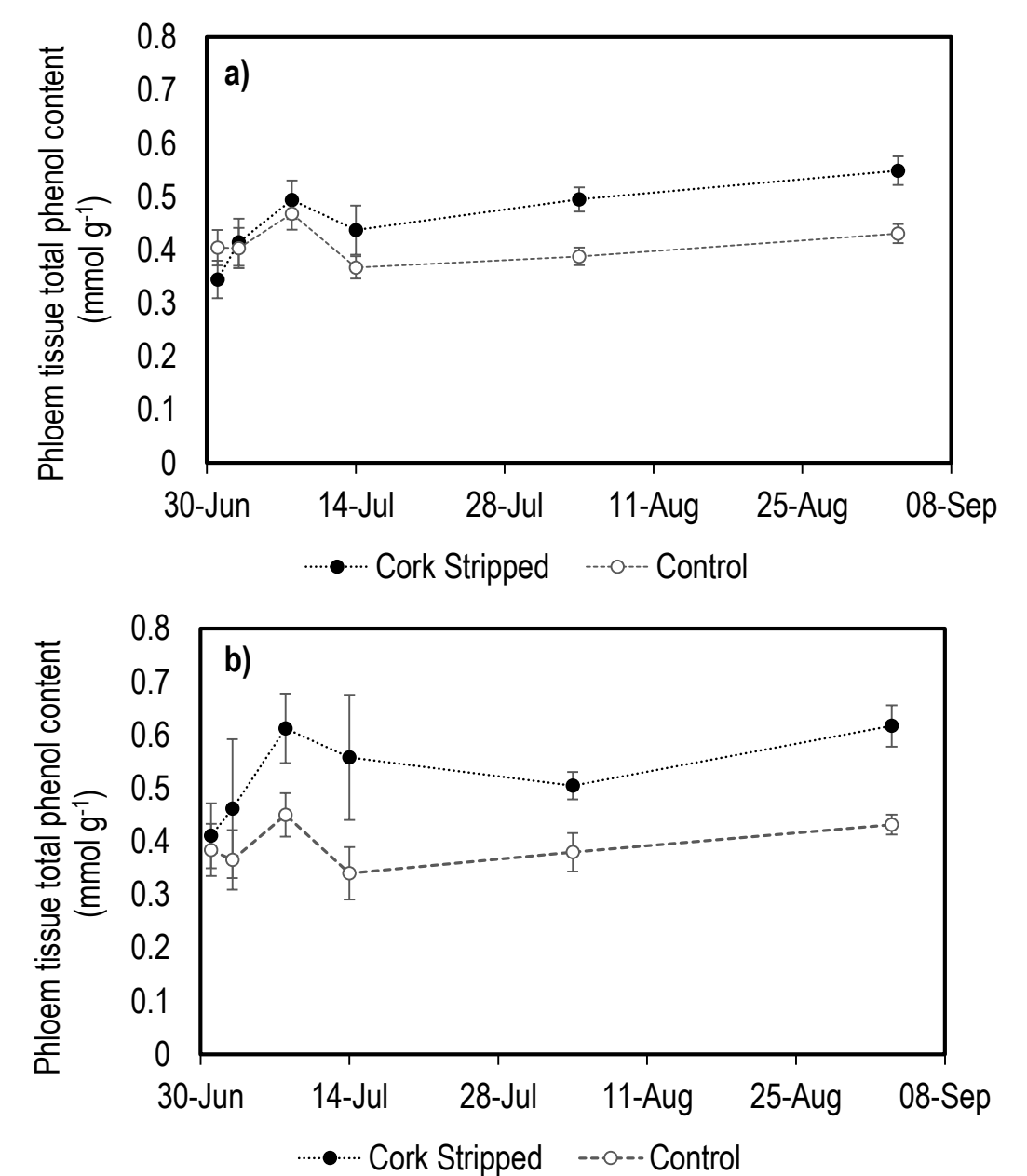


Fig. 2: Total phenolic compounds in the phloem tissue. Considering all studied trees (a), restricting the analysis in each group to the trees that were simultaneously experiencing higher levels of water stress and classified as producers of good quality cork (b). Error bars are standard errors.

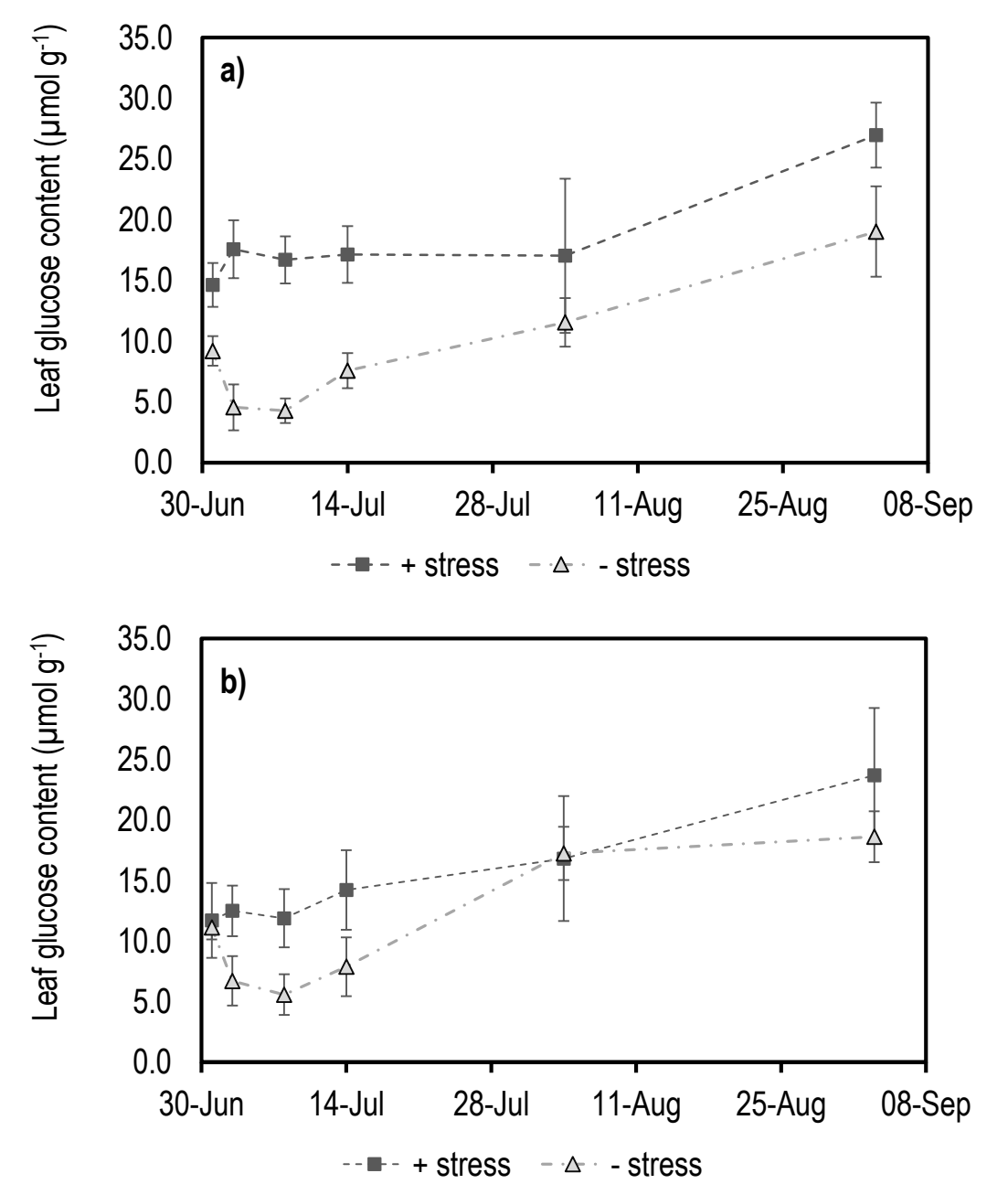


Fig. 5: Glucose content in the leaves of the studied *Q. suber* trees analysed according to the water stress level: Cork Stripped (a) and Control (b). Error bars are standard errors.

ACKNOWLEDGEMENTS

The research was done with financial support from grants: SFRH/BD/39058/2007 (A.C. Correia) and SFRH/PBD/111801/2015 (F. Costa-e-Silva). Fundação para a Ciência e a Tecnologia partially funded this experiment through the project PTDC/AGR-FOR/4360/2012 "Pegada de carbono da cortiça: das árvores aos produtos".

The authors wish to thank to António Gonçalves Ferreira and Alfredo Gonçalves Ferreira and Grupo Amorim for their support with field facilities and ITQB-Nova for lab facilities.

CONCLUSIONS

The increase of phenolic compounds in the phloem tissue likely results from a physiological response to cork harvesting, although mainly driven by the progression of drought. Similarly, sucrose content increase in the phloem tissue of control trees may be reflecting differences in phloem capacity to translocate sugars, following cork harvesting, and in phellogen activity throughout the summer in response to water stress. Contrary to water stress, cork harvesting does not seem to affect glucose content in the leaves. So far, our results suggest that cork harvesting is likely triggering a biochemical response, however, summer drought seems to be the main driver for the physiological stress experienced by *Q. suber* trees.

Preliminary results on the use of reflectance spectroscopy and artificial intelligence techniques to automatically identify *Vitis* species

Margarida Pires, Andreia Figueiredo, Pamela Teubig, Nuno Burnay, Pedro Mariano, Jorge Marques da Silva

University of Lisbon, Faculty of Sciences, BioISI – Biosystems and Integrative Sciences Institute, Campo Grande, 1749-016 Lisboa, jmlsilva@fc.ul.pt

INTRODUCTION

Grapevine (*Vitis vinifera* L.) is the most widely cultivated and economically important fruit crop in the world [1]. One of the major risks for viticulture is the infection by fungal pathogens. Enhancing the resistance of cultivated grapevine, while keeping a good berry quality, constitutes a major goal for breeders. Breeding approaches are quite time consuming and resource-intensive until the expression of the trait is observable in the progeny, due to the grapes' long generation cycle [2]. Moreover, the selection of resistant offspring is based on controlled inoculations, where thousands of plants have to be tested. Thus, the discovery of diagnosis methodologies that will allow a quick and accurate identification of the seedlings that inherited the resistant trait would have a major impact for grapevine breeders.

We used a diagnostic assay based on an optical technique – VIS/NIR reflectance spectroscopy - and an artificial intelligence technique – decision trees - to automatically classify two grapevine species presenting different resistance towards fungal diseases [3]. This approach is non-invasive, time- and cost-effective, being a valuable tool for high-throughput plant resistance phenotyping.

METHODOLOGIES

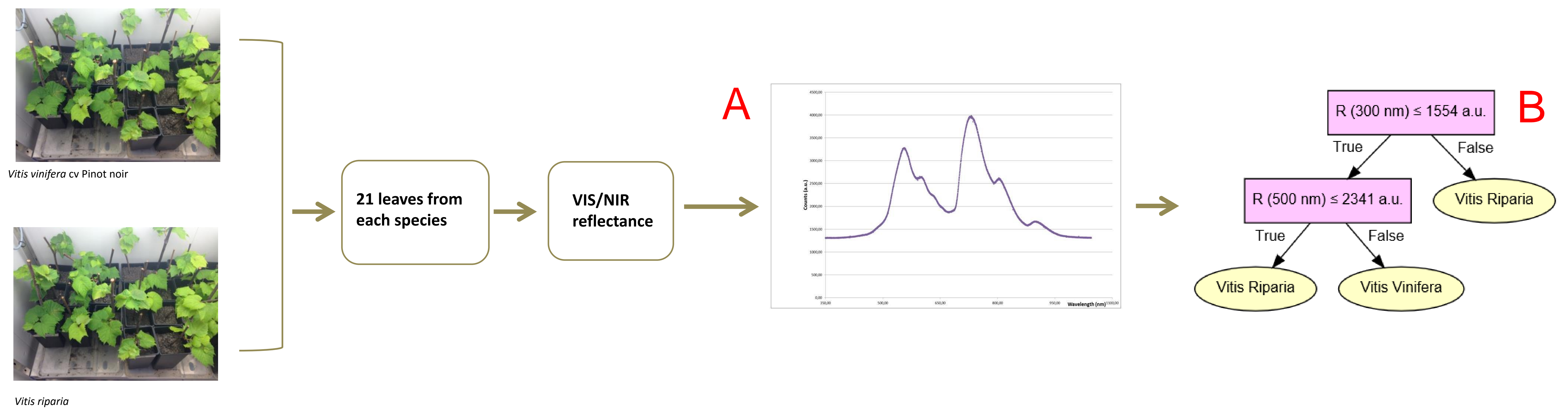


Fig. 1: A leaf in each plant was illuminated with a Vis-NIR wavelength range source (350-1050 nm); the reflected light was gathered by an optical fiber equipped with a collimator and analyzed by an Ocean Optics USB4000 spectrometer, with high resolution (A). The measured data was divided in two data sets: training dataset and a testing dataset. The decision tree is grown according to the following process: Given the dataset at the current node, a feature to split the dataset is selected such that the ability to discern the classes is maximum. For each division of the dataset, a node is created and the process repeats until a stopping criteria is met. Possible stopping criteria are: all the samples in dataset belong to the same class; the dataset has a minimum number of samples; depth of the node is maximum. Decision trees were built using the training dataset. Different parameters were varied: depth of the tree, minimum number of samples to split a dataset in a tree node. The obtained decision tree was evaluated in the testing dataset (B).

RESULTS AND DISCUSSION

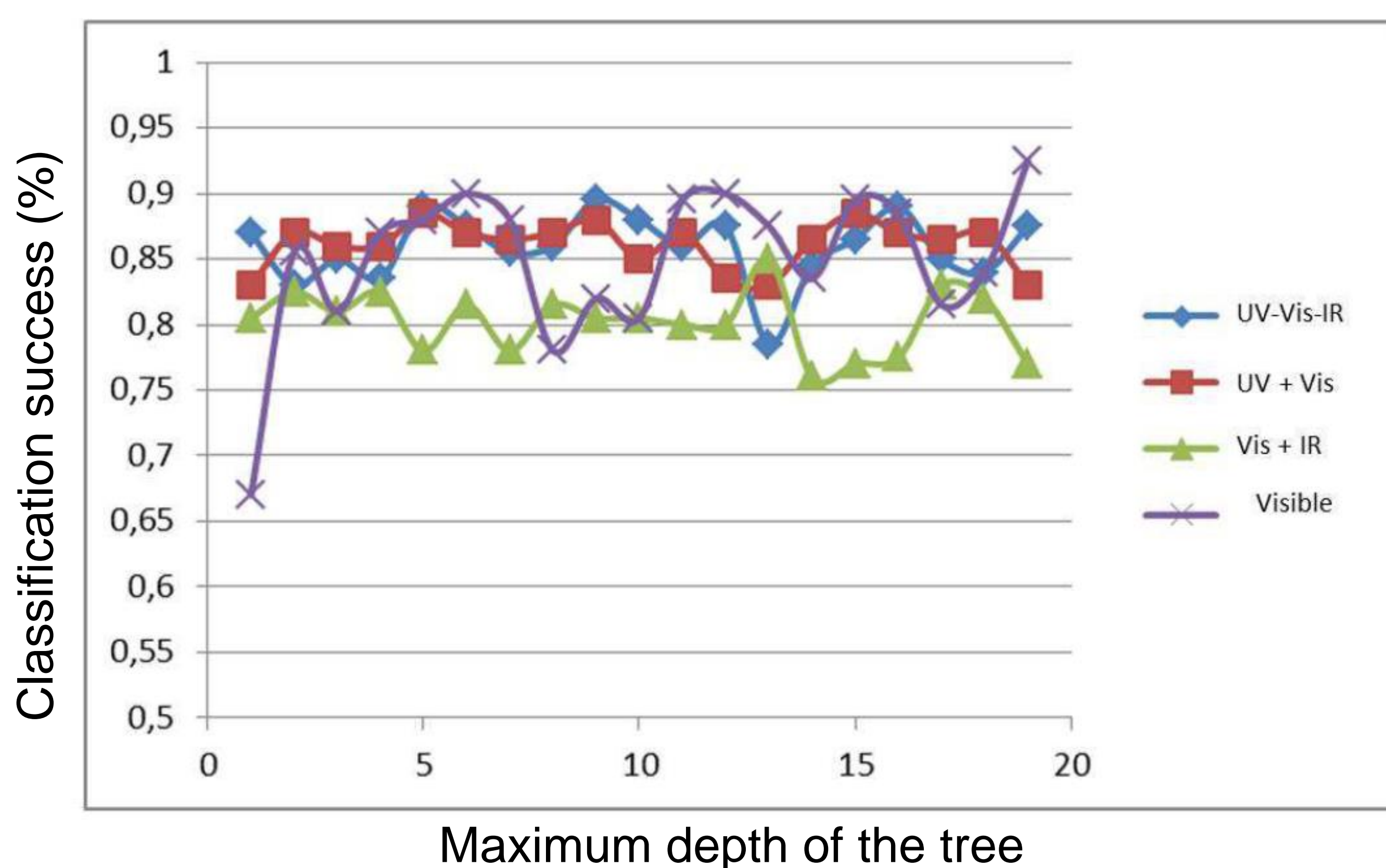


Fig. 2: Percentage of success of the classification of leaves of *Vitis riparia* and *Vitis vinifera* based on Vis/NIR reflectance, as a function of the maximum depth of the trees.

CONCLUSIONS

VIS/NIR reflectance spectroscopy is a promising technique to select *Vitis* species with different resistance backgrounds to fungal infections. In particular, the near-UV band of the spectrum has increased potential for the non-invasive discrimination of tolerant genotypes. The application of decision trees to the spectroscopic data facilitates the inclusion of this technique in high throughput plant phenotyping platforms.

REFERENCES

- [1] Organisation of Vine and Wine. 2016. 2016 OIV Statistical Report on World Vitiviniculture.
- [2] Gessler, C., I. Pertot, and M. Perazzolli. 2011. Plasmopara viticola: a review of knowledge on downy mildew in different time-points. Plant Sei. 191-192: 100-107
- [3] Gameiro C, Pereira S, Figueiredo A, Bernardes da Silva A, Matos AR, Pires MC, Teubig P, Burnay N, Moniz L, Mariano P, Marques da Silva J (2016) Preliminary results on the use of chlorophyll fluorescence and artificial intelligence techniques to automatically characterize plant water status. Proceedings of the XIII Simposio Hispano Português de Relaciones Hídricas en las Plantas

P73 PhenomicsNL, the Dutch Plant Phenotyping Network

Rick van de Zedde

Wageningen University & Research Centre, The Netherlands

The global population is growing and fossil fuels are becoming scarce. This is why it is important to grow crops that can be cultivated efficiently and have high yields, whether these are grains, vegetables, fruits or raw materials for bioplastics. But this is easier said than done. The agricultural sector is experiencing the results of climate change all across the globe; from floods in Bangladesh and droughts in the Horn of Africa, to the arrival of new plant diseases in Europe. Research groups at Wageningen University & Research are currently studying the behaviour of plants at different levels: from model and individual plants to the growth of crops in greenhouses and on the field.

Speeding up developments: Combining all knowledge, expertise and facilities in the field of phenomics into one single PhenomicsNL platform speeds up developments which enable chain partners to strengthen their position on the international market. Through this platform, Dutch companies will be informed about join large-scale initiatives. Wageningen University & Research has established several public-private partnerships and has been a partner in notable European initiatives such as SPICY, the COST action Phenomenall and the European Plant Phenotyping Network (EPPN). With PhenomicsNL, Wageningen University & Research is involved in many new programmes including those of the International Plant Phenotyping Network (IPPN), EMPHASIS and EU-project EPPN 2020. The EMPHASIS initiative develops and/or improves new and existing facilities and makes them widely accessible so that a clear image of the response of crops to climate change can be created through collaboration. EMPHASIS is part of Roadmap 2016 created by the European Strategy Forum for Research Infrastructures (ESFRI).

Phenotyping as a tool to screen the plant growth and symptom expression in sensitive, tolerant and resistant potato genotypes infected with Potato virus Y

M. Pompe-Novak, M. Dermastia, K. Gruden
National Institute of Biology, Ljubljana, Slovenia



INTRODUCTION

Potato virus Y (PVY) is of extreme economic importance as it is responsible for yearly losses in production of crops from family *Solanaceae* in Europe, and thus the subjects of investigation in many research groups all over the world. The tuber necrotic strain of Potato virus Y (PVY^{NTN}) causes potato tuber necrotic ringspot disease (PTNRD) in sensitive potato (*Solanum tuberosum* L.) cultivars that is responsible for great losses in crop industry. Sensitive cultivars of potato infected with PVY^{NTN} show growth inhibition, faster senescence and leaf drop, chlorotic ringspots and/or spot necrosis on inoculated leaves, crinkles and mosaics on systemic infected leaves and necrotic ring spots on tubers. Viruses from PVY^{N-Wi} group can also cause severe symptoms on potato.



RESULTS

Differences in growth inhibition, senescence, leaf drop and symptom appearance on leaves appeared between four potato cultivars after the infection with two isolates of Potato virus Y, PVY^{NTN} and PVY^{N-Wi}.

Symptoms on leaves 2 weeks post inoculation ranged from mild to severe symptoms, expressed as chlorotic ringspots and/or spot necrosis of different size and shapes or vein necrosis.

5 weeks post inoculation symptom expression depended on potato cultivar,, faster leaf drop (palm tree effect) and decline of plants were observed.



CONCLUSIONS

- Symptom development and their severity depend on the isolate of PVY and potato cultivar.
- The results were complemented with microarray and quantitative real-time PCR analyses of differentially expressed genes.

REFERENCES

- Kogovšek et al. (2016) PloS one, ISSN 1932-6203.
Baebler et al. (2014) Journal of Experimental Botany 65: 1095-1109.
Baebler et al. (2011) PloS one, doi: 10.1371/journal.pone.0029009.
Kogovšek et al. (2011) Phytopathology 101: 1292-1300.
Kogovšek et al. (2010) Plant Pathol. 59: 1121-1132.

Hemp (*Cannabis sativa* L.) is an important fibre crop used in the textile and construction sectors. The stem of hemp cultivars grown for biomass production presents hypolignified extraxylary fibres rich in crystalline cellulose. The hypocotyl development was followed between 6 (H6) and 20 (H20) days after sowing. It was demonstrate that the hemp hypocotyl is a suitable model to study the molecular events associated with the dynamics of the cell walls in relation with the primary and secondary growth (Behr et al, 2016) and the molecular events accompanying lignification. Lignin and lignans are two macromolecules deriving from the monolignol pathway. Despite the similarity of their building blocks, they fulfil different functions *in planta*. Lignin strengthens the tissues of the plant, while lignans are involved in plant defence and growth regulation. Their biosyntheses are tuned both spatially and temporally to suite the development of the plant (water conduction, reaction to stresses). The present work confirms the validity of this system, by using it to study the regulation of lignin and lignan biosyntheses.

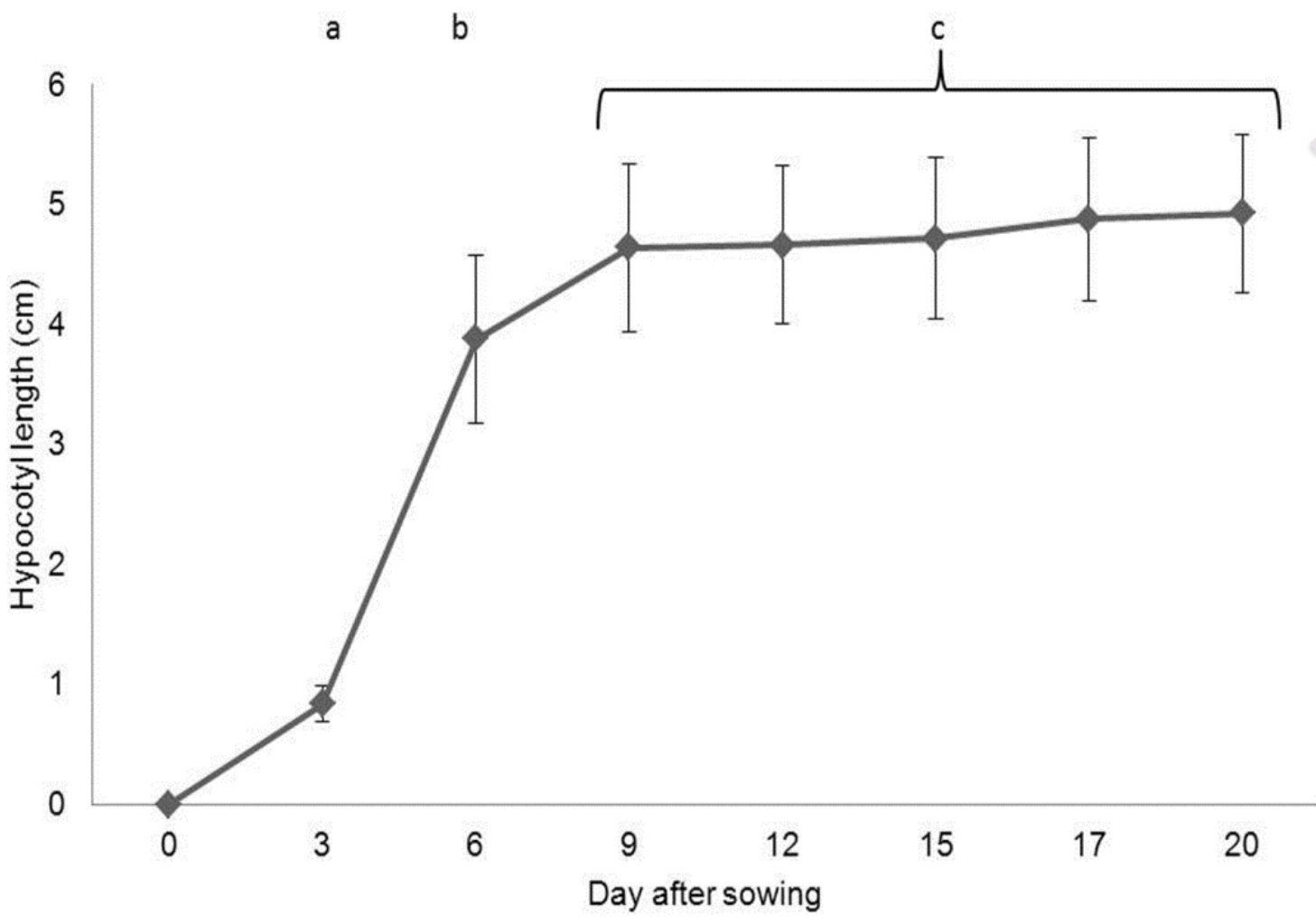
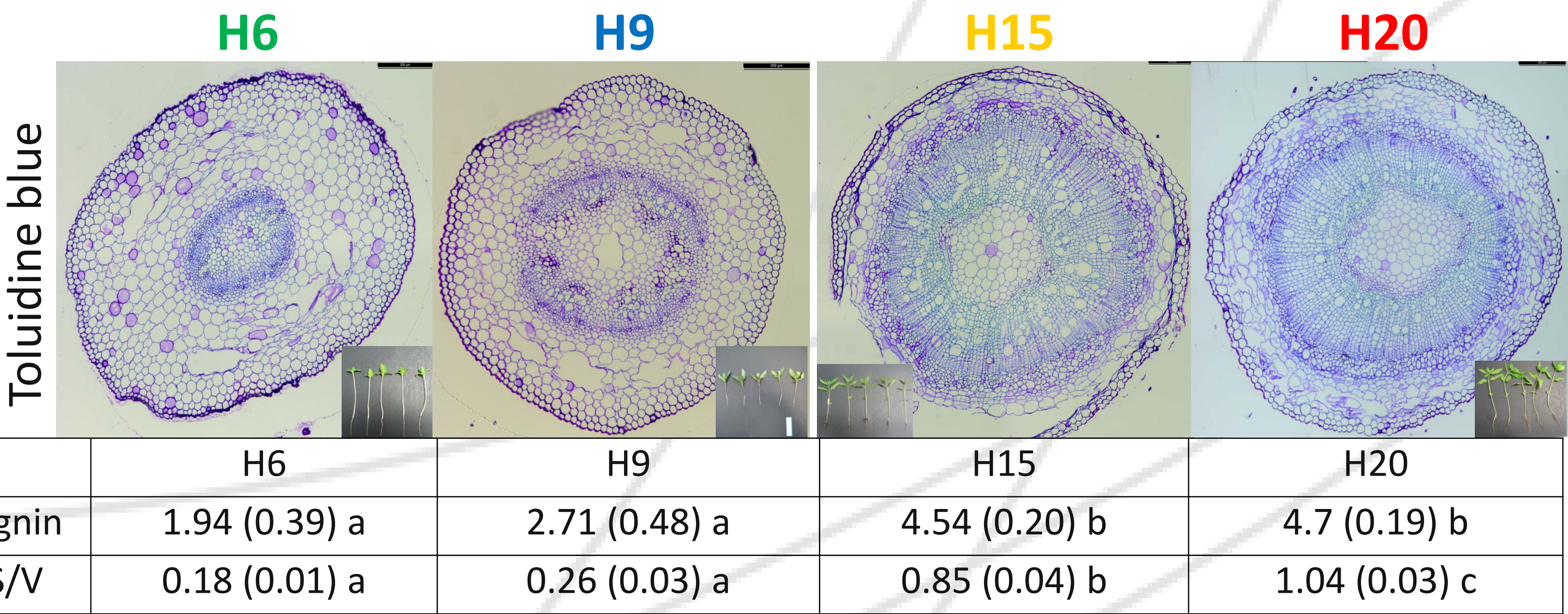


Fig. 1: Length of the hypocotyls (mean values +/-SD, n=15) with value of Tukey post-hoc test at p=0.05.

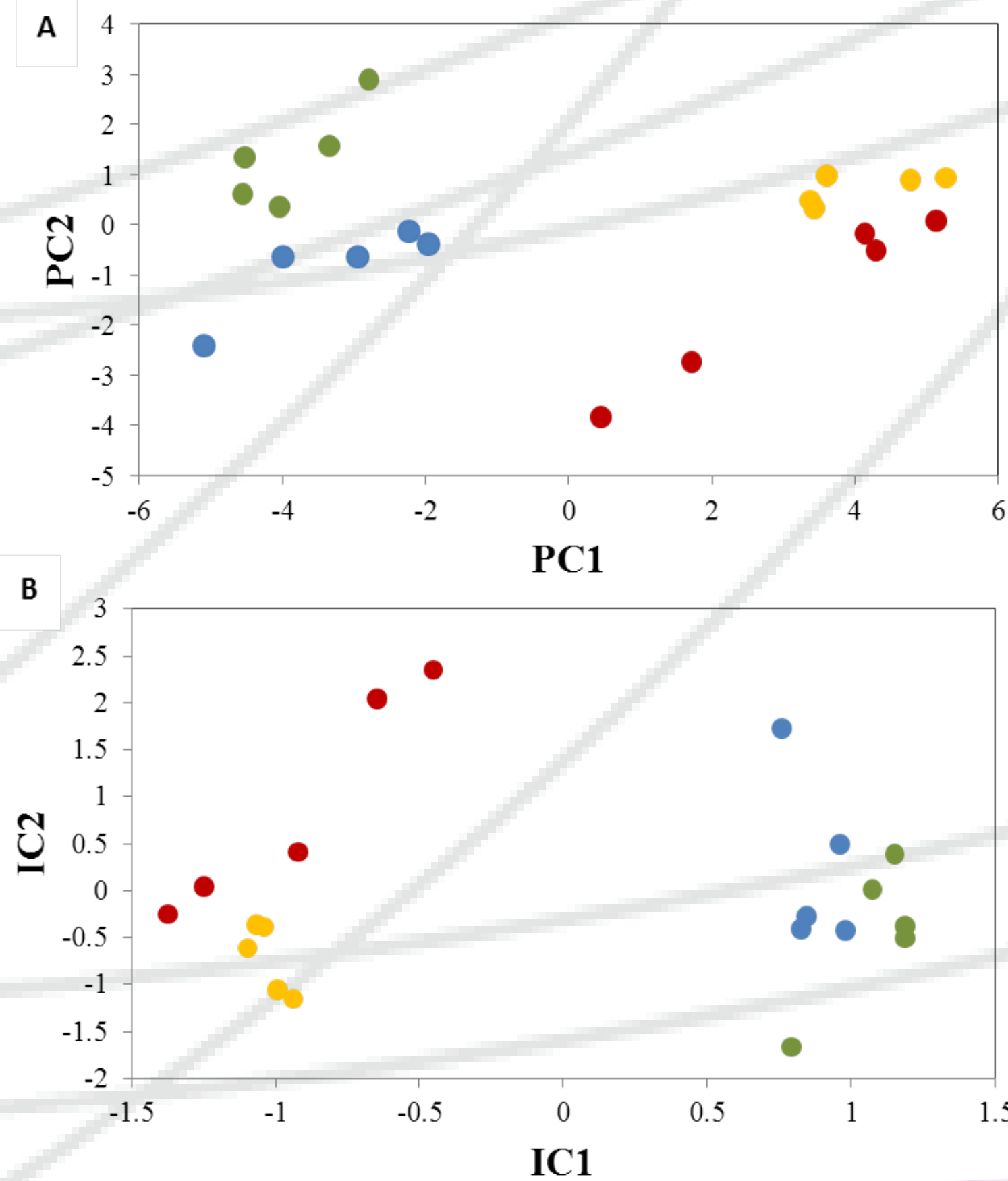
Fig. 2: Cross-sections of Cannabis stems at H6, H9, H15 and H20 stained with toluidine blue (magnification 10 x) and the corresponding content in lignin (%CWR, average (SD)) and the ratio S/V : V vanillin, S syringaldehyde.



Growth measurements (Fig.1), observations at the microscope and lignin analysis (Fig.2), gel-based and gel-free proteomics (Fig.3 and 4), together with targeted RT-qPCR, *in situ* laccase and peroxidase activity assays were carried out to understand the dynamics of lignan/lignin synthesis during the development of the hemp hypocotyl.

RT-PCR was performed on dirigent-like protein, laccase, pinorensinol reductase 1, dirigent protein, NAC secondary cell wall thickening 1, methionine synthase 1, S-adenosylmethionine synthase, peroxidase, pinorensinol-lariciresinol reductase.

In H15 and H20, no laccase activity signal was observed in the primary xylem but a strong peroxidase signal was instead visible. This may suggest that a peroxidase-driven lignification occurs after the polymerisation of monolignols by laccases.



	Tukey PC1	Tukey PC2
Anova p-value	2.39e-08	0.0034
H6	a	c
H9	a	ab
H15	b	bc
H20	b	a

	Tukey IC1	Tukey IC2
Anova p-value	1.52e-11	0.039651
H6	b	ab
H9	b	ab
H15	a	a
H20	a	b

Fig.4: NSAF relative quantities of proteins involved in cell wall biogenesis assessed by LC-MS. The group I (in yellow) includes proteins which are more abundant in H15 or H20 as compared to younger hypocotyls. The proteins of the group II (in magenta) are more abundant in H20, including the majority of the proteins involved in the phenylpropanoid and monolignol biosynthetic pathways, as well as in lignin polymerisation. Finally, the proteins present in the group III (in blue) are more abundant in young hypocotyls. They are mainly devoted to the modification of the cell wall to ensure the extensibility of the hypocotyl.

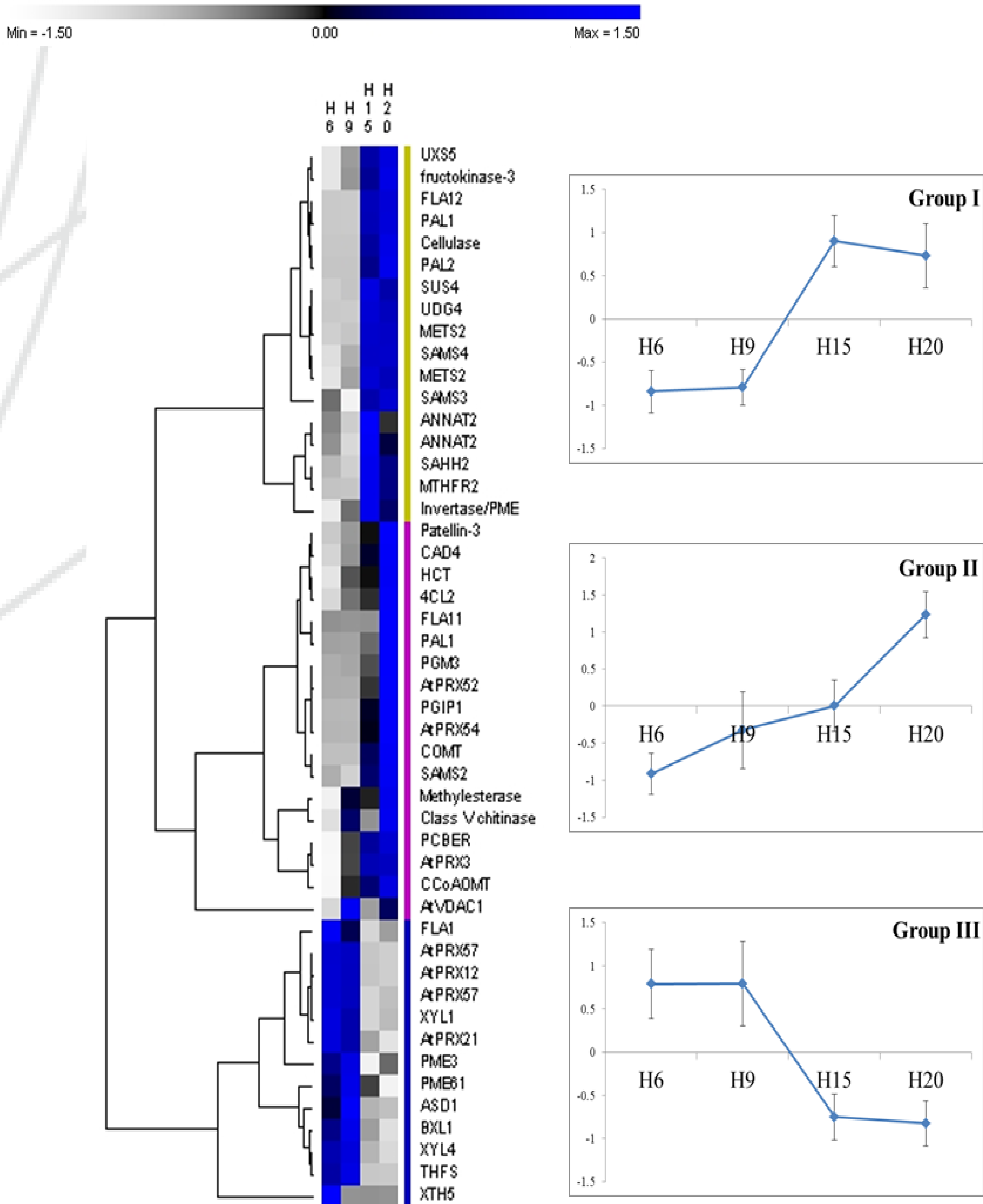


Fig.3: Variability of the proteome profiles. A: Principal component analysis of the time points assessed by 2D-DIGE. B: Independent component analysis of the time points computed with the NSAF values from LC-MS. In both panels, the significance of the coordinates was assessed using a Tukey post-hoc test, values with different letters within one column are significantly different .

We suggest a role for the hemp dirigent and dirigent-like proteins based on phylogenetic analysis and targeted gene expression. The complementary approach adopted identifies the main players (genes and proteins) involved in the biosynthesis of monolignols and their oxidative coupling (class III peroxidases and laccases), in lignin deposition (dirigent-like proteins) and the stereoconformation of lignans (dirigent proteins). Our work sheds light on how the growing hemp hypocotyl regulates, at the transcriptional and proteomic level, the provision of the precursors needed to synthesize the aromatic biopolymers lignin and lignans.

UDP-xylose synthase 5 (UXS5), fructokinase-3, fasciclin-like arabinogalactan 12 (FLA12), pal1, cellulase, sucrose synthase 4 (SUS4), UDP-glucose dehydrogenase 4 (UDG4), methionine synthase 2 (METS2), S-adenosylmethionine synthases 3-4 (SAMS3-4), S-adenosyl-L-homocysteine hydrolase 2 (SAHH2), methylenetetrahydrofolate reductase 2 (MTHFR2), annexin 2 and one invertase/PME. PAL1, 4CL2, HCT, CAD4, COMT, CCoAOMT, PHENYLCOUMARAN BENZYLIC ETHER REDUCTASE (PCBER), and orthologs of AtPRX52, AtPRX54 and AtPRX3. Patellin-3, phosphoglucosyltransferase 3 (PGM3), FLA11, polygalacturonase inhibiting protein 1 (PGIP1), methyltransferase, class v chitinase, voltage dependent anion channel 1 (VDAC1). Orthologs of AtPRX49, AtPRX52 and AtPRX72. FLA1, PRXS, PMES, xyloglucan endotransglucosylase/hydrolase 5 (XTH5), alpha-xylosidase 1 (XYL1), beta-xylosidase 1-4 (BXL1, XYL4), and alpha-L-arabinofuranosidase 1 (ASD1). 10-formyltetrahydrofolate synthetase (THFS)